Tomás Caldeira Lourenço
Licenciado em Ciências de Engenharia Civil

Anomalies detection in adhesive wall tiling systems by infrared thermography

Dissertação para obtenção do Grau de Mestre em
Engenharia Civil – Perfil de Construção

Orientador: Luís Manuel Cordeiro Matias, Investigador Auxiliar, Laboratório Nacional de Engenharia Civil

Co-orientadora: Maria Paulina Faria Rodrigues, Professora Associada, Faculdade de Ciências e Tecnologia da Universidade Nova de Lisboa

Júri:

Presidente: Prof. Doutor Carlos Manuel Chastre Rodrigues

Arguente: Prof. Doutor Fernando Manuel Anjos Henriques

Vogal: Doutor Luís Manuel Cordeiro Matias

FACULDADE DE CIÊNCIAS E TECNOLOGIA
UNIVERSIDADE NOVA DE LISBOA

Dezembro 2016

Anomalies detection in adhesive wall tiling systems by infrared thermography

Acknowledgements

I would like to thank some persons and organizations to whom I owe the possibility of bringing forth this masters dissertation.

Firstly I would like to express my gratitude to Doctor Luís Matias (LNEC) and Prof. Doctor Paulina Faria (FCT/UNL) for the orientation and co-orientation of this work respectively, for the help and engagement through the learning process of this thesis and useful comments.

I would also like to acknowledge Doctor Luís Silva and Mr. Miguel Mendes from Weber Saint-Gobain, for supporting this work not only by providing material and applying it on the external panels but also to the suggestions and interest shown during the process.

To Eng. Helena Afonso from Revigrés, for providing the tiles used in this study.

To Mr. José Carlos Matos and to Mr. Manuel Sadio to all the help with the measuring equipment.

To Mr. José Fernandes Costa for the help and transmittance of practical knowledge on the specimens' preparation.

To all the staff from LNEC's Buildings Department who participated in the project by wittingly supporting me, sharing their time and knowledge: Doctor Carlos Pina dos Santos, Engª. Maria Alexandra Costa, Engª. Sofia Malanho, Mrs. Vanda Cardoso, Mr. Acácio Monteiro, Mr. Bento Sabala and Mr. Carlos Raposo Saldanha.

I would like to thank Eng. Vitor Silva for the valuable help to this dissertation's presentation.

I am also very grateful to all my friends and colleagues for the good moments, friendship and cooperation though out this course.

A special thanks to my mother, father and brother for all the love, support, encouragement, care, trust and teaching through all the stages of my life. This work is dedicated to them.

Abstract

Tiling systems for building facade coatings are widely used all over the world. Despite very common, mainly due to its aesthetic characteristics, this kind of cladding is characterised by a complex application, given the fact that it is a system in direct contact with a support (the rendered wall) and composed by three different components with specific characteristics and technical requirements: the tiles, the adhesive grout, and the joint grout. This complexity can result in several possible anomalies, as it is the case of detachment, the most common onerous one and probably the most difficult anomaly to early diagnosis in this type of cladding.

Infrared thermography is a non-destructive testing method with a broad applicability in buildings' inspection. The method consists in using a thermal camera that, by detecting thermal radiation, reads thermal variations that can indicate the presence of anomalies.

Taking into account this diagnosis method's potential, it was developed in LNEC a wide study where the results of thermographic surveys on laboratory specimens, exterior panels cladded with tiles with controlled anomalies and case studies of real situations are presented.

In order to characterize the claddings behaviour and the anomalies' detectability using this method, in a first phase eight specimens were studied in laboratory with differences in terms of: colour, thickness, kind of support, finishing and presence of anomaly.

In a second phase, four panels divided into two experimental cells, located in LNEC's campus, aiming to evaluate the diagnostic technique in exterior facades with differences in terms of tiles' colour and support of application.

As a complement of the laboratory surveys (indoors and outdoors) certain features of this kind of cladding were characterized, such as their emittance and reflectance.

In order to evaluate infrared thermography's diagnosis capability in real and unfamiliar situations, two real cases of buildings in Lisbon, cladded with ceramic tiles, were studied.

The results obtained in the form of thermal differentials between "normal" and "anomalous" zones in a tiled facade or specimen proved that Infrared Thermography can be a valuable tool to early identification of anomalies, mainly detachments, in this kind of coating systems.

Keywords: Non-destructive testing method**,** Anomaly, Tile, Detachment, Infrared Thermography, Facade.

Resumo

O revestimento de fachadas de edifícios com ladrilhos é uma técnica bastante usada em todo mundo. Apesar de bastante comum, principalmente devido às suas características estéticas, este tipo de revestimento tem uma aplicação complexa, dado ser um sistema em contacto direto com o suporte (parede) e composto por três diferentes componentes com características e requisitos técnicos específicos. Esta complexidade pode resultar em diversas anomalias, como é o caso do destacamento, a anomalia mais comum e mais gravosa neste tipo de revestimentos e, provavelmente, a mais difícil de identificar precocemente.

A termografia de infravermelhos é um método de diagnóstico não destrutivo com uma vasta aplicação na inspeção de edifícios. Este método baseia-se na leitura de temperaturas através da deteção de radiação térmica, cujas diferenças podem ser indício de anomalia.

Tendo em conta o potencial deste método foi desenvolvido no LNEC um estudo amplo do qual se apresentam os resultados obtidos em ensaios termográficos realizados em provetes e painéis exteriores revestidos com ladrilhos, com anomalias controladas e em casos reais com anomalias desconhecidas.

Para uma caracterização do comportamento do revestimento e da detetabilidade das anomalias com termografia foram em primeiro lugar executados e estudados em laboratório oito provetes, com diferenças em termos de: cor, espessura, acabamento, tipo de suporte e presença de anomalia.

Numa segunda fase foram estudados quatro painéis divididos em duas fachadas de células experimentais localizadas no *campus* do LNEC, com o objetivo de avaliar a técnica de diagnóstico em fachadas exteriores com ladrilhos de diferentes cores e diferentes suportes de aplicação.

Como complemento ao estudo dos sistemas (realizado no interior e no exterior) foram caracterizadas os parâmetros emitância e refletância dos ladrilhos de revestimento utilizados.

Para validar a capacidade de diagnóstico da termografia em situações reais foram estudados três edifícios com revestimentos cerâmicos em Lisboa.

Os resultados obtidos, sobre a forma de diferenciais de temperatura entre zonas “normais/sãs” e “anómalas” de uma parede revestida com ladrilhos, mostram que a termografia de infravermelhos é uma ferramenta capaz de identificar anomalias, sobretudo destacamentos, neste tipo de revestimento.

Termos-chave: Método não destrutivo de diagnóstico, Anomalia, Ladrilho, Destacamento, Termografia de infravermelhos, Fachada.

Index

Appendix

Figures Index

Tables Index

Symbols

General abbreviations

AIRT – Active Infrared Thermography

APICER – Associação Portuguesa da Industria de Cerâmica

ASTM – American Society for Testing and Materials

ATS – Adherent Tiling System

BS – British Standard

CDT – Cooling Down Thermography

CG – Cementitious Grout

EDCP – European directive for construction products

EN – European Norm

EPS – Expanded Polystyrene

ETICS – External Thermal Insulation Composite System

FIR – Far infrared

FPA – Focal Plane Array

GL – Glazed

HgTeCd – Mercury - Cadmium - Tellurium

IMPIC – Instituto dos Mercados Públicos do Imobiliário e da Construção

InSb – Indium antimonide

IPQ – Instituto Português da Qualidade

IR – Infrared Radiation

IRT – Infrared Thermography

ISO – International Organization for Standardization

LNEC – Laboratório Nacional de Engenharia Civil

LT – Lock-in Infrared Thermography

VT – Vibrothermography

NDT – Non-destructive Testing

MIR – Medium Infrared

NIR – Near Infrared

NMF – Nonnegative Matrix Factorization

NP – Norma Portuguesa

NRI – Núcleo de Revestimentos e Isolamentos

PbS – Lead sulphide

PCA – Principal Component Analysis

PIRT – Passive Infrared Thermography

PT – Pulsed Infrared Thermography

q-QIRT – Quasi-quantitative Infrared Thermography

RG – Reaction resin Grout

SIS – Simple Image Subtraction

SH – Step Heating Infrared Thermography

td-PIRT – Time-dependent Passive Infrared Thermography

UGL – Unglazed

UV – Ultra-violet Radiation

XPS – Extruded polystyrene

Experimental symbols

A - Area [m2]

a - Thermal Diffusivity [m^2/s]

α - Coefficient of absorption

b - Thermal effusivity [$J/(K \cdot m^2 \cdot s^{0.5})$]

c – Light speed [m/s]

c_p - Specific Heat [J/(kg·K)]

Dist – Distance to the target [m]

ΔT – Temperature differential [°C]

Δx - Thickness [m]

E - Total Emissive Power

E_λ - Spectral emissive power [W/m^2]

E^0 - Total emissive power of a blackbody [W/m^2]

E^0_λ - Spectral emissive power of a blackbody [W/m^2]

E_{atm} – Radiation emitted by the atmosphere [W/m^2]

E_{obj} – Emission from the object in study [W/m^2]

E_{refl} – Radiation reflected by the object [W/m^2]

ε - Emittance / Total (hemispheric) emittance

ε' - Directional (total) emittance

ε_λ - Spectral (hemispherical) emittance

ε'_λ - Spectral directional emittance

f - Frequency [Hz]

G_a - Absorbed Radiation

G_i - Incident radiation or irradiation

G_r - Reflected Radiation

G_t - Transmitted Radiation

HR – Relative humidity [%]

h – Plank's constant [$6.6260693(11)x10^{-34}$ J·s]

h_c – the heat transfer coefficient (W/(m2·K)

k – Boltzman's constant [$1.3806503x10^{-23}$ J/K]

L – Radiance [$Wm^{-2}sr^{-1}$]

L_λ - Spectral radiance [$W \cdot m^{-2} \cdot sr^{-1}$]

L^0_λ - Spectral radiance from a black body [$W \cdot m^{-2} \cdot sr^{-1}$]

L^0 - Total radiance from a black body [$W \cdot m^{-2} \cdot sr^{-1}$]

λ - Thermal Conductivity [W/(m·°C)]

λ_{max} - maximum wavelength [μm]

λ - Wavelength [μm]

Q - Heat [W]

q - Heat Flow [W/m2]

q' – Heat generated per unit of volume (W/m^3)

q_{conv} – Heat flow by convection (W/m^2)

ρ - coefficient of reflection

T - Temperature [ºC or K]

T_{atm} – Atmospheric temperature [°C]

T_{refl} – Reflected temperature [°C]

τ - Coefficient of Transmission

τ_{atm} - Atmosphere's transmittance

σ - Stefman-Boltzman constant [$5.67x10^{-8}$ $W \cdot m^{-2} \cdot K^{-4}$]

Θ - Angle

Ω - Direction

Specimens' abbreviations

Blad – Black laboratory specimen with adherent tiles

Wnat – "White natural" laboratory specimen with detached tile

Bnat – "Black natural" laboratory specimen with detached tile

Wpol – "White polished" laboratory specimen with detached tile

Wl – "White light" laboratory specimen with detached tile

Bl – "Black light" laboratory specimen with detached tile

Wti – White laboratory specimen with detached tile over thermal insulation support

Bti – Black laboratory specimen with detached tile over thermal insulation support

TDet – Temperature of the non-adherent obtained with thermography

TAd - Temperature of the adherent zone obtained with thermography

TcDet - Temperature of the non-adherent zone obtained using a thermocouple

TcAd - Temperature of the adherent zone obtained using a thermocouple

Outdoors panels' abbreviations

C1_W – White panel from cell 1

C1_B – Black panel from cell 1

C2_W – White panel from cell 2

C2_B – Black panel from cell 2

Tc_Bad – Temperature measured with a thermocouple under an adherent black tile

Tc_Bdet – Temperature measured with a thermocouple under a detached black tile

Tc_Wad – Temperature measured with a thermocouple under an adherent white tile

Tc_Wdet – Temperature measured with a thermocouple under a detached white tile

Tc_Bs – Temperature measured with a thermocouple on the surface of an adherent black tile

Tc_Ws – Temperature measured with a thermocouple on the surface of an adherent white tile

Tint – Temperature measured with a thermocouple in the interior of the experimental cell

Det – Average temperature from detached tiles measured by thermography

Ad - Average temperature from adherent tiles measured by thermography

1 Introduction

1.1 Framework

With the increasing importance given to building rehabilitation comes the need to create simple, fast and non-destructive testing methods (NDT) to identify potential anomalies. Tiling systems are one of the most typical kinds of exterior wall cladding in several countries; its history goes back from The Egyptian Empire, with the earliest known examples dating from 4000 BC. Portugal, despite not being the biggest producer, was the European country that used ceramic claddings the most in its buildings from the XVI century [W5]).

This type of building facade coating, though being quite often used due to its aesthetic and architectural characteristics, is one of the most complex that can be applied given the several parts from which it is composed. Hence, it is also one of the most difficult to correctly diagnose with expeditious methods. From the numerous anomalies associated with adherent tiling systems, the detachment of tiles is probably the most common and difficult to identify and it is also definitely the one that can compromise security the most. In this study, the term detachment will be used for tiles with lack of adhesion to the support.

Despite this diagnostic testing being often seen as unnecessary, according to Martarelli et al. (2014), the economic effort required for the realization of diagnostic testing will be repaid during the repair intervention: previous studies have, in fact, shown that 1 € spent in preliminary tests can allow a saving of 10 € during the development of works (Bosiljkov et al. 2010). Thus, it is necessary to study a process of inspection more efficient and economic than the currently used, which often consist of destructive or semi-destructive methods, that can only be used in a small part of the building at a time, allowing some assumptions on what can the rest of the cladding be like.

Infrared thermography (IRT) is an NDT technique, with a wide variety of applications in building inspections, that is becoming commonly used to identify anomalies related with thermal variations in the inspected surfaces, without impairing its future usefulness (Maladague et al. 2001). When compared with other classical NDT techniques, such as C-Scan, ultrasonics or X-Rays, this technique is safe, nonintrusive and noncontact, allowing the detection of relatively shallow subsurface defects under large surfaces and in a fast manner (Ibarra-Castanedo et al. 2007). Although all the mentioned advantages of this inspection method, it has been considered as an expensive method due to the equipment required. However, a thermal camera for building diagnostic, which was an instrument mostly owned and used by research institutes and large size laboratories, has become affordable for every consultant almost all over the world (Lehmann et al; 2013).

Few authors have studied the application of IRT in anomalies associated with ceramic claddings claiming that the presence of air or water beneath the superficial layer will influence the heat transfer in a way that can be detected in both a qualitative and a quantitative way by the thermal camera, providing information about the state of the wall in a much broad area per trial than other methods commonly used nowadays. Considering the previous work developed in this field, this dissertation aims to be a step forward to improve this diagnostic method's recognition, encouraging its use and, possibly, promoting the creation of testing standards by studying its capacities and limitations in the detection of anomalies in tiling systems under different conditions.

1.2 Objectives and methodology

The main goal of this dissertation is to prove and validate infrared thermography's capacities in detecting anomalies in wall tiling systems. As detachment is considered the most important anomaly to study on this kind of cladding, this dissertation will be especially focused on its study. However some other anomalies, such as moist presence, cracking and glaze detachment, will also be analysed.

As a complement of the main objective, a research on the different kinds of claddings and their most usually associated anomalies will also be presented. Another part of the research for this work is on infrared thermography, being the objective to gain a better understanding of the testing method/equipment, its capacities and requirements.

Considering the above, a study in LNEC (Laboratório Nacional de Engenharia Civil) with the support of Weber Saint-Gobain and Revigrés has been developed, using laboratory specimens, outdoor panels from experimental buildings and case studies, to verify infrared thermography's capacity in detecting anomalies in tile claddings.

This study will be focused on ceramic claddings as these are the most commonly tiling systems used in walls and the anomalies' identification process using thermography is considered to be similar as in other kinds of tiling systems.

As it will be presented, there are numerous types of ceramic cladding from which the porcelain tiles were chosen to this study's laboratory survey. Hence, using this tiles eight laboratory specimens were made to study differences in thermal behaviour due to colour, finishing, type of support, thickness, presence of detachments and presence of moisture. In order to study the cladding's behaviour in exterior conditions four panels were made with changes in terms of colour and type of support at LNEC's campus.

As the method of diagnosis under study consists in reading thermal radiation emitted by the objects, a research on this kind of radiation and how it interacts with bodies has been done, not only for a better understanding of the method's fundaments but also for a better understanding of the parameters needed to input on the equipment (thermal camera) in order to make proper thermal readings.

Aiming to solidify the work and testify infrared thermography's applicability in real situations, two buildings with ceramic claddings were inspected in Lisbon.

1.3 Work structure

This dissertation is divided into six chapters:

The present chapter contains a brief introduction framing the work subjects, objectives and how the dissertation is structured.

The second chapter is a bibliographic research on tiling systems, their characteristics, how they are classified and applied, their most common anomalies and respective diagnosis methods.

The third chapter is also a product of bibliographic research, but this time the subject is infrared thermography. Firstly, in order to understand the phenomena concerned, some concepts about heat transfer, particularly about radiation, are exposed. Then, a research on infrared thermography is presented, how it has been applied to building inspections and more particularly some studies on

how thermography can be used to identify anomalies in tile claddings or other closely related subjects.

Chapter four presents how the non-destructive method will be tested and all the other complementary procedures.

The fifth chapter contains the analysis of the results obtained both experimentally (indoors and outdoors) and in real cases inspections. The results of some parameters' determination will also be presented.

Seventh chapter presents the conclusions of all the work and some proposals for future works.

This document comes to an end with the bibliographic references, followed by the appendix where some complementary information can be found.

2 Tiling systems

2.1 General considerations

Ceramic claddings consist in a type of facade coating composed by three main components: the ceramic tiles (EN 14411:2016), the adhesive layer (EN 12004:2014) and the joint filling grout (EN 13888:2009).

This type of cladding has been used for decades as a wall coating not only due to its aesthetic features but also because of its high resistance towards environmental conditions, cleanability, good resistance to humidity and low maintenance cost (Campante et al. 2001). According to Campante et al. (2001) and Shohet et al. (1996), comparing this type of cladding with others such as cementitious mortars, synthetic mortars and stone, its superiority in terms of durability is obvious (table 1).

Table 1 - Cladding types' lifespan estimation in years
(adapted from Campante et al. 2001; Shohet et al. 1996)

Environment category	Cementitious mortar	Synthetic mortar	Ceramic cladding	Stone
Non-corrosive	10 - 15	12 – 15	Above 15	Above 25
Corrosive	5	8 – 12	10 - 15	Above 25

Despite having a reasonable lifespan, sooner or later anomalies (situations where the cladding no longer presents the expected performance requirements, failing in attending the users necessities (Canpante et al. 2001)) occur in this kind of cladding as well as in all the others, either naturally due to the claddings wearing or due to human-related causes such as problems in the project or respective application.

As a part of a construction, tiles claddings shall respect to the following fundamental requirements according to the European Directive for Construction Products (89/106/CEE):

- mechanical resistance and stability;
- safety in case of fire;
- hygiene, health and the environment;
- safety in use;
- protection against noise;
- energy economy and heat retention.

Besides these fundamental requirements, tile cladding systems shall also obey to the requirements correspondent to their primary function of coating such as (Apicer; 2003 and Campante et al. 2001):

- compatibility with the support;
- visual and tactile comfort;
- durability;
- regular using adaptation;
- protection of the building envelope.

2.2 Tiles

According to EN 13888:2008, wall and floor tiles are "tiles made out of ceramic or natural and agglomerated stones". More specifically, as this work is focused on ceramic tiles, according to EN 14411:2016, a ceramic tile is a "slab made from clays and/or other inorganic raw materials", whit a plane configuration, which is usually used for cladding walls or pavements.

The tiles are usually built by extrusion or dry pressing at atmospheric temperature but they can also be moulded by other processes. Then, tiles are *cooked* at the required temperature depending on the desired characteristics.

Tiles are rigid, fireproof and unaffected by light materials; they can be characterized according to its surface vitrification as glazed (GL) or unglazed (UGL) (Bento; 2010 and EN 14411:2016). Glazed tiles are known in Portugal as *azulejos*. Amongst other, the degree of vitrification is one of the most important characteristics of this kind of cladding, not only due to aesthetic reasons but also its influence on the tile's superficial porosity.

It is often claimed that the technical performance level rises with the vitrification degree. The exception is the mechanical resistance to the impact that reduces with vitrification, resulting in a higher fragility of the glided tiles (Bento; 2010). Besides the vitrification, tiles' surfaces can also be engobed ("given a clay-based covering with a matt finish which can be permeable or impermeable" (EN 14411:2016) or polished ("surface of a glazed or unglazed tile which has been given a glossy finish by mechanical polishing carried out after firing" (EN 14411:2016).

According to EN 14411:2016, "ceramic tiles are divided according to their method of manufacture and their water absorption".

When the method of manufacture is concerned, ceramic tiles can be divided into extruded tiles (method A) and dry-pressed tiles (method B). As to the water absorption, there are three groups of tiles: of low water absorption (group I), of medium water absorption (group II) and of high water absorption (group III). These three groups are then divided as follows (table 3):

a) Tiles of low water absorption (Group I), E ≤ 3 %

a1) Extruded tiles:

1) E ≤ 0.5 % (Group AI_a),

2) 0.5 % < E ≤ 3 % (Group AI_b).

a2) Dry-pressed tiles:

3) E ≤ 0.5 % (Group BI_a),

4) 0.5 % < E ≤ 3 % (Group BI_b).

b) Tiles of medium water absorption (Group II), 3 % < E ≤ 10 %

b1) Extruded tiles:

1) 3 % < E ≤ 6 % (Group AII_a, Parts 1 and 2),

2) 6 % < E ≤ 10 % (Group AII_b, Parts 1 and 2);

b2) Dry-pressed tiles:

3) 3 % < E ≤ 6 % Group BII_a,

4) 6 % < E ≤ 10% Group BII_b.

c) Tiles of high water absorption (Group III), E > 10 %

Table 2 shows some examples of products corresponding to the categories indicated in EN 14411:2016.

Table 2 – Some ceramic tiles examples (adapted from Apicer; 2003 and Vaz; 2003)

	A – Extrusion		B – Dry-pressed
Group I E≤0.5%	 Extruded Stoneware [W6]	Group I_a E≤0.5%	 Porcelain
		Group I_b 0.5%≤E<3%	 Porcelain Stoneware [W7]
Group II_a 3%<E≤6%	 Klinker	Group II_a 3%≤E<6%	 Single-fired flooring [W7]
Group II_b 6%<E≤10%	 Terrakota [W9]	Group BII_b 6%≤E<10%	 Single-fired coating [W7]
Group III E>10%	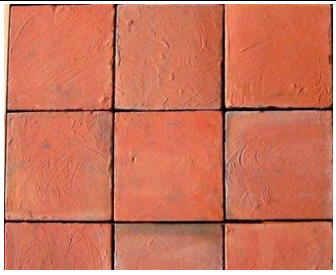 Rustic cotto [W10]	Group BIII E>10%	 Faience [W8]

Table 3 - Classification of ceramic pavements and claddings
(Adapted from Apicer; 2003; EN 14411:2016)

Manufacture method	Group AI E≤3%		Group AII_a 3%<E≤6%	Group AII_b 6%<E≤10%	Group AIII E > 10 %
A **Extrusion**	Extruded stoneware		Extruded stoneware Klinker Rustic cotto	Rustic cotto Terracotta	Rustic cotto
Manufacture method	Group BIa E≤0.5%	Group BI_b 0.5%<E≤3%	Group BII_a 3%<E≤6%	Group BII_b 6%<E≤10%	Group BIII E > 10 %
B **Dry- pressed**	Stoneware flooring Klinker Porcelain	Stoneware flooring Klinker Fired ceramic flooring	Single-fired flooring	Single-fired coating	Faience
Manufacture method	Group CI E≤3%		Group CII_a 3%<E≤6%	Group CII_b 6%<E≤10%	Group CIII E > 10 %
C **Other processes**			Rustic flooring	Rustic flooring	Faience Rustic flooring

2.3 Tiles' application

Besides the tile itself, another important part of this cladding system is the attachment process that can be either by contact or mechanical fixation.

2.3.1 Mechanical fixation

In the case of mechanical fixation systems can be divided according to the purpose of the cladding: if its destiny is ventilated facades or raised access floors. Both these cases are used due to their advantages in terms of ventilation, maintenance, safety, comfort (eliminating thermal bridges and raising the thermal inertia and consequently reducing the energy consumptions for acclimatization), attenuation of the facade's aging process and its applicability over almost all kinds of existing supports, making this kind of application fit not only to new buildings but also for rehabilitation (Apicer; 2003). These tiles are generally thicker than the ones for fixation by contact.

2.3.2 Fixation by contact

This is the most typical kind of fixation that consists in creating adhesion between the two parts of the cladding (tile and support) by the creation of cohesive molecular forces. These forces come from the development of crystalline structures within the pores that maintain the components connected (Apicer; 2003). Hence, the characteristics of the adhesive material rely mainly on the tiles and support's porosity but also in other factors like the tiles' dimension, the application process and the positioning (outdoors/indoors and vertical walls/pavements). According to the mentioned characteristics, these kinds of adhesives, in the case of ceramic tiles, shall be applied in all the area, either in a single layer (in the tile or in the support) or a double layer (in both the tile and support).

Traditional mortar

The oldest method of fixation used in this system is with traditional mortars composed by a mix of binder, aggregates and water. These mortars are usually mixed *in situ* and then applied in a thick

layer which allows the compensation of the traditional tiles' variation of thickness and the support's irregularities.

This mortar presents some disadvantages in relation to the majority of the most recent ones such as (Apicer; 2003):

- lower adhesion tension;
- higher overcharge to the structure;
- higher probability of human error as they are prepared *in situ*;
- suitable only for highly porous tiles, since the application is purely by physical action.

Cementitious adhesives (C)

Cementitious adhesives are the most used nowadays; this kind of binding material consists in a mixture of hydraulic binding agents, aggregates and organic additives. These materials are usually pre-dosed, ready to mix with water or liquid admixtures and use. (EN 12004:2014)

Depending on performance exigencies there are five main kinds of cementitious adhesives available (Apicer; 2003):

- with organic and inorganic additives;
- of cellulosic derivatives;
- of mixed organic and inorganic binders;
- aluminous with mixed binders;
- of two components with resins.

Dispersion adhesives (D)

Dispersion adhesives consist of a "mixture of organic binding agent(s) in the form of aqueous polymer dispersion, organic additives and mineral fillers". This kind of adhesive comes in a ready to use mixture.

Reaction resin adhesives (R)

Reaction adhesives consist of a "mixture of synthetic resin, mineral fillers and organic additives in which hardening occurs by chemical reaction". Therefore, they are available in one or more components.

The price and the capacities of the adhesives rise from the traditional to the R class.

2.4 Joint filling grouts

Despite the name of the chapter that makes sense in the context of this dissertation on adherent ceramic tiles, the ceramic tiles systems not always have a joint filling grout as a component. For example in the case of ventilated facades, it makes no sense to fill the joints between tiles, disabling the ventilation process. However, in the context of adhesive tiles, the ceramic tile filling grout (defined in EN 13888:2008 as "any suitable product to be used to fill the joints between all types of ceramic tile") is indispensable to provide the system with resistance to water, to prevent the construction joints from being filled with dirt and to attenuate tensions from the components' dimensional variations.

According to the standard EN 13888:2008, there are four types of joint filling products:

- Cementitious grout (CG) – “mixture of hydraulic binding agents, aggregates, inorganic and organic additives” (the grout has only to be mixed with water or liquid admixture just before use).
- Reaction resin grout (RG) - “mixture of synthetic resin, aggregates, inorganic and organic additives in which hardening occurs by chemical reaction” (they are available in one or more component forms).
- Liquid admixture or latex additive – “special aqueous polymer dispersion to be mixed with a cementitious grout on site”.

Besides these grouts, Silvestre et al. (2009b) also consider the traditional grout, usually prepared on site in an apparent volumetric proportion of 1:2 (cement : medium humid sand) for joints up to 10mm (the incorporation of hydrofugue materials should also be considered in exterior claddings). This kind of filling material when compared with the most recent solutions presents problems due to the lack of control in production, problems of retraction and high stiffness.

There are two main types of joints (Apicer; 2003):

- Laying joints – the most common ones, used between tiles. The sizing of these joints must be set by the ceramic cladding’s manufacturer.
- Construction joints – divided in structural joints (crossing all over the building and aiming to absorb structural movements), peripheral joints (used on the edges of the cladded surface panels) and intermediate joints (these joints are used on large surfaces to attenuate the coating’s dimensional variations and should penetrate the totality of the regularization mortars’ depth). It is important to mention that this kind of joints should not be grouted with the products mentioned above but with specially designed products.

2.5 Anomalies in tiling systems

As mentioned previously, tiling systems are one of the most used cladding systems due to aesthetic, technical and economic reasons. However, as in all claddings, the durability relies on the system’s capacity withstanding the aging processes. In order to avoid anomalies, systems shall be designed according to their purpose and environment. Thus, it is necessary to have a good project with the right materials and well defined application technics.

A good project should take into account:

- the cladding’s purpose;
- the kind of support where the cladding will be applied;
- the aggressiveness of the environment (for example in terms of humidity and corrosive agents’ presence);
- the temperatures that the element will achieve (minimum temperatures when freeze-thaw is a possibility and maximum thermal amplitudes for thermal expansion purposes);
- tile’s characteristics, such as weight/size (influencing on the kind of attachment system (Apicer; 2003)) or the colour (influencing the thermal absorption and consequently thermal expansion, which might be attenuated with construction joints (Barros; 2010));
- the possibility of other attacks (such as mechanic impacts);
- The aging process of the system.

Detachment

According to Dufour (1948), detachment represented always more than 50% of the totality of anomalies in this kind of cladding. The percentage has not changed much currently. It is also probably the most studied anomaly not only due to the consequences it brings in terms of aesthetics loss and functional requirements (usually implying the total functional loss of the cladding, compromising the durability of the support) but also due to the safety concerns it can rise (Abreu; 2005). According to Tan et al. (1994), a 250 g tile falling from a 10th floor reaches the soil with the same destructive power as a firearm projectile.

Detachment consists in the loss of adhesion between two or more layers of the cladding system (support, adhesive mortar and tile) which can result in the separation of the tiles (or the tiles and the adhesive) from the rest of the system. Detachments can be divided into three different types/phases according to what happens to the tile:

- the first type is the non-visible detachment where, despite the existence of a void beneath the tile, differences between attached and detached tiles are not visible to the naked eye; these detachments are usually detected by their hollow sound when tapped (ASTM D4580);
- the second is the detachment with buckling (fig. 1a) which "occurs when compressive forces induced into the tile system overcome the bond between the tile and substrate. The compressive forces are typically the result of expansive forces created during moisture or thermal exposure, and the effect from these forces may be exacerbated by restraining forces from inherent shrinkage of concrete substrates or the lack of movement joints" (Bart B. Barrett et al.);
- finally there is the detachment with the total separation of the cladding from the support (fig. 1b), resulting in the release of the tile (by gravity on walls or by "explosive release" in floors (Silvestre et al. 2004)); this is obviously the final phase of the detachment and also the one that most compromises not only the facade but the security.

Figure 1 – Examples of detachments in glazed tiling systems in Lisbon: with buckling (a) and with the falling of tiles (b)

As these three "phases" of detachment are connected, sooner or later the total release of the tile will happen. So, it is considered that the gravity of these situations is identical for all in terms of consequences for the cladding system and necessity of repair (Silvestre et al. 2004).

There are several probable causes for this kind of anomaly (Lucas, 2001 and Silvestre et al. 2008):

- deficient preparation of the support (presence of dust and dirt);
- wrong choice of materials;

- faulty gluing of the tiles;
- awry sizing of the joints;
- excessive deformations of the support or of the tiles;
- presence of humidity or corrosive agents;
- aging;
- disrespect of the "open time" (EN 12004:2014) at which tiles can be embedded in the adhesive (Peixoto de Freitas et al. 2008).

Despite being described as different probable causes, these are often connected, for example, the "open time" depends overall on the right choice of the adhesive and weather conditions (such as the temperature, humidity and wind speed (Apicer; 2003)). According to Silvestre et al. (2006a), in Portugal most of the construction done has been on the coastline (in the first semester of 2015, just Lisbon and Porto represented over 50% of the construction sector (IMPIC; 2015)), suggesting that there is a great probability of a high influence of factors such as solar incidence or wind speed in the adhesive's "open time".

One of the problems of this anomaly is that there is no way of solving it but removing and re-gluing the tiles, which in some cases is very difficult due to dimensional variations.

According to Silvestre et al. (2008), the best way to diagnose this anomaly is the percussion method. However, the sphere-crash test, ultrasounds, the pull-off test and thermographic inspection are also valuable inspection methods.

Cracking

It consists in the opening of breaches (fig. 2) in the surface of the cladding that can either be superficial, in the tile glazing or the tile layer, or deeper, up to the adhesive mortar layer. The cracking results from the occurrence of tensile stress in the tiles layer greater than the tensile strength of the tiles. This phenomenon mainly occurs each time the adhesion strength between the tiles and the mortar is high. When that adhesion strength is low, the tensile stress in the tiles layer causes the detachment of this element (Silvestre et al. 2008, 2009a).

The most common causes of this anomaly are (Lucas; 2001 and Silvestre et al. 2008):

- awry sizing of the joints;
- excessive deformations of the support, tiles or adhesive mortar;
- poorly attached tiles rupture by bending;
- presence of humidity;
- impacts.

Figure 2 – Example of cracking in one of the case studies that will be presented

Crushing or delamination of the tiles' edges

This anomaly (fig. 3) is mainly due to differential movements of the support/cladding that result in the tiles compression and consequently the edges' crushing (Carvalho Lucas; 2001).

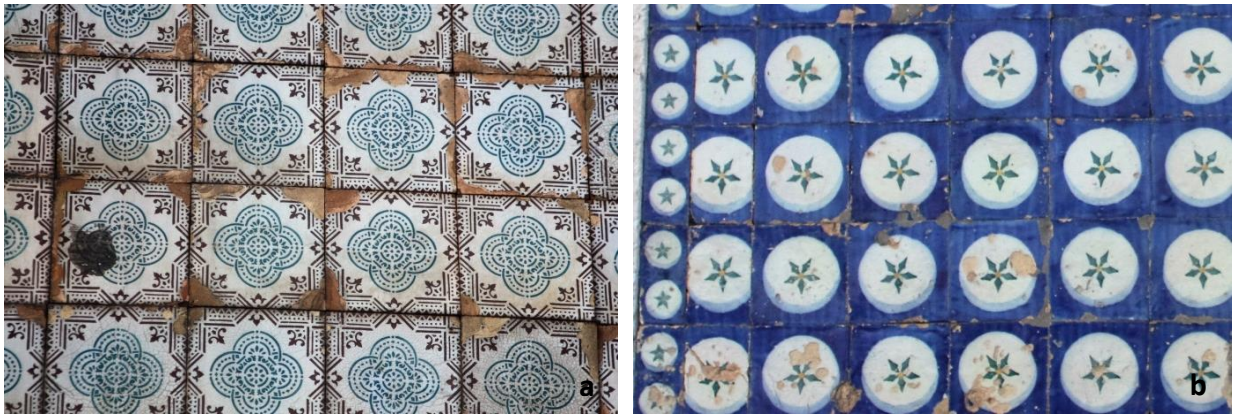

Figure 3 – Two examples of glazed tiles edges' crushing

Staining

This anomaly consists in the cladding´s colour alteration mainly due to dust trapping or chemical attacks (fig. 4). This phenomenon happens usually when there is a poor selection of products or when pores open because of the materials' wear.

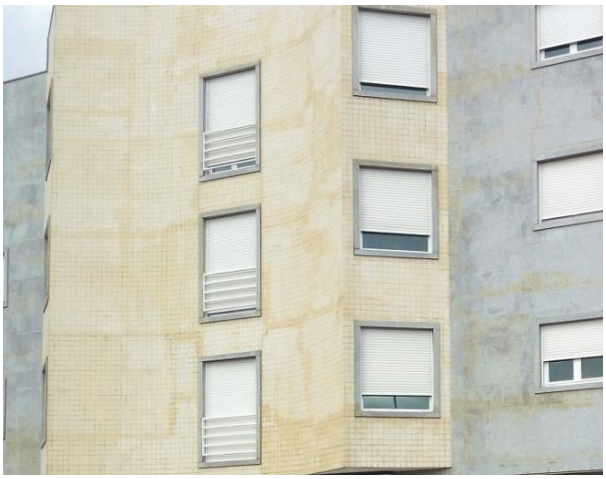

Figure 4 - Example of staining by chemical attack (wrong choice of hydrofugue treatment)

Glaze detachment/cracking

Glaze detachment/cracking consists in the appearing of craters or superficial cracks in the tile´s surface, often leading to its partial or global loss, owing to a lack of resistance from the tile's outer layer against actions such as freeze-thaw, impact or excessive tile's deformation (fig. 5). This anomaly not only has aesthetic impact but it can also compromise the cladding's efficiency, once the most water resistant layer of the tile can be lost.

Figure 5 - Two examples of glaze detachment/cracking

Flatness deficiencies

The irregularities in the cladding flatness are usually caused by the incorrect application of the tiles or a faulty preparation of the support. It can also be a sign of the cladding's buckling/detachment (fig. 6).

Figure 6 – Example of a building with flatness deficiencies, probably a sign of detachment

Moisture related anomalies

As humidity often implies dimensional variations of the building's materials, or in some cases freeze-thaw actions, it can be the cause of some already mentioned anomalies such as cracking or detachment. However, it can also cause some other anomalies, especially when water is able to penetrate the wall through some particular point affecting the cladding's layers. These anomalies are:

- Microorganisms colonies – Moist provides microorganisms such as algae, lichens or moss with the perfect development conditions (fig. 7a). This phenomenon happens mainly in the joints or cracks of shadowed and moist areas. More rarely, the formation of vegetation (with roots beneath the cladding (fig. 7b) that will obviously accelerate the process of degradation) can happen (Silvestre et al. 2006a).
- Efflorescences - This phenomenon consists in the appearing of whitish stains on the coating's surface due to crystallization of salts that usually are transported in the water from the inside layers of the wall (fig. 7c).
- Subflorescences – An anomaly very similar to efflorescences but usually more severe due to the fact that crystallization happens in the inner layers of the cladding, not being visible until the time it provokes the tiles buckling or cracking that can progress into a detachment.

Figure 7 – Three examples of moisture related anomalies (bio-contamination (a), vegetation growth (b) and efflorescences (a))

Anomalies in joints

Anomalies in joints, despite being often disregarded due to a low visual impact, are very important to study, as joints are the most vulnerable component of a tiling system and its degradation usually leads to more severe anomalies that affect the overall health of the system, for example through the loss of watertightness. Silvestre et al. (2007) divided joint anomalies in:

- efflorescences;
- colour change;
- cracking (fig. 8a);
- detachment of the grout (fig. 8b);
- biodeterioration (fig. 8c);
- dust trapping.

Figure 8 – Examples of Joint's cracking (a), detachment of the grout (b) and biodeterioration (c)

2.5.1 Anomalies' causes statistics

As seen, anomalies can happen due to various causes. Silvestre et al. (2006a) divided the causes in:

- project errors;
- execution errors;
- exterior mechanical actions;
- ambient actions;
- maintenance failures;
- alteration of initial conditions (such as using destination or structure's loading conditions).

After this division, the authors analysed 64 cases of tiling systems in Portugal and came up whit relative occurrence frequency graphics respective to the anomalies causes (fig. 9).

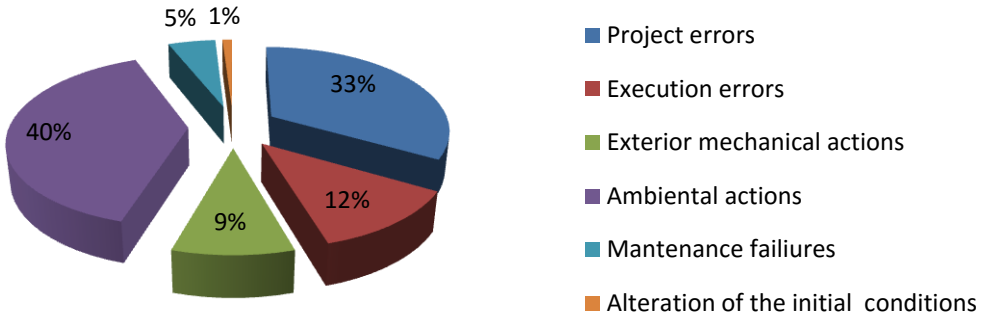

Figure 9 – Percentage of occurrence of the causes groups in facades (adapted from Silvestre; 2005 and Silvestre et al. 2006a)

The same authors conducted a statistical study on the same causes but this time specifically on joint related anomalies (fig. 10).

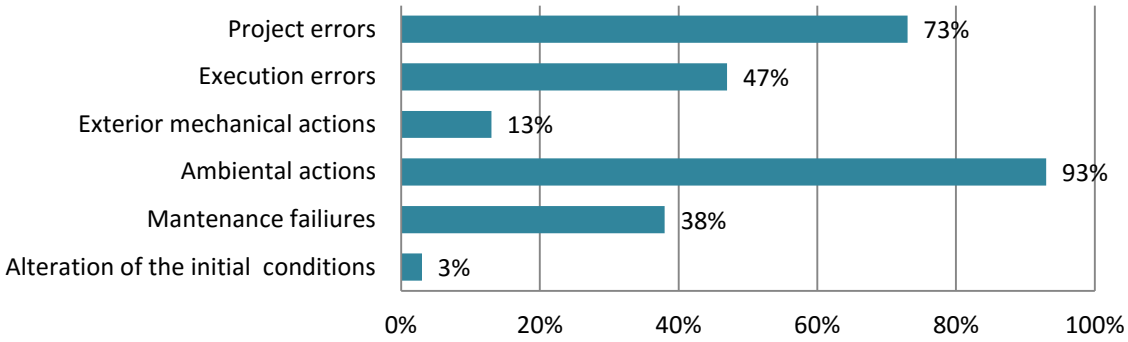

Figure 10 – Relative frequency of the probable causes of anomalies in joints (Adapted from Silvestre et al. 2007)

2.5.2 Recommendations to minimize anomalies

Abreu (2005) made a compilation of some recommendations that must be taken into account to minimize the risk of detachments in ceramic claddings. However, some of these good practices can help to avoid the appearance of many other anomalies, contributing to the health of tiling systems:

- Adherent tiling systems must be avoided in supports with lack of cohesion, dimensional instability and susceptibility to cracking or excessive deformations. The support must also be clean from dust (to promote adhesion) and have the least number of contaminants as possible (to avoid anomalies such as efflorescences). According to Silva et al. (2015), it is imperative to ensure that the mechanic behaviour of the support is compatible with the cladding's attachment system, with a minimum value of adhesion towards perpendicular traction of 0.3 N/mm^2 (DTU 26.1).
- Higher porosity favours the penetration of the adhesive in the tiles' bottom, improving the adherence to the support. Furthermore, more porous tiles are usually less rigid, reducing the tensions transmitted from the support.
- Thicker tiles are usually more rigid, requiring the use of more flexible joint filling grouts.
- Low water absorbent tiles are usually preferable, as it will promote moisture expansion (the term used to describe the expansion of ceramic materials due to the adsorption of water), which usually occurs slowly and is relatively small. But it can damage the ceramic tiles

adhesion to the underlayment, craze the glaze and lead to the development of cracks on ceramic tiles (Mendonça et al. 2012).

- The adhesive and gluing method shall be adequate to the surface to clade, to the location, the use, the degree of exposure to corrosive agents and the tiles. The gluing recommendations usually provided by the fabricant shall be respected.
- Thicker and more flexible adhesives may contribute to a higher independence to the support of the tiles, reducing the possibility of transmitting tensions and decreasing the physical restraints to deformations.
- A higher number of joints may be beneficial as it reduces tensions that tend to develop.
- Joints must be thick enough to facilitate the grout filling's entrance and to efficiently absorb deformations and tensions. Excessive flexibility or inexistence of the filling grout is not advisable, as tensions on the surface might drop, or even becoming null, giving place to peaks of tension perpendicular to the surface and of shear stress, which in turn would free the cladding from shoaling but facilitate the tiles detachment from their edges. The non-filling or incomplete filling of the joints will reduce the watertightness and expose the tiles' edges to mechanical impacts and dirt penetration.
- The cladding project must define precisely the construction joints' placing.
- Protective profiles shall be used in particular zones such as building's edges susceptible to mechanical impacts.
- Watertightness elements shall be used in particularly exposed zones such as upper boundary edges of exterior walls or junctions between different claddings.
- Time periods between each construction phase shall be respected according to each construction characteristics and weather conditions. "Open time" defined by EN 12004:2014 as "maximum interval after application at which ties can be embedded in the applied adhesive and meet the specified tensile adhesion strength requirement", and measured by the method described in EN 1346:2007 shall be respected; otherwise detachments may occur.
- After the cladding's application, characteristics such as alignment of the tiles and joints, flatness and verticality of the cladding and adherence of the tiles shall be analysed before the building's entry in service.

2.5.3 Diagnostic methods

Silvestre et al. (2008) have conducted a study on adhered ceramic tiling systems (ACTS) from which a part consisted in creating a matrix of correlation between anomalies and diagnosis methods (this matrix only includes diagnosis methods that can be used by the inspector at the moment of inspection (Silvestre et al. 2006b)). Table 4 presents an adaptation of the mentioned matrix where:

- **0 – No relation** – There is no relation between the anomaly and the diagnostic method (correspondent to empty cells on table 4).
- **1 – Small relation** – Diagnostic method fitted to the anomaly's characterization but with some limitations in terms of technical execution or cost, reducing its applicability.
- **2 – High relation** – Diagnosis method adequate to the anomaly's characterization, with minimum technical exigence and accessible equipment.

Table 4 – Matrix of correlation between anomalies and diagnosis methods (Adapted from Silvestre et al. 2008).

Anomaly	Visual assisted analysis		Mechanical techniques	Ultrasonic methods	Acoustic methods	Thermal methods	stress / deformation techniques	
	Fissurometer	ATS's inclination measuring	Sphere crash	Ultra-sounds	Percussion	Thermography	Gypsum testimonies	*Pull-off*
Detachment			1	1	2	1		1
Cracking - outer layer	2		1		2			
Cracking - ATS	2				2		2	
Crushing or delamination of the tiles' edge		1						
Efflorescence / Subflorescence		2						
Joints deterioration		1						
Aesthetic anomaly		1				1		

3 Infrared thermography

Infrared thermography is a non-destructive technique that is evolving day by day proving its capacities in many fields, including building inspections. To understand this testing method and how it can be applied in order to detect anomalies in ceramic claddings there is a need to perceive some basic principles, related with thermal radiation and heat transfer.

3.1 Heat transfer

Heat is a kind of energy that flows between systems every time there is a temperature differential. Thus, in order to achieve the thermal equilibrium, the heat flows always from the hotter to the colder system. The heat transfer can occur in three different ways: Conduction, Convection or Radiation.

3.1.1 Conduction

Conduction is the heat transfer process that happens every time there is a temperature differential between two solid or fluid bodies in contact or between two points of one body due to its particles agitation (for every material, a higher temperature corresponds to a higher state of molecular agitation) (Henriques, 2011).

The heat Q (W) or heat flow q (W/m^2) that is transferred by conduction is generally explained by Fourier's law of thermal conduction (fig. 11) that is commonly used as shown in equation 3.1 (Matias, 2001; Henriques, 2011):

$$Q = qA = -\lambda \frac{A \cdot \Delta T}{\Delta x} \tag{3.1}$$

Thereby, for example considering a tile whose exterior surface is in contact with air at a temperature T_1 and whose bottom is in contact with a wall at a lower temperature T_2, the heat that flows through its area, A (m^2) perpendicular to the flow's direction, depends on the temperature differential, ΔT (°C), between T_1 and T_2, its thickness, Δx (m), and its thermal conductivity, λ (W/(m·°C)).

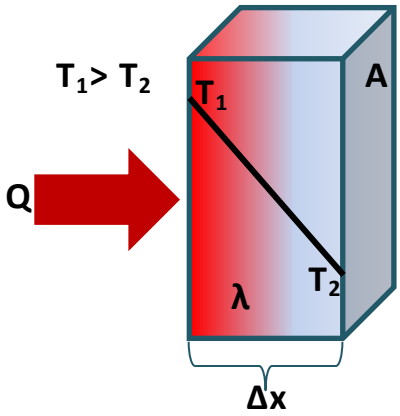

Figure 11 - Fourier's law of heat conduction

Thermal conductivity is thus the parameter that can define different material's capacity to conduct heat, being set as the heat energy transferred per unit of time, surface area and temperature gradient that flows through a unitary length perpendicular to the area (fig. 11).

However, in real situations, the heat transfer is not unidirectional (being usually considered in three directions (*∂x, ∂y, ∂z*); it depends on the time and if there is an internal production of heat (by the body in study). So, assuming that thermal conductivity is constant, the equation to be considered when studying this heat transfer type is the simplification of the general equation of thermal diffusion known as Fourrir-Biot´s equation (eq. 3.2) (Henriques 2011).

$$\frac{\partial^2 \mathrm{T}}{\partial \mathrm{x}^2} + \frac{\partial^2 \mathrm{T}}{\partial \mathrm{y}^2} + \frac{\partial^2 \mathrm{T}}{\partial \mathrm{z}^2} + \frac{q'}{\lambda} = \frac{1}{a}\frac{\partial \mathrm{T}}{\partial \mathrm{t}} \tag{3.2}$$

In this equation:

- *T* – temperature
- *q'* – heat generated per unit of volume (W/m^3)
- *λ* – thermal conductivity
- *a* – thermal diffusivity
- *t* – time

Besides thermal conductivity there are also some materials' characteristics variations that can influence its behaviour (table 5), such as the specific heat, c_p (amount of thermal energy necessary to raise a material´s temperature in 1 °C), thermal diffusivity, *a* (capacity of a material to transmit a thermal variation in its interior) and thermal effusivity, *b* (amount of thermal energy that a material is capable of absorbing or releasing). These characteristics are represented in table 5 for air and water.

Table 5 - Some thermal characteristics of air and water (Rempel et al. 2013).

Parameters	Water	Air
λ [W/(m·K)]	0.6	0.025
c_p [J/(kg·K)]	4187	1000
a [m^2/s]	0.14x10^{-6}	20x10^{-6}
b [J/(K·m^2·s$^{0.5}$)]	1580	5

Looking at table 5 it is possible to state that water can conduct heat better than air, needs more energy to rise its temperature, has a lower capacity to transmit heat in its interior and is able to absorb and release more energy.

Considering that, as mentioned above, when the detachment of ceramic tiles takes place, the voids created between the cladding layers are filled with air or water. Alongside with the fact that thermal conductivity takes different values for different materials, comes the assumption that the presence of one or both these elements in a wall will, even in an almost imperceptible way, cause variations on the overall thermal behaviour of the wall.

According to Alba et al. (2011), the heat is transferred more quickly throughout the most cohesive materials and/or materials with greater thermal effusivity. Differences in surface temperature due to different thermal properties of elements such as timber, bricks, stone, and mortar, can be visualized using IRT at proper time as a "footprint" of their shapes projected on the overlapping plaster. Any thin delamination of the coating and detachment of the finishing layer strongly reduces the heat transfer and adds its signal to that given by the structure.

3.1.2 Convection

Convection is a similar process that can only occur in fluids and that involves a mass variation and a rearrange of the fluid's molecules' relative positioning.

The principle behind this heat transfer method is that for different temperatures fluids are presented in different densities and, consequently, different masses. These differences cause the fluid´s molecules to move. Two great examples of these movements are the wind and sea currents.

The heat flow by convection, q_{conv} (W/m^2) between a surface at a temperature *T1* and the ambient, at a temperature *T2*, is given by Newton's law of cooling (eq. 3.3) (Henriques, 2011).

$$q_{conv} = h_c(T_1 - T_2) \tag{3.3}$$

Being h_c the heat transfer coefficient (W/(m2·K)), a characteristic that is not specific for the fluid in study but that depends on specific circumstances such as the geometry of the surface, the fluid's nature and the type of movement of the fluid's particles.

Knowledge of this heat transfer method can be useful to this study because it is, for example, one of the causes of the building's facades temperatures presenting higher temperatures for the lower floors. Despite the mentioned possibility of a fluid such as air or water in the gap caused by a detached tile, it does not come in a volume enough to give this heat transfer method such a significant role on this study.

3.1.3 Radiation

Radiation is the result of the energy emitted by all bodies above the absolute zero temperature (0 K). The energy is emitted due to the object's particles rotational movements and it travels in the form of electromagnetic radiation with no need for a material vehicle of transfer.

Despite all the heat transfer methods having a role in this study, the most important to understand is radiation, as it stands on the basis of infrared thermography.

There are two main approaches to describe heat transfer by radiation. The first one, by Maxwell, considers that radiation happens when electromagnetic waves (eq. 3.4) characterized by a wavelength, λ (*m*), and frequency, *f* (*Hz*), propagate at light speed, *c* (*m/s*) (Maladague; 2001).

$$c = \lambda \cdot \mathrm{f} \tag{3.4}$$

The second approach, known as Planck's quantic theory (eq. 3.5), considers electromagnetic radiation as a particles' (*photons*) waving flow. This theory also considers that radiant energy is not emitted continuously but in discrete quantities named *quantum*. This energy, *E* (J), can be obtained using equation 3.5 where *h* (*J/s*) is the Plank's constant.

$$E = h \cdot \mathrm{f} \tag{3.5}$$

Relating both theories comes equation 3.6, where it is possible to understand that the bigger the wavelength, the lower the radiated energy.

$$E = \frac{h \cdot c}{\lambda} \tag{3.6}$$

Both these approaches are valuable. However, Plank's quantic theory is mainly used to describe gasses' radiative properties, while Maxwel's approach allows a better understanding of solid and liquid material's radiative properties.

3.2 Electromagnetic spectrum

Electromagnetic radiation is usually presented in the electromagnetic spectrum according to its wavelength, λ, and frequency, f. In the electromagnetic spectrum presented in figure 12, it is possible at first sight to notice from the left to the right the high energy waves like gamma rays and ultra-violet radiation. With shorter wavelength there is the visible radiation, with wavelengths comprehended between 0.4 µm and 0.78 µm, and then the infrared radiation and other weaker waves with longer wavelengths, as microwave and radio waves.

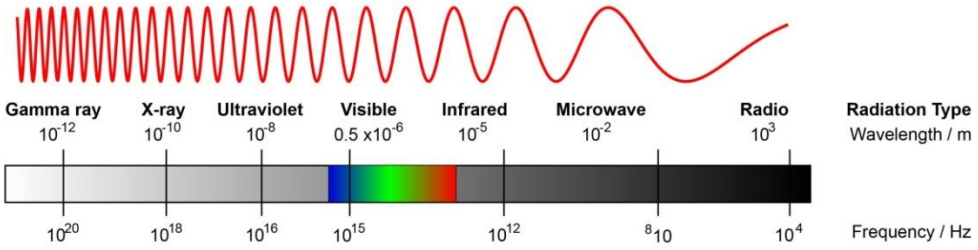

Figure 12 - Electromagnetic spectrum [W1]

3.3 Thermal radiation

As this study is focused on thermal behaviours, it is logical that the part of the electromagnetic spectrum that is more interesting is the thermal radiation. This is the part of the spectrum that concerns when heat transfer is taken into account (Henriques; 2011).

It was in 1973 that William Herschel through an accidental experiment discovered the infrared radiation. He used a prism to separate the colours from blue to red and thermometers with blackened bulbs, as he moved the thermometer from violet to red in the rainbow created by sunlight passing through the prism. He noticed that the hottest temperature was actually beyond red light where no radiation was visible, and that the distance where the heating was greatest had a specific location, which in turn lead to the conclusion that it depends on the wavelength. Herschel termed this invisible radiation "calorific rays". Today, it is known as infrared radiation. (Maladague; 2001 and Barreira et al. 2012).

Thermal radiation comprehends wavelengths from 0.1 µm to 100 µm. Thereby it comprehends a small part of *UV* radiation (0.1 µm to 0.4 µm), the visible radiation (detectable by the human eye, 0.4 µm to 0.78 µm) and a big portion of infrared radiation (0.78 µm to 100 µm).

The infrared thermal radiation is the most interesting part of the spectrum to this study, not only because the wavelengths with more energy emitted by bodies at the ambient temperature (around 25°C) are in the infrared zone but because, for that same reason, these are the wavelengths that are detected by thermal cameras.

The spectral range of Infrared radiation (fig. 13) is comprehended between 0.78 µm and 102 µm (Maladague; 1994). Infrared radiation can also be divided into three regions (that can slightly vary according to the author) (Maladague; 2001):

- Near infrared (NIR), from 0.78 µm to 1.5 µm;
- Medium infrared (MIR), from 1.5 µm to 20 µm;

- Far infrared (FIR), from 20 µm to 102 µm.

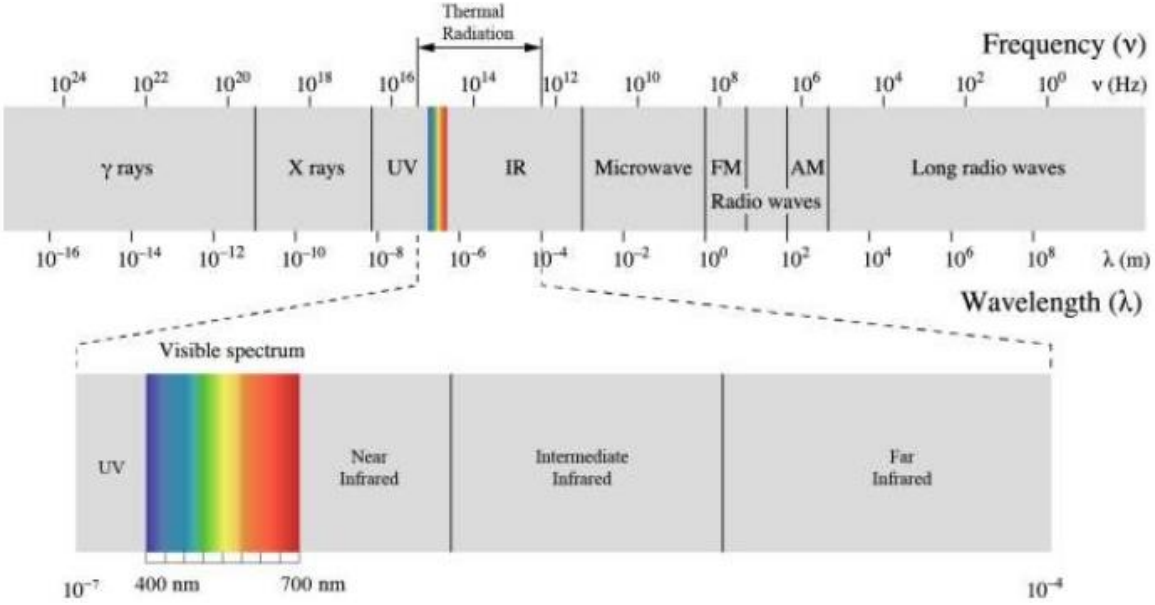

Figure 13 - Thermal radiation within the electromagnetic spectrum [W2]

3.4 Blackbody's radiation

A fundamental concept that is needed in order to understand radiation is the total emissive power, *E*, of a body, which is the total quantity of energy emitted per unit of surface (W/m^2). "In order to quantify the flux passing through small surface, *dA* within small solid angle *dΩ* around a direction making angle θ with the normal to the surface" the term radiance, *L* ($Wm^{-2}sr^{-1}$), is used (Maladague; 1994).

There are three fundamental laws in which IRT is based on, and to understand them it is needed to first know what is a blackbody: a physical abstraction characterized by absorbing the totality of the incident radiation, regardless of the wavelength and direction (Henriques, 2011). The three laws described below, though being applied to a blackbody, can be used to understand the current body's behaviour.

Planck's law

Planck's law describes the spectral distribution of the radiation emitted from a blackbody. This law shows that, for a given wavelength, the emitted radiation increases with the temperature and that the higher the temperature, the shorter the wavelength at which the maximum occurs (Hart; 1991). The law is described by equation 3.7 in order to the spectral emissive power:

$$E_{\lambda T} = \frac{2\pi \cdot h \cdot c^2}{\lambda^5 \cdot [exp\left(\frac{h \cdot c}{\lambda \cdot k \cdot T}\right) - 1]} \quad (3.7)$$

In this equation:

- $E_{\lambda T}$ – Spectral distribution of energy emitted by a blackbody;
- λ – Wavelength (µm);
- T – Temperature (K);
- h – Plank's constant ($6.6260693(11)x10^{-34}$ J·s);
- c – Light velocity (m/s);
- k – Boltzman's constant ($1.3806503x10^{-23}$ J/K).

This law is often represented by figure 14.

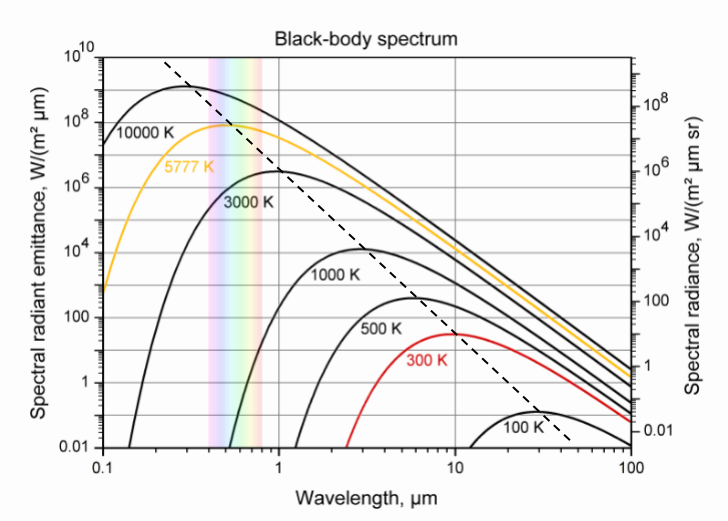

Figure 14 - Spectral emissive power of a black body [adapted from W3]

Wien's law

Represented by the dashed line in figure 14, that shows that for a given temperature there is a maximum spectral emissive power correspondent to a specific wavelength, λ_{max}, the equation that describes Wien's law (eq. 3.8) is obtained deriving Planck's law in order to the wavelength.

$$\lambda_{max} = \frac{2898}{T} \tag{3.8}$$

Analysing the graphic on figure 14 or using the equation above (eq. 3.8), it is noticeable that for temperatures around 25°C (298K) the maximum emissive power corresponds to a wavelength of 9.7µm. As it will be presented in chapter 5, for the ceramic tiles' superficial temperatures obtained in this study that range from 15°C (288K) to 70°C (343K), corresponding to maximum emissive power wavelengths between 10.1 µm and 8.5 µm. These wavelengths are placed in the medium infrared region and, as it will be shown, in the thermal camera's operational range.

Stefman-Boltzman's Law

By integrating the Planck's formula from λ=0 to λ=∞ comes the Sefman-Boltzman equation which states that the total emissive power of a blackbody, E^0, is proportional to the fourth power of its absolute temperature as in equation 3.9 (Hart; 1991).

$$E^0 = \sigma \cdot T^4 \tag{3.9}$$

Using this equation, where the constant of proportionality σ represents the Stefman-Boltzman constant (5.67×10^{-8} W·m^{-2}·K^{-4}), it is possible to calculate the maximum radiance (the black body's radiance) for a given temperature.

3.4.1 Radiative properties of a current surface

In order to characterize the interaction of a surface with the incident radiation it is essential to perceive that, for a current body, the incident radiation or irradiation, G_i, can be divided into three fractions (fig. 15): absorbed radiation (G_a), transmitted radiation (G_t) and reflected radiation (G_r) (eq. 3.10) (Henriques, 2011).

$$\mathrm{Gi} = \mathrm{Ga} + \mathrm{Gt} + \mathrm{Gr} \tag{3.10}$$

When the material is opaque, the transmitted radiation equals zero, remaining (eq. 3.11):

$$\mathrm{Gi} = \mathrm{Ga} + \mathrm{Gr} \tag{3.11}$$

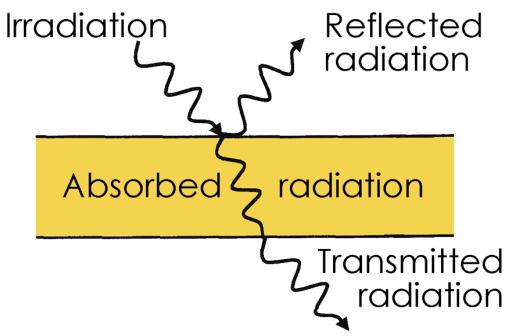

Figure 15 - Schematic representation of irradiation's division when reaching a body [W4]

To characterize a body's behaviour when irradiated there are three coefficients, each one corresponding to one of the three fractions of radiation mentioned above: the coefficient of absorption α, the coefficient of reflection ρ, and the coefficient of transmission τ, given by the equations 3.12, 3.13 and 3.14:

$$\alpha = \frac{G_a}{G_i} \tag{3.12}$$

$$\rho = \frac{G_\rho}{G_i} \tag{3.13}$$

$$\tau = \frac{G_\tau}{G_i} \tag{3.14}$$

Therefore (eq. 3.15):

$$\alpha + \rho + \tau = 1 \tag{3.15}$$

And in the case of opaque materials (eq. 3.16):

$$\alpha + \rho = 1 \tag{3.16}$$

All these properties depend not only on the wavelength λ of the incident radiation's direction θ, and of the temperature T, but also of the material's surface characteristics such as the roughness and the presence of dirt or other surface contaminants. Despite these characteristics may vary, for the same wavelength, incident radiation's direction and temperature, their sum is equal to one (Hagentoft; 2001).

According to Modest (2003) the terminology used to describe the radiative properties of a surface shall end in "tivity or ssivity" when the surface is completely flat and in "tance" when there is any kind of roughness or contamination.

One example that is often used to explain material's radiative characteristics facing the wavelength of the incident radiation is the case of glass. This material, though being transparent for visible radiation (letting it pass through), has an almost unitary coefficient of absorption towards infrared radiation (with bigger wavelengths), behaving almost as a black body for this radiation (Henriques; 2011). This characteristic is the main reason for the greenhouse effect. Thermal radiation gets in through a glass (namely solar radiation), heating the inside (car or building compartment, for instance) that in turn emits thermal radiation, mainly infrared with bigger wavelengths. The temperature will then rise quite rapidly as this radiation cannot get out because of the glasses' opacity towards it.

Being the great majority of construction materials opaque and rough, it is considered of more importance the parameters of reflectance and absorptance.

The reflectance of the surface is influenced by factors such as:

- Exposure conditions – According to Prado et al. (2005), meteorological conditions such as the intensity of the radiation, the presence of wind, rain or the relative humidity are factors that can influence a surface reflectance.
- Wavelength of the incident radiation - As stated above, surfaces' absorption depends on the wavelength of the incident radiation; accordingly, as the reflectance is the remaining of the radiation incident in an opaque body, this characteristic will also depend on it.
- Surface colour – brighter colours such as white are more reflective in the region of visible and near infrared radiation, which does not mean the same to other wavelengths (Berdahl et al. 1997).
- Surface roughness – This characteristic plays an important role in reflection. When a surface is completely flat, the reflection can be described by the law of reflection (fig. 16)). Otherwise, it can be considered a diffuse reflection (corresponding to a perfect diffusor, a physical abstraction that does not really exist) or a disperse reflection where reflection is partially diffused regarding the surfaces' irregularities (fig. 17).

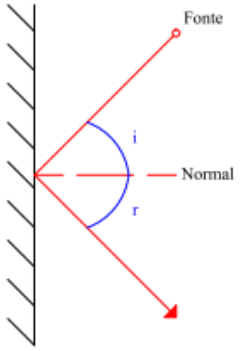

Figure 16 - Reflection's law (RYER, 1998)

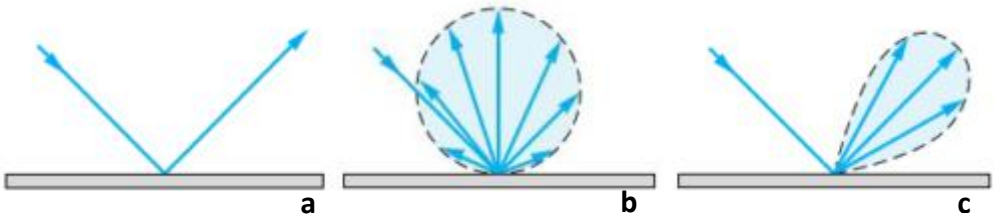

Figure 17 - Specular reflection (a), diffuse reflection (b) and disperse reflection (c) (RYER, 1998)

- Surface's condition – The presence of any kind of contamination such as dust will obviously impact the behaviour of the surface towards the incoming radiation, not only because of the actual presence of a different material but also because of the weariness it will cause, eventually changing surface's characteristics such as colour or roughness.

3.4.2 Non-black body radiation (emittance)

According to Kirchhoff's law of thermal radiation (applicable only for systems in thermodynamic equilibrium and without irradiance from the sun), for a specific temperature, T, and wavelength, λ, the spectral emissivity and spectral absorptivity are equal at any given temperature and wavelength (Hart; 1991).

As a blackbody is a perfect absorber, from this law comes that it is also capable of emitting radiation at all wavelengths, and naturally, it has the maximum value of emissive power (E^0)

correspondent to an absolute temperature. Thus, here comes the concept of emittance (ε) of a current body ("common body"), which consists in the percentage of the emissive power in relation to the blackbody (eq. 3.17).

$$\varepsilon = \frac{E}{E^0} \tag{3.17}$$

E (W·m^{-2}) is the emissive power of the surface and E^0 (W·m^{-2}) the total emissive power of a blackbody.

Emittance can thereby be considered a body's efficiency emitting energy (Henriques; 2011) in comparison with the black body's capacity (which has the maximum efficiency, ε=1).

There are four emittance parameters defined regarding the wavelength and direction of the incident radiation (Maladague; 1994):

- Total (hemispheric) emittance (eq. 3.18):

$$\varepsilon = \frac{E}{E^{0\prime}} \tag{3.18}$$

- Directional (total) emittance (eq. 3.19):

$$\varepsilon' = \frac{L}{L^{0\prime}} \tag{3.19}$$

where L (W·m^{-2}·sr^{-1}) is the surface's radiance and L^0 (W·m^{-2}·sr^{-1}) the total luminance from a black body.

- Spectral (hemispherical) emittance (fig. 18; eq. 3.20):

$$\varepsilon_\lambda = \frac{E_\lambda}{E_\lambda^{0\prime}} \tag{3.20}$$

where E_λ (W·m^{-2}) is the spectral emissive power of the surface and $E^0{}_\lambda$ (W·m^{-2}) the spectral emissive power of a blackbody.

- Spectral directional emittance (eq. 3.21):

$$\varepsilon'_\lambda = \frac{L_\lambda}{L_\lambda^0} \tag{3.21}$$

where L_λ (W·m^{-2}·sr^{-1}) is the surface's spectral radiance and $L^0{}_\lambda$ (W·m^{-2}·sr^{-1}) the spectral radiance from a black body.

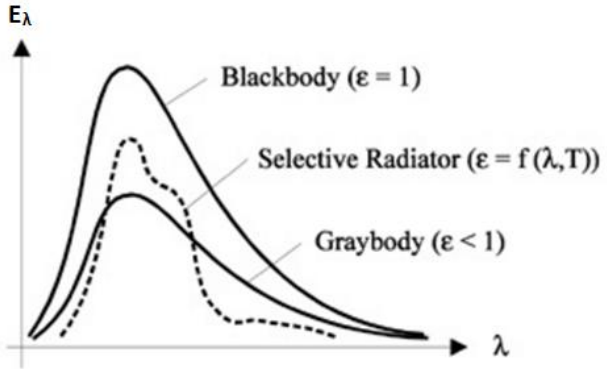

Figure 18 - Spectral radiant emittance of three types of radiators [W11]

As it has been proven, the emittance is a complex question given all the parameters in which it depends on. Therefore, to simplify the analysis of this parameter, two assumptions can be made regarding the surface (Gonçalves; 2014):

- The surface is grey and so, the radiative properties do not depend on the wavelength.
- The surface is diffuse and so, the radiative properties do not depend on the direction of the emitted radiation.

In table 6, the values and simplifications of the radiative properties of different surfaces are represented (Hart; 1991)

Table 6 – Spectral emittance, reflectance and transmittance of different surfaces (Hart; 1991)

	ε_λ	ρ_λ	τ_λ
Black body	1	0	0
Transparent body	0	0	1
Grey body	ε_λ and E_λ constant		
Opaque surface	$\varepsilon_\lambda+\rho_\lambda=1$		
Perfect mirror	0	1	0

3.5 Solar radiation

As all bodies at a given temperature emit electromagnetic radiation, the sun is no exception. Radiation needs no material medium to flow; so, the radiation from the sun can easily reach earth's atmosphere, where its radiation is filtered, protecting life as it is of common knowledge.

Solar radiation's spectrum comprehends wavelengths between 0.28 µm and 3.0 µm (Castro; 2002), and its maximum emissive power corresponds to wavelengths around 0.5 µm (fig. 19). The characterization of the solar emissive spectrum is of extreme importance to this study. Its importance will be shown for example in the characterization of the thermal camera, in the characterization of the pyranometers that were used to measure the claddings' reflectance, and overall because it is the thermal properties of this radiation that allow the highlight of anomalous areas, allowing in turn their detection using thermography.

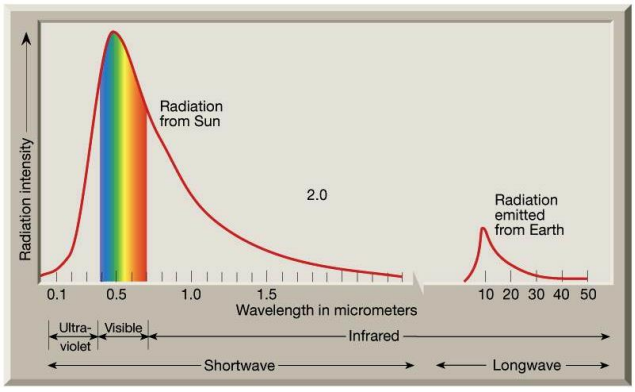

Figure 19 - Solar and terrestrial radiation spectrum

3.6 Infrared thermography in building inspections

As stated above, all bodies at a given temperature emit some radiation depending on their emissivity. "Thermography literally means "writing with heat", just as photography implies "writing with light"" (Barreira et al. 2012). Hence, this non-destructive diagnosis method consists in using an infrared camera that is able to detect infrared radiation and to create a thermal image by converting the different wavelengths of radiation detected in electrical signals that are displayed as a thermal image called thermogram, which shows, with different colours, the thermal variation of the surface that is being inspected.

Infrared thermography has been proven to be a valuable tool in many areas such as medicine or the military and also in building inspections, allowing a fast and reliable inspection without having to

physically interact with the object of inspection. In buildings, it has been used to "identify structural changes, structural abnormalities, the lack of insulation, degradation (cracks), air leakage sources, heat losses, moisture. The infrared measurement gives a qualitative image of the thermal protection level of buildings envelope and identifies the week zones hidden from eye visual contact" (Pleşu; 2012).

Despite still considered by some as kind of an unknown method, IRT has a long story. Approximately thirty years after the infrared discovery the first detector using this type of radiation ("thermopiles", based on the same principles of the thermocouples) was developed. Between 1870 and 1920, the first quantum detectors (based on the interaction between radiation and matter), were developed, changing the detection nature (the electrical signal created by the effect of thermal radiation gave place to a direct conversion of radiation into electrical signals) improving considerably the response time and measurement accuracy (Barreira et al. 2012).

Between the decades of 30 and 60 several infrared detectors were developed, essentially for military purposes. The wavelengths range that the infrared detectors were sensitive depended on the materials used in its manufacture (such as Lead sulphide (PbS), Indium antimonide (InSb) or Mercury-Cadmium-Tellurium (HgTeCd)) However, all these detectors were working with optical-mechanical scan systems and requiring cryogenic cooling (Barreira et al. 2012).

"The first commercial infrared cameras appeared by the end of the 60's. In the '90s a new generation of equipment with array detectors appeared in the market. This new equipment allowed a simultaneous temperature reading at different points and did not require cryogenic cooling systems" (Barreira et al. 2012).

But not all the radiation that comes from the surface is emitted; as previously explained, a portion of it will be reflected radiation. Hence, it is required to know the equipment and how to proceed in order to use the adequate kinds of inspection and to minimize errors.

Before starting an infrared survey, it is recommended to decide which kind of analysis the data obtained will be subjected to. There are two main kind of analysis to choose from: The qualitative and the quantitative.

A qualitative analysis is based on the evaluation of thermal differences on the inspected subject. This method is the most simple to use and does not require a great quality in the data obtained, as the differences can usually be visible even if the temperatures are not exactly correspondent to the reality. The simplicity of this method makes it very suitable for *in situ* inspections, providing information about possible anomalies in real time, just from the thermogram visual observation.

In order to make a quantitative survey it is required much more quality in the data, as this method relies on real temperatures. This method is often used in laboratory to study material's behaviour. The accuracy needed in the thermograms to make this kind of analysis raises also the need of a better accuracy of the parameters to set in the camera, as well as taking all the measures to minimize possible errors.

Some crucial aspects must be kept in mind when leading an IRT survey, as the thermogram obtained can be severely influenced by several factors such as:

- surface characteristics;
- camera characteristics and positioning;
- external factors' influence like the weather or presence of neighbouring elements;

- atmospheric attenuation between the object studied and the camera.

Despite thermograms showing only the superficial temperature, it is possible to make some assumptions about the condition of the inspected element if the principles of heat transfer and inspection conditions are understood. When a building has some heat related anomaly, although it can be behind the surface, it will affect the heat transfer through the element analysed and it will cause thermal variations in the surface. Depending on the thermal camera sensitivity, those variations will be noticed in the thermogram. That is why, based on these basic principles, IRT has been used as a NDT to identify anomalies like air leakage, thermal bridges, lack of thermal insulation, presence of humidity (Matias; 2012 and Maladague; 2001) and anomalies in roof waterproofing systems (Melrinho; 2014) or claddings, especially when related with presence of air or water in the intermediate layers of the studied element (Hart; 1991).

3.6.1 Thermal camera

Nowadays, thermal cameras are digital devices that use sensors/detectors to transform infrared radiation into an electronic signal with a voltage proportional to the received radiation. There are two main families of detectors: uncooled microbolometric detectors and cooled detectors used for high sensitivity cameras. In order to obtain the two-dimensional measurements, cameras can be characterized in two types: single sensor, where the camera uses a rotating mirror that scans the information into a single sensor; and focal plane array (FPA), were cameras use an array of detectors (each providing information about the radiation at one point) called a focal plane array (the resolution of these cameras is defined by the number of these detectors) (Usamentiaga et al. 2014).

Another very important defining parameter of thermal cameras is the spectral range where they work, which should be chosen according to the kind of readings the camera is destined to make. Presumably, short or mid wavelength systems are more sensitive to high temperatures (above ambient), whereas long wavelength systems are more sensitive to lower temperatures (ambient and below). Cameras usually work in bandwidths either between 3 µm and 5 µm or between 7.5 µm and 13 µm.

Besides these features, thermal cameras are also characterized for example by their field of view, thermal sensitivity, temperature range, accuracy and many other technical features.

All the thermographic surveys presented in this dissertation were achieved using as equipment the infrared camera (fig. 20) available on LNEC (*NRI - Núcleo de Revestimentos e Isolamentos*). The model is the *ThermaCAM P640* from *FLIR Systems*, characterized by a spectral range between 7.5 µm and 13 µm and a FPA system with uncooled microbolometric detectors. Other technical specifications of this camera are presented on the appendix A.1.

Figure 20 – Thermal camera *ThermaCAM P640* from *FLIR Systems*

When using a thermal camera, the first thing to do in order to have a correct reading of temperatures is to set the following parameters in the camera:

- ε – Emittance of the surface;
- T_{refl} – Reflected temperature (°C);
- Dist – Distance to the target (m);
- T_{atm} – Atmospheric temperature (°C);
- HR – Relative humidity (%).

After setting these parameters, it will be needed to define other features such as the range of colours and temperatures desired for the thermogram. Finally, after focusing the image it is time to shoot, just like in a photographic camera.

When the shot is taken, the radiation that comes to the sensor is transformed into electrical signals that are analysed and transformed into a thermogram. According to Usamentiaga (2014), the total radiation received by a thermal camera (W_{tot}) comes from three sources (fig. 21):

- E_{obj} – the emission from the object in study;
- E_{refl} – the radiation reflected by the object;
- E_{atm} – the radiation emitted by the atmosphere.

These parameters are then affected by the atmosphere's transmittance τ_{atm}, which can be estimated using the distance from the camera to the object and the air relative humidity and which values are usually close to one (Usamentiaga; 2014).

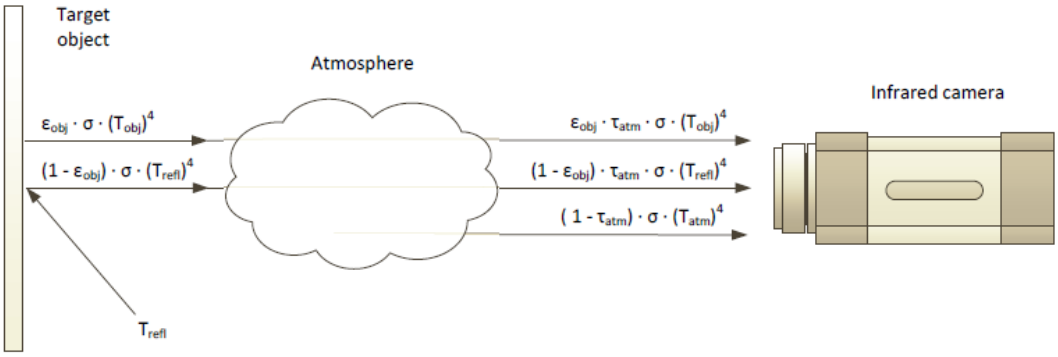

Figure 21 - Radiation received by the infrared camera (Usamentiaga; 2014)

The three portions of radiation captured by the camera can be calculated by equations 3.22, 3.23 and 3.24:

$$E_{obj} = \varepsilon_{obj} \cdot \tau_{atm} \cdot \sigma \cdot (T_{obj})^4 \quad (3.22)$$

$$E_{refl} = \rho_{obj} \cdot \tau_{atm} \cdot \sigma \cdot (T_{refl})^4 = (1 - \varepsilon_{obj}) \cdot \tau_{atm} \cdot \sigma \cdot (T_{refl})^4 \quad (3.23)$$

$$E_{atm} = \varepsilon_{atm} \cdot \sigma \cdot (T_{atm})^4 = (1 - \tau_{atm}) \cdot \sigma \cdot (T_{atm})^4 \quad (3.24)$$

The sum of these three equations (eq. 3.25) equals the total incident radiation (just like in equation 3.15). In turn; this equation can be put in order to the object's temperature (eq. 3.26) which is then displayed on a graphic: the thermogram.

$$W_{tot} = \varepsilon_{obj} \cdot \tau_{atm} \cdot \sigma \cdot {T_{obj}}^4 + (1 - \varepsilon_{obj}) \cdot \tau_{atm} \cdot \sigma \cdot {T_{refl}}^4 + (1 - \tau_{atm}) \cdot \sigma \cdot {T_{atm}}^4 \quad (3.25)$$

$$T_{obj} = \sqrt[4]{\frac{W_{tot} - (1-\varepsilon_{obj}) \cdot \tau_{atm} \cdot \sigma \cdot {T_{refl}}^4 - (1-\tau_{atm}) \cdot \sigma \cdot {T_{atm}}^4}{\varepsilon_{obj} \cdot \tau_{atm} \cdot \sigma}} \quad (3.26)$$

3.6.2 Emittance and reflected apparent temperature's measurement

From the mentioned parameters that are required to input in the camera to make a proper inspection there are two that stand out not only because of their importance but also because they are the least usual parameters to lead with in building inspections. These parameters are emittance and reflected temperature.

Emittance

Despite being possible to make a thermographic qualitative inspection without defining precisely the material's emittance, using an approximate value taken for example from an emissivity table, correct temperature readings and so, quantitative results, are typically not possible to attain without knowledge of the materials' emissivity values. In view of this, this parameter is usually obtained either approximately, on a table such as the one below (table 7), or more accurately, using one of two current methods.

Table 7 - Table of emissivity (Adapted from [G] and FLIR Systems; 2006)

Material	Feature	Emissivity	Material	Feature	Emissivity
Aluminium	Oxidized	0.30	Human skin		0.98
	Polished	0.02-0.04	Graphite	Oxidized	0.20-0.60
Brass	Oxidized	0.50	Plastic	Non-transparent	0.95
	Polished	0.02-0.05	Rubber		0.95
Gold		0.01-0.10	Plastic cement		0.85-0.95
Iron	Oxidized	0.70	Concrete		0.95
Steel	Oxidized	0.7-0.9	Cement		0.96
Asbestos		0.95	Soil		0.90-0.98
Plaster		0.80-0.90	Mortar		0.89-0.91
Asphalt		0.95	Brick		0.90-0.96
Rock		0.70	Marble		0.94
Wood		0.90-0.95	Textile		0.90
Charcoal	Powdered	0.96	Paper		0.95
Carbon		0.85	Sand		0.90
Lacquer work	Lacklustre	0.97	Clay		0.92-0.96
Carbon Cement		0.90	Glass		0.85-0.92
Soap Bubble		0.75-0.80	Oil		0.94
Water		0.93	Wool	Natural	0.94
Snow		0.83-0.90	Lead	Oxidized	0.50
Ice		0.96-0.98	Sandstone	Polished	0.91
Frozen Foods		0.95		Rough	0.94
Ceramics		0.95	Water	Distilled	0.96
Limestone		0.98	Porcelain	Glazed	0.92
Paint		0.93		Shiny	0.70-0.75

The first method uses an emissometer and it can be based on ASTM C 1371-04a (Gonçalves; 2014).

The second method, the black tape method (a method used by Bauer et al. (2014) and based on an ASTM standard (ASTM E1862)), consists in attaching a piece of black tape (with already known emittance) to the target and, after heating both to the same temperature, take a thermogram and change the emittance value on the configurations until the temperature of the target achieve the same value as the temperature of the tape (Usamentiaga; 2014).

This last method is not flawless; so, for low emittance objects - such as chromed metals where small emittance variations can lead to bigger variations than in the case of the most usual construction materials (to whom emittance value rounds 0.8-0.9 and slight variations in the chosen value will only cause minor changes in temperature) (Usamentiaga; 2014) -, emittance shall be obtained using a more accurate method.

Reflected apparent temperature

Reflected apparent temperature, or just reflected temperature, is a parameter used to make corrections on the thermogram by estimating the radiation that is being reflected by the target. As seen before, according to Kirchhoff's law, from the emissivity value (that equals the absorbance value without solar radiation incidence) it is possible to find the reflectance value. But as equation 3.23 shows, the camera's software uses Stefman-Boltzman's law (eq. 3.9) where a temperature is needed to calculate the portion of reflected radiation. Hence, reflected temperature, also known as thermal background, respects to the amount of thermal radiation (in the form of temperature) that surrounds the target and that can be reflected depending on its reflectance (obtained by the camera using emissivity's value).

This parameter is very important to define, especially when low emissivity materials are being tested, as their reflectance is higher.

To set reflected temperature's value there are two methods suggested in the thermal camera's manual (FLIR Systems; 2006):

- Direct method – this is the most difficult and consequently the less used method. The method is divided into three stages:
    1. Looking for possible reflection sources (1) considering that the angle of reflection (b) equals the angle of incidence (a) (fig. 22):

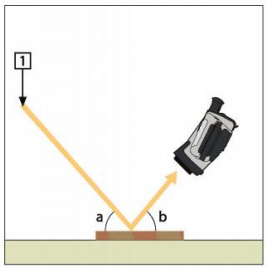

Figure 22 – Reflected temperature measuring – direct method (step 1)

    2. Modifying the source with a cardboard if it is a "spot source" (fig. 23):

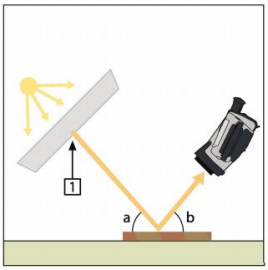

Figure 23 – Reflected temperature measuring – direct method (step 2)

3. Measuring the reflected temperature from the reflecting source with the emissivity and distance to object set to 1 and 0m respectively (fig. 24):

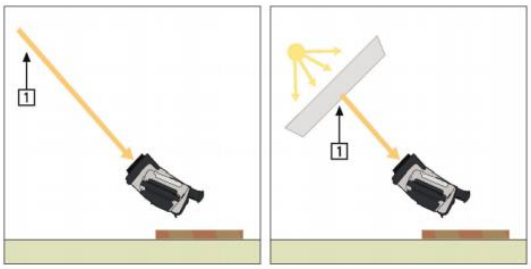

Figure 24 – Reflected temperature measuring – direct method (step 3)

- Reflector method – this is a much more common method, as it is easier to apply and provides better results (Usamentiaga; 2014). The method consists of (FLIR Systems; 2006):
  1. crumbling and reflating a piece of aluminium foil and attaching it to a cardboard or a calibrated reflected standard, such as gold metallic coating (with 95% constant reflectivity from 2 to 20µm), according to Usamentiaga (2014);
  2. positioning the cardboard in front of the object with the aluminium side pointing the camera (fig. 25);
  3. measuring the reflected temperature of the aluminium foil with the emissivity set to 1.

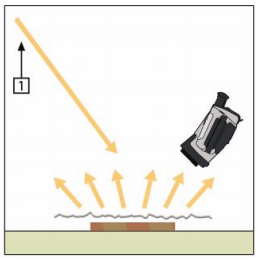

Figure 25 – Reflected temperature measuring – reflector method

3.6.3 Imaging techniques

Two kinds of diagnosis techniques can be used: the passive infrared thermography (PIRT) and the active infrared thermography (AIRT).

PIRT consists in the interpretation of superficial temperatures without the appliance of any mean of thermal variation. Thereby, the thermal variations that can lead to a diagnosis are usually caused either by the solar incidence or by a heat flow through the inspected element.

AIRT on the other hand consists in applying a thermal variation on the specimen for example through the incidence of radiation from a lightbulb. This method studies the thermal variation

caused by the imposed action that can either be from the side of the reading (reflexion method, used to find more superficial anomalies) or the opposite side (transmission method, used on more deep anomalies). This kind of IRT can further be divided in (Maladague; 2001):

- Pulsed IRT (PT) – Consists in applying a short thermal stimulation pulse and studying the temperature decay curve.
- Step Heating (SH) – Also known as long pulse IRT, it relies, as it is named of, on a long thermal stimulation pulse.
- Lock-in IRT (LT) – Is a technique in which thermal waves are imposed inside a specimen for example by periodic disposition of heat; this kind of AIRT is named after the need to precisely monitor the time between the input and the output signal.
- Vibrothermography (VT) – Is based on the effect of mechanical vibrations induced on the specimen, which result in heat creation that can be read by the thermal camera; this technique is especially effective in showing cracks or delamination zones where friction can cause a higher thermal variation.

3.7 Review of the research done so far

Despite being a NDT that has been applied to building inspections as a valuable diagnostic tool (Freitas, S. et al. 2014), IRT has potential applications that have not been completely explored and valuated yet. One of these applications is the detection of detachments/moisture in facades that is not at the time covered by any standards like other construction related areas are (Edis et al. 2013, 2014). Nevertheless, other building related anomalies, such as thermal irregularities or air infiltration problems, are well-developed and inspection procedures and conditions are defined in standards, such as ASTM C 1060-90:200, ISO 6781:1983 and EN 13187:1998.

Few efforts have been made in order to turn this inspection technique in a viable alternative to the other ones in use. However, there are some researchers that have given the first steps in order to make it possible: some have studied anomalies on ceramic tiling systems such as detachments (Bauer et al. 2014; Edis et al. 2014) or moisture detection (Edis e. al; 2013, 2015b; Barreira et al. 2008) and others have studied closely related subjects (Bauer et al. 2015; Freitas, S. et al. 2014; Theodorakeas et al. Melrinho et al. 2015; Freitas, J. et al., 2014).

For example Theodorekas et al. (2014) have analysed plastered mosaic detection by means of IRT. In this study, the researchers have quantitatively analysed five assorted panels in laboratory assuming that IRT would be “able to detect hidden mosaics, presented with temperature variations on the surface, due to the dissimilar diffusion that each layer renders”. They used a method named Cooling Down Thermography (CDT) that allows to analyse the decay of temperatures as a function of time after heating. This technique has proven to be “very well suited” for the investigation of plastered mosaics demonstrating thermal contrast among “mosaic-consisted and mosaic-free areas” in all inspections. The research prove that numerical computation applied to the thermal images can be useful as it is not only able to provide information about the thermal response of the investigated structure (confirming or predicting results acquired through experimental testing) but also it makes possible to “acquire information regarding the influence of specific parameters variations to the produced detectability, as well as to estimate the detection limits under specific testing conditions” (Theodorakeas et al. 2014). With this research the authors claim that IRT can be

applied efficiently to detect plastered mosaics for example in cases of cultural heritage inspection. A similar survey was taken by Avdelidis et al. (2006) with analogous results.

Edis et al. (2014) have also done some research on this NDT using quantitative analysis to study detachment of adhered ceramic cladding by Time-dependent PIRT. With this purpose in mind authors inspected two buildings in Lisbon not only with IRT but also recurring to other testing methods such as tapping control by hand and by hammer. They also used some other instruments to evaluate some of the climatic and the facade's conditions like the wind speed, the intensity of the sunlight and the moisture content in the facade. The time-dependent PIRT (td-PIRT) improved the accuracy of the inspection results. Three different quantitative analysis methods were used: simple image subtraction (SIS), nonnegative matrix factorization (NMF) and principal component analysis (PCA). The td-PIRT is a method to enhance thermograms used in medium to high rise building where AIRT is not viable. The method consisted in taking thermograms with half an hour intervals gathering information on how the surfaces temperatures variate and relating it to the other data mentioned above. At the end, results were crossed with the quantitative IRT and the tapping tests. It came to conclusion that td-PIRT is the most appropriate technique to detect detachments in adhered ceramic cladding, since new areas with detachments "were identified during supplementary tapping controls performed with indications in the thermograms and quantitative analysis results being taken into account" (Edis et al. 2014). The PCA analysis technique was the one who proved to be the most efficient showing high consistency in different time periods and environmental conditions. They also claim that the greatest advantage of td-PIRT over PIRT is its consistent performance in showing defective areas when proper analysis methods are used. More general conclusions were taken such as the effectiveness of the IRT in detecting delamination before detachment occurs.

Freitas, S. et al. (2014) conducted a study to verify the viability of IRT in the detection of facade polymeric plaster detachments. Despite not being the same type of cladding as ceramics, the principle is the same: detachment creates an air gap that increases thermal resistance to heat flow. To this purpose physical models were created in laboratory with artificial detachments. Specimens were formed by a concrete sample cladded with a layer of plastic with air bubbles (in the zone of the induced anomaly) simulating the air gap between the support and the fine polymeric plaster. The technique used for testing was a qualitative AIRT where "thermograms were obtained on a minute-by-minute basis in three phases: without a heat source; with the heat source switched on (for 30 min) and after the heat source was switched off (for 70 min)" (Freitas, S. et al. 2014). From the laboratory tests the authors concluded that PIRT is not a viable method for laboratory testing because "without the action of the heat source, the detachment created in the sample is not visible" (Freitas, S. et al. 2014). However, when the heat source is switched on, there is an increase in surface temperature throughout the sample, particularly in the area of defect. Similarly, "when the heat source is switched off, the temperature drop is greater in the detached area" (Freitas, S. et al. 2014).

After the laboratory survey, in situ measurements were done on the southern facade of a residential building in Porto with occasional detachments. Similarly to the experimental campaign taken by Edis et al. (2014), PIRT was used and then crossed with the results from a tapping control inspection. "Thermograms were obtained hourly in three phases: without sunlight falling on the facade, with sunlight falling directly on the facade and after the sun had been on it" (Edis et al. 2014). Simultaneously, a numerical simulation was done using the program WUFI Pro 5.3 and the characteristics of the facade studied in situ. Comparing the results from the numerical simulation with the ones obtained in situ, it is claimed that "the temperature change in the numerical

simulation is analogous to the change in surface temperature obtained by IRT, both in the area without detachment and in the area with detached plaster; that is, on a southward-facing facade, at the end of the morning, the temperature of the detachment zone is higher than that of the facade and, in early evening, the temperature in the detachment area is lower" (Edis et al. 2014). Once more, IRT was proven to be a valuable tool to detect early detachment situations.

Bauer et al. (2014) have likewise done some work on this field. Authors created a model for laboratory testing composed by a slab cladded with three ceramic tiles with different thickness. The detachment was simulated by a middle flaw zone with a width of 20 mm in which adhesive mortar was lacking. Using a long pulse AIRT technique it was proven by a quantitative analysis that, as expected, the thicknesses of the cladding influences the thermal variations of the surface since a higher thermal variation between the normal zone and the faulty zone was noticed on the thinner tile. From the quantitative analysis another important conclusion was obtained: when the thermal variation considered is between the faulty zone and the whole tile, they noticed that the thickest tile verified the lower thermal variation. This observation lead the researchers to claim that thermal variation factor alone does not serve as a defining parameter of anomalies and that is necessary to consider also the facade´s temperature, the materials characteristics and the existing heat flows.

The year after, Bauer et al. (2015) continued the study of detachment detection by means of IRT, this time using the specimen created by Freitas, S. et al. (2014). The same specimen was studied using two different infrared cameras aiming "to assess the effect of the specific adjustments and acquisition characteristics of the equipment" (Bauer et al. 2015). After once more confirming this method's capacity to detect detachments, the authors claim that "when the quantitative criterion ΔT between regions was being assessed, the differences between the two cameras were very small. Thus, quantitative IRT can be used for the assessment of damage and anomalies in facades" (Bauer et al. 2015). They also state that "in field inspections, when PIRT is being used, different thermal flow regimes need to be implemented. Thus, assessing the facade under different temperature conditions (under the action of the sun, at night, amongst others) it is possible to identify damages and anomalies comparatively by applying quantitative criteria" (Bauer et al. 2015).

Sfarra et al. (2016) conducted a study on an innovative hybrid thermographic (HIRT) approach combining both the time component and the solar source to obtain quantitative information such as the defect depth in Santa Maria Collemaggio church (L'Aquila, Italy). The authors conclude that an inspection shall be divided into two main phases, beginning with a passive and qualitative approach to verify the state of conservation of the facade and then a more deep analysis, for example using the proposed hybrid method, useful for the estimation of the depth of small defects which appeared inside vertical known structures. The authors also conclude that a "recording of many thermograms during a sunny day that is preceded by sunnier ones, and at a time of the day when the sun directly irradiates the inspected surface tends to minimize the operator's discretional contribution during the interpretation of the defects present in a thermogram. It also minimizes the miscalculation during a measurement focused on the defect depth retrieval". Another particularity of this work is that among the anomalies verified in the church (sometimes difficult to analyse due to the geometric pattern of the tiles, or in a specific region because of the reintegration of the tiles using a different type of mortar and having a lower thermal diffusivity) was the detachment of some tiles.

Moisture related presence in ceramic claddings was analysed by Edis et al. (2013). Authors presented a research based on results from numerical simulations and *in situ* inspections

performed to verify the viability of passive infrared thermography in a prelaminar identification of moisture in tiled facades before any visible signs occur. Authors concluded that given the increased heat capacity of the moist material it was possible to identify moisture using solar heat gain. Despite finding out that "the greater the moisture content difference between the moist and dry areas, the higher the observed surface temperature variation will be", authors claim that this method can only be used for a preliminary identification because of its qualitative nature. Regarding the best period of the day to identify moisture problems, it is claimed that the maximum magnitude between moist and dry areas is at midday, whereas at night the differential is smaller.

The same authors (Edis et al. 2015b) continued the study on moisture detection but this time using a "quasi-quantitative" (q-QIRT) approach and crossing the infrared data with hammer-tapping control and surface moisture measurements to access IRT capacity to detect moisture variations. For this, the facade of a building block in Lisbon (Portugal) with a pre-identified rising damp problem was inspected by IRT during daylight hours at ½ h intervals, and the IRT data was then analysed by three different quantitative methods for different time periods and intervals. As conclusions authors claim that the quasi-quantitative method "has a great potential to detect moisture variation above ca. 36%" and that "half-day daytime IRT inspection during or after solar exposure either at ½ h or 1 h intervals is sufficient to identify areas with increased moisture content by q-QIRT using a principal component analysis (PCA). The PCA analysis has also proved to be useful in eliminating false indications caused by reflection and shade that could not be eliminated at the time of inspection.

Melrinho et al. (2015) studied a method for the detection and mapping of anomalies in flat roofs, more specifically waterproof related problems, with IRT. The efficacy of the NDT was proven again. One interesting conclusion from the survey is that one of the factors that can influence the image obtained is the angle of observation. However, through the experimental campaign it was verified that although some error may occur from the angle variation, it is not significant. Therefore, together with the use of a simple support during the campaigns, turns this type of inspection extremely viable for application on real cases.

Another interesting survey taken by Freitas, J. et al. (2014) aimed to verify the possibility of using IRT to detect cracks on rendered facades *in situ*. Authors claim that, despite not being able to identify all the failure zones with IRT alone, when using a computational program to overlap the thermogram and the digital image, as well as inputting the surface temperature in points of interest, it is possible to claim that IRT is a highly capable technique to evaluate and diagnose problems in facades' claddings.

Critical analysis

Without many weak points to appoint on the research done so far, it is necessary to say that some of the results obtained may lack the supposedly necessary number of specimens to test, often being only one specimen tested. Despite this, all the surveys studied in this study revealed similar conclusions regarding the applicability of the diagnosis method in question.

The crossing between traditional testing methods such as the tapping method and IRT proved to be valuable not only to verify the accuracy of the "new" method but also to compare the efficiency of both methods. As well as testing techniques as the one mentioned above, numerical simulation before the actual survey may help to foresee the results, eliminating possible errors. Despite its complexity, a quantitative analysis taking into account as many aspects as possible proves to be a useful tool to ensure the credibility of the data obtained.

In the case of ceramic claddings there is an additional problem for the use of IRT to assess detachments due to the high reflectance characteristic of some tiles, the thermal differences between tiles (when they are not from the exact same colour), the thermal differences between tiles and joints and the height that the facades can have.

3.8 Recommendations for a thermographic survey

Considering all the research made, there are some recommendations that should be taken into account while leading a thermographic survey:

- Before the survey, all the possible information about the element to inspect shall be gathered in order to eliminate possible mistakes.
- Similarly, all the information about the surroundings shall be gathered, such as possible sources of radiation or reflection, or shadowing elements.
- The period/position of the camera or the type of thermography (active or passive) shall be chosen according to the type of anomaly that is expected to identify, i.e. according to the deepness and thermal behaviour of the anomalous zone.
- The already mentioned parameters to input in the equipment shall be measured as accurately as possible, especially when leading a quantitative survey.
- Thermograms shall be taken as near to the element to inspect as possible.
- Inspections to partially shadowed or partially subjected to reflections shall be avoided.
- Avoid direct solar incidence in the camera's lenses.
- Maintain the camera levelled (using a tripod for example) and focused on the target.
- Avoid angles higher than 60° between the camera and the normal to the surface.

After the thermograms being taken, a correct analysis shall be made in order to achieve proper results. This analysis shall take into account:

- The targets' characteristics already gathered, such as the existence of thermal bridges or the existence of particularities such as heating equipment in contact with the element of inspection.
- Possible shadows/reheated zones (by reflection or a secondary heat source) must be taken into account.
- When inspecting building elements there are some particularities to take under consideration:
    - The heat-flow through the element.
    - The upward movement of warm air from radiators or other heat sources and the cold air down from the windows can cause distortions in surface temperatures (Barreira et al. 2008).
    - The *chimney effect* that causes infiltrations on the lower floors and exfiltrations on the upper floors, leading to the cooling of the walls on the lower floors and heating the upper floors.
    - The wind presence can pressurize/depressurize the facades, causing infiltrations/exfiltrations through the windows. It can also reduce the superficial thermal resistance to the heat flow, cooling the surface, especially on the buildings' corners, causing therefore a differential cooling and compromising thermograms (Barreira et al. 2008).
    - Transparent/semi-transparent objects' temperatures (such as windows) are usually very difficult, if not impossible, to read, as the portion of transmitted radiation is not considered as so by the measuring equipment.

Taking these factors into account the thermogram shall be analysed by inputting the right parameters if not already introduced in the equipment at the inspection moment and considering that, in order to correctly interpret the thermogram, it might be required a rearrangement of the thermal scale/spectre and the colours' pallet so that smaller thermal variations can be visualized.

4 Study methodology

4.1 Introduction

As mentioned above, usually an anomaly implies a change in the element's constitution, such as the voids that are created between the cladding layers which are filled with air or water when a detachment occurs. The presence of one or both these elements in a wall (air, water) will, even in an almost imperceptible way, cause variations in the overall thermal behaviour of the wall. This assumption is what in theory will enable an infrared camera to detect anomalous zones – in the present case, areas of low adhesion between the tile and the support.

As the differences in terms of thermal behaviour provoked by the appearance of an anomaly may differ according to the element's characteristics, this study aims to characterize, both under controlled conditions (indoors and outdoors) and in real cases, the influence of colour, thickness, kind of support, finishing, presence of moisture and day period in a thermographic inspection of tiling systems. Hence, eight specimens and four exterior wall panels containing simulations of anomalies were tested in LNEC and two real cases of tiled facades were studied *in situ*.

In this section, the methods of testing used to approve thermography´s capacity in detecting ceramic tiles related anomalies are presented. With this purpose, firstly some preliminary testing has been done in order to characterize the functioning of the thermographic camera, as well as environment conditions and parameters to setup the camera. The tests aimed to define:

- the temperature and time the heating plate, used in laboratory tests, takes to stabilize;
- the kind of heating (by conduction or radiation);
- the duration of heating and cooling required to test the specimens;
- the emissivity of the specimens;
- the best way to find the apparent reflected temperature.

Afterwards, the main testing of the diagnosis method has been taken care of, with the testing of eight laboratory specimens and four exterior wall panels with controlled detachments.

Finally, two case studies of real situations will be presented.

4.2 Laboratory testing

4.2.1 Specimens´ preparation

For the laboratory survey eight specimens were prepared with different characteristics in terms of tile's colour, surface finishing (polished or natural/unpolished), thickness, kind of support and presence of detachment. The specimens produced are described in table 8.

All the specimens were created using thermal paving slabs as base/support (fig. 26). The slabs were composed by an extruded polystyrene (XPS) board covered by a mineral mortar layer – the paving side. However, six specimens had the tiles applied to the paving slab side, while two specimens had the tiles applied to the thermal insulation side, simulating an ETICS solution (External Thermal Insulation Composite System).

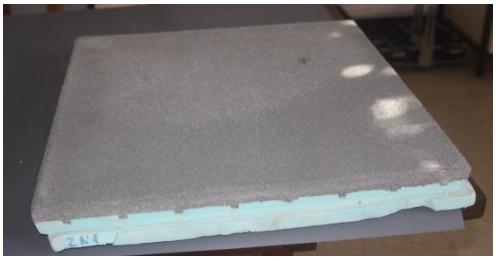

Figure 26 - Thermal paving slab

Table 8 - Specimen's characteristics

Code	Designation	Tiles´ commercial designation and original dimension (cm x cm)	Tiles' colour	Surface finishing	Support	Presence of detachment	Tile's thickness [mm]
Blad	Black light adherent	Revigrés LIGHT FLINT SPPERT R 30X60 [TS6]	Black	Natural	Paving slab	No	5.4-5.6
Wnat	White natural	Revigrés CROM.BRANCO RECT 30X30 [TS7]	White	Natural	Paving slab	Yes	8.1-8.3
Bnat	Black natural	Revigrés CROM.PRETO RECT 30X30 [TS7]	Black	Natural	Paving slab	Yes	8.1-8.3
Wpol	White polished	Revigrés CROM.BRANCO POL 30X30 [TS7]	White	Polished	Paving slab	Yes	7.6-7.8
Wl	White light	Revigrés LIGHT FLINT MARFIM R 30X60 [TS6]	White	Natural	Paving slab	Yes	5.4-5.6
Bl	Black light	Revigrés LIGHT FLINT SPPERT R 30X60 [TS6]	Black	Natural	Paving slab	Yes	5.4-5.6
Wti	White over thermal insulation	Revigrés CROM.BRANCO RECT 30X30 [TS7]	White	Natural	Thermal insulation	Yes	8.1-8.3
Bti	Black over thermal insulation	Revigrés CROM.PRETO RECT 30X30 [TS7]	Black	Natural	Thermal insulation	Yes	8.1-8.3

In the case of the specimens simulating an ETICS solution with ceramic coating, whose tiles were applied over the insulation side of the slabs, a preparation has been given before applying the tiles. The preparation consisted of two thin layers of *weber.therm pro* [TS1] (a mortar designed for gluing and coating thermal insulation boards) with an anti-alkaline fiberglass mesh (*weber.therm rede normal*) in between. The coating applied to the XPS side of the slab simulates what is usually used in an ETICS solution. Figure 27 shows the simulation of the ETICS.

Figure 27 - Preparation of the ETICS specimens

After preparing the supports (after being cleaned, dried and plane), came the application of the tiles.

As it is possible to see on table 8, tiles provided by *Revigrés* are dimensioned between 30 cm x 30 cm and 30 cm x 60 cm. Hence, in order to be applied in a 60 cm x 60 cm thermal slab, with the

disposition presented in figure 28a, tiles had to be cut. The cutting was done using a manual tile cutter (*RUBI TS-60 PLUS*, as suggested by *Revigrés*) (figure 28b).

Figure 28 - Tiles display and marking before application (a) and tile cutter (b)

The first specimen to be done was *Plad*, a control specimen without any provoked anomaly, following the specifications in the technical sheet of the adhesive mortar (*Weber.col flex* [TS2], a cementitious flexible tile adhesive, design to tiles without water absorption, with surfaces up to 1500 cm^2 for either indoor or outdoor walls or pavements). The tile adhesive was applied with an 8mm notched trowel. Figure 29 shows the sequence of the application.

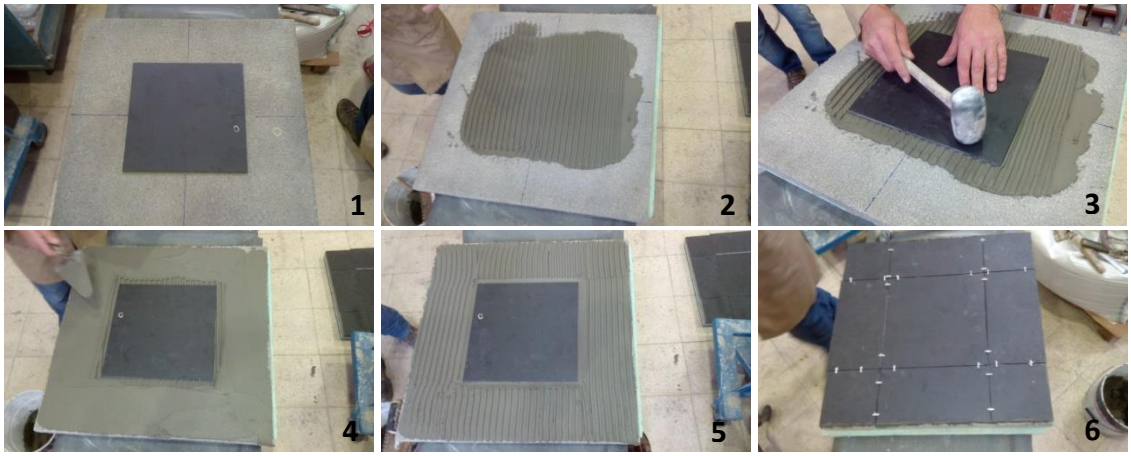

Figure 29 - Sequence of the tiles' application (specimen *Blad*): 1-Marking; 2- Application of the adhesive mortar on the support destined to the middle tile's appliance; 3- Middle tile application and pressing with a rubber hammer; 4 and 5- Application of adhesive mortar for the following tiles; 6- Application of following tiles with 2mm joint spacers.

The difference that sets the mentioned specimen apart from the others is the application of the middle tile. In this specimen, the tile is well adhered to the support, whereas in the other specimens anomalies have been intentionally provoked. A natural and at the same time controlled detachment is not easy to create in laboratory. However, after some research, the method chosen consisted of leaving an empty space between the middle tile and the support with lack of adhesive mortar. This empty space was achieved applying adhesive mortar only in the corners of the middle tile as it can be seen in the sequence of figure 30.

Figure 30 - Production of the anomaly on the middle tile of specimen *Bnat* (application of the adhesive in the zone correspondent to the corners of the middle tile (a), placing the tile (b), empty space created beneath the tile (c)

The rest of the specimens with provoked anomalies were executed using the same method.

In short, the general sequence of application per specimen was:

1. tiles' cutting;
2. tiles' positioning and marking over the support;
3. weighting of 3.6kg of adhesive mortar (powder, 5.5kg/m^2);
4. mixing the powder with 0.94l of clean water (0.26l/kg) using an electric mixer until the mixture is homogenate and without grumps;
5. let the mortar lay down for 2min and then mix it again;
6. spread a thin and tight layer of adhesive mortar over the support (where the middle tile will be placed in first place) in order to waterproof it, using a flat trowel;
7. using an 8mm notched trowel, spread the mortar in the space where the tile will be placed (this procedure will depend if it is an adherent or non-adherent tile as mentioned above);
8. place the tile and press it against the support crushing the mortars' threads;
9. using a rubber hammer hit the tiles for a better crushing of the threads;
10. repeat the process 6, 7, 8 and 9 for the area destined to receive the remaining tiles (the remaining tiles positioning will be set using 2mm cross-shaped spacers);
11. let the mortar slightly dry and clean the joints;
12. after one day clean the specimen to avoid staining.

After the specimen´s drying, the 2mm joints between tiles were filled with *Weber.color premium* [TS3] (cement mortar with organic and inorganic admixtures and mineral pigments, waterproof and reinforced with fibres), a mortar designed for a flat joint finishing, between 2 and 15 mm, both for indoor and outdoor conditions. The joint filling process was the same for all the specimens. In figure 31 it is possible to see the aspect of three finished specimens (the rest of the black and white non-polished specimens are similar in aspect to the ones from figures 31a and 31b).

Figure 31 – Specimens *Bti* (a), *Wl* (b) and *Wpol* (c)

4.2.2 Characterization of the heating plate

After the tiles preparation came the need to define how to test them. But as there are no specific methods to verify thermography's capacity in the detection of this kind of anomalies, the testing procedures would have to be studied so that they can be applicable to all the specimens in equal terms.

As mentioned in the previous chapter, active thermography is the most suitable method for laboratory testing, as specimens need to be heated in order to show differences between normal and anomalous zones.

A heating plate used in several research studies for example Melrinho's (2014) and Gonçalves' (2014) Msc dissertations, with a surface area equivalent to the specimen's, was available in LNEC and was chosen as the heating mechanism.

The heating plate consists of a box with an electric resistance inside that heats specimen through a black surface. In figure 32 there is an image of the heating plate and a thermogram where it is possible to see the electric resistance and confirm the uniformity of the heating.

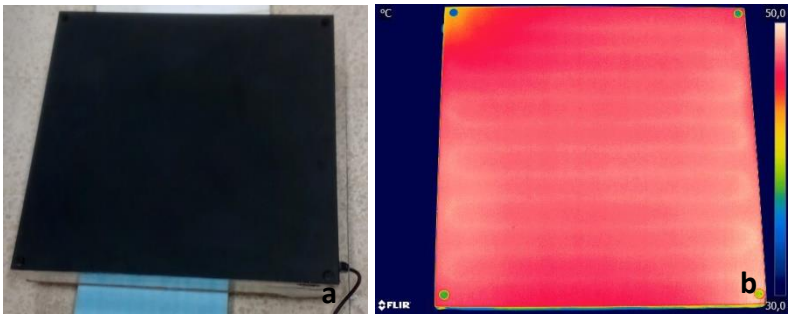

Figure 32 - Heating plate (a) and thermography of the heating plate (b)

Before the actual heating of the specimens, the characterization of the plate was taken care of, leading to the following conclusions:

- the plate reaches temperatures rounding 50°C (fig. 34);
- the temperature stabilizes at about 40-50 min of heating;
- the heating is the most even when it is done with the plate horizontally placed but it also reaches a lower medium temperature (fig. 33).

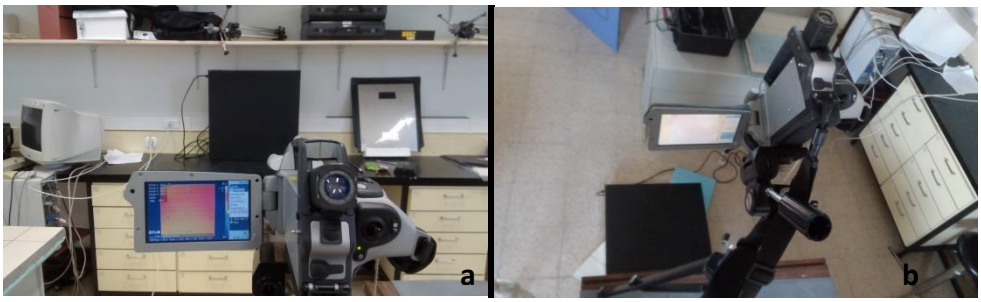

Figure 33 - Thermographic analysis of the heating plate in a vertical position (a) and in an horizontal position (b)

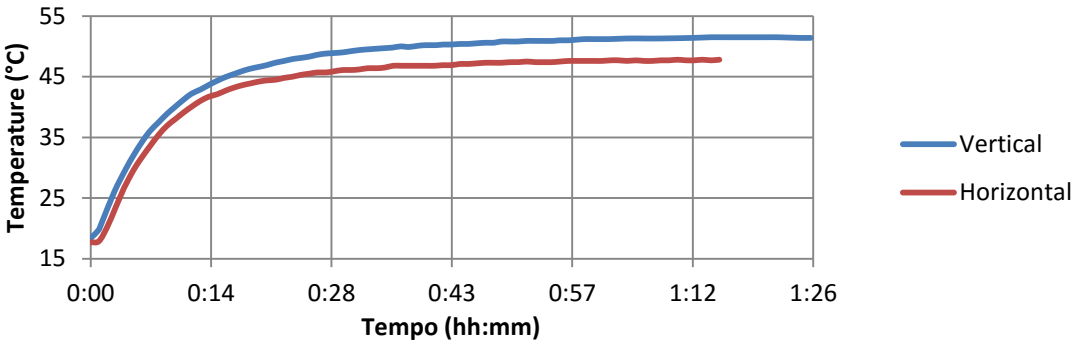

Figure 34 – Heating plate's heating in two different positions

Type of heating

Two methods of heating were studied: without contact and with a 3 mm sponge between the plate and the specimen.

The specimens were heated for 15 min and thermograms were taken of the cooling down process during 15 minutes (fig. 35). Afterwards, the temperature decay was measured continuously using thermocouples.

The results showed that:

- specimens reach higher temperatures in the anomalous zone;

- higher temperatures were obtained for the no contact method;
- the polished specimen reached higher temperatures, especially for the no contact type of heating;
- after 15 minutes of heating the temperatures stabilized only after about 1h30 of cooling.

Figure 35 - Specimen's cooldown thermographic survey

4.2.3 Emissivity definition

In order to determine the tiles' emissivity, a procedure based on ASTM E 1933-99 (ASTM, 1999) was used. The method is known as black tape method and, as the name suggests, it consists in using a tape (usually black) with a previously determined emissivity to find the material's emissivity (Bauer et al. 2014). The tape used had its emissivity determined for Gonçalves' (2014) MSc dissertation using a portable emissometer, at Universidade Politecnica de Madrid. The value obtained for the tape's emissivity was ε=0.88.

The black tape method consists in taking a thermogram from the heated surface with the tape stuck on it (fig. 37) - and so, at the same temperature. This thermogram is taken with the camera setup to the tape's emissivity. Despite both the surface and the tape being at the same temperature, the temperatures obtained in the thermogram will probably differ due to a difference of emissivity. Thus, after the thermogram being taken, the temperature of the tape should then be written down and, by an iterative method, the emissivity on the camera's setup must be changed to equalize the temperature of the surface to the temperature of the tape. The emissivity that equals these two values is the surface's emissivity.

This parameter definition only had to be done once per specimen, since the procedure taken will raise the tiles' temperature to a temperature of the same order as the expected on the rest of the survey. Furthermore, as figure 36 shows, the emittance would not change significantly from the range of temperatures expected.

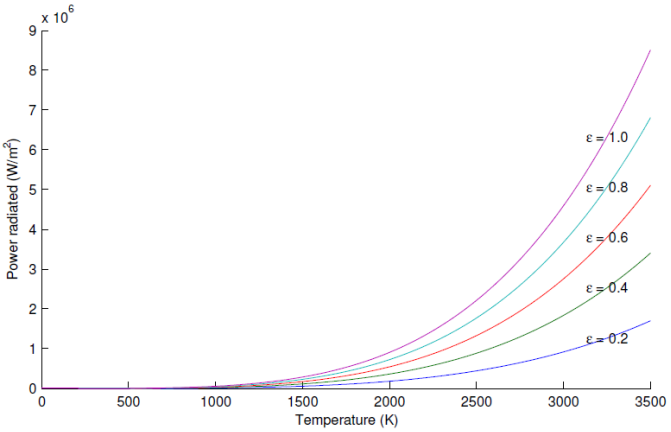

Figure 36 - Power radiated by grey body with different emissivities (Usamentiaga; 2014)

Figure 37 - Specimen *WI* prepared for emittance determination using the black tape method

4.2.4 Reflected apparent temperature

As opposed to the emissivity determination, the reflected temperature was determined before every thermographic testing because this parameter does not depend on the materials characteristics but on its surroundings.

The method used to determine reflected temperature was the reflector method (described in section 3.6.2), using a piece of aluminium foil attached to a cardboard, as shown in figure 38.

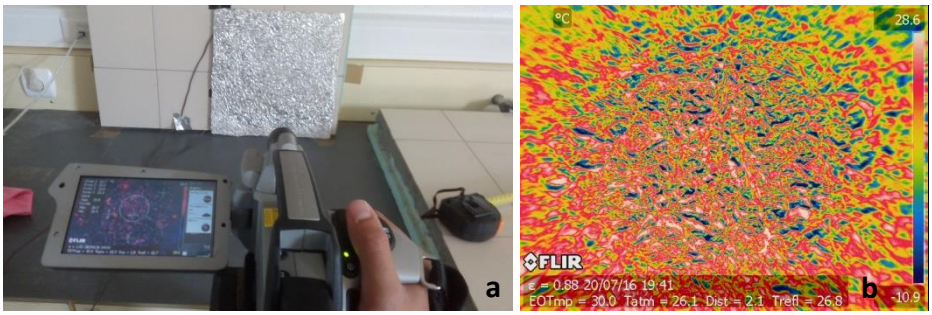

Figure 38 - Determination of the reflected temperature (a) and the respective resulting thermogram (b)

4.3 Laboratory survey

Regarding the results from the preliminary experimental campaign, a testing method was defined to apply to all the specimens mentioned. The method's sequence was:

1. switch on the heating plate for 50 min;
2. lay the heating plate (facing down) over the specimen (placed horizontally with the tiles facing up) (fig. 39);
3. heat the specimen for 20 min;
4. stop the specimen heating and place it in a vertical position facing the thermal camera (positioned 2 m from the specimen) (fig. 40);
5. run a program on the thermal camera where thermograms are taken every 2 min for the first 45 min of cooling, after which the time between thermograms will be 5 min;
6. the test ends after 2 hours of cooling.

It is important to mention that two thermocouples were glued to each specimen's surface using a black tape (one in the middle of the detached tile and one in the middle of the adherent tile positioned below the previously mentioned one).

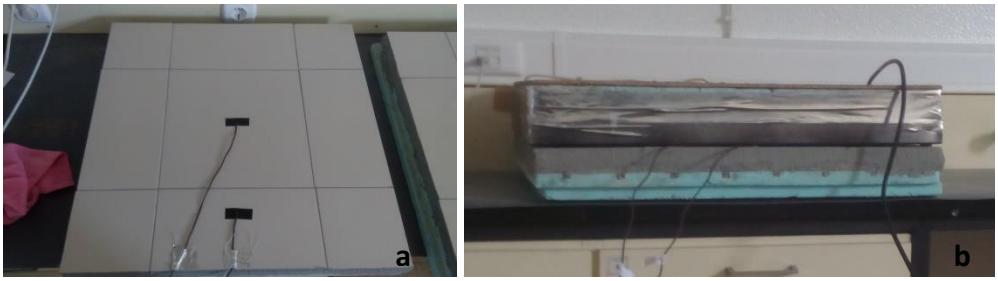

Figure 39 - Specimen's preparation (with thermocouples) (a) and heating (b)

Figure 40 - Thermographic analysis of the specimen's cooldown (a) and ambient temperature and relative humidity monitoring with *Rotronic hygrolog*

4.4 *In situ* testing under controlled conditions

4.4.1 The outdoor panels

Thermographic inspections are extremely dependent on the weather conditions. Therefore it is very important to characterize this testing method outdoors, subjecting facade's simulations to real weather conditions.

To this purpose, four outdoor wall panels were created in two experimental cells built in LNEC's campus (fig. 41), with differences in terms of support and tile's colour. Before the tiles being applied, the western facades of both cells were cleaned using a pressure washer.

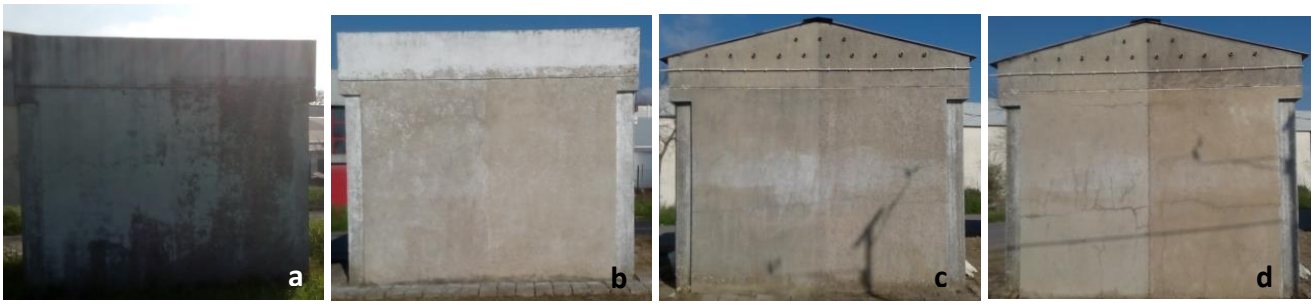

Figure 41 - Experimental cell 1 before (a) and after (b) washing and cell 2 before (c) and after (d) washing

Both the cells' West facing facades were cladded with two panels of tiles (one white and one black). The difference between the cells is that cell 1 facade was previously coated with a common ETICS solution, being the tiling its finishing coat, while cell 2 had the facade simply rendered with, a mineral mortar system.

In order to verify the thermographic method, the panels of cell 1 after the ETICS's application were instrumented with thermocouples. The positioning of the thermocouples and the schematic representation of the anomalies is shown in figure 42. Despite thermocouples being only present in cell 1, due to logistic reasons, the schematic representation of the anomalies' positioning is the same for the two cells.

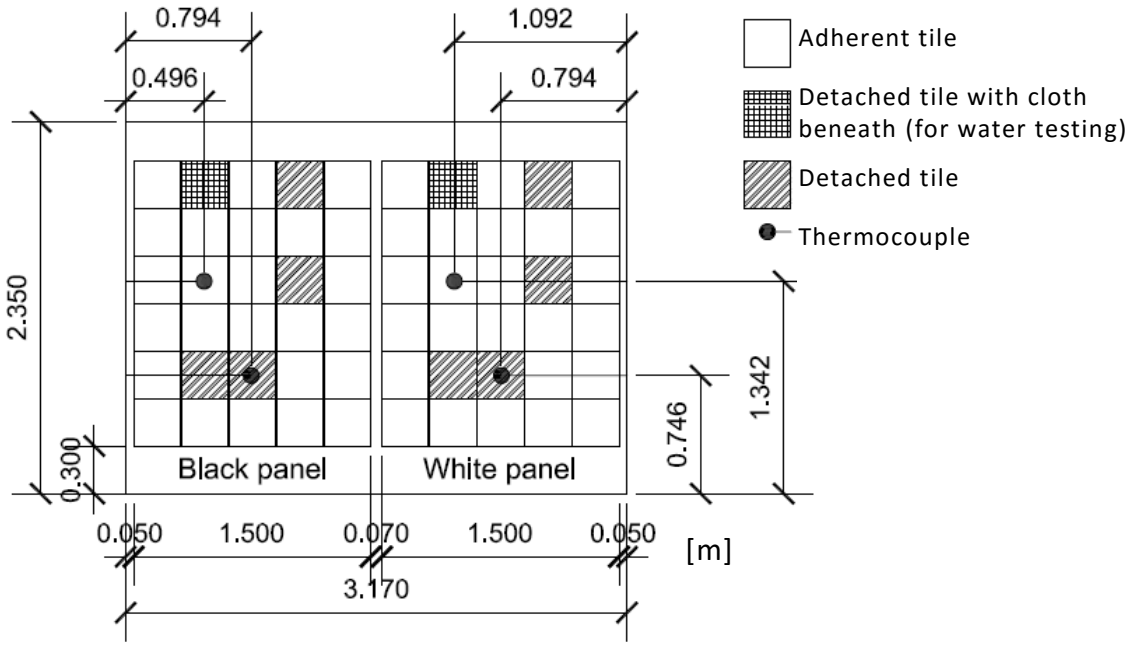

Figure 42 - Schematic representation of the outdoor panels with thermocouples and provoked anomalies

Table 9 presents the designation of the outdoor experimental panels, the cell where they are applied, the type of support, the tiles´ colour, commercial designation and original dimension and the testing that was performed.

Table 9 - Designation and characteristics of the exterior panels

Code	Experimental cell	Support	Tiles' colour	Tiles´ commercial designation and original dimension (cmxcm)	Testing methods
C1_B	1	ETICS	Black	Revigrés CROM.PRETO RECT 30X30 [TS7]	Thermocouples & Thermography
C1_W	1	ETICS	White	Revigrés CROM.BRANCO RECT 30X30 [TS7]	Thermocouples & Thermography
C2_B	2	Rrender	Black	Revigrés CROM.PRETO RECT 30X30 [TS7]	Thermography
C2_W	2	Render	White	Revigrés CROM.BRANCO RECT 30X30 [TS7]	Thermography

The ETICS application in cell 1, as well as the tiles' application in both cells 1 and 2 was done by Weber Saint-Gobain personnel. The material used to attach the insulation (4 cm of EPS) to the wall, as well as to clade the EPS, was the same used in the "ETICS specimens" described in section 5.2 (*Weber.therm pro* and a fiberglass mesh - *Weber.therm rede normal* –inserted between the two layers applied on top of the EPS). The system's production sequence was the following:

1. marking and fixation of the bottom base aluminium profile (fig. 43_1);
2. mixing of the synthetic-mineral adhesive mortar (fig. 43_2);
3. mortar spreading using a notched trowel (9 mm) on the EPS insulation boards(fig. 43_3/4);
4. pressing the EPS boards towards the wall (fig. 43_5), crushing the mortar's threads (repeat the process from the base of the wall to its top taking care of leaving a flat surface);
5. let the mortar dry (fig. 43_6);
6. using a scrapping trowel, scrape the insulation until it is completely flat (fig. 43_7);

7. drill holes to insert the plastic mechanic fixations and hammer them into place (fig. 43_8/9);
8. cover the mechanical fixations with the adhesive mortar (fig. 43_10);
9. using a notched trowel spread the same mortar over the EPS (fig. 43_11);
10. apply the fiberglass mesh on the fresh mortar layer and a new layer of mortar (fig. 43_12);
11. reinforce the corners with double mesh;
12. flatten the mortar layers (with the incorporated mesh) using the flat side of the trowel and let it dry (fig. 43_13);
13. place the thermocouples according to figure 43_14 and reinforce the cables with double mesh (letting the thermocouple tips hanging out);
14. apply a final layer of *Weber.therm pro* using a flat trowel (and without covering the thermocouples) (fig. 43_15/16).

Figure 43 - Sequence of the ETICS application on cell 1

After applying and drying the ETICS, the ceramic tiles were applied to both cells. The tiles' application process was similar to the one used on laboratory specimens. The process used for tiles' assembly consisted in a single gluing (using *Weber.col flex M,* applied on the support with a 9mm notched trowel). The anomalies were created using the same method as in the anomalous specimens (fig. 44a). However two of the tiles had anomalies created differently: on the second tile (left to right) from each panel's top line of tiles, a thin absorbent cloth was inserted in the empty space (created likewise other anomalies) with the purpose of testing with water, simulating humidity (fig. 44b). The piece of sponge tissue was applied because of its absorptivity that would trap the water and "distribute" it evenly beneath the tile. Furthermore, each panel's tile positioned in the fifth row, fourth line (top to bottom, left to right), was wittingly badly applied (fig. 44c) by letting the mortar dry for a few minutes, creating a skin, and then pressing it into the wall (simulating something that often happens in construction and that can influence the cladding's behaviour, especially in long term).

Figure 44 - Detachment simulation (a), positioning of the thin absorbent cloth beneath a tile for humidity simulations (b) and simulation of an awry application case (c)

After the panels drying, the 5 mm joints were closed using *Weber.color premium* and a rubber trowel. Nevertheless, testing was also performed before joints treatment.

The extremities of each panel were sealed using an elastic and waterproof polyurethane sealant (*Weber.flex PU* [TS4]). The zone above the panels, where eventually water could enter, was painted using *Weber.dry lastic* [TS5], a waterproofing liquid membrane (fig. 45).

Figure 45 - Joints' closing (a), edges' sealing (b) and top waterproofing (c)

After the joint filling, the grout's excess was cleaned and the panels looked as presented on figure 46.

Figure 46 - Finished experimental cells 1 (a) and 2 (b)

4.4.2 Outdoor panels testing

Characterization of the panels' properties

The tiles applied in the outdoor panels had the same reference and lot that the ones used in laboratory specimens. Therefore, parameters such as emissivity were already determined. However, despite in laboratory conditions simplifications such as Kirchhoff's law can be taken (for a specific temperature and wavelength, the spectral emissivity and spectral absorptivity are equal), this assumption cannot be applied in outdoor conditions (with solar radiation). Thus, for the outdoor testing, emissivity and absorptivity are different.

Nevertheless, according to Garcia (2014), quoting Barreira et al. (2012), despite surfaces' colours not affecting significantly the emittance value, they can have a greater impact when a facade is exposed to the sun, as they affect the solar radiation's absorption.

Insofar as the bodies in study are opaque, and so, the incident radiation equals the sum of reflected radiation and absorbed radiation, measuring the bodies' reflectance it is possible to know their absorptance.

Measuring the panel's reflectance

In order to study the cladding's reflectance, it was used an adaptation of ASTM E1918 – 06, a standard designed for measuring the solar reflectance of horizontal and low-sloped surfaces in field. Despite being a standard designed for horizontal surfaces, the method was adapted to obtain the vertical panels' reflectance.

The method consists in using a pyranometer ("an instrument (radiometer) used to measure the total solar radiant energy incident upon a surface per unit time and unit surface area" (ASTM E1918 – 06)) to measure the ratio between reflected and incident radiation.

Despite the standard procedure consisting in using only one pyranometer, which must be pointed firstly upwards (measuring solar radiation) and then downwards (measuring reflected radiation), the procedure adopted uses two pyranometers mounted in parallel and back to back. Therefore, the incoming and reflected radiation can be measured simultaneously. The instruments used were two *Kipp & Zonen CM5 Pyranometers* (Appendix A.2.), mounted as shown in figure 47.

Figure 47 - Reflectance measuring on panel C1_B

After the pyranometers' calibration, a first test was done to determine the best time of the day to measure reflectance. According to the standard (ASTM E1918 – 06), "the test shall be done in conditions where the angle of the sun to the normal from the surface of interest is less than 45°. For flat and low-sloped surfaces, this limits the test to between the hours of 09h00 and 15h00 local standard time; this is when solar radiation is at least 70 % of the value obtained at solar noon for that day." However, as the inspected surfaces are vertical, the angle of the sun to the normal from the surface is less than 45° from 15h00 until the sun sets (for a West facing wall). On this first test it was noticed that after 16h00, the shadowing from the equipment on the panels starts influencing the readings leading to a greater error. Hence, the best time window to do this testing on a West facing vertical wall is considered to be between 15h00 and 16h00.

Another aspect that was thought to influence the readings is the fact that the pyranometer that is facing the wall might not only be reading the reflected radiation but also the emitted radiation. However, the spectral range of the pyranometers is limited by the transmission of its glass domes

(Kipp & Zonen), which ranges from around 0.3 µm to 2.8 µm (Appendix A.2). This makes complete sense, as like mentioned in chapter 2, sun's higher emissive power corresponds to wavelengths around 0.5 µm.

Withal, according to Plank / Wien's laws, the maximum emissive powers correspondent to the verified temperatures range from around 8 µm to 11 µm, emitting very weak (negligible) radiation in the range that is captured by the pyranometers (see Plank's law graphic representation on chapter 3 (fig. 14)).

To verify this theoretical principle, a test was conducted using the heating plate in a dark room. Using the same setup as the one used for measuring reflected radiation, the pyranometer was placed facing the already mentioned heating plate. The heating was turned on and the variation of the radiation that hits the pyranometer was read. The heating plate reached temperatures around 50°C. However, no significant variations in the radiance readings were noticed, proving this theory.

In sum, the radiation emitted by the cladding would not be read by the pyranometers, distorting the reflectance value. Hence, despite some possible errors that might occur due to the panels' reduced dimensions, in theory, everything was set in order to successfully read the material's reflectance (in a qualitative context) using this ASTM adaptation. Hence, the readings were done between 15h00 and 16h00 with the equipment positioned 0.5 m from the panels, as recommended in the standard.

Continuous temperature measuring with thermocouples

In order to verify the thermographic method, as well as to continuously record the temperatures on the tiles, thermocouples (*type T* (Copper/Constantan)) were placed strategically, as mentioned above.

The temperatures recorded would overall help to, ensure the reproducibility of results. Despite being a useful method, this procedure was only applied in experimental cell 1 because of logistic reasons (as mentioned before).

Temperatures measured were coded regarding their position (see fig. 42) in the panels as follows:

- Tc_Bad – thermocouple under an **adherent black** tile
- Tc_Bdet – thermocouple under a **detached black** tile
- Tc_Wad – thermocouple under an **adherent white** tile
- Tc_Wdet – thermocouple under a **detached white** tile
- Tc_Bs – thermocouple on the **surface** of an adherent **black** tile
- Tc_Ws – thermocouple on the **surface** of an adherent **white** tile
- Tint – thermocouple in the **interior** of the experimental cell

Thermographic surveys

Detachment's detection

In order to verify thermography's capacity in detecting detachments four surveys were conducted on the outdoors panels: one before closing the joints between tiles (under clean sky (19/06/2016)), one after closing the joints (with a clean sky and dry wall (20/07/2016)), and two where controlled quantities of water were introduced in the facade to prove the capacity of moisture detection (27/09/2016 and 28/09/2016 respectively).

Both the four surveys consisted in five thermograms taken periodically and perpendicularly to each experimental cell: two thermograms (3.6 m from the panel) in which firstly the top three rows of tiles were captured and then the bottom three; two similar thermograms to the other panel in the same cell; and finally a general thermogram containing both the two panels.

Simultaneously with every thermographic inspection, both the reflected temperature, using the reflective thermographic method, and the humidity and temperature, using a thermo-hygrometer (*HygroLog digital*) were measured.

Humidity inspections

Despite infrared's thermography capacity in detecting moisture problems has already been proven both in tiling systems (Barreira et al. 2008; Edis et al. 2013; Edis et al. 2015b) and other claddings (Pina dos Santos et al; 2003, Matias; 2006, Matias et al; 2007, 2008; Magalhães et al. 2008), as well as the fact that humidity is not an anomaly specifically related with tiling systems, as it can happen in almost all kinds of constructive solutions, it is considered that it is important to study the humidity detection in this kind of cladding.

The two main reasons that lead to believe that humidity detection in tiling systems is considerably different from its detectability in other coating systems is that, in first place the different characteristics between this system's component, that have already been presented as a challenge to an infrared inspection.

In second place, the very low water absorption of some tiles (especially the porcelain tiles in study) which makes it almost impossible to the water to reach the surface from the inside. Hence, unlike in other kinds of outdoor coating systems such as renders or porous stones, water will only be present either beneath the tile, over the tile (visible to the human eye and consequently of no interest to study using thermography) or in the joint, but not within the tile.

However, as water evaporation is an endothermic reaction inducing local surface cooling (Barreira et al. 2008; Matias et al; 2007, 2008; Magalhães et al. 2008), it is considered that a cooler zone will be noticed when water is introduced in the panels.

In order to test humidity detectability water was introduced using a 10 ml syringe beneath each of the two top detached tiles of each panel (fig. 48): on the left, tiles that were applied with a spongious cloth (CT); on the right, tiles with a void (DT). The elasticity of the waterproof polyurethane sealant (*Weber.flex PU*) used to seal the panel's edges allowed the use of syringes to introduce water without damaging the system.

Figure 48 - Injection of water beneath a tile

The humidity testing was made in two phases. The first phase consisted in introducing a small amount of water beneath the tile (40 ml) corresponding to 50% of the cloth's water absorption

capacity (previously tested in laboratory). The second phase consisted of the introduction of a maximum amount of water beneath each panel (total of 120 ml).

In order to ensure that the panels were watertight and that the testing would be done injecting water on dry panels, thermograms were taken after a rainy day. As there was no thermal differential indicating rain infiltrations on these thermograms the panels were considered watertight. Besides these thermograms, thermal inspections using thermography were also done right before the water injection aiming to, together with the thermograms taken in the detachments' detection survey, serving as comparison.

Both the two phases had the water introduced in the morning and thermograms taken during the rest of the day. It is also important to refer that the two surveys were done in sunny days and the water used was left in a bucket outside to, as close as possible, equal the water temperature with the tiles' temperatures.

4.5 *In situ* inspections

One of the principal parts of this study was the inspections on real buildings, not despising the previous work, where important characteristics of this diagnostic method were analysed. It is by confirming the capacity of anomalies' detection in real cases that this inspection method can be properly recognised.

To this purpose, some buildings' facades were analysed:

- Firstly some tile cladded facades from *Edifício Manuel Rocha*, in LNEC's campus, comprising coloured glazed tiles (fig. 49a).
- Secondly both the Western and Eastern facing facades from a residential building in *Parque das Nações, Lisboa*, cladded with ochre klinker tiles (fig. 49b).

Figure 49 – Eastern facing facades from *Edifício Manuel Rocha* (a) and from a residential building in *Parque das Nações* (b)

The thermographic data was analysed qualitatively and then verified for each building using other methods according to each building's particularities.

Edifício Manuel Rocha's East facing tiled facade was chosen not only because of its location (and proximity to the laboratory) or the coloured glazed tiles that challenged the infrared survey, but also because their ground level tiled walls were already known to have some anomalies (cracking of tiles, cracking/detachment of the glaze, non-visible lack of adhesion, inexistence of some tiles (already detached due to lack of adhesion) and replaced tiles). As the tiled facades were easily accessible, the accessory method chosen was the *tapping control,* as known as percussion method,

which consists in tapping the tiles in search of hollow sounds correspondent to anomalous (detached) zones.

The second case was inspected because of already known problems of detachments. In this case, a perimeter was set around the Western facade to prevent people from passing close to it, as the tiles were actually in risk of falling and, therefore, compromising the security (fig. 50). This inspection aimed to determine more specifically the detached zones in order to decide the future of the cladding, i.e. if the cladding should be totally replaced or only partially, in the identified zones. Despite the building being only cladded with ceramic tiles between the first and fourth floors, there were some bulked tiles visible especially when the sun was sideward to the facade, projecting their shadows. The infrared data was therefore compared with photos in a first phase. In order to prove the thermographic method more accurately it is intended to make a tapping control inspection using an auto-crane to access the tiled floors.

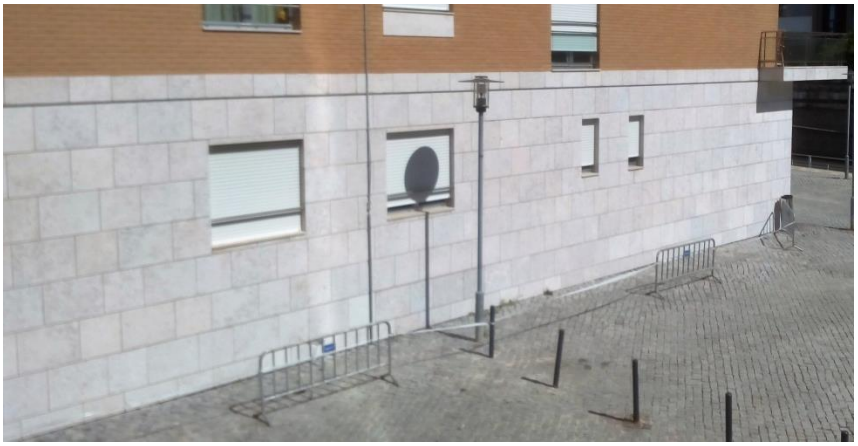

Figure 50 – Perimeter set to prevent passers from being hit with detached tiles

5 Results and analysis

5.1 Introduction

After conducting all the experiments mentioned in the previous chapter, a numerical analysis was done. Despite the fact that thermograms in general qualitatively speaking for themselves, this numerical analysis serves the purpose of proving scientifically thermography's capacity in detecting detachments on ceramic claddings, as well as assessing its accuracy and the results reproducibility.

5.2 Emittance

As mentioned in the previous chapter, this parameter was only measured once for each kind of tile (polished/non-polished, black/white). Surprisingly, in the cases of the non-polished specimens, there was no need of making iterations to find the tiles' emittance as with the emissivity set for 0.88 (the black tape's emissivity), after heating, the temperatures obtained were the same in the black tape as in the area of tile that surrounds it. Figure 51 shows the thermograms where it is possible to see the temperatures obtained in three of the specimens.

Figure 51 - Emittance testing using the black tape method for the specimens *Wnat* (a), *Bnat* (b) and *Wpol* (c)

Despite the value obtained being very convenient, it makes sense, as it is a value close to the defined to the generality of these materials. As it is possible to see, in the two first thermograms above (fig. 51a and 51b), the temperature of the black tape positioned in the middle is equal to the temperature of the surrounding area (correspondent to the detachment area), making it hard to distinguish between the two materials.

However, in the case of the polished specimen, *Wpol*, the black tape's temperature is slightly different from the tile's temperature. Thus using the iterative method mentioned, its emittance value was determined as 0.76. This lower value makes sense as it is obvious that this specimen reflects more radiation than the previous ones. Furthermore, it is also expected when looking at some emittance tables that classify ceramic materials in polished and non-polished, setting lower emittance values for the polished ones.

5.3 Laboratory survey

There are several aspects that must be taken into account when analysing the data obtained:

- As each specimen testing requires much time, in order to properly study its cooldown, it was only tested one specimen per day.
- With the summer coming, temperatures inside the laboratory raised slightly (different testing conditions) which might have provoked small deviations on the results.
- Despite the procedure being the same for every specimen's production, the space created between the tile and the support may vary slightly, possibly inducing to some small errors when comparing results between specimens.

Data was analysed, providing two kinds of results, function of the measuring equipment in use (presented on appendix B):

- Two thermocouples measured the temperatures in both the middle of the detached tile and on the middle of the bottom adherent tile. This equipment was not only useful in laboratory for comparing temperatures between the two measuring methods but also to provide the temperature variations in the heating phase, where thermography was not applicable given the chosen contact method.
- Thermography assessed the thermal variations for the specimen's entire surface but only during its cooldown phase.

Therefore, for each of the eight specimens, four curves of temperature were obtained in function of cooldown time. These curves were abbreviated as follows:

- TDet – Temperature of the non-adherent obtained with thermography;
- TAd - Temperature of the adherent zone obtained with thermography;
- TcDet - Temperature of the non-adherent zone obtained using a thermocouple;
- TcAd - Temperature of the adherent zone obtained using a thermocouple.

Before presenting the results from the anomalous specimens' behaviour, it is important to show how a specimen without any anomaly (fig. 52) behaves under the same conditions (time and temperature of heating and respective cooldown).

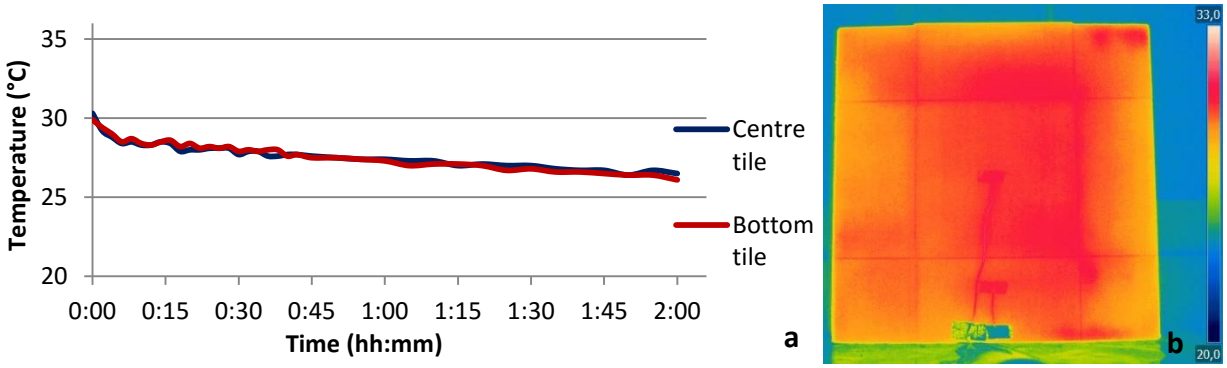

Figure 52 - *Blad* cooldown in laboratory conditions (a) and respective first thermogram (b).

On the graphic above (figure 52), despite all the tiles being adherent, the temperatures were measured in a similar way as in the anomalous specimens (similar positioning of measuring points). Thus, the two temperatures displayed correspond to the temperatures measured in the centre of the specimen (which would correspond to a detached area in an anomalous specimen), and to the temperatures on the centre of the bottom tile.

As it was expected, the temperatures are the same in both the two zones. Another aspect that is possible to verify when comparing this specimen with the other specimens is that the temperatures are much more stable during the two hours of testing.

After observing the "normal" specimen's behaviour it is time to verify the possibility of detecting the detachments on the anomalous specimens.

Right after the first attempt of using thermography on these heated specimens it came clear that the anomalous zones could be detected very easily as it can be seen on the thermogram and respective horizontal middle height thermal profile of figure 53, where higher temperatures correspond to the detached zone. However, it is also important to verify the differences that this diagnosis method presents when applied to different kinds of tiles.

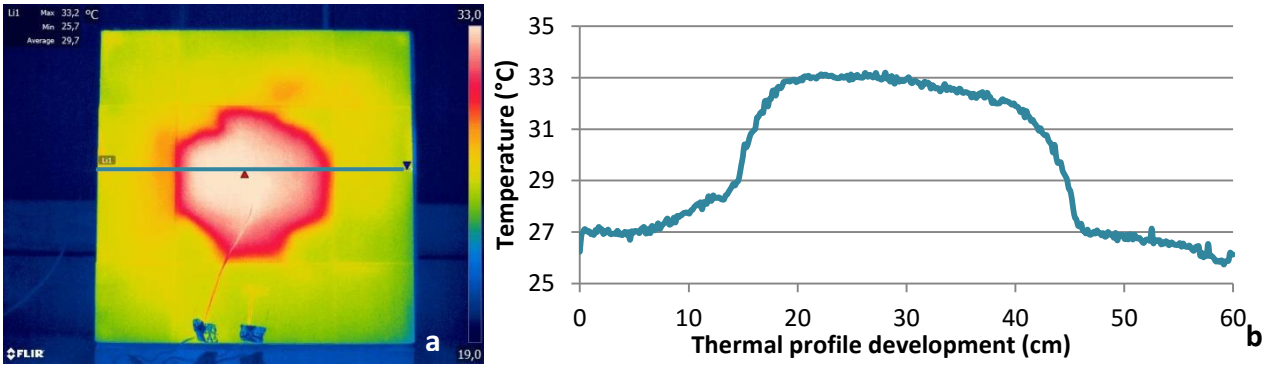

Figure 53 – First thermogram after *Wnat*'s heating with representation of the horizontal thermal profile (a) represented graphically (b).

The two first tiles to analyse were *Wnat* (fig. 54) and *Bnat* (fig. 55), to verify if there was any difference in detecting anomalies between black and white porcelain tiles with a natural (non-polished) finishing.

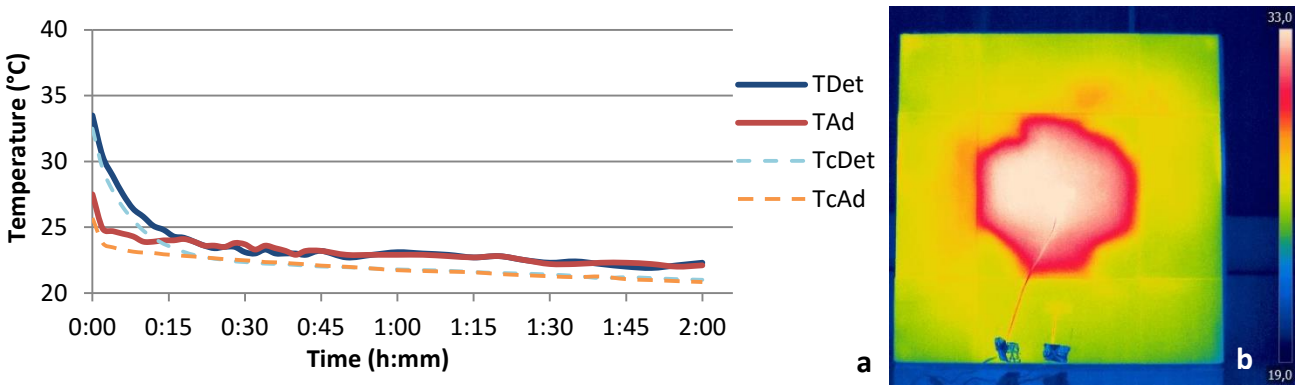

Figure 54 - *Wnat* cooldown in laboratory conditions (a) and respective first thermogram (b).

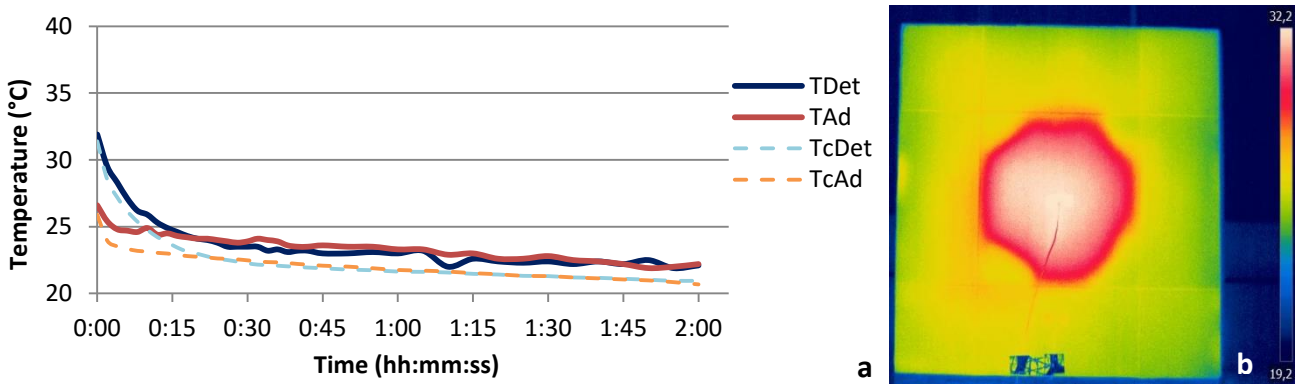

Figure 55 - *Bnat* cooldown in laboratory conditions (a) and respective first thermogram (b).

Before comparing the different behaviours caused by colour differences, it is possible to notice a common behaviour. In the beginning of the cooldown, in the first 20 minutes, temperature drops quickly (faster in the detachment than in the adherent zone). After these 20 minutes the temperature on the detachment drops slightly below the adherent area and, soon after, temperatures stabilize (with similar values). This behaviour proves that the higher thermal diffusivity of the air, or the lower thermal inertia provoked by the air space, makes the detachment's temperature vary faster. This faster variation is the fundamental theoretic principle behind this study, as it will enable detachment´s detection using this thermal method.

Once the temperatures of both areas are equal, the cooldown slows its pace because of the proximity between the ambient temperature and the tiles'.

After comparing the two specimens there were no substantial differences. Despite the temperature obtained after heating being 1°C higher for the white specimen, this is not considered to be a substantial difference, as errors (mentioned in the beginning of this section) may occur. Despite this, the differences between attached and detached zones are very similar for both specimens.

The polished specimen (fig. 56) was destined to test if there is any difference in the tile's behaviour due to the finishing. Indeed there was a difference, but not really in terms of the obtained temperatures as they were similar to the two previous specimens (besides a slightly bigger difference between the adherent and detached area). The difference is more in the inspection time, as the polished surface reflects much more making it difficult to read the actual temperatures.

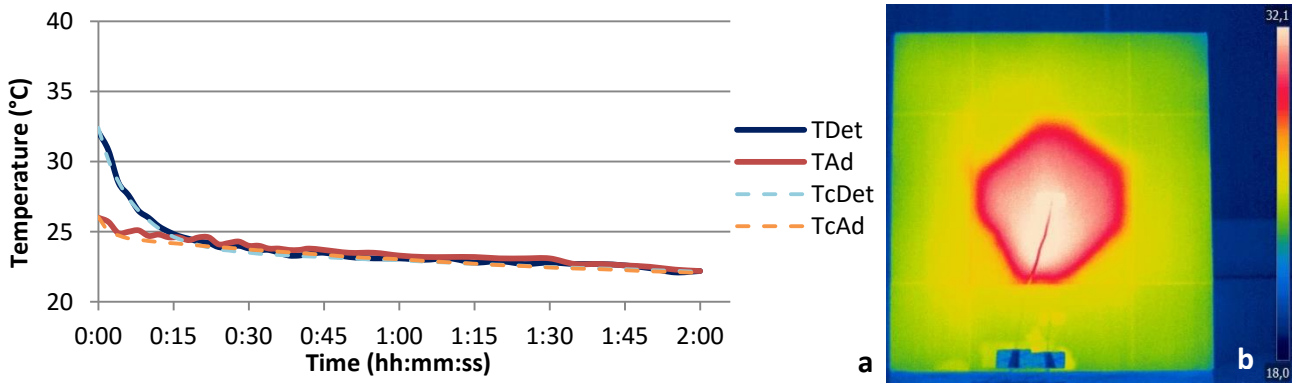

Figure 56 - *Wpol* cooldown in laboratory conditions (a) and respective first thermogram (b).

As it can be seen in figure 57, unless there is no source of reflection (such as a human body, or even the camera's lenses, that mirrors the specimen's temperature creating a reflection cycle that results in a higher thermal reading) the readings are not reliable. Reflection errors are reduced when the specimen is heated; even if there is a source of reflection its temperature is probably similar to the specimen's and, thus, the reflected wavelengths are similar to the ones emitted by the specimen. To minimize this error, the method of inspection consisted of running a timed program in the thermal camera, with no need for an operator to take the thermogram, as well as in the other specimens.

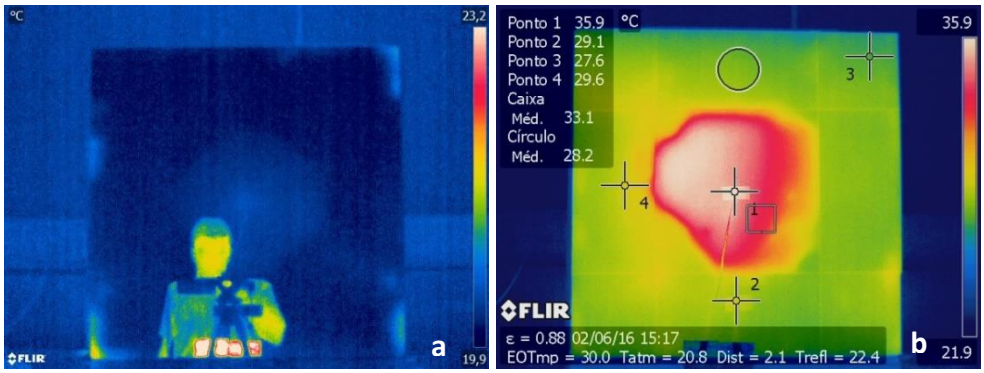

Figure 57 - On the left a thermogram showing the reflections
and on the right a thermogram taken during the actual survey

Besides the surface's finishing, another important characteristic of the cladding whose impact in the readings should be analysed is the tiles' thickness. Therefore, two thinner (light) tiles were analysed (fig. 58 and 59).

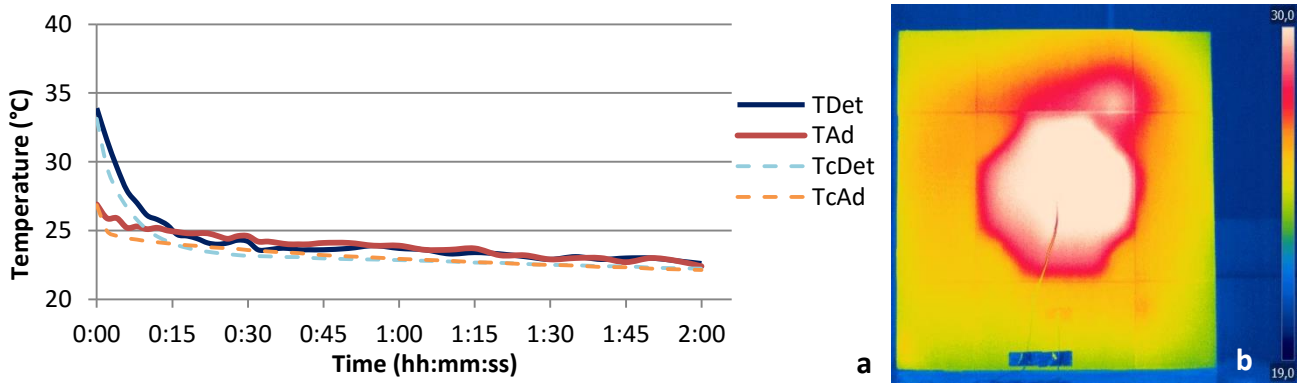

Figure 58 - *WI* cooldown in laboratory conditions (a) and respective first thermogram (b).

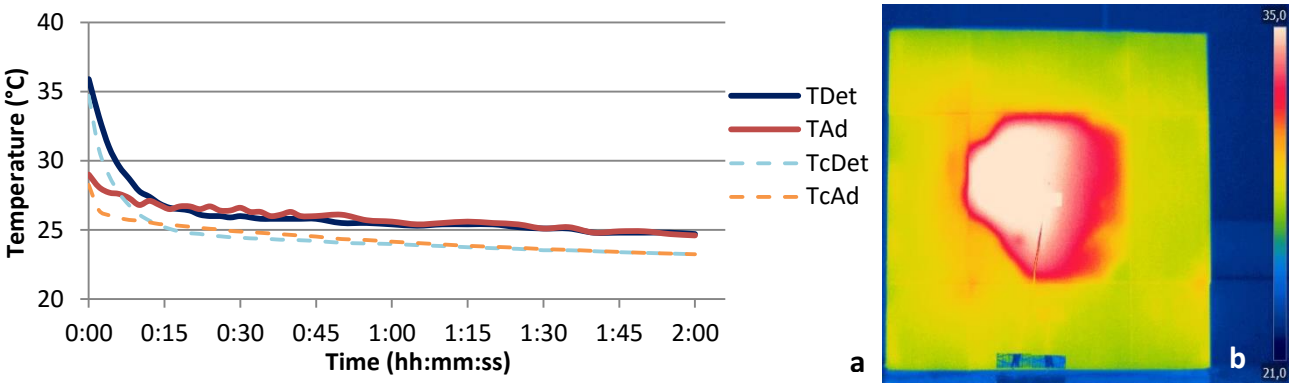

Figure 59 - *BI* cooldown in laboratory conditions (a) and respective first thermogram (b).

The two thinner tiles analysed vary between themselves only in terms of colour. As expected, as well as results obtained for *Wnat* and *Bnat* show, the colour is not a characteristic of great impact in the readings. Confirming the fact that colour is not very important when the readings are made in interior conditions, as the material's colour is not a selective parameter for infrared radiation.

Comparing the results obtained between the thicker and the *light* tiles, the most expectable difference would be in the temperature decreasing rate, i.e. temperatures would be expected to drop quickly in the thinner tiles, and therefore, the temperatures of the detached zones would equal the temperatures on the adherent zones more quickly.

In fact, the drop in the temperatures was faster in the thinner tiles, but only 2/4 minutes faster. The reduced difference may be taken as prove of what would be expected, given the also reduced difference of thickness between tiles (around 3 mm), despite being an almost negligible difference.

One factor that has always been taken as a characteristic that can seriously have an impact on the cladding's behaviour is the support over which it is applied. Thus, the differences between cementitious supports (already analysed) and thermal insulation supports that are used in ETICS solutions were studied (fig. 60 and 61).

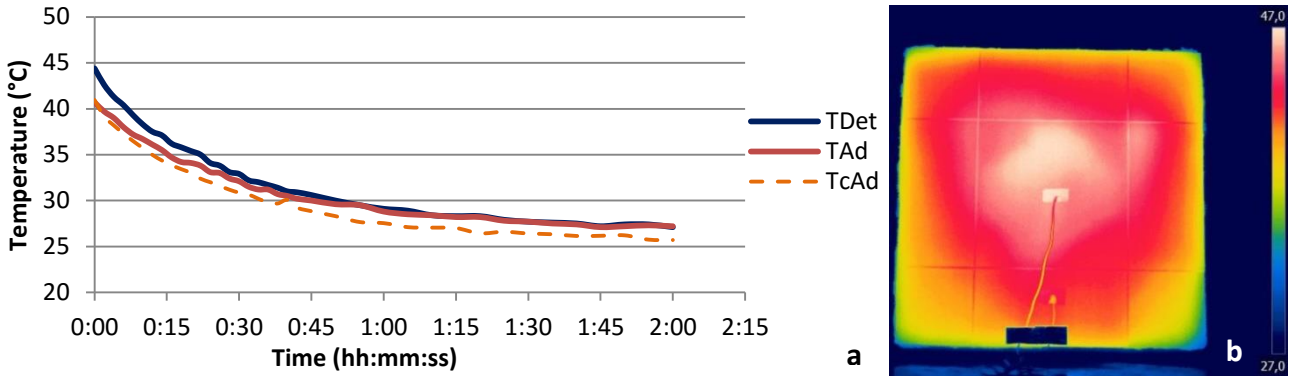

Figure 60 - *Wti* cooldown in laboratory conditions (a) and respective first thermogram (b).

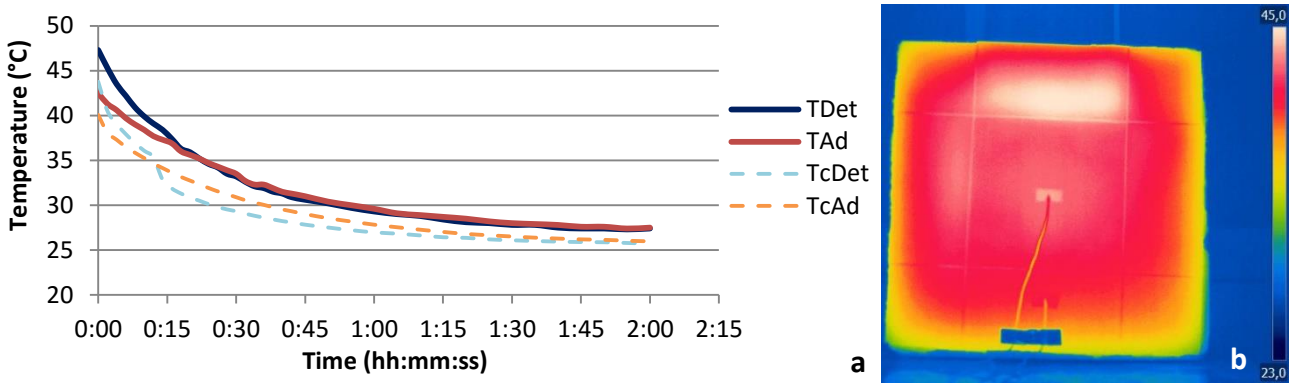

Figure 61 - *Bti* cooldown in laboratory conditions (a) and respective first thermogram (b).

Once again, comparing the results between the two colours, there are no great differences as the specimens are being tested in laboratory.

When comparing these two specimens with the previous five with detached tiles it is possible to observe two noteworthy differences. Firstly, the temperature the specimens reach after heating, which is approximately 10°C higher in the ETICS-like specimens, an expected result, as the thermal insulation acts like a barrier "trapping" the heat and rising the tiles' temperature.

The second remarkable difference is that the difference between the detached and adherent zones is lower. This happens probably because, as the thermal resistance of the support is much higher, the thermal diffusivity of the thin layer of air is not high enough to make such a considerable difference of temperatures as seen in the cementitious rendered based specimens.

When analysing the maximum temperature obtained for each specimen's detached and adherent areas it is possible to observe on figure 62 that these differences rely overall on the type of support.

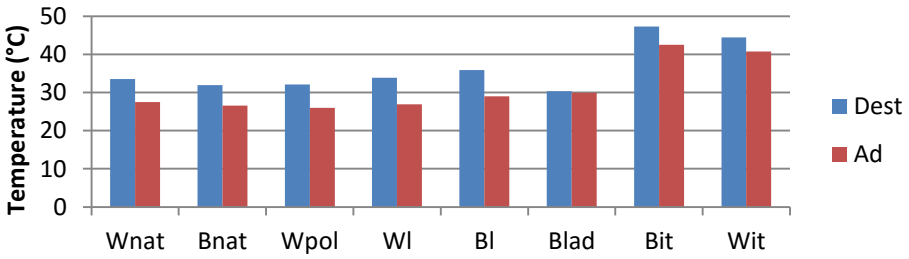

Figure 62 - Maximum temperatures obtained after 20 min of heating for all the specimen's detached and adherent zones

The detectability of the anomalies is mainly ensured by the thermal difference between detached and adherent tiles. Comparing the maximum thermal differential between detached and adherent

areas (fig. 63), the higher differential is obtained for the specimens with cementitious render, as mentioned above.

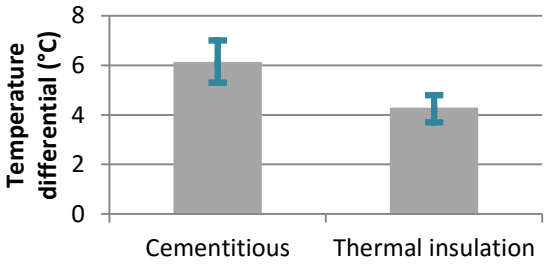

Figure 63 - Thermal differential between adherent and detached zones according to the specimen's support

Another important data to analyse is the amount of time it took until the temperatures of the detached and adherent areas became the same (fig. 64).

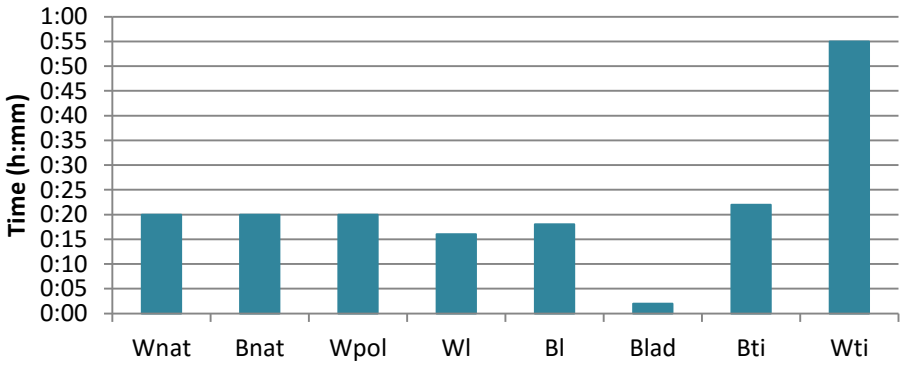

Figure 64 – Elapsed time until the temperatures of the detached d and adherent areas became the same

As already mentioned, the elapsed time was slightly (almost negligible) lower for the thinner specimens. Surprisingly the temperatures took much more time to equal on the specimen *Wti*. Despite having no explanation for this, it is possible to say that the thermal differential around the 20 min off cooldown had a value of 1°C, a difference that can be argued in terms of the anomalies' detectability.

5.4 *In situ* testing under controlled conditions

As mentioned before, four major experimental campaigns were made sequentially in outdoor conditions:

- one with the joints still opened and a clear sky (Appendix C.1.);
- one with the panels finished (treated joints) and clear sky (Appendix C.2.);
- two after water injection beneath the two top detached tiles from each panel (Appendix C.3. and C.4.).

As seen in the previous experiments there were no major differences resulting from the tiles' colour. Therefore, to explain the differences expected to obtain in exterior conditions it was needed to define either each tiles' absorbance or its "opposite", their reflectance.

5.4.1 Reflectance

In order to define the tiles' reflectance, after the pyranometers' calibration (using a previously calibrated pyranometer) and the first test done (to determine the best period to make the readings), the previously mentioned setup was placed during 30 min in front of the panels *C1_B*

and *C1_W* (cell 1 with ETICS – black and white panel). The readings were very steady, giving reflectance coefficients of 0.23 and 0.55 for the black and white tiles, respectively.

The results obtained were no surprise. Besides proving the effectiveness of the reading method, from these results it is proven that black tiles reflect much less than white tiles. Thus, even though having the same emittance, the black tiles will absorb more thermal radiation and also release more of this radiation. The results predict a higher maximum temperature to be achieved by the black panels. As a higher thermal variation will be even higher in the case of the detachments (as concluded on the laboratory survey), the difference between anomalous and "normal" tiles is also expected to achieve higher values on black panels.

5.4.2 First survey: opened joints and clear sky

Infrared thermography is a graphic method of inspection. Thus, an experimental campaign using this method results in images / coloured graphics that by themselves can allow the anomaly's detection. However, despite most of the times the graphics' analyses being quite simple, it is important in this phase of the methods' study to prove its capacity with concrete data.

On figures 65 and 66 and there are two sequences of thermograms where the thermal variations during the same day are presented for each experimental cell in study. The thermal differences are easily detectable, as higher temperatures are represented on white and lower temperatures on blue, according to the scale on the right side of each thermogram.

Therefore, on figure 65 there are three general thermograms of the experimental cell 1 (with ETICS), each with the black panel (C1_B) on the left and the white panel (C1_W) on the right. Similarly, figure 66 contains three thermograms of cell 2 with a black panel (C2_B) on the left and a white panel on the right (C2_W). In the thermograms, black panels appear in reddish colours due to the higher emitted temperature when compared with the white panels (represented in bluish colours). It is of note that thermograms from figures 65 and 66 are not exactly on the same colour scale.

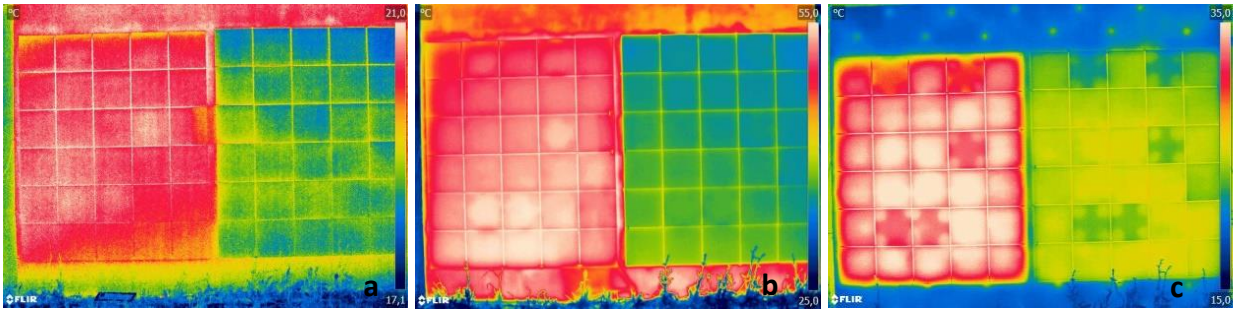

Figure 65 - Thermograms taken from cell 1 at 09h10 (a), 15h30 (b) and 20h30 (c)

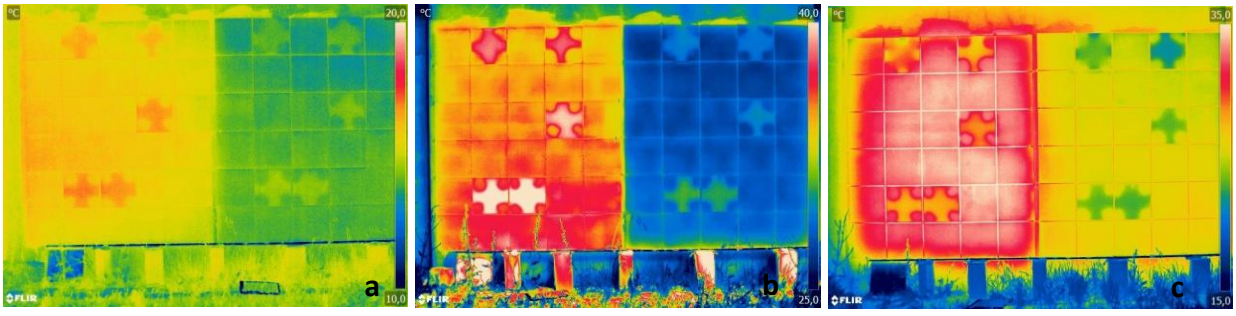

Figure 66 - Thermograms taken from cell 2 at 09h10 (a), 15h30 (b) and 20h30 (c)

Looking at the thermograms it is possible to take conclusions such as:

- Comparing the thermograms with the schematic representation of the anomalies (fig. 42) it is observable that, in general, detached tiles are easily detected on the thermograms.
- Anomalies are easy to detect on the beginning of solar radiation's incidence (15h30) and in the beginning of the cooldown (20h30) on both experimental cells.
- Temperatures are higher on darker panels.
- Temperatures obtained for cell 1 (ETICS) are superior to the ones registered on cell 2.
- Anomalies detection is easier on cell 2, without thermal insulation.
- In the heating phase (two first thermograms) the detached tiles are hotter than the adherent ones; contrariwise, on the cooldown phase, detachment are presented as colder spots.

As can be seen, the detachments' identification, in general, is quite simple; yet, to analytically prove the differences, an analysis has been done using the software *FLIR Tools.*

To this analysis, the two thermograms taken from a position closer to the panels were used. This option is justified not only due to a better resolution but also because when a thermography contains two panels with different colours (as the ones presented above) the scale has to be enlarged to be adequate to both panels' temperatures simultaneously, which in time will difficult the reading of smaller thermal differences.

After obtaining the average temperature for each tile (in a uniform central area) an average temperature was calculated to the detached tiles and to the adherent tiles. These two average temperatures were then analysed for each panel.

The temperatures' variation with time for the four panels is presented in figures 67 and 68.

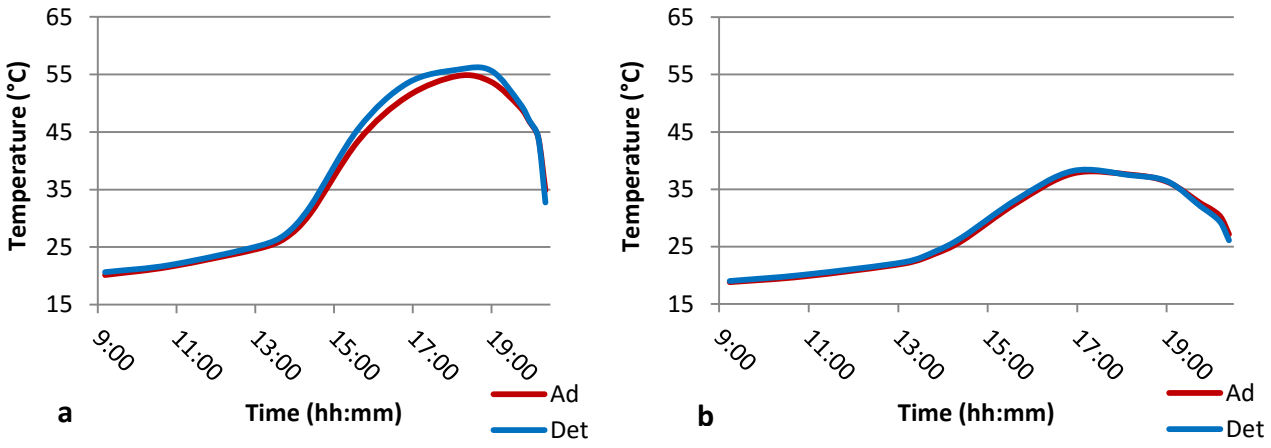

Figure 67 - Evolution of adherent (Ad) and detached (Det) tiles' average temperatures in **cell 1** black panel (a) and white panel (b)

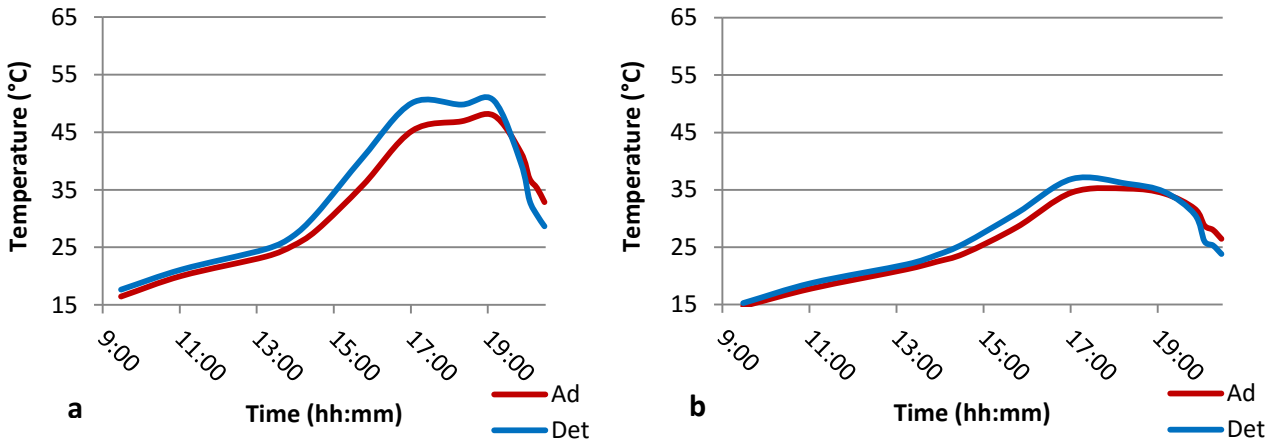

Figure 68 - Evolution of adherent (Ad) and detached (Det) tiles' average temperatures in **cell 2** black panel (a) and white panel (b)

By observing these figures (fig. 67 and 68) it is notable that the curves are similar for all the specimens. During the morning temperatures rise because of the incidence of diffuse radiation and the increasing ambient temperature; proximately at 14h00, the curves' slope rises as thermal radiation from the sun starts reaching the wall. Temperatures reach their maximum value between 17h00 and 18h00 and then start decreasing on the account of the decrease in the ambient temperature and also a decrease in the incident radiation. In fact when sun sets, despite the irradiated energy remaining the same, as the sun is more perpendicular to the wall, the distance that radiation has to overcome through atmosphere is much higher and so, as atmosphere also absorbs a part of radiation, its intensity will be much lower at the end of the afternoon.

When the differences between adherent tiles of different colours are analysed, as expected and seen in the thermograms, black panels reach higher temperatures than white panels (about 17°C above on cell 1 – with thermal insulation - and 13°C above on cell 2).

Regarding the differences between the two cells (fig. 69), i.e. with different supports, the ETICS solution reaches the higher temperatures. In the case of black panels, ETICS based panels' temperatures are 7°C higher, while in the case of white panels the difference is only 3°C for the two supports.

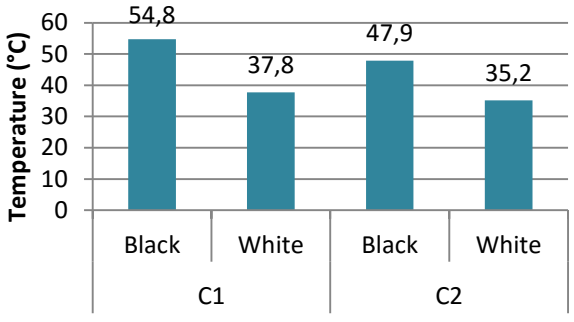

Figure 69 - Maximum average temperatures obtained in all panels' adherent tiles

After analysing the temperatures evolution in the adherent claddings, the difference between adherent and detached tiles was studied. On figure 70 the thermal differential between detached and adherent tiles is represented in function of time for all the four panels.

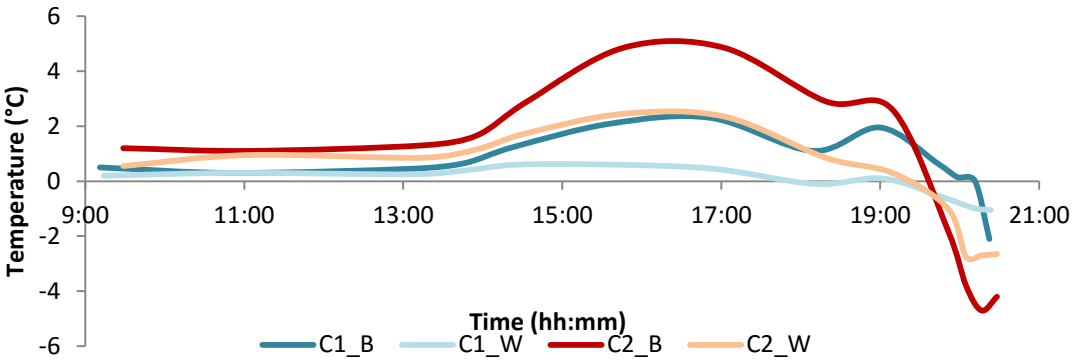

Figure 70 - Thermal differentials between detached and adherent tiles

It can be observed that the differential depends not only on the adopted cladding solution but, above all, on the period of the day where the inspection is made. Despite temperatures achieving maximum values between 17h00 and 18h00, the maximum differential occurs around 15h30, after 1h30 of direct solar incidence. Another observation was that when the sun starts setting, as the air gap (behind detached tiles) temperature varies quicker, there is an inversion of thermal differential and the detachment's temperature drops below the temperature of the adherent tiles.

The maximum (correspondent to the heating phase) and minimum (correspondent to the cooldown phase) temperatures are represented in figure 71.

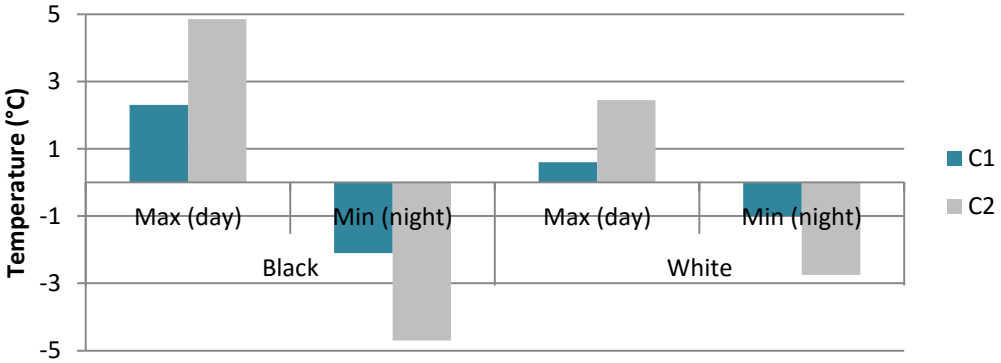

Figure 71 - Maximum and minimum thermal differentials between adherent and detached tiles

This graphic (fig. 71) shows that cell 2 presents bigger thermal differentials between adherent and detached zones, which leads to the conclusion that an ETICS solution difficults the detachments' detection.

A higher thermal differential is also observable in the black panels. The reason for this is that a higher absorption of radiation leads to a higher and faster thermal variation, a behaviour that is fostered by detachments.

In sum, after the survey it is possible to state that:

- Infrared thermography is a capable diagnostic method regarding detachments´ detection on ceramic claddings with open joints.
- The verification of thermography as a capable tool leads to the assumption that detachments are also detectable on finished walls and facades whose joints are degraded.
- The anomalies detection is easier when:
  - Facades are not exteriorly thermally insulated;
  - Facades are darker.

- For a better quality, thermographic inspections shall be made during a sunny and windless day, at the beginning of the solar direct incidence (between 30min and 1h after incidence) or in the beginning of the cooldown (approximately 1h after the facade's shadowing).

5.4.3 Second survey: closed joints

After closing the joints of the cladded panels, the main measuring campaign has been done on a day with clear sky. The survey was similar in every aspect of the testing performed with opened joints. Despite the differences on the panels (closed joints), the results were consistent with the ones obtained with open joints.

Likewise in the previous section, the following figures show a sequence of three thermograms taken to experimental cell 1 (fig. 72) and cell 2 (fig. 73).

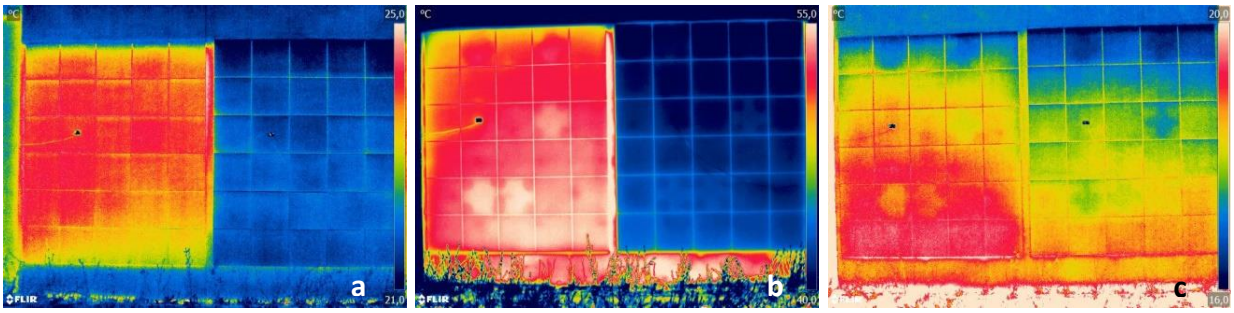

Figure 72 - C1 at 9h30 (a), 15h30 (b) and 22h15 (c)

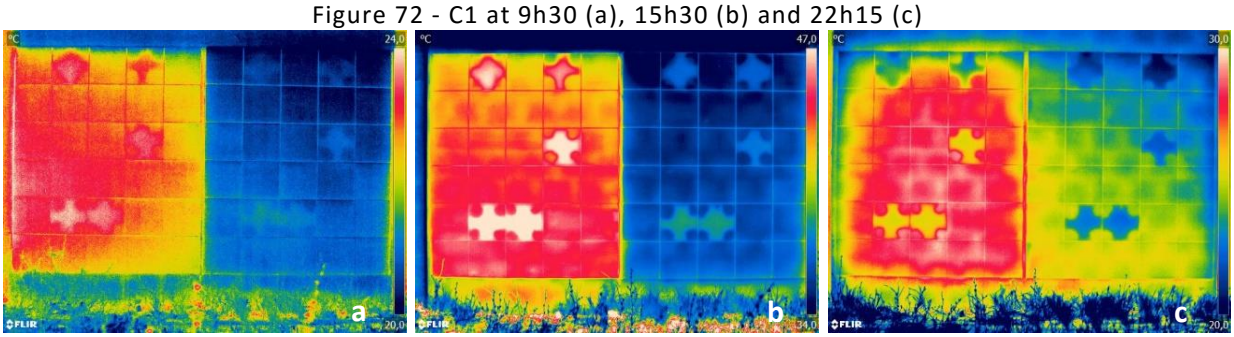

Figure 73 - C2 at 9h30 (a), 15h30 (b) and 22h15 (c)

As it is possible to see detachments are much clearer on cell 2 than on cell 1, which is consistent with the results obtained with open joints. However, the differences between detached and adherent tiles appear to be lower this time, i.e. with the joints closed it appears to be more difficult to identify some detachments.

Converting the thermograms into numbers, using the same procedures as before, figures 74 and 75 were obtained.

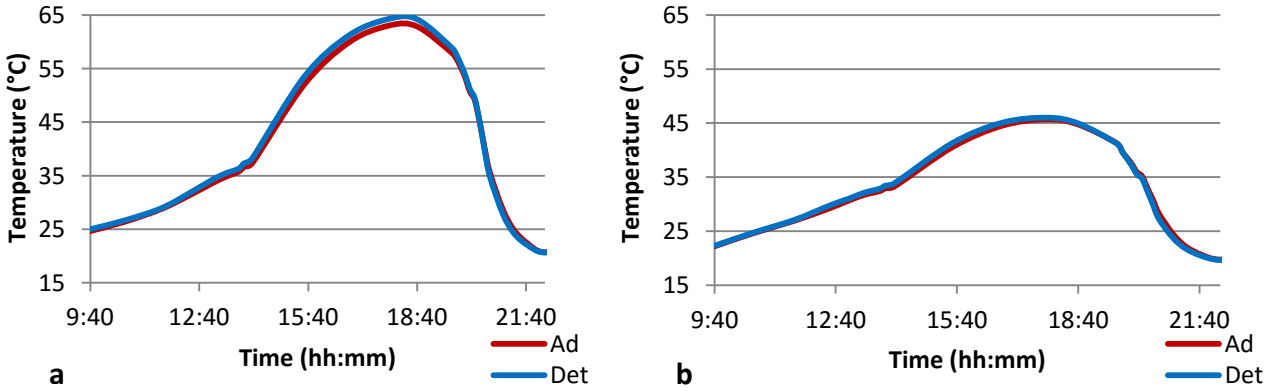

Figure 74 - Evolution of adherent (Ad) and detached (Det) tiles' average temperatures in **cell 1** black panel (a) and white panel (b)

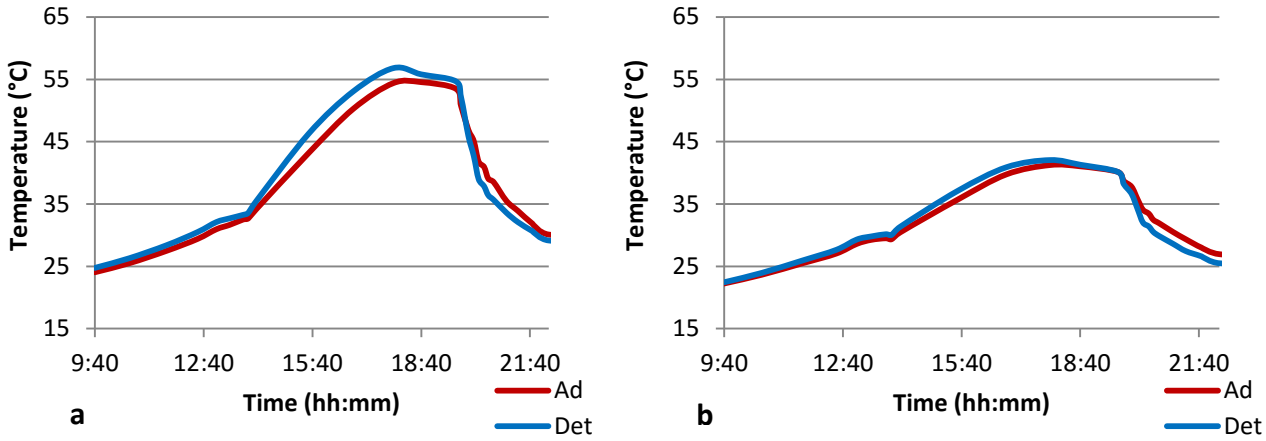

Figure 75 - Evolution of adherent (Ad) and detached (Det) tiles' average temperatures in **cell 2** black panel (a) and white panel (b)

After analysing both the thermal evolution graphics and the thermograms it is possible to take some similar conclusions regarding the behaviour of the tiles. As well as it was mentioned concerning the thermograms, it clearly stands out that differences between attached and detached tiles are lower when joints are closed.

When looking only to this campaign's results it is possible to observe the following aspects:

- The temperature of the panels starts rising at a faster pace after around 14h00, when the solar radiation starts to directly reach the facades.
- It is also in the beginning of the solar incidence that differences between detached and adherent tiles start to get clearer as detached tiles get warmer.
- Temperatures reach a maximum at around 18h00.
- When temperatures start dropping, especially after 19h45 (when the walls start getting shaded) the detached tiles drop below the adherent tiles' temperature.
- The thermal differential between detached and adherent tiles start to fade at around 21h00 (after around 1h15 without solar incidence).

In the following bars graphic (fig. 76) it is possible to compare detached and adherent tiles' maximum temperatures verified during the survey.

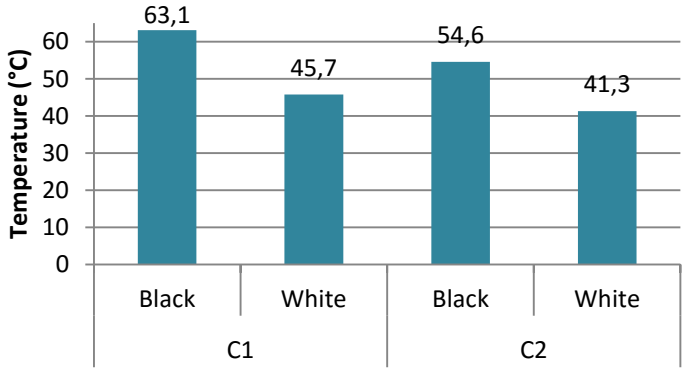

Figure 76 - Maximum average temperatures obtained in all panels' adherent tiles

Comparing adherent tiles' temperatures, the results show that (fig. 76):

- Black panels reach higher temperatures than white panels (17°C higher in C1 and 13°C in C2).
- ETICS based panels reach higher temperatures (9°C higher in black panels and 4°C in white panels).

Figure 77 likewise as presented for the preceding survey (fig. 70), shows the variation of the thermal differential between detached and adherent tiles with time. As well as in the previous survey, the figure evidences the existence of different phases:

- In the morning there is no great difference between anomalous and normal tiles.
- After 14h00 the differential starts rising until it reaches its peak at around 15h30 (after 1h30 of solar incidence).
- The differential drops slowly until 18h30/19h00.
- The differential changes from a positive value (detachments' temperatures higher) to a negative value (detachments' temperatures lower).
- While temperature drops and the sun sets the differential also drops reaching its minimum at around 20h30.
- After reaching the minimum the differential fades.

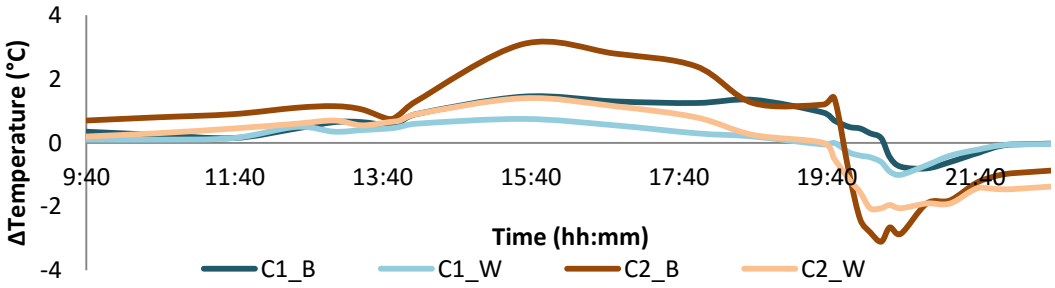

Figure 77 - Thermal differentials between detached and adherent tiles

Figure 78 shows the maximum and minimum differentials manifested during this survey.

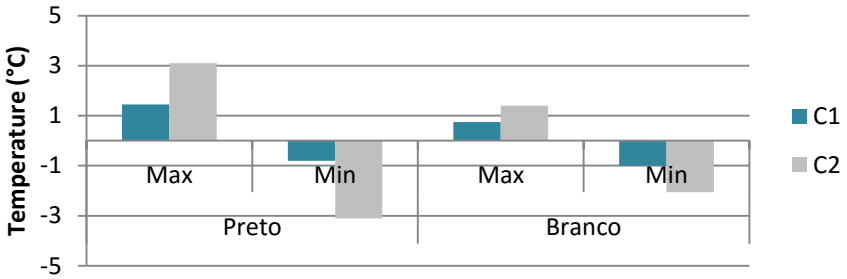

Figure 78 - Maximum and minimum thermal differentials between adherent and detached tiles

From figure 78 and previous surveys it is possible to identify certain particularities about the thermal differential between detached and adherent tiles:

- The thermal differential is always superior in cell 2 (C2) which once again indicates that cementitious render supports favour the detachments location.
- In cell 2 (render) differentials are higher on the black panel (C2_B).
- In cell 1 (with thermal insulation) maximum differentials are higher on the black panel; however, minimum differentials are slightly higher on the white panel.
- In cell 1, the differentials are very low (close to 1°C) which leads to some doubts regarding the detachments detectability on real cases where the inspector does not know if detachments exist and where they are located.
- The best case scenario to identify a detachment is on a black tiles cladding based on a rendered wall after 1h30 of solar incidence.
- When the joints between tile are not closed, thermal differentials are more pronounced, facilitating the detachment's detection.

As an example of these maximum and minimum thermal differentials figure 79 presents two thermograms taken to the bottom half of the black panel from cell 2 (C2_B) during the day (maximum differential) and at night (minimum differential).

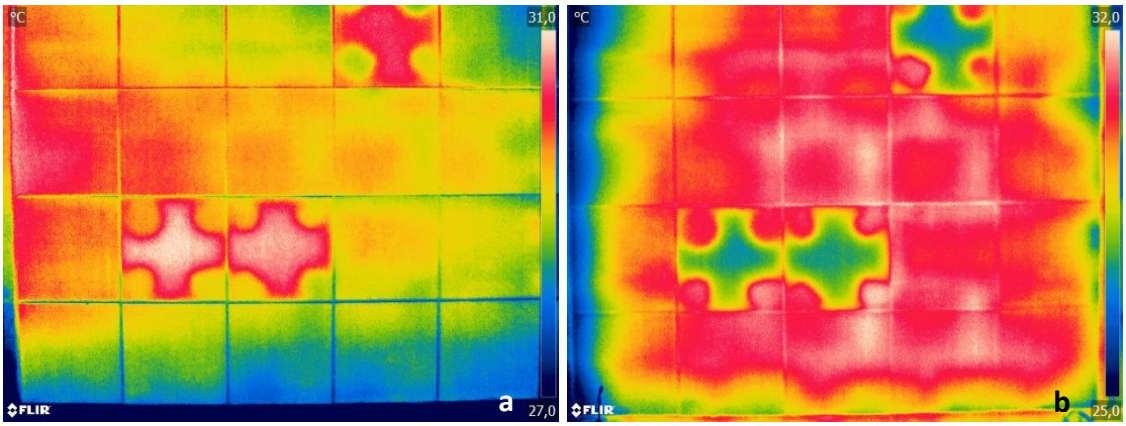

Figure 79 - Thermograms from the bottom half of cell 2's black panel taken at midday (a) and at night (b)

These thermograms, taken closer to the panel, are significant not only for the improvement of definition but overall because as only one colour of tiles is present the temperature scale can be narrowed, facilitating the interpretation of thermal differentials. Hence it is possible to verify that, as shown before in the numerical analysis, the thermal differential is positive during the heating phase (day) and negative after some time of cooldown (night); i.e. in the first thermogram it is possible to see higher temperatures in the detached tiles (reddish/whitish coloured in the thermogram) and in the second the opposite, as detached tiles are colder (bluish).

An interesting feature that is visible, especially in the second thermogram, is that, besides the differences in terms of detachments thermogram, it is possible to notice the contours of the brick masonry behind the tiles. This phenomenon happens because of two main factors: the heat absorption by the masonry that is being released and the heat flow that at the moment of the thermogram was from the inside to the outside of the experimental cell. Thus, as the heat is flowing from the masonry to the exterior, the thermal resistance created by the air gap difficults its passage, provoking lower surface temperatures on the detached tiles.

5.4.4 Thermocouples data

As mentioned in the previous chapter, thermocouples were used not only to reinforce the thermographic results but also to verify the thermal differentials between detached and adhered zones continuously. Temperatures were measured for over a month continuously (figure 80 presents one day of measuring as an example).

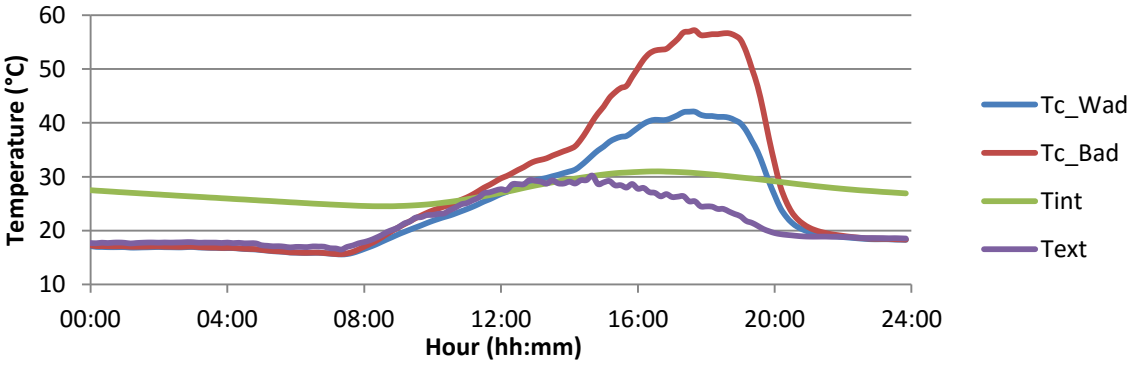

Figure 80 – Temperatures measured with the thermocouples on the 30th of August on the adherent white and black tiles (*Tc_Wad* and *Tc_Bad*), interior of cell 1 (*Tint*) and exterior (*Text*)

Analysing figure 80 it is possible to verify some already expected behaviours. Firstly it is possible to see that the panel's temperatures are higher than both the interior and ambient temperatures (especially in the black panel) in the irradiation period. It is also possible to notice that the interior temperature is almost always higher than the exterior temperature. This happens because the experimental cell suffers very small thermal losses, only having a small window facing south (which in the summer contributes mainly for the heat gains) and being highly thermally insulated. The effect of thermal inertia is also visible as the exterior thermal peaks are verified before the interior's peaks.

Regarding the thermal differences between the detached and adherent tiles, during the same day, as in figure 80, it was possible to observe the following differentials (fig. 81).

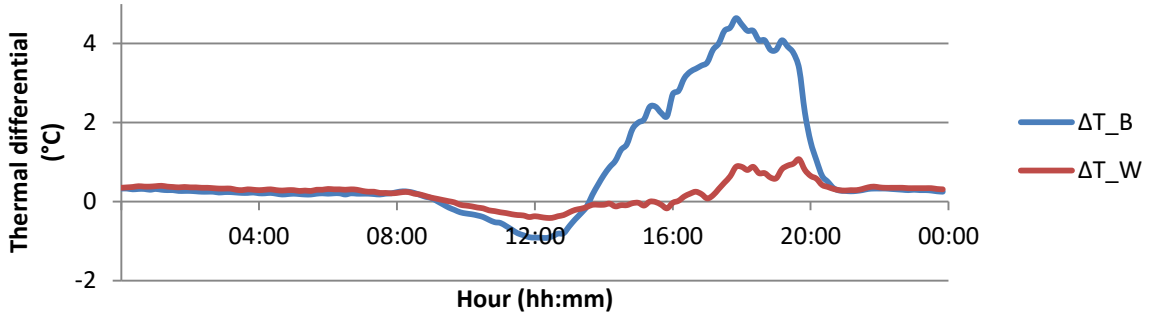

Figure 81 – Thermal differentials between detached and adherent tiles in the 30th of August for the black (ΔT_B) and white (ΔT_W) panels of cell 1

From figure 81 it is possible to verify the following behaviours:

- At night, between 21h30 and 08h00, as expected from the thermographic data analysis, a very small (negligible) thermal differential is visible between detached and attached tiles.
- Contrariwise to what was verified in the thermographic surveys, a negative thermal differential was verified in the morning period. This negative differential indicates that detached tiles are cooler than adherent tiles. This behaviour happens because of the additional thermal resistance created by the air gap beneath the detached tile, which delays the heating of the thermocouple placed beneath it. In other words, as the heat is conducted faster in the case of the adherent tile, its thermocouple is heated faster conducting to higher temperature readings and, therefore, a negative differential. However, this thermal differential is considered too small and so, negligible.
- As expected from the thermographic surveys, thermal differentials are more pronounced on black tiles; however, the thermal differential peak happens later in the thermocouples' readings (between 17h00 and 18h00) probably because of thermal inertia.
- Once more, unlike in the thermographic inspection, where in the cooldown phase detached tiles appeared cooler than adherent tiles for a small period, a negative thermal differential is not visible in the thermocouples' data.

In conclusion, some differences can be noticed between thermocouples and thermographic readings mainly due to the fact that thermography reads superficial temperatures while thermocouples are placed in contact with the panel's support, reading more deep temperatures. In the morning (beginning of the heating phase) the heat is conducted faster to the thermocouple beneath the adherent tile being held on the detached tiles' surface and, therefore, provoking a positive thermal differential with thermography and a negative differential for thermocouples. After this first phase of equilibrium, redden temperatures both using thermocouples and thermography have a similar progress. In the cooldown phase a negative thermal differential is

verifiable in the thermography for a short period; on the contrary, thermocouples do not register this differential due to the higher thermal resistance in the detached tile that holds the heat on the inside, provoking a delay on its temperature drop.

When the whole month's temperatures were analysed together it was verified that, according to figure 82, thermal differentials between detached and adherent tiles do not vary much and, therefore, thermographic results would be reproducible for different days/conditions.

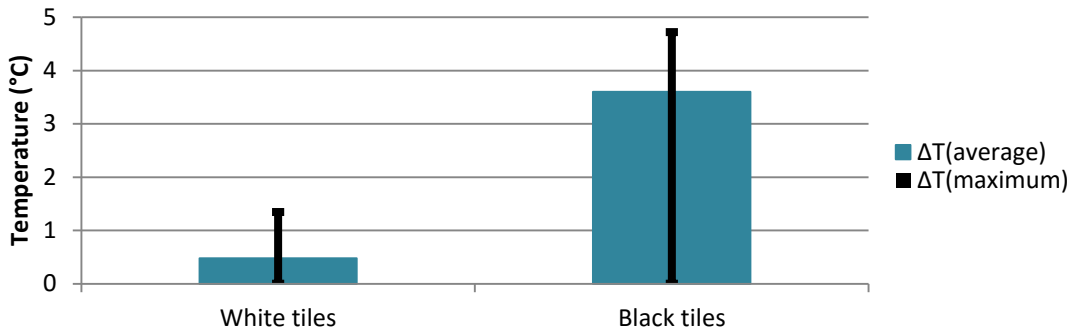

Figure 82 – Average and maximum thermal differentials between detached and adherent tiles measured with thermocouples during 30 days

All considered and despite the mentioned differences, thermocouples confirm that:

- temperatures verified during the day between adherent and detached ties are different;
- the highest thermal differential is verified in darker tiles as they absorb more thermal energy;
- the best period of the day to verify a detachment is after 1h30 of solar incidence.

5.4.5 Humidity inspection

First Survey

As mentioned previously, the first phase of humidity testing consisted in introducing 40 ml of water beneath each top detached tile. Before water being introduced in the panels, thermograms were taken in order to enable a comparison (fig. 83).

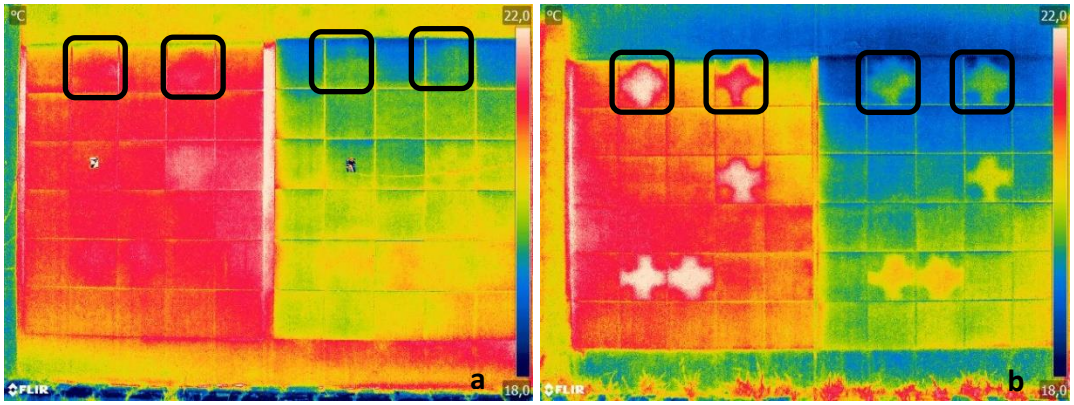

Figure 83 – Thermograms taken before water insertion (beneath the tiles signalized with a black square) on cell 1 (a) and cell 2 (b)

In the thermograms of figure 83 it is possible to verify that besides the differences between adherent and detached tiles, specially in cell 2 (already presented and confirmed once more), there are no significant thermal differences in each panel.

The actual survey started at 10:h00 with the water introduction beneath the tiles. Right after injecting the water on the black panels it was possible to verify a thermal difference (on the tiles

signalized using a black square of figure 84). This thermal difference appeared as a colder (bluish) zone on the top part of the tile with the cloth, CT (on the left) and on the bottom of the simply detached tile, DT (on the right).

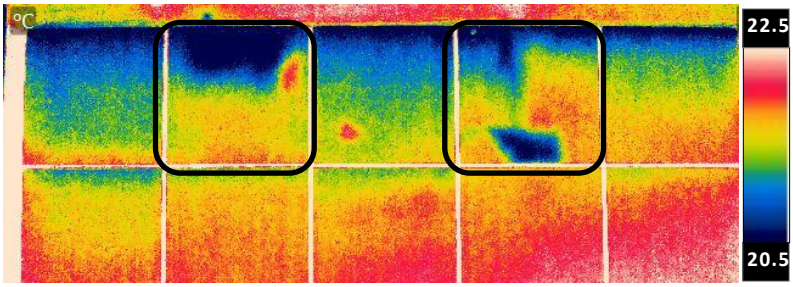

Figure 84 - Thermogram taken right after the water injection (signalized tiles) on panel *C1_B*

The water stayed on the top part of the left tile because of the cloth, which absorbed the water preventing it from reaching the bottom; unlikewise, on the ‘‘simply detached’’ tile, it is possible to see the water runoff from the top (place of injection) to the bottom where it stayed deposited. Despite this behaviour being the expected, in the black panels, after about two minutes from the water injection, it escaped through very thin cracks on the joints (fig. 85). This phenomenon only happened on black tiles with no cloth beneath, firstly because, as mentioned, the cloth spread the water more evenly through the tile’s area, preventing it from reaching the joints in such quantity, but also because as black panels reach higher temperatures, the tension it causes on the cladding materials (more specifically on the joints) is higher making them more susceptible to cracking.

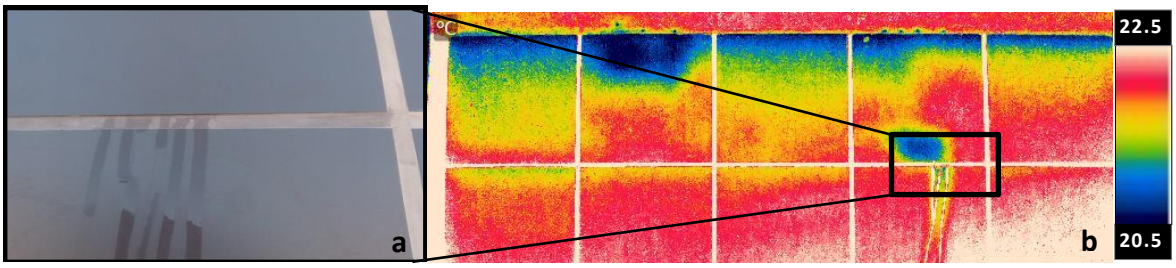

Figure 85 – Water escaping through the joint of the simply detached tile of panel *C1_B*
(Close-up photo (a) and thermogram (b))

Despite being important to know how the water is spread on this specific cladding solution, the main goal of this survey was to analyze if it is possible to identify (not visible) humidity within the cladding using infrared thermography. As mentioned it is possible to verify thermal differences when water is injected; however, this phenomenon only happens because the claddings temperature is different to the water. Thus, when the water is injected at a lower temperature (despite the water had been placed outside for days in order to equalize as much as possible its temperature with the claddings, there is always small differences especially when the more absorbent black tiles are concerned) it will absorb the tiles thermal energy, lowering it and allowing its detection using thermography.

When white tiles are concerned the behaviour is different; when water is injected, the temperature remains unchanged. This happens because the water’s temperature is closer to these panels temperature.

With these first thermograms it was possible to confirm that, as expected, when water is at a different temperature it is possible to detect it using thermography. Thus, this inspection method is once more confirmed to be a valuable tool to detect for example infiltrations of water at a different temperature from the wall, such as leaks on plumbing systems. But what if the humidity has a more stationary character, reaching temperatures similar to the wall’s? In this case, theoretically it would

only be possible to detect humidity if the thermal variation of the humid zone is different from the dry zone, i.e. if when the inspected element is in a process of heating or cooldown and the behaviour of the humid part is different from the rest, verifying different temperatures.

After approximately one hour from the water's injection the thermograms were repeated (fig. 86 and 87).

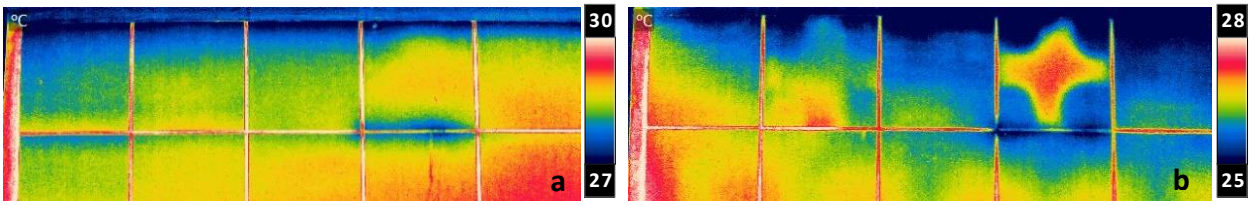

Figure 86 – Thermograms taken to the **black panels** (C1_B (a) and C2_B (b)) after 01h20 from the water injection

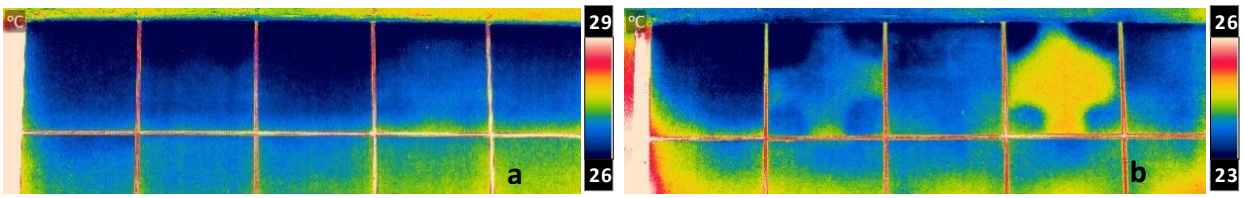

Figure 87 - Thermograms taken to the **white panels** (C1_W (a) and C2_W (b)) after 01h20 from the water injection

Despite these thermograms have been taken before the panels being directly irradiated by the sun, enhancing the anomalous zones, it is possible to take some conclusions from their analysis:

- Once again it is confirmed that anomalies are more visible in the rendered support (cell 2).
- As water takes more time than air to vary its temperature, a detachment where the empty space is filled with water instead of air takes more time to vary its temperature; so, its behaviour became similar to the adhesive tiles'. Thus, the presence of water beneath the tile with cloth disguises the detachments making them very difficult to detect.
- Regarding the tiles with no cloth beneath there are two different behaviours:
    - White tiles do not present any thermal difference indicative of humidity, with results very similar to the ones obtained in the dry surveys.
    - In the case of black tiles it is possible to verify a cooler zone on the joints and surroundings indicating the presence of water.

While detachments can be classified using a simple numerical method, the same is complicated to do in the case of water, because of its variations in terms of quantity and positioning beneath the cladding. Therefore, in order to characterize the behaviour of the panels when water is injected a more qualitative approach was used, where the two tiles where water was injected (CT and DT) on each panel were classified indicating what is visible in the thermograms. The classification was done using the following parameters (exemplified on figures 88, 89, 90 and 91 and presented in table 10):

0. **No difference** between the anomalous and the normal tiles.
1. It is **very hard** to notice a detachment.
2. It is **hard** to notice a detachment.
3. Clear **detachment.**
4. Presence of **water** (non-visible to the human eye) **hindering the detachment's detection.**
5. Presence of **water in the joint and surroundings** (non-visible to the human eye).
6. **Clearly humid area** (non-visible to the human eye).
7. Humid zone with **superficial runoffs** (visible).

Table 10 – Classification of the phenomena visible on the thermograms from the first humidity survey

Hour	Observations	White panels				Black panels			
		C1		C2		C1		C2	
		CT	DT	CT	DT	CT	DT	CT	DT
9:30	Before the water injection	1	1	2	2	1	1	3	3
10:15	20min after the water injection	4	2	4	3	4	7	4	7
11:45		1	1	4	3	4	5	4	5
13:45	Beginning of the solar incidence	4	2	4	3	4	5	4	3
15:00		4	2	4	3	4	5	4	3
17:00		0	0	4	3	4	2	4	3

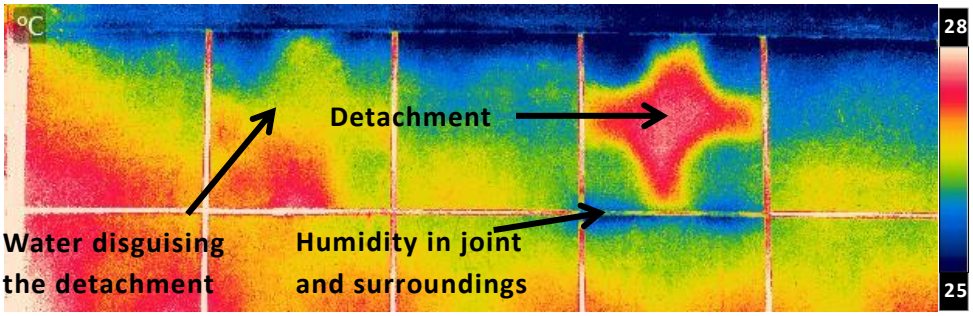

Figure 88 - Thermogram taken from *C2_B* at 11h45 - the classification of the anomalous tiles is presented in table 10, where CT is classified with a 4 and DT with a 5

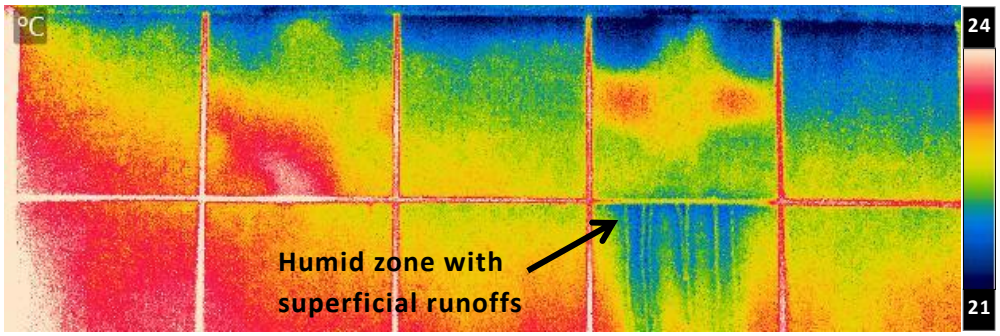

Figure 89 - Thermogram taken from *C2_B* at 10h15 - the classification of the anomalous tiles is presented in table 10, where CT is classified with a 4 and DT with a 7

Using this classification method it is possible to gather some information that despite not describing the thermal differences quantitatively, allows some conclusions about the water presence and its detectability during the day:

- CT tiles tend to, as expected, absorb the water and, consequently, as it is more evenly distributed beneath the tiles, disguises the detachment making it harder to identify
- It was very difficult to verify the presence of water in the white DT tiles, possibly because the amount of water introduced was not enough to allow its identification.
- As already mentioned, black DT tiles suffered from leaks through cracks in the joints. These leaks provoked the water runoff visible on the thermograms taken after the water injection. This water runoff drought leaving efflorescences that despite being visible in the thermograms were not considered as a runoff (even if the water presence is superficial it could not be detected visually).
- After the superficial water drought, it was possible to verify thermal variations mainly in the joints from where water had escaped, as the porous material from the joints traps some water. However, the thermal differences extended to the joints' surroundings, either because of thermal transferences (conduction) between the joint and its surroundings or because these surroundings were actually humid.

- As humid zones are colder than both detached and normal zones it can be more difficult to detect water in a detached tile, as the negative thermal differential between the humid and dry zones is compensated by the positive thermal differential the detached and attached zones.
- Probably because of the low amount of water introduced under the tiles, there were no thermograms showing wide humid areas.

Second survey

Besides some small differences in terms of weather conditions considered as negligible, the main difference in this survey was the amount of water introduced. In a previous laboratory test, it was found that the cloth used beneath the tile was able to absorb approximately 80 ml of water; after these 80 ml it started dropping water. In addition to this, the approximate space to hold water beneath the detached tiles was about 120 ml (considering an empty area of 200 x 200 mm^2 and a thickness of 3 mm). Therefore, the amount of water considered to this survey was of 120 ml per tile, corresponding to 12 syringes.

Injecting higher water contents, it was expected to achieve the point where the water would spread beneath the tiles even through the normal (adherent) zones. Despite this, it was also expected some leakage through the joints, especially in the most damaged joints from the black panels. However, the leakage happened for every tile where water was injected after a few minutes, indicating that the joints were not watertight enough to prevent pressured leaks/infiltrations.

In order to simplify the description of the panels' behaviour facing the injection of a higher amount of water, the same classification method as in the first survey was used (table 11).

Table 11 - Classification of the phenomena visible on the thermograms from the second humidity survey

Hour	Observations	White panels				Black panels			
		C1		C2		C1		C2	
		CT	DT	CT	DT	CT	DT	CT	DT
09:30	Before the water injection	0	0	1	1	0	1	3	3
11:30	30min after the water injection	8	6/7	4&7	4&7	5	7	7	7
12:00		4&5	5	4&5	6	4&5	6/7	4&5	6/7
13:45	Beginning of the solar incidence	4&5	5	4&5	5	4&5	6	4&5	6
14:00		4&5	5	4&5	5	4&5	6	4	5
15:00		4&5	2	4	3	4&5	5	4	5
16:14		4&5	2	4	3	4&5	5	4	5

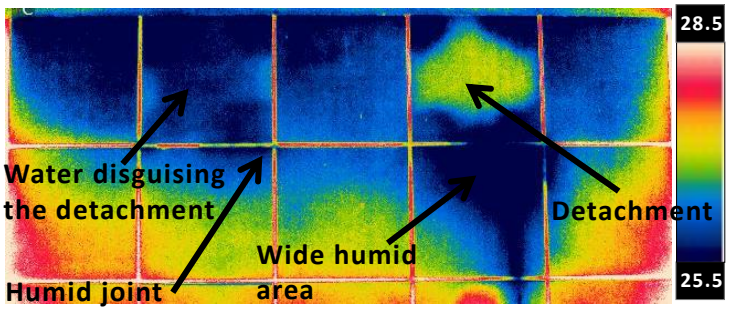

Figure 90 - Thermogram taken from *C2_W* at 12h00 - the classification of the anomalous tiles is presented in table 11, where CT is classified with a 4 and DT with a 6

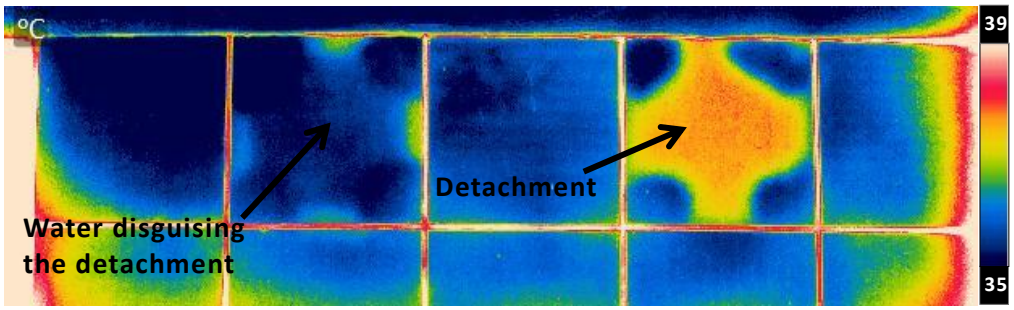

Figure 91 - Thermogram taken from *C2_W* at 15h00 – the classification of the anomalous tiles is presented in table 11, where CT is classified with a 4&5 and DT with a 3

From the analysis of table 11 it is possible to conclude that:

- Despite, as mentioned, every tile having verified some water leakage from the joints, being classified as so in the thermograms taken 30 min after the injection, the leakage from C1_B's CT did not appear visible on the thermogram.
- Tiles with a cloth beneath (CT) verified, in general, both presence of water hindering the detachment's detection and presence of water in the joint and surroundings.
- Simply detached tiles, in general, presented a wide humid area after the injection, sometimes partially hindering the detachment's detection (only partially because the water was only present in the bottom half of the tile (fig. 90)).
- With the heating of the panels during the day, it was possible to verify a diminution of the wide humid area, with the humidity being presented only in the joints and its surroundings.

In sum, after the results analysis from both the surveys it is considered that:

- Moisture is definitively possible to identify in porcelain tiling systems. As this type of tiling system is one of the least absorbent, it is considered that other kinds of ceramic claddings should also allow humidity identification using infrared thermography.
- The "cloth method" proved to be an efficient way to "trap" humidity, simulating a more even distribution.
- Joints were able to prevent just a determined amount of water, but when the pressure was too high with 120 ml of water injected), they started leaking.
- As moisture increases heat storage capacity, or decreases thermal resistance (Edis et al. 2015), it helps to cause surface temperature variations (manifested as lower temperatures during the day) allowing its detection.

5.5 *In situ* inspections – case studies

Accordingly to what was mentioned in the fourth chapter, the two case studies' inspection results will now be presented (some other results are presented in appendix D).

Case study 1 – *Edifício Manuel Rocha*

Despite the existence of various anomalies in this tiling system, the main goal was to identify the non-visible detachments as it is the only non-visible present anomaly. The thermographic surveys were done within the first 1h30 of solar incidence, as suggested by the inspections under controlled conditions (fig. 92). According to the previous work, detached areas would have to be noticed for their higher temperatures.

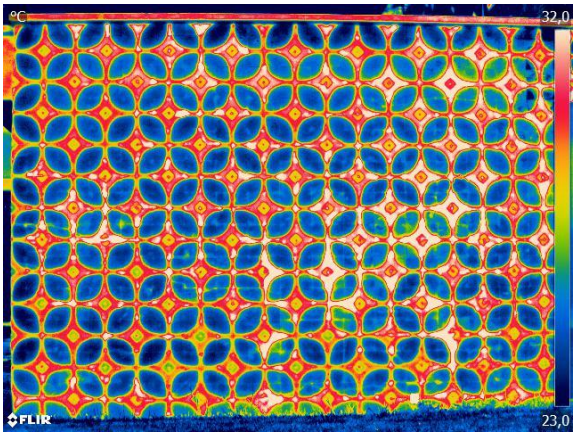

Figure 92 – Untreated thermogram

Right away, the presence of different colours (yellow, white and blue) in the tiling system appeared as a challenge to the inspection as darker areas achieved higher temperatures (fig. 92). Thus, different thermal scales and colour pallets had to be adopted in order to allow the visualization of thermal differences within the different coloured zones (fig. 93 and appendix D.1.). The yellow zones were despised because of their reduced presence in the facade.

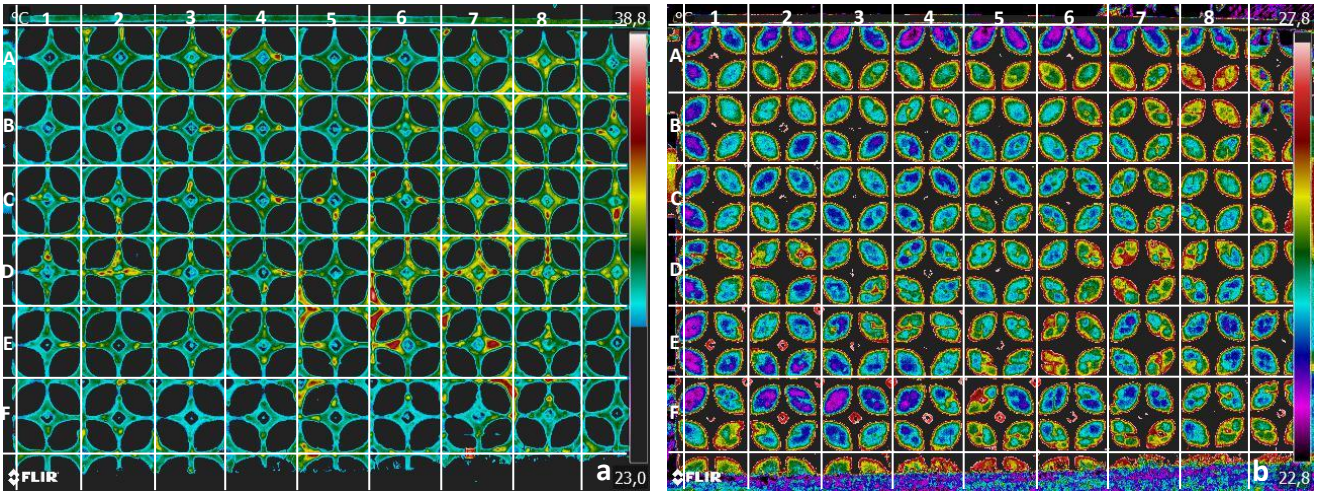

Figure 93 - Thermograms treated to visualize anomalies in different coloured zones (thermogram (a) is scaled to higher temperatures than thermogram (b))

As it is possible to see, even after the scale arrangement, the thermal differentials are hard to identify. However, there are some zones where higher temperatures are visible.

In the thermogram on the left (fig. 93a), black zones correspond to the cooler areas (correspondent to the white part of the tiles), while the coloured areas (from blue to white according to the scale) show the temperatures of the blue part of the system. Analogously, on the right (fig. 93b), the thermogram is only coloured in the areas correspondent to the white areas of the system.

In order to simplify the thermograms' analysis, a grid (with identification of lines and columns) was designed over the thermograms. Regarding thermogram from figure 93a some zones with high temperatures are identified, for example in the crossing between cells D5, D6, E5 and E6. This, as well as other similar hot spots, were afterwards identified by *tapping control* as detachments. For the same zone, it is visible that in thermogram from figure 93b that the same tiles were not considerably hotter than the rest of the cladding. This happened because, as suggested by the

tapping control, the tiles only were detached (sounded hollow) in their edges (crossing between cells D5, D6, E5 and E6).

On the contrary, for example on the superior left corner from cell F5, higher temperatures are verified in both the two thermograms, suggesting the detachment of almost all the tile.

The identification of some detachments using thermography was then considered once more possible. However, when the thermograms were more deeply analysed it was found that not all the warmer areas corresponded to detachments of the cladding. The small hot spots verified for example on cell C5 were not identified as detachments in the *tapping control;* instead, they were identified as zones where the glaze was starting to detach, creating blisters on the tiles' surface. The higher temperatures in these spots are due to the same principle as the explained for the detachments (chapter 3) where the air gap, this time between the glaze and the rest of the tile, raises the thermal resistance, therefore provoking a thermal differential.

As the two anomalies verified in the cladding were presented at the same temperatures there is no specific way to distinguish one from the other without a closer look. However it is possible to predict that small and well defined spots correspond to glaze problems, as these problems usually comprise smaller areas and more superficial, and so more defined.

Regarding the existent cracks, it is possible to state that, despite the obstacles imposed by different colours and reflectant tiles, they are identifiable: comparing the photography with the thermography on figure 94 it is possible to see an orange line correspondent to the crack. However, given their dimension and the fact that the contrast between these anomalous zones and the rest of the cladding is higher in a photography, or that they are easily identifiable by the naked eye, sets infrared thermography as a less practical mean of identification. Nevertheless, it is important to know they are present when analysing a thermogram to eliminate possible mistakes.

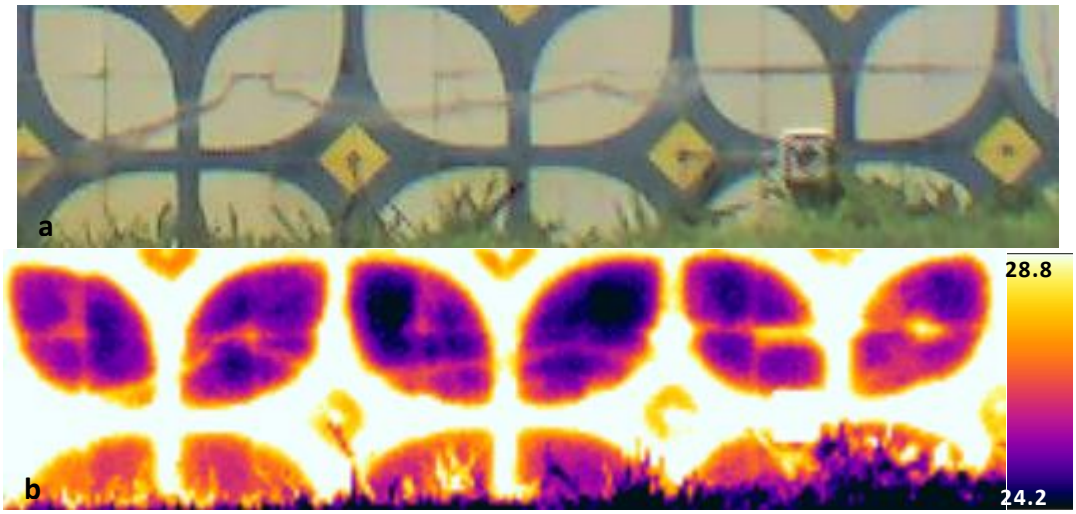

Figure 94 – Image of a crack (a) and respective thermogram (b)

Case study 2 – Building in *Parque das Nações*

As mentioned, it was not possible to access the raised floors in order to a close inspection; so the presented results are only based on the crossing between thermograms and photos.

Although the tiling system in this case had no major colour variations, the interpretation of the thermograms was also challenging. Firstly because temperatures vary considerably with the height of the building, not only because of the existent convection (chimney effect) but also because of

the location of the building whose Eastern façade was facing a large plane with no roughness facing the wind – the river *Tejo*'s estuary; secondly because of the existence of two kinds of construction elements, the masonry and the concrete structure; the third problem consisted in the existence of reflections and shadows from the surrounding buildings. Hence, similarly to what happened in the first case study, various scales had to be adopted in order to correctly diagnose each portion of the building.

Despite these challenges, following the recommendations from chapter 3.8 it was possible to successfully analyse this building's tiled facades using the non-destructive method.

As the thermal camera's optic angle is not wide enough to take a thermogram comprising all the building from a reasonable distance, several thermograms were taken to small portions of the facade at a time. Afterwards it was possible to arrange the thermograms in panoramas recurring to the software *FLIR Reporter* (fig. 95). However, despite thermograms being taken from a fixed point and predicting the overlap, as suggested by *FLIR,* it was found that panoramic thermograms were not appropriate to a rigorous analysis as the overlapping of the thermograms was not always successful. Thus, the analysis was made thermogram by thermogram (fig.96).

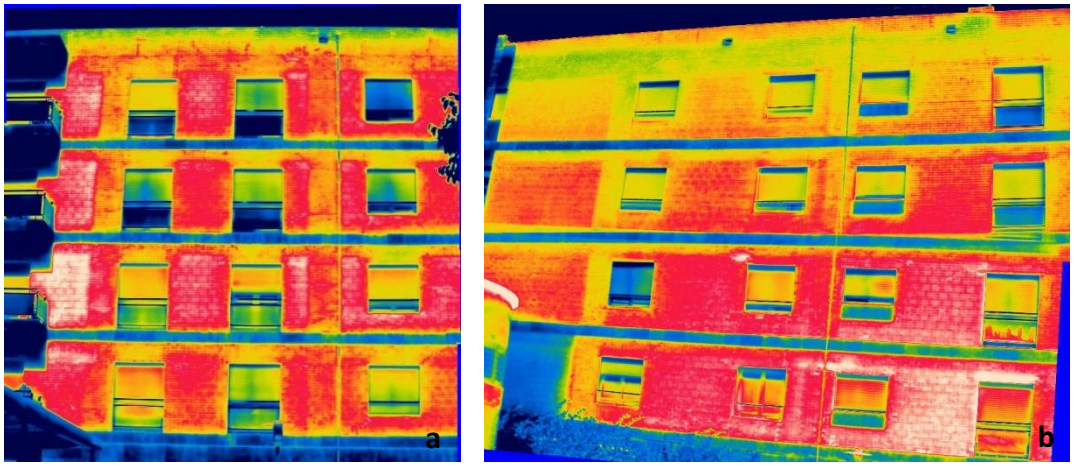

Figure 95 – Two panoramic thermograms from the eastern (a) and western (b) facades executed with the aid of the software *FLIR Reporter*

As an example a portion of the western facade will be presented containing both visible bulked tiles and non-visible thermally identified detachments (fig. 96Figure 96).

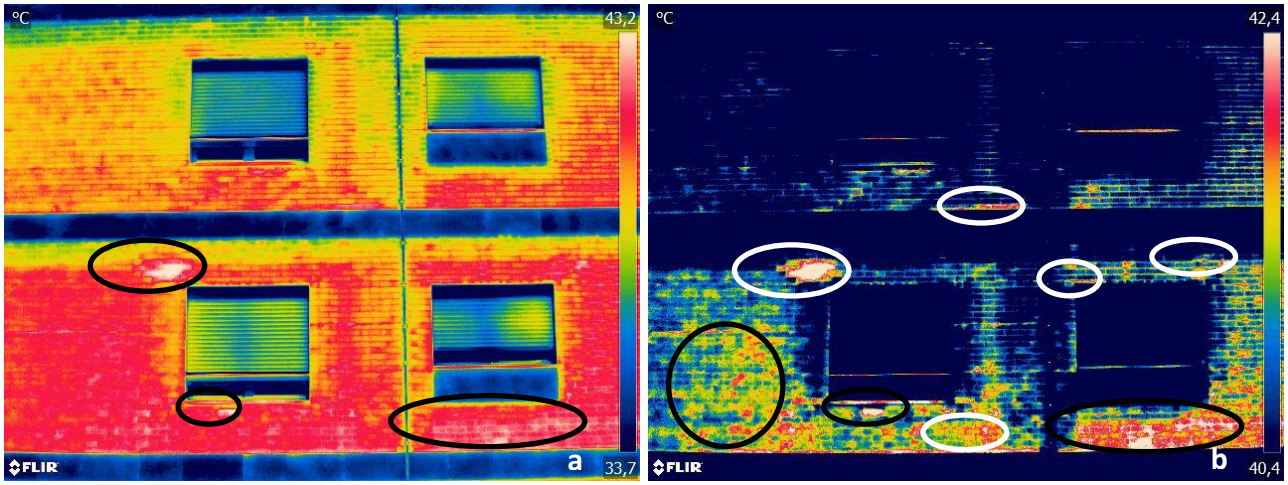

Figure 96 – Thermograms without rearrangement of the scale (a) and with a rearranged scale (b) (the detachments are identified by black/ white circles)

With this example (fig. 96) it is obvious that the thermal scale has to be changed (redefining the window of temperatures presented on the thermal graphic with more suitable scales to each area of the building, i.e. with smaller temperatures for colder zones such as the top floors and with higher temperatures for the lower floors masonry areas which were naturally hotter) in order to identify possible detachments, as thermogram (b) allows the identification of five more possible detachments than thermogram (a).

Figure 97 shows a photography taken to the same area as the thermograms from figure 96. In this photography it is possible to visually identify two (circled) detachments: first an area with bulked tiles (superior left corner of the left window) and the secondly an already fallen tile below the same window. The fact that both these two detachments (as well as the great majority of the other visible detachments) are easily identifiable in the thermograms from figure 96 allows the assumption that at least thermography is a valuable tool to confirm the existence of detachments in this case.

Figure 97 – Photography with visible detachments identified by circles

As mentioned, the presence of reflections/shadows from the surroundings affected the thermograms' quality in a way that this zones verified different temperatures that could not be analysed separately as in the case of differences between structure/masonry because of their non-stationary character. Some examples of these problems are presented in figure 98.

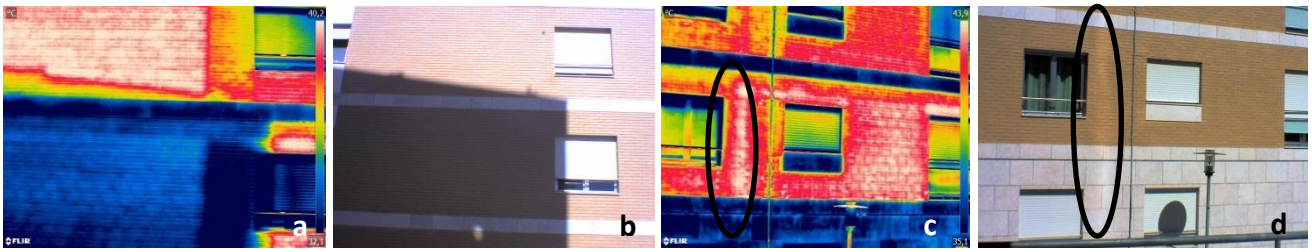

Figure 98 – Example of a shadowed surface (thermogram (a) and photography (b)) and of a signalized (circled) reflection (thermogram (c) and photography (d))

Figure 98 shows both an example of a shadowed surface clearly at a lower temperature and a zone of reflection where temperature is higher. It is important to say that this reflection came from the adjacent buildings' mirrored windows that reflected the sun "behaving as a secondary heat source". Thus, the effect of a higher temperature in the thermograms is not because of a reading of reflected radiation but because the temperature is actually higher as the zone is being heated from "two heat sources". As these shadows/reflections changed place with the sun's rotation it was possible to study these zones in different time periods.

As a final product of the inspection, two photographs (one from the Eastern facade (fig. 99) and other from the Western (fig.100)) were coloured with the identified detachments.

Figure 99 – Eastern facade with identified anomalous zones (green – visible anomalies; red – anomalies identified in thermograms)

Figure 100 - Western facade with identified anomalous zones (green – visible anomalies; red – anomalies identified in thermograms)

6 Conclusions

6.1 Final remarks

This work had, as main objective, the verification of infrared thermography's capacity in the detection of anomalies in tile cladded walls. After all the research, laboratory work and *in situ* inspections presented, the main conclusion is that it is possible to detect anomalies, mainly detachments and moisture, in this type of wall coating systems using the mentioned non-destructive method.

However, besides the main objective, there were other specific objectives of study, such as assess the influence of colour (black or white), surface finishing (polished or unpolished), thickness of the tiles, kind of support (with thermal insulation or just a render) and joints' condition (opened or closed), presence of humidity, weather conditions and period of the day in detachment's detectability. Studying these parameters it was possible to conclude:

- It is very important to understand the influence of the cladding's colour when leading a thermographic survey, as temperatures will reach higher values for darker (more absorbent) colours and consequently higher thermal differentials between attached and detached zones.
- Regarding the colours it is also very important to understand that tiles with several colours difficult the use of thermography, as differences in absorption and reflection will result in different temperatures, which in turn will difficult a colour scale definition that can evidence detachments in all the colours.
- The kind of support has a great impact in detachments' detectability. When the support is rendered, the thin air layer provoked by a detachment raises the thermal resistance to the heat flow, causing a thermal difference in the detached zone (higher temperatures in the heating phase). In the other hand, when the support is an insulating system (ETICS), the thermal resistance increase is hardly enough to enable to distinguish detached zones from adherent zones.
- Considering the tiles available, there were no greater differences in detectability of anomalies caused by different thicknesses, probably because the thickness difference was not high enough. However, there was a small difference in the thermal variation rate that suggests that, as expected, temperature vary faster for thinner tiles.
- The kind of surface finishing given to the tiles is also of great importance, as polished/gladded tiles tend to reflect more and, therefore, will difficult the survey, especially if there are reflection sources in the surroundings or if flatness deficiencies are present.
- The weather conditions play an essential role in this method's efficiency. Given the fact that the sun is the main responsible for the facade's heating and consequently for the thermal differentials between detached and adherent zones, it is evident that on a cloudy day the detection of detachments is harder. Hence, it is possible to say that detachments' detectability is proportional to the solar radiation intensity.
- Despite during the study period there were no fully clouded day, making it impossible to study the influence of this kind of weather conditions, it may be considered that a cloudy day can be compared to the morning period on West facing facades (as the ones studied), where only reflected and diffused radiations reach the facade. As in the morning period there were some small differences between attached and detached areas (when the support was not "insulator"), it is possible to admit that in a cloudy day detachments might be distinguishable. However, it is not recommendable to make a thermographic survey with a cloud covered sky.

- There are two recommendable day periods to inspect a facade in search of detachments: in the first 1h30 of direct solar incidence or in the beginning of the cooldown (after sunset or after the complete facade's shading).
- During inspections, conditions like wind speed, solar incidence, ambient temperature and existence of reflections/shadows must be taken into account to minimize possible errors.
- Moisture in walls can be identified as areas with lower temperatures because of the evaporative cooldown. As expected, its identification is easier if the water content in the wall is higher or if the cladding is darker (provoking higher differentials).
- As most of the anomalies that can happen in a facade imply a change in the wall's thermal behaviour, such as cracking, efflorescences or the glaze detachment/cracking, their identification using infrared thermography is usually possible. In practice, this can difficult the thermograms' interpretation. However, these anomalies are also usually visibly identifiable, enabling to separate them from the non-visible anomalies (such as detachments) for example by comparing the thermogram with photography. This makes a photographic parallel survey of extreme importance.
- It is also important to say that when two anomalies with opposite thermal behaviours, such as moisture presence and detachment, happen at the same time it is possible that the thermal differential can be null, hindering any of the anomalies' identifications. This aspect reinforces the need of making inspections under different conditions.
- The excessive temperatures verified especially in black claddings makes their adoption in exposed to sun radiation walls inadvisable, as with time it will certainly result in problems related to thermal variations such as cracking or detachment.
- Thermocouple data has proven to be valuable as the continuous thermal readings proved the existence of thermal differentials between anomalous and "healthy" areas for different days/weather conditions. Nevertheless, its use in inner layers is limited to experimental studies.
- Regarding the analogous experiment developed during this project to evaluate reflectance in vertical walls, it is possible to state that this parameters' determination using the adapted method has shown positive results. However, in order to achieve more precise readings, the surface to analyse shall have a larger area and shadows shall be minimized for example by improving the pyranometers' support.

Given the complexity and all the problems existent in this widely used adherent cladding system, together with the proven capacities of the thermographic inspection method, it is considered that the creation of standards dedicated to tiling systems' inspections shall be considered in order to help this diagnosis technique to gain a proper recognition and promoting the monitoring of these claddings in order to prevent severe anomalies.

6.2 Proposals for future works

Aiming to expand the knowledge both in the thermographic inspection of buildings and in ceramic claddings the following themes are proposed:

- Evaluation of anomalies in other kinds of ceramic tiles´ claddings using infrared thermography.
- Evaluations of thermographic analysis/data acquisition methods to eliminate the thermograms' "contaminations", such as shadows/reflections or different colored areas.
- Analysis of more case studies in different weather conditions, in facades with different orientations and with different tiling systems.

- Analysis of the consequences of the high temperatures verified on solar exposed cladding systems.
- Evaluation of the aging process of ceramic tiled facades with different characteristics.
- Development of the thermographic analysis software.
- Analysis of the accuracy of different data acquisition methods such as thermocouples or pyrometers.

Despite not being considered as an objective of this work, the thermocouples placed in different parts of the cladding were surprisingly useful. Readings of the temperatures achieved by the adhesive grouts under different weather conditions and for different cladding characteristics (colour and kind of support) are not available in the bibliography. The results still to analyse will provide information on the temperatures achieved by different components of the system, allowing the calculation of the stress these materials are subjected to, which is known to be a cause of numerous anomalies.

Several parts of the present study were presented by the author in two conferences (Lourenço et al. 2016a; Lourenço et al. 2016b) and one submitted article to Construction and Building Materials (Lourenço et al. n.d.).

References

Abreu, M.M. (2005) – **Revestimentos cerâmicos colados: recomendações para a minimização do risco de descolamento.** LNEC, Portugal.

Alba, M. I., Barazzetti, L., Scaioni, M., Rosina, E., Previtali, M. (2011) – **mapping infrared data on terrestrial laser scanning 3d models of buildings.** Remote Sensing, Vol. 3, pp. 1874-1870.

Avdelidis, N.P., Moropoulou, A. (2003) – **Emissivity considerations in building thermography.** Energy and Buildings, Vol. 35, pp. 663–667.

Avdelidis, N.P., Koui, M., Ibarra-Castanedo, C., Maldague, X. (2007) – **Thermographic studies of plastered mosaics.** Infrared Physics & Technology Vol. 49, pp. 254–256 (doi: 10.1016/j.infrared.2006.06.027).

APICER (2003) – **Manual de aplicação de revestimentos cerâmicos**. Associação Portuguesa da Indústria Cerâmica (APICER), Coimbra.

ASTM D4580 / D4580M - 12 – **Standard practice for measuring delaminations in concrete bridge decks by sounding.** Technical report, American Society for Testing and Materials, West Conshohocken, PA. (DOI: 10.1520/D4580_D4580M-12).

ASTM C1060-90:2003 – **Standard practice for thermographic inspection of insulation installations in envelope cavities of frame buildings.** West Conshohocken: American Society for Testing and Materials, PA.

ASTM E1862:1997 – **Standard test methods for measuring and compensating for reflected temperature using infrared imaging radiometers** (Reapproved 2010). Technical report, American Society for Testing and Materials, West Conshohocken, PA.

ASTM E1918:2006 – **Standard test method for measuring solar reflectance of horizontal and low-sloped surfaces in the field**. Technical report, American Society for Testing and Materials, West Conshohocken, PA.

Bart B. Barrett, P.E., James M. Falls, E.I. – **Common perils of ceramic floor tile systems.** Article, Nelson Architectural Engineers, Dallas Parkway, Plano, Texas.

Barreira, E., Freitas, V.P., Delgado, J.M.P.Q., Ramos, N.MM. (2008) – **Thermography applications in the study of buildings hygrothermal behaviour.** LFC − Building Physics Laboratory, Civil Engineering Department, Faculty of Engineering, University of Porto Portugal.

Barreira, E., de Freitas, V.P., Delgado, J.M.P.Q., Ramos, N.M.M. (2012) – **Thermography applications in the study of buildings hygrothermal behaviour, infrared thermography**, Raghu V Prakash (Ed.), ISBN: 978- 953-51-0242-7, InTech.

Barreira, E., Almeida, R. (2015) – **Drying evaluation using infrared thermography.** Energy Procedia Vol. 78, pp. 170–75. (DOI: http://dx.doi.org/10.1016/j.egypro.2015.11.135).

Barros, R.M. G.M., Uchôa, S.B.B., Moraes, K.A.M. (1998) – **Estudo da temperatura superficial de fachadas de edifícios edifícios.** XIII Encontro Nacional de Tecnologia do Ambiente Construído, Canela – RS, Brasil.

Bauer, E., Castro, E. K., Leal, F. E., Antunes, G. R. (2011) – **Identification and quantification of failure modes of new buildings facades in Brasília**, Proceedings of XII International Conference on Durability of Building Materials and Components, FEUP Edições, Vol. 3, pp. 1089-1096.

Bauer, E., Castro, E. K., Oliveira Filho, A. H., Pavón, E. (2014) – **Criteria for application of passive infrared thermography as an auxiliary technique in the diagnosis of pathologies on the facades of buildings**. Iº Encontro Luso-Brasileiro de Degradação de Estruturas em Betão Armado, Salvador, Bahia, Brasil, (2014), pp. 266-277.

Bauer, E., Freitas, V., Mustelier, N., Barreira, E., Freitas, S. (2015) – **Infrared thermography – evaluation of the results reproducibility**. Structural survey, Vol. 33 (1), pp. 20-35 (doi: 10.1108/SS-05-2014-0021).

Berdahl, P., Bretz, S.E. (1997) – **Preliminary survey of the solar reflectance of cool roofing materials.** Energy and Buildings, Vol. 25 (2), pp. 149–158.

Bento, J. (2010) – **Patologias em revestimentos cerâmicos colados em paredes interiores de edifícios.** MSc dissertation, Faculdade de Engenharia, Universidade do Porto.

Bosiljkov, V., Uranjek, M., Zarnic, R., Bokan-Bosiljkova, V. (2010) – **An integrated diagnostic approach for the assessment of historic masonry structures**. Journal of Cultural Heritage Vol. 11, (3), pp. 239–249 (http://dx.doi.org/10.1016/j.culher.2009.11.007).

Castro, A. (2002) – **Análise da refletância de cores de tintas através da técnica espectrofotométrica**. Msc dissertation, Universidade Estadual de Campinas.

CSTB (2008) - DTU 26.1 – **Enduits aux mortiers de ciments, de chaux et de mélange plâtre et chaux aérienne.** Paris, France.

EN 1346:2007 – **Adhesives for tiles. Determination of open time**. Brussels: European Committee for Standardization.

EN 12004:2014 – **Adhesives for tiles - requirements, evaluation of conformity, classification and designation**. Brussels: European Committee for Standardization.

EN 13187:1998 – **Thermal performance of buildings – qualitative detection of thermal irregularities in building envelops – infrared method.** Brussels: European Committee for Standardization.

EN 13888:2009 – **Grout for tiles; Requirements, evaluation of conformity, classification and designation.** Brussels: Committee European de Normalization (CEN).

EN 14411:2016 – **Ceramic tiles; Definition, classification, characteristics, assessment and verification of constancy of performance and marking.** Brussels: Committee European de Normalization (CEN).

Dufour, J., Della Giustina, G. – **La patologie des carregales**. Paris, ITBP. Annales de l'ITBP No 426, Julliet-Août 1948, Série Questiones Générales 162.

Edis, E., Flores-Colen, I., Brito, J. (2013) – **Passive thermographic detection of moisture problems in facades with adhered ceramic cladding.** Construction and Building Materials Vol. 51, pp. 187–197 (http://dx.doi.org/10.1016/j.conbuildmat.2013.10.085)

Edis, E., Flores-Colen, I., Brito, J. (2014) – **Building thermography: detection of delamination of adhered ceramic claddings using the passive approach**. Journal of Nondestructive Evaluation, Vol. 34, article 268. (http://link.springer.com/10.1007/s10921-014-0268-2).

Edis, E., Flores-Colen, I., Brito, J. (2015a) – **Time-dependent passive building thermography for detecting delamination of adhered ceramic cladding**. J. Nondestructive Evaluation, Vol. 34 (2), article 24 (doi: 10.1007/s10921-015-0297-5).

Edis, E., Flores-Colen, I., Brito, J. (2015b) – **Quasi-quantitative infrared thermographic detection of moisture variation in facades with adhered ceramic cladding using principal component analysis.** Building and Environment, Vol. 94 (1), pp. 97-108.

FLIR Systems (2006) – **Manual do utilizador**. Publ. No 1558561 Ver. A147

Freitas, J., Carasek, H., Cascudo, O. (2014) – **Utilização de termografia infravermelha para avaliação de fissuras em fachadas com revestimento de argamassa e pintura**. Ambiente Construído, Vol. 14 (1), pp. 57-73.

Freitas, S.S. Freitas, V. P., Barreira, E. (2014) – **Detection of facade plaster detachments using infrared thermography - A nondestructive technique**. Construction and Building Materials, Vol. 70, pp. 80-87. (doi: 10.1016/j.conbuildmat.2014.07.094).

Garcia, J. (2014) – **Potencialidades da termografia para o diagnóstico de patologias em edifícios.** MSc dissertation, Universidade do Porto.

Gaussorgues, G. (1999) – **La thermographie infrarouge – principes, technologies, applications.** 4th Édition, TEC & DOC, Paris, France.

Gonçalves, L. (2014) – **Avaliação do desempenho térmico de tintas reflectantes em fachadas por análise termográfica.** MSc dissertation, Universidade Nova de Lisboa.

Hagentoft, C. (2001) - **Introduction to building physics.** Student Litteratur, Sweden.

Hart, J. M. (1991) – **A practical guide to infra-red thermography for building surveys**. Building Research Establishment Report. ISBN: 0 85125 448 9.

Henriques, F. M. A. (2011) – **Comportamento higrotérmico de edifícios**. Version 11.5. Universidade Nova de Lisboa. ISBN: 978-989-20-3993-0.

Ibarra-Castanedo, C., Genest, M., Piau, J.M., Guibert, S., Bendada, A., Maldague, X.P.V. (2007) – **Active infrared thermography techniques for the non-destructive testing of materials.** Ultrasonic and Advanced Methods for Nondestructive Testing and Material Characterization, ed. Chen CH: 325–48.

IMPIC (Instituto dos Mercados Públicos, do Imobiliário e da Construção). (2015) – **O sector da construção em Portugal.** Relatório Semestral do Sector da Construção em Portugal.

ISO 6781:1983 – **Thermal insulation – qualitative detection of thermal irregularities in building envelopes – infrared method.** Switzerland: International Organization for Standardization.

Kipp & Zonen – **Pyranometer for outdoor installation - Model CM5 - CM6 - Directions for use**

Lehmann, B; Ghazi Wakili, K., Frank, Th., Vera Collado, B., Tanner, Ch. (2013) – **Effects of individual climatic parameters on the infrared thermography of buildings.** Applied Energy, Vol. 110, pp.29–43 (http://dx.doi.org/10.1016/j.apenergy.2013.03.066).

Lourenço, T., Matias, L., Faria, P. (2016a) – **Anomaly diagnosis in ceramic claddings by thermography - A review**. 7th International Conference on Safety and Durability of Structures (ICOSADOS), UTAD, Portugal (ISBN:978-989-20-6683-7).

Lourenço, T., Matias, L., Faria, P. (2016b) – **Deteção de anomalias em revestimentos de ladrilhos por termografia de infravermelhos.** QIC 2016 - 2° Encontro Nacional Sobre Qualidade e Inovação na Construção, Lisboa, LNEC.

Lucas, J. A. C. (2001) – **Anomalias em revestimentos cerâmicos colados**. ITCM 28. LNEC. ISBN: 972-49-1886-6.

Magalhães, A., Veiga, M.R., Santos, C., Matias, L., Vilhena, A. (2008) – **Methodology for diagnosis of rendering anomalies due to moisture in walls.** Conservar Património, Vol. 7, pp. 45-54. Associação Profissional de Conservadores Restauradores de Portugal (ARP).

Maldague, X.P.V., (1993) – **Nondestructive evaluation of materials by infrared thermography**, Springer-Verlag, Berlin.

Maladague, X. (1994) – **Infrared methodology and technology**. Nondestructive testing monographs and tracts, Vol. 7. Editor-in-Chief: W. J. McGonnagle. Gordon and Breach Science Publishers. ISBN: 2-88124-590-0.

Maladague, X**.** (2001) – **Theory and practice of infrared technology for nondestructive testing**. Ed. K. Chang. Wiley-Interscience. ISBN 0-471-18190-0.

Maldague, X. P. V., Streckert, H. H., Trimm, M. W. (2001) – **Introduction to infrared and thermal testing: Part 1. Nondestructive testing.** Nondestructive Handbook, Infrared and Thermal Testing, Vol. 3, X. Maldague technical ed., P. O. Moore ed., 3rd edition, Columbus, Ohio, ASNT Press, 2001, pp. 718.

Martarelli, M., Castellini, P., Quagliarini, E., Seri, E., Lenci, S., Tomasini, E.P. (2014) – **Nondestructive evaluation of plasters on historical thin vaults by scanning laser doppler vibrometers.** Research in Nondestructive Evaluation, Vol. 25, pp. 218–234.

Matias, L. (2001) – **Avaliação do desempenho térmico de protecções reflectantes aplicadas em coberturas inclinadas.** Msc dissertation, Universidade de Lisboa.

Matias, L. (2006) – **Aplicação da análise termográfica em edifícios antigos em viana do alentejo.** (Projecto FCT nº POCTI/ECM/46323/2002), 2ª campanha experimental. Ministério das Obras Públicas, Transportes e Comunicações. Laboratório Nacional de Engenharia Civil, Departamento de Edifícios, Núcleo de Revestimentos e Isolamentos.

Matias, L., Magalhães, A.C., Vilhena, A., Pina dos Santos, C. A., Veiga, M.R. (2007) – **ensaio de capilaridade e análise termográfica para visualização da secagem de um murete de alvenaria de pedra.** (Projecto FCT nº POCTI/ECM/46323/2002). Ministério das Obras Públicas, Transportes e Comunicações. Laboratório Nacional de Engenharia Civil, Departamento de Edifícios, Núcleo de Revestimentos e Isolamentos.

Matias, L., Vilhena, A., Santos, C., Veiga, R., Magalhães, A. (2008) – **Infrared thermography applied to the evaluation of moisture in ancient buildings.** Historical Mortars Conference (HMC 2008), Livro de resumo pág. 75. Lisboa, LNEC.

Matias, L. (2012) – **Testing techniques for structures inspection**. DURATINET project. Lisbon, LNEC.

Melrinho, A. (2014) – **Anomalias em impermeabilizações de coberturas em terraço: Detecção por termografia de infravermelhos**. MSc dissertation, Universidade Nova de Lisboa.

Melrinho, A., Matias, L., Faria, P. (2015) – **Detecção de anomalias em impermeabilizações de coberturas em terraço através da termografia de infravermelhos**. TECH ITT, Vol. 13 (37), pp. 29-38.

Mendonça, A.M.G.D., Cartaxo, J.M., Menezes, J. M. R. R., Santana, L.N.L., Neves, G. A., Ferreira, H. C. (2012) – **Moisture expansion of ceramic tiles produced using kaolin and granite wastes.** Cerâmica, Vol. 58, pp.216-224.

Modest, M. F. (2003) – Radiative heat transfer. Academic press.

Peixoto de Freitas, V., Alves, S. (2008) – **Patologia de argamassas**. APFAC. Tektónica.

Pleşu, R., Teodoriu, G., Ţăranu, G. (2012) – **Infrared thermography applications for building investigation.** Universitatea Tehnică „Gheorghe Asachi" din Iaş 1(LXII), pp.1–12.

RYER, A. (1998) - **Light measurement handbook**. International Light Inc.

Pina dos Santos, C. A., Matias, L. (2002) – **Aplicação laboratorial da análise termográfica para visualização da absorção capilar e da secagem de um provete de parede de alvenaria de tijolo cerâmico furado.** Relatório 144/02 – NCCt, Ministério das Obras Públicas, Transportes e Comunicações. Laboratório Nacional de Engenharia Civil, Departamento de Edifícios, Núcleo de Revestimentos e Isolamentos.

Pina dos Santos, C. A., Matias, L. (2003) – **Aplicação laboratorial da análise termográfica para visualização da absorção de água e da secagem de uma parede de alvenaria de blocos de betão de argila expandida.** Relatório 37/2003, Ministério das Obras Públicas, Transportes e Comunicações. Laboratório Nacional de Engenharia Civil, Departamento de Edifícios, Núcleo de Revestimentos e Isolamentos.

Prado, R. Ferreira, F. (2005) – **Measurement of albedo and analysis of its influence on the surface temperature of building roof materials.** Energy and Buildings, Vol. 37 (4), pp. 295–300.

Rempel, A.R., Rempel, A.W. (2013) – **Rocks, clays, water, and salts: Highly durable, infinitely rechargeable, eminently controllable thermal batteries for buildings.** Geosciences. pp. 63 - 101

Sfarra, S., Marcucci, E., Ambrosini, D., Paoletti, D. (2016) – **Infrared exploration of the architectural heritage: from passive infrared thermography to hybrid infrared thermography (hirt) approach.** Materiales de Construcción, Vol. 66 (323), pp. 1-16. (ISSN-L: 0465-2746 http://dx.doi.org/10.3989/mc.2016.07415).

Silva, L., Sequeira, P., Gonçalves, L. (2015) – **Avaliação de suportes em contexto de colagem de elementos cerâmicos em fachada.** TECH ITT, Vol.13 (37), pp. 4-10.

Silvestre, J., Brito, J. (2004) – **Classificação de Anomalias em Sistemas de Revestimentos Cerâmicos Aderentes.** Conference paper, Construção 2004, FEUP, Porto, Portugal.

Silvestre, J.D. (2005) – **Sistema de apoio à inspecção e diagnóstico de anomalias em Revestimentos Cerâmicos Aderentes**. MSc dissertation, Instituto Superior Técnico, Lisboa.

Silvestre J. D., Brito, J. (2006a) – **Diagnóstico de revestimentos cerâmicos em fachadas de edifícios.** Article, Instituto Superior Técnico, Portugal

Silvestre J. D., Brito, J. (2006b) – **Diagnóstico e reparação de anomalias em revestimentos cerâmicos aderentes (RCA).** Article, Instituto Superior Técnico, Portugal

Silvestre J. D., de Brito J. (2007) – **Análisis estadístico de los defectos de juntas cerámicas.** Materiales de Construcción Vol. 57, pp. 285-292 (ISSN: 0465-2746).

Silvestre, J. Brito, J. (2008) – **Inspecção e diagnóstico de revestimentos cerâmicos aderentes**. Revista Eng. Civil - U. Minho, Vol. 30, pp. 67-82.

Silvestre J. D., de Brito J. (2009a) – **Ceramic tiling inspection system**. Construction and Building Materials, Vol. 23 (2), pp. 653-668.

Silvestre J. D., de Brito J. (2009b) – **Juntas em revestimentos cerâmicos aderentes (RCA): da construção à manutenção.** Article, Instituto Superior Técnico, Portugal

Silvestre J. D., de Brito J. (2011) – **Ceramic tiling in building facades: Inspection and pathological characterization using an expert system**. Construction and Building Materials, Vol. 25 (4), pp. 1560-1571 (DOI: 10.1016/j.conbuildmat.2010.09.039).

TAN, K. S. et ai. (1994) – **Non-destructive assessment of voids in tiled walls**. In: International Conference on Building Envelope Systems and Technology, Singapore. Proceedings. Singapore, CIDBNTU, pp. 91-96.

Theodorakeas, P., Avedelidis, N.P., Cheilakou, E., Koui, M. (2014) – **Quantitative analysis of plastered mosaics by means of active infrared thermography**. Construction and Building Materials, Vol. 73, pp. 417-425 (doi: 10.1016/j.conbuildmat.2014.09.089).

Usamentiaga, R., (2014) – **Infrared thermography for temperature measurement and non-destructive testing**. Sensors, Vol. 14, pp. 12305-12348 (doi:10.3390/s140712305).

Vaz, E. (2003) – **Aplicação de revestimentos cerâmicos aderentes**. MSc dissertation, Instituto Superior Técnico.

Websites:

[W1] http://www.sciencemadesimple.co.uk (21/09/2016)

[W2] http://www.slideshare.net (21/09/2016)

[W3] http://how-it-looks.blogspot.pt (21/09/2016)

[W4] http://www.ceramicx.com (21/09/2016)

[W5] http://www.anfacer.org.br (21/09/2016)

[W6] http://www.archiexpo.es/ (26/09/2016)

[W7] http://www.archiproducts.com/ (26/09/2016)

[W8] http://www.magmatextil.com.br/ (26/09/2016)

[W9] http://www.mouzinho.com/ (26/09/2016)

[W10] http://vasfer-businesssources.blogspot.pt/ (26/09/2016)

[W11] https://spie.org/publications/ (30/09/2016)

Technical sheets:

[TS1] http://www.weber.com.pt/uploads/tx_weberproductpage/FT_w.therm_pro_2014.pdf

[TS2] http://www.weber.com.pt/uploads/tx_weberproductpage/FT_col_flex_M_2010.pdf

[TS3] http://www.weber.com.pt/uploads/tx_weberproductpage/FT_color_premium.pdf

[TS4] http://www.weber.com.pt/uploads/media/FT_weber.flex_PU_01.pdf

[TS5] http://www.weber.com.pt/uploads/tx_weberproductpage/Ficha_Tecnica_weber.dry_lastic.pdf

[TS6] http://www.revigres.pt/getfile.php?xp=2&src=file50_pt&ext=pdf

[TS7] http://www.revigres.pt/getfile.php?xp=2&src=file51_pt&ext=pdf

Appendix A - Characteristics of the equipment

A.1. ThermaCAM FLIR P640

Table A.1 - FLIR P640 Technical Specifications

Imaging and optical data	
Field of view (FOV) / Minimum focus distance	24° × 18° / 0.3 m
Spatial resolution (IFOV)	0.65 mrad
Thermal sensitivity / NETD	30 mK @ +30°C
Image frequency	30 Hz
Focus	Automatic or manual (electric or on the lens)
Zoom	1–8× continuous, digital zoom, including panning
Focal Plane Array (FPA) / Spectral	Uncooled microbolometer / 7.5–13 µm
IR resolution	640 × 480 pixels
Image presentation	
Display	Built-in widescreen, 5.6 in. LCD, 1024 × 600 pixels
Viewfinder	Built-in, tiltable LCD, 800 × 600 pixels
Automatic image adjustment	Continuous / manual; linear or histogram based
Manual image adjustment	Level /span / max / min
Image modes	IR-image, visual image, thermal fusion, picture in picture, thumbnail gallery
Thermal fusion	IR image shown above, below or within temp interval on visual
Picture in Picture	Resizable and movable IR area on visual image
Reference image	Shown together with live IR image
Measurement	
Temperature range	–40°C to +500°C
Accuracy	±2°C or ±2% of reading
Measurement analysis	
Spotmeter	10
Area	5 boxes or circles with max. / min. / average
Automatic hot / cold detection	Max / Min temp. value and position shown within box, circle or on a line
Isotherm	2 with above / below / interval
Profile	1 live line (horizontal or vertical)
Difference temperature	Delta temperature between measurement functions or reference temperature
Reference temperature	Manually set or captured from any measurement function
Emissivity correction	Variable from 0.01 to 1.0 or selected from editable materials list
Measurement corrections	Reflected temperature, optics transmission, atmospheric transmission and external optics
Measurement function alarm	Audible/visual alarms (above / below) on any selected measurement function
Set-up	
Set-up commands	Configurable measurement tools menu; configure information to be shown in image; 2 Programmable buttons; user profiles; local adaptation of units, language, date and time formats

Storage of images	
Image storage	Standard JPEG, including measurement data, on memory card Built-in RAM for burst recording
Image storage mode	IR / visual images; simultaneous storage of IR and visual images Visual image is automatically associated with corresponding IR
Periodic image storage	Every 10 seconds up to 24 hours
Panorama	For creating panorama images in FLIR Reporter Building software
Image annotations	
Voice	60 seconds stored with the image
Text	Predefined text or free text from PDA (via IrDA) stored with the
Image marker	4 on IR or visual image
Video recording and streaming	
Radiometric IR-video recording	Real-time to built-in RAM, transferable to memory card.
Non-radiometric IR-video recording	MPEG-4 to memory card
Non-radiometric IR-video streaming	MPEG-4 to PC using USB or WLAN (optional)
Digital camera	
Built-in digital camera	3.2 Mpixel, auto focus, and video lamp
Laser pointer	
Laser	Activated by dedicated button
Data communication interfaces	
Interfaces	USB-mini, USB-A, IrDA, composite video, headset connection
Power system	
Battery	Li Ion, 3 hours operating time
Charging system	In camera (AC adapter or 12 V from a vehicle) or 2-bay charger
Power management	Automatic shutdown and sleep mode (user selectable)
Environmental data	
Operating temperature range	–15°C to +50°C
Storage temperature range	–40°C to +70°C
Humidity (operating and storage)	IEC 68-2-30/24 h 95% relative humidity +25°C to +40°C
Encapsulation	IP 54 (IEC 60529)
Bump	25 g (IEC 60068-2-29)
Vibration	2 g (IEC 60068-2-6)
Physical data	
Camera weight, incl. lens and battery	1.8 kg
Cameras size, incl. lens (L × W × H)	324 × 144 × 147 mm
Tripod mounting	UNC ¼"-20

A.2. Pyranometers Kipp & Zonnen CM5

Specifications

The pyranometer CM 5 is designed for measuring the irradiance on a plane surface, which results from the direct solar radiation and from the diffuse solar radiation incident from the hemisphere above.

Reflected solar radiation can be measured with the pyranometer in the inverted position.

The pyranometer CM5 complies with the specifications for a 'first class' pyranometer, as published in the 'Guide to meteorological instruments and methods oi observation', Fifth edition, 1983, from the Secretarial oi the World Meteorological Organization (WMO)-Geneva, Switzerland.

Table A.2 - Table of WMO-Classification of pyranometers

Class	*First class*
Resolution (smallest detectable change in W m-2)	±5
Stability (percentage of full scale, change/year)	±2
Cosine response (percentage deviation from ideal at 10° solar elevation on a clear day)	<±7
Azimuth response (percentage deviation from the mean at 10º solar elevation on a clear day)	<±5
Temperature response (percentage maximum error due to change oi ambient temperature within the operating range)	±2
Non-linearity (percentage oi lull scale)	±2
Spectral sensitivity (percentage deviation from mean absorptance 0.3 to 3 µm)	±5
Response time (99% response)	<1 min

Connection to measuring equipment

The pyranometer is provided with a two-core output cable. Black is the negative and blue the positive.

Extension cables with a length up to some hundreds oi metres may be used but care has to be taken that these are provided with a shield and that the cable resistance is lower than 0.1% of the impedance of the read-out equipment. Connect the shield at one end only to 'ground' in order to prevent shield currents.

Operating

The irradiance level (in W/m2) outside the pyranometer in the plane of the sensing element can be computed when the output voltage (µV) is divided by the sensitivity (in µV/Wm^{-2}) of the pyranometer.

The sensitivity can change slightly with temperature, irradiance, tilt angle, direction of radiation, etc. Some typical curves (of relative sensitivity) are shown in figure 1.

The spectral range of the instrument is limited by the transmission of the glass domes. See figure 2. The black paint oi he sensor has a constant absorptance in this range.

Small offset voltages can arise due to lack of thermal equilibrium in the instrument. E.g. at clear windless nights the infrared emission to the cold sky results in a zero offset of down to -50 µV.

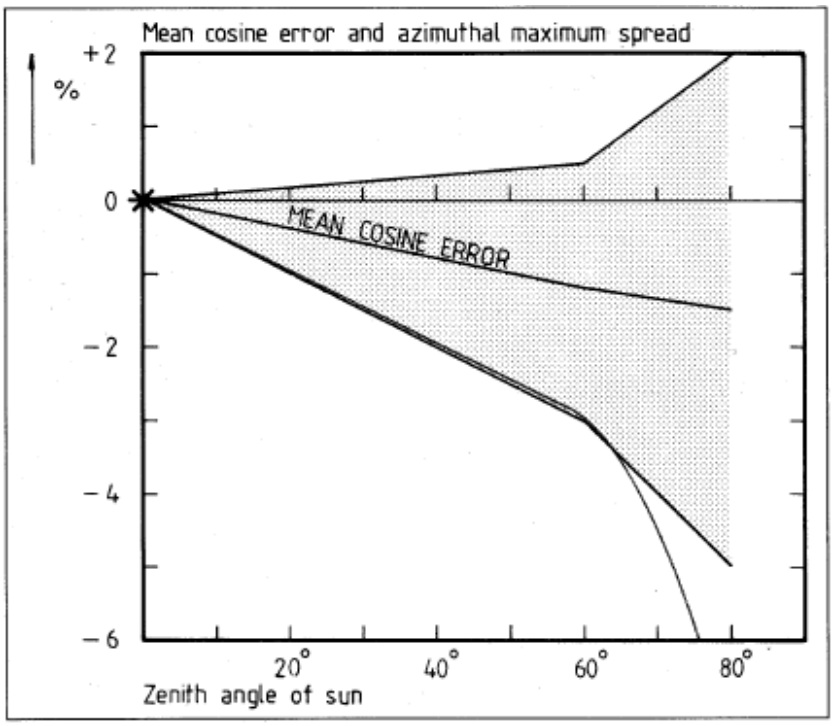

Figure A.1 – Mean cosine error and azimuthal maximum spread

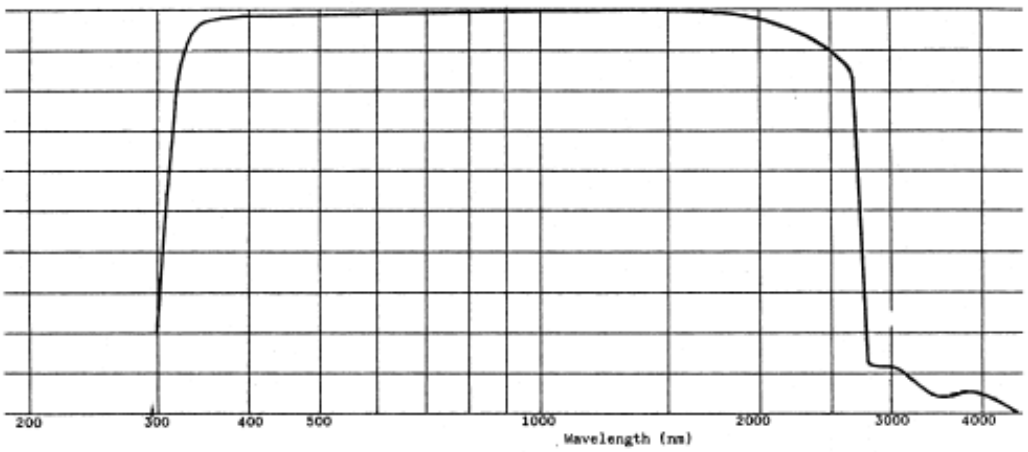

Figure A.2 - Relative transmittance vs. wavelength of two Schott K5 glass domes, each 2mm thick, as used in the CM 5. Four surface reflections (normal incidence), taking into account the index change with wavelength.

Appendix B – Results from the Interior laboratorial Surveys

C.1. – Specimen *Wnat*

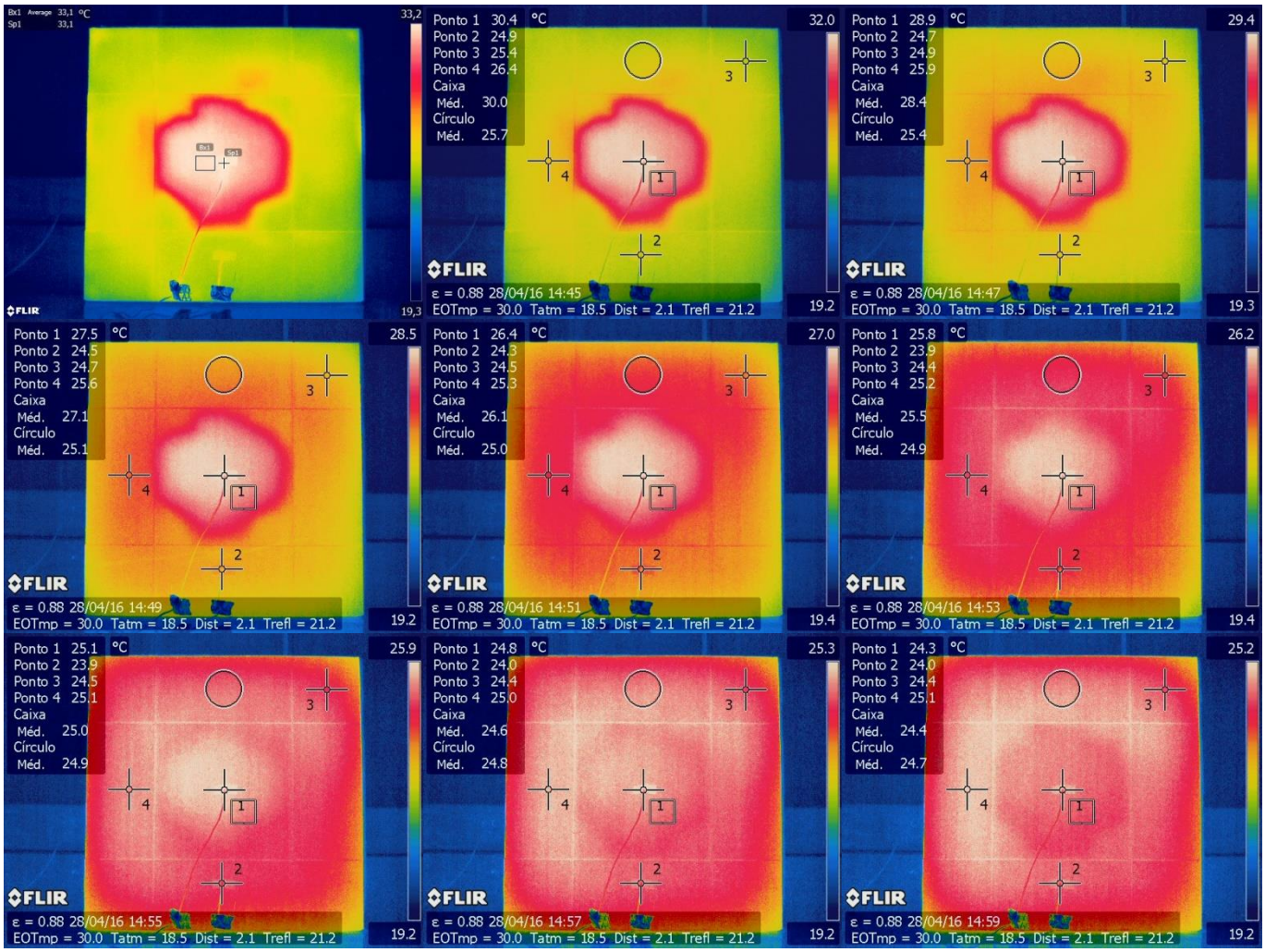

Figure B.1 – *Want* - Thermograms obtained during the first 18 min of survey

Table B.1 – Results from specimen *Wnat*

Phase	Accumulated time [hh:mm:ss]	Thermography												Thermocouples	
							Temperature [°C]							Temperature [°C]	
		ε	Trefl [°C]	Dist. [m]	Tamb [ºC]	Hr [%]	TDet	TAd	ΔT (Det-Ad)	Sp3	Sp4	Bx1	El1	TcDet	TcAd
Heating	00:00:00	-	-	-	-	-	-	-	-	-	-	-	-	26,53	23,83
	00:01:00	-	-	-	-	-	-	-	-	-	-	-	-	29,95	27,54
	00:02:00	-	-	-	-	-	-	-	-	-	-	-	-	30,84	28,05
	00:03:00	-	-	-	-	-	-	-	-	-	-	-	-	31,68	28,32
	00:04:00	-	-	-	-	-	-	-	-	-	-	-	-	32,48	28,52
	00:05:00	-	-	-	-	-	-	-	-	-	-	-	-	33,2	28,77
	00:06:00	-	-	-	-	-	-	-	-	-	-	-	-	33,87	28,99
	00:07:00	-	-	-	-	-	-	-	-	-	-	-	-	34,55	29,18
	00:08:00	-	-	-	-	-	-	-	-	-	-	-	-	35,1	29,43
	00:09:00	-	-	-	-	-	-	-	-	-	-	-	-	35,61	29,65
	00:10:00	-	-	-	-	-	-	-	-	-	-	-	-	36,04	29,85
	00:11:00	-	-	-	-	-	-	-	-	-	-	-	-	36,48	30,09
	00:12:00	-	-	-	-	-	-	-	-	-	-	-	-	36,86	30,33
	00:13:00	-	-	-	-	-	-	-	-	-	-	-	-	37,25	30,55
	00:14:00	-	-	-	-	-	-	-	-	-	-	-	-	37,59	30,79
	00:15:00	-	-	-	-	-	-	-	-	-	-	-	-	37,9	31,01
	00:16:00	-	-	-	-	-	-	-	-	-	-	-	-	38,24	31,27
	00:17:00	-	-	-	-	-	-	-	-	-	-	-	-	38,53	31,49
	00:18:00	-	-	-	-	-	-	-	-	-	-	-	-	38,81	31,73
	00:19:00	-	-	-	-	-	-	-	-	-	-	-	-	39,08	31,95
	00:20:00	-	-	-	-	-	-	-	-	-	-	-	-	39,34	32,16
Cooldown	00:23:10	0,88	21,2	2,1	18,5	61,9	33,5	27,5	6,0	26	27,6	32,1	26,7	32,5	25,7
	00:25:10	0,88	21,2	2,1	18,5	61,9	30,4	24,9	5,5	25,2	26,3	30	25,7	29,45	23,8
	00:27:10	0,88	21,2	2,1	18,5	61,9	28,9	24,7	4,2	24,7	25,8	28,4	25,4	27,76	23,47
	00:29:10	0,88	21,2	2,1	18,5	61,9	27,5	24,5	3,0	24,7	25,6	27,1	25,1	26,51	23,29
	00:31:10	0,88	21,2	2,1	18,5	61,9	26,4	24,3	2,1	24,6	25,2	26,1	25	25,55	23,14
	00:33:10	0,88	21,2	2,1	18,5	61,9	25,8	23,9	1,9	24,7	25,1	25,5	24,9	24,74	23,07
	00:35:10	0,88	21,2	2,1	18,5	61,9	25,1	23,9	1,2	24,4	25,2	25	24,9	24,2	23,04
	00:37:10	0,88	21,2	2,1	18,5	61,9	24,8	24,0	0,8	24,3	25	24,7	24,8	23,73	22,94
	00:39:10	0,88	21,2	2,1	18,5	61,9	24,3	24,0	0,3	24,4	25	24,4	24,7	23,43	22,89
	00:41:10	0,88	21,2	2,1	18,5	61,9	24,2	24,1	0,1	24	24,8	24,1	24,5	23,12	22,82
	00:43:10	0,88	21,2	2,1	18,5	61,9	23,9	23,9	0,0	24,1	24,6	23,9	24,5	22,89	22,77
	00:45:10	0,88	21,2	2,1	18,5	61,9	23,6	23,6	0,0	24	24,7	23,6	24,3	22,75	22,7
	00:47:10	0,88	21,2	2,1	18,5	61,9	23,4	23,6	-0,2	23,9	24,5	23,5	24,3	22,6	22,64
	00:49:10	0,88	21,2	2,1	18,5	61,9	23,5	23,5	0,0	23,9	24,4	23,5	24,2	22,53	22,57
	00:51:10	0,88	21,2	2,1	18,5	61,9	23,5	23,8	-0,3	23,9	24,4	23,5	24,2	22,4	22,53
	00:53:10	0,88	21,2	2,1	18,5	61,9	23,1	23,7	-0,6	23,7	24,4	23,4	24,1	22,35	22,48
	00:55:10	0,88	21,2	2,1	18,5	61,9	23,0	23,3	-0,3	23,5	24,3	23,3	24	22,28	22,43
	00:57:10	0,88	21,2	2,1	18,5	61,9	23,3	23,6	-0,3	23,6	24,3	23,3	24	22,23	22,35
	00:59:10	0,88	21,2	2,1	18,5	61,9	23,0	23,4	-0,4	23,6	24,2	23,2	23,9	22,21	22,33
	01:01:10	0,88	21,2	2,1	18,5	61,9	23,0	23,2	-0,2	23,4	23,9	23,1	23,8	22,18	22,28
	01:03:10	0,88	21,2	2,1	18,5	61,9	23,0	22,9	0,1	23,3	24,1	232	23,8	22,13	22,23
	01:05:10	0,88	21,2	2,1	18,5	61,9	22,9	23,2	-0,3	23,5	23,9	23,2	23,8	22,08	22,18
	01:08:20	0,88	21,2	2,1	18,5	61,9	23,2	23,2	0,0	23,2	24,1	23,1	23,6	22,01	22,08
	01:13:20	0,88	21,2	2,1	18,5	61,9	22,7	22,9	-0,2	23,1	23,9	23	23,4	21,96	21,99
	01:18:20	0,88	21,2	2,1	18,5	61,9	22,9	22,9	0,0	22,7	23,5	22,8	23,3	21,86	21,86
	01:23:20	0,88	21,2	2,1	18,5	61,9	23,1	22,9	0,2	22,8	23,5	22,9	23,3	21,79	21,73
	01:28:20	0,88	21,2	2,1	18,5	61,9	23,0	22,9	0,1	22,9	23,4	22,8	23,2	21,74	21,67
	01:33:20	0,88	21,2	2,1	18,5	61,9	22,9	22,8	0,1	22,6	23	22,7	23,1	21,69	21,62
	01:38:20	0,88	21,2	2,1	18,5	61,9	22,7	22,7	0,0	22,7	22,9	22,6	22,9	21,59	21,57
	01:43:20	0,88	21,2	2,1	18,5	61,9	22,8	22,8	0,0	22,5	22,9	22,7	22,9	21,52	21,44
	01:48:20	0,88	21,2	2,1	18,5	61,9	22,5	22,5	0,0	22,3	22,6	22,5	22,7	21,47	21,35
	01:53:20	0,88	21,2	2,1	18,5	61,9	22,3	22,2	0,1	22,1	22,5	22,3	22,5	21,4	21,27
	01:58:20	0,88	21,2	2,1	18,5	61,9	22,4	22,2	0,2	22	22,6	22,3	22,5	21,3	21,2
	02:03:20	0,88	21,2	2,1	18,5	61,9	22,2	22,3	-0,1	22,4	22,6	22,3	22,5	21,13	21,25
	02:08:20	0,88	21,2	2,1	18,5	61,9	22,0	22,3	-0,3	22,2	22,4	22,2	22,4	21,2	21,05
	02:13:20	0,88	21,2	2,1	18,5	61,9	21,9	22,2	-0,3	22,1	22,4	22,1	22,2	21,13	20,98
	02:18:20	0,88	21,2	2,1	18,5	61,9	22,1	22,0	0,1	21,9	22,2	22,1	22,3	21,05	20,9
	02:23:20	0,88	21,2	2,1	18,5	61,9	22,3	22,1	0,2	21,8	22,1	22,1	22,2	21	20,83
	22:06:29	0,88	21,2	2,1	18,4	64,1	18,8	19,0	-0,2	18,7	18,8	18,8	18,7	18,74	18,71

C.2. – Specimen Bnat

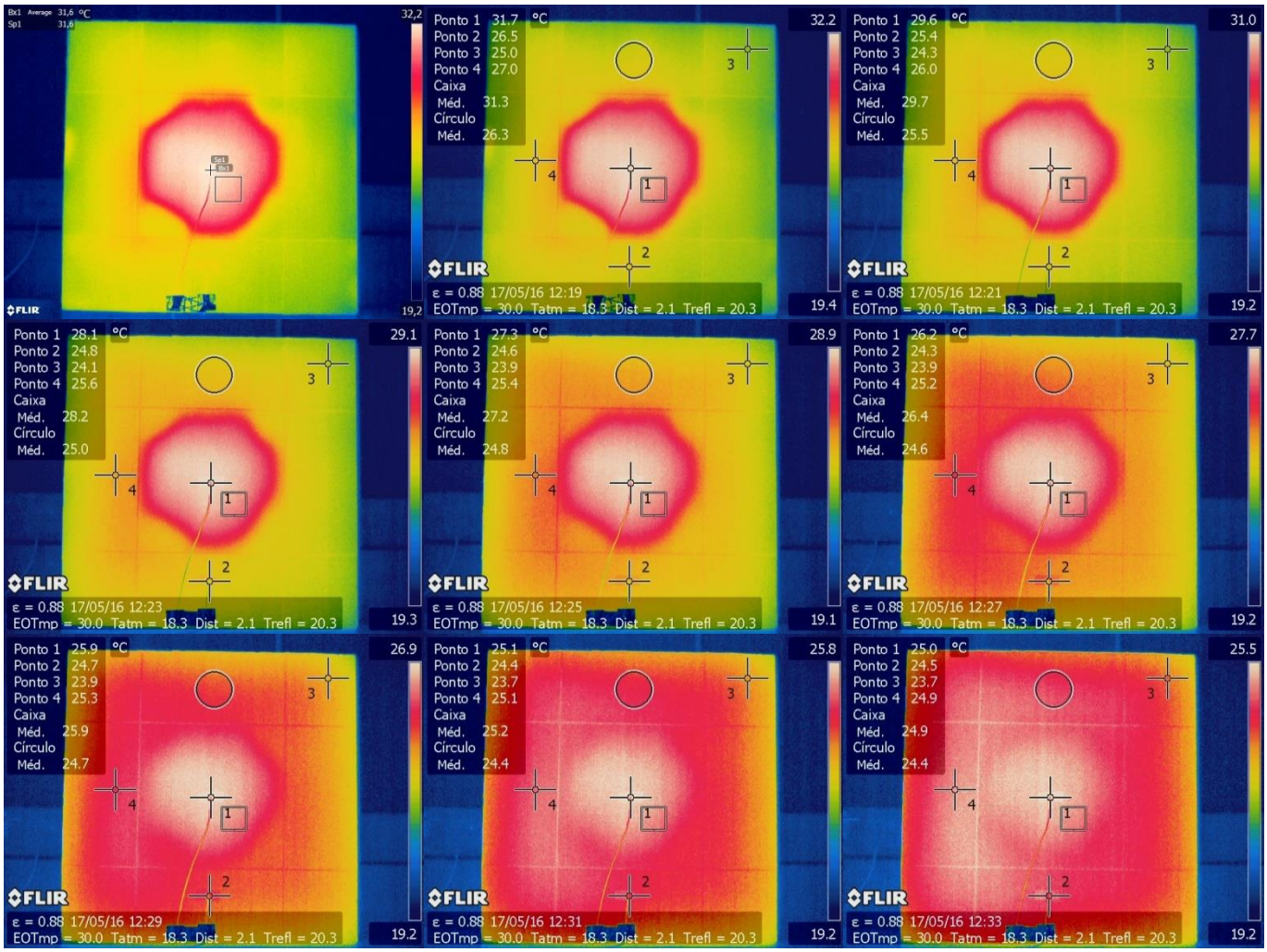

Figure B.2 – *Bnat* - Thermograms obtained during the first 18 min of survey

Table B.2 - Results from specimen Bnat

Phase	Accumulated time [hh:mm:ss]	Thermography												Thermocouples	
							Temperature [°C]							Temperature [°C]	
		ε	Trefl [°C]	Dist. [m]	Tamb [ºC]	Hr [%]	TDet	TAd	ΔT (Det-Ad)	Sp3	Sp4	Bx1	El1	TcDet	TcAd
Heating	00:00:00	-	-	-	-	-	-	-	-	-	-	-	-	19,09	27,76
	00:01:00	-	-	-	-	-	-	-	-	-	-	-	-	29,5	28,94
	00:02:00	-	-	-	-	-	-	-	-	-	-	-	-	30,4	29,21
	00:03:00	-	-	-	-	-	-	-	-	-	-	-	-	31,06	29,41
	00:04:00	-	-	-	-	-	-	-	-	-	-	-	-	31,73	29,63
	00:05:00	-	-	-	-	-	-	-	-	-	-	-	-	32,43	29,8
	00:06:00	-	-	-	-	-	-	-	-	-	-	-	-	33,06	30
	00:07:00	-	-	-	-	-	-	-	-	-	-	-	-	33,63	30,19
	00:08:00	-	-	-	-	-	-	-	-	-	-	-	-	34,19	30,38
	00:09:00	-	-	-	-	-	-	-	-	-	-	-	-	34,67	30,6
	00:10:00	-	-	-	-	-	-	-	-	-	-	-	-	35,15	30,81
	00:11:00	-	-	-	-	-	-	-	-	-	-	-	-	35,56	31,01
	00:12:00	-	-	-	-	-	-	-	-	-	-	-	-	35,97	31,2
	00:13:00	-	-	-	-	-	-	-	-	-	-	-	-	36,33	31,44
	00:14:00	-	-	-	-	-	-	-	-	-	-	-	-	36,72	31,63
	00:15:00	-	-	-	-	-	-	-	-	-	-	-	-	37,03	31,87
	00:16:00	-	-	-	-	-	-	-	-	-	-	-	-	37,39	32,12
	00:17:00	-	-	-	-	-	-	-	-	-	-	-	-	37,71	32,31
	00:18:00	-	-	-	-	-	-	-	-	-	-	-	-	37,97	32,53
	00:19:00	-	-	-	-	-	-	-	-	-	-	-	-	38,28	32,74
	00:20:00	-	-	-	-	-	-	-	-	-	-	-	-	38,57	32,96
Cooldown	00:21:00	0,88	20,3	2,1	18,3	66,3	31,9	26,6	5,3	25,2	27	31,4	26,4	31,39	25,89
	00:23:00	0,88	20,3	2,1	18,3	66,3	29,5	25,4	4,1	24,4	26	29,6	25,5	28,52	23,95
	00:25:00	0,88	20,3	2,1	18,3	66,3	28,3	24,8	3,5	24,1	25,6	28,2	25	27,19	23,53
	00:27:00	0,88	20,3	2,1	18,3	66,3	27,1	24,7	2,4	24,1	25,3	27,2	24,8	26,16	23,34
	00:29:00	0,88	20,3	2,1	18,3	66,3	26,2	24,6	1,6	23,9	25,3	26,4	24,7	25,38	23,19
	00:31:00	0,88	20,3	2,1	18,3	66,3	25,9	24,9	1	24	25,3	25,9	24,6	24,76	23,14
	00:33:00	0,88	20,3	2,1	18,3	66,3	25,3	24,4	0,9	23,6	25,3	25,3	24,5	24,22	23,04
	00:35:00	0,88	20,3	2,1	18,3	66,3	24,9	24,5	0,4	23,7	25	24,9	24,4	23,83	22,99
	00:37:00	0,88	20,3	2,1	18,3	66,3	24,6	24,3	0,3	23,5	24,7	24,5	24,3	23,43	22,89
	00:39:00	0,88	20,3	2,1	18,3	66,3	24,3	24,2	0,1	23,6	24,7	24,2	24,2	23,14	22,8
	00:41:00	0,88	20,3	2,1	18,3	66,3	24,1	24,1	0	23,6	24,6	24,1	24,2	22,97	22,75
	00:43:00	0,88	20,3	2,1	18,3	66,3	24	24,1	-0,1	23,6	24,7	24	24,2	22,77	22,7
	00:45:00	0,88	20,3	2,1	18,3	66,3	23,8	24	-0,2	23,4	24,6	23,8	24,1	22,6	22,62
	00:47:00	0,88	20,3	2,1	18,3	66,3	23,5	23,9	-0,4	23,3	24,4	23,6	24	22,5	22,6
	00:49:00	0,88	20,3	2,1	18,3	66,3	23,5	23,8	-0,3	23,4	24,3	23,5	24	22,38	22,55
	00:51:00	0,88	20,3	2,1	18,3	66,3	23,5	23,9	-0,4	23,1	24,4	23,5	23,9	22,26	22,48
	00:53:00	0,88	20,3	2,1	18,3	66,3	23,5	24,1	-0,6	23,2	24,4	23,5	24	22,16	22,4
	00:55:00	0,88	20,3	2,1	18,3	66,3	23,2	24	-0,8	23,1	24,2	23,3	23,8	22,13	22,35
	00:57:00	0,88	20,3	2,1	18,3	66,3	23,3	23,9	-0,6	22,9	24,2	23,3	23,8	22,08	22,33
	00:59:00	0,88	20,3	2,1	18,3	66,3	23,1	23,6	-0,5	23,1	24,1	23,2	23,7	22,03	22,28
	01:01:00	0,88	20,3	2,1	18,3	66,3	23,2	23,5	-0,3	23	24	23,2	23,7	21,99	22,21
	01:03:00	0,88	20,3	2,1	18,3	66,3	23,2	23,5	-0,3	22,9	23,8	23,1	23,6	21,94	22,16
	01:06:00	0,88	20,3	2,1	18,3	66,3	23	23,6	-0,6	22,8	23,8	23,1	23,5	21,89	22,08
	01:11:00	0,88	20,3	2,1	18,3	66,3	23	23,5	-0,5	23	23,8	23,1	23,5	21,79	22,01
	01:16:00	0,88	20,3	2,1	18,3	66,3	23,1	23,5	-0,4	22,5	23,6	23	23,4	21,74	21,89
	01:21:00	0,88	20,3	2,1	18,3	66,3	23	23,3	-0,3	22,4	23,6	22,9	23,3	21,64	21,76
	01:26:00	0,88	20,3	2,1	18,3	66,3	23,2	23,3	-0,1	22,1	23,4	23	23,2	21,62	21,71
	01:31:00	0,88	20,3	2,1	18,3	66,3	22	22,9	-0,9	22,4	23,2	22,8	23	21,57	21,64
	01:36:00	0,88	20,3	2,1	18,3	66,3	22,6	23	-0,4	22,5	23	22,7	22,9	21,47	21,52
	01:41:00	0,88	20,3	2,1	18,3	66,3	22,4	22,6	-0,2	22,4	23	22,5	22,8	21,42	21,44
	01:46:00	0,88	20,3	2,1	18,3	66,3	22,3	22,6	-0,3	22,1	22,6	22,4	22,7	21,32	21,32
	01:51:00	0,88	20,3	2,1	18,3	66,3	22,4	22,8	-0,4	22	23	22,5	22,7	21,3	21,3
	01:56:00	0,88	20,3	2,1	18,3	66,3	22,2	22,5	-0,3	21,9	22,4	22,3	22,5	21,2	21,2
	02:01:00	0,88	20,3	2,1	18,3	66,3	22,4	22,4	0	22	22,6	22,3	22,5	21,17	21,13
	02:06:00	0,88	20,3	2,1	18,3	66,3	22,2	22,2	0	21,9	22,5	22,3	22,4	21,1	21,05
	02:11:00	0,88	20,3	2,1	18,3	66,3	22,5	21,9	0,6	21,8	22,4	22,2	22,3	21,03	20,98
	02:21:00	0,88	20,3	2,1	18,3	66,3	22,1	22,2	-0,1	21,8	22,2	22,1	22,2	20,95	20,68

C.3. – Specimen *Wpol*

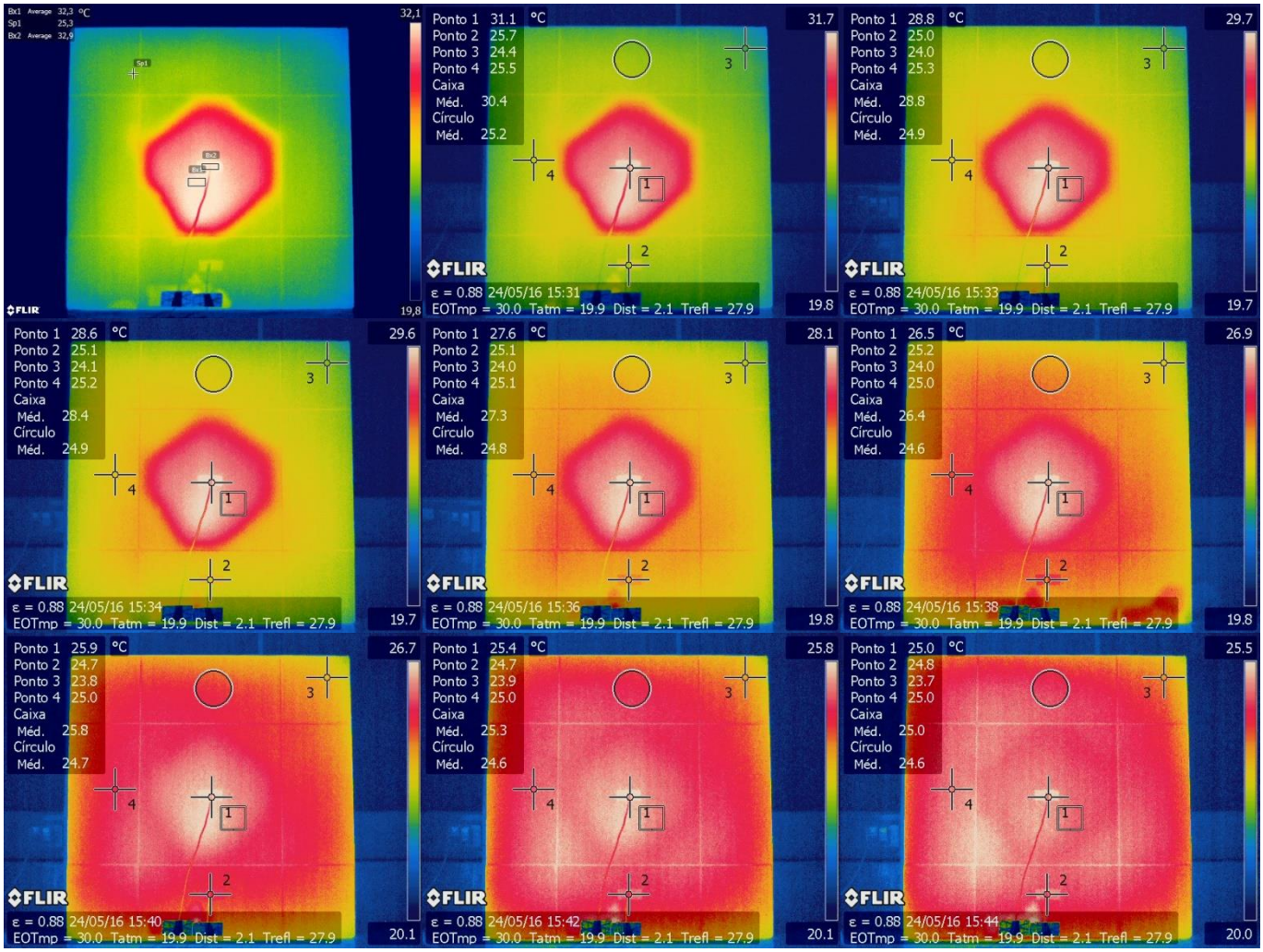

Figure B.3 – *Wpol* - Thermograms obtained during the first 18 min of survey

Table B.3 - Results from specimen Wpol

Phase	Accumulated time [hh:mm:ss]	Thermography												Thermocouples	
							Temperature [°C]							Temperature [°C]	
		ε	Trefl [°C]	Dist. [m]	Tamb [ºC]	Hr [%]	TDet	TAd	ΔT (Det-Ad)	Sp3	Sp4	Bx1	El1	TcDet	TcAd
Heating	00:00:00	-	-	-	-	-	-	-	-	-	-	-	-	20,17	20,17
	00:01:00	-	-	-	-	-	-	-	-	-	-	-	-	29,7	28,86
	00:02:00	-	-	-	-	-	-	-	-	-	-	-	-	31,03	30,91
	00:03:00	-	-	-	-	-	-	-	-	-	-	-	-	32,16	31,22
	00:04:00	-	-	-	-	-	-	-	-	-	-	-	-	33,18	31,39
	00:05:00	-	-	-	-	-	-	-	-	-	-	-	-	34,12	31,59
	00:06:00	-	-	-	-	-	-	-	-	-	-	-	-	34,93	31,75
	00:07:00	-	-	-	-	-	-	-	-	-	-	-	-	35,66	31,95
	00:08:00	-	-	-	-	-	-	-	-	-	-	-	-	36,31	32,19
	00:09:00	-	-	-	-	-	-	-	-	-	-	-	-	36,91	32,4
	00:10:00	-	-	-	-	-	-	-	-	-	-	-	-	37,42	32,65
	00:11:00	-	-	-	-	-	-	-	-	-	-	-	-	37,9	32,86
	00:12:00	-	-	-	-	-	-	-	-	-	-	-	-	38,33	33,13
	00:13:00	-	-	-	-	-	-	-	-	-	-	-	-	38,77	33,39
	00:14:00	-	-	-	-	-	-	-	-	-	-	-	-	39,13	33,66
	00:15:00	-	-	-	-	-	-	-	-	-	-	-	-	39,44	33,87
	00:16:00	-	-	-	-	-	-	-	-	-	-	-	-	39,78	34,14
	00:17:00	-	-	-	-	-	-	-	-	-	-	-	-	40,09	34,4
	00:18:00	-	-	-	-	-	-	-	-	-	-	-	-	40,42	34,67
	00:19:00	-	-	-	-	-	-	-	-	-	-	-	-	40,7	34,93
	00:20:00	-	-	-	-	-	-	-	-	-	-	-	-	40,96	35,18
Cooldown	00:22:00	0,88	27,9	2,1	19,9	67,9	32,1	26	6,1	24,5	25,8	31,1	25,4	32,4	26,04
	00:24:00	0,88	27,9	2,1	19,9	67,9	30,8	25,7	5,1	24,3	25,6	30,4	25,2	30,09	25,03
	00:26:00	0,88	27,9	2,1	19,9	67,9	28,5	24,9	3,6	24,1	25,4	28,3	24,8	28,57	24,74
	00:28:00	0,88	27,9	2,1	19,9	67,9	27,6	25	2,6	24	25,1	27,2	24,8	27,39	24,52
	00:30:00	0,88	27,9	2,1	19,9	67,9	26,5	25,1	1,4	24,1	25,1	26,4	24,6	26,51	24,44
	00:32:00	0,88	27,9	2,1	19,9	67,9	26	24,7	1,3	23,8	25	25,8	24,7	25,82	24,34
	00:34:00	0,88	27,9	2,1	19,9	67,9	25,4	24,8	0,6	23,8	25	25,3	24,6	25,25	24,27
	00:36:00	0,88	27,9	2,1	19,9	67,9	25	24,6	0,4	23,7	25	24,9	24,6	24,81	24,2
	00:38:00	0,88	27,9	2,1	19,9	67,9	24,7	24,6	0,1	23,6	24,9	24,7	24,6	24,49	24,15
	00:40:00	0,88	27,9	2,1	19,9	67,9	24,5	24,4	0,1	23,6	24,8	24,4	24,4	24,25	24,07
	00:42:00	0,88	27,9	2,1	19,9	67,9	24,3	24,6	-0,3	23,6	24,8	24,3	24,5	24,05	24,02
	00:44:00	0,88	27,9	2,1	19,9	67,9	24,2	24,6	-0,4	23,5	24,9	24,2	24,4	23,88	23,95
	00:46:00	0,88	27,9	2,1	19,9	67,9	23,9	24,1	-0,2	23,5	24,5	24	24,3	23,73	23,9
	00:48:00	0,88	27,9	2,1	19,9	67,9	23,9	24,2	-0,3	23,4	24,5	23,9	24,2	23,66	23,85
	00:50:00	0,88	27,9	2,1	19,9	67,9	24	24,3	-0,3	23,4	24,5	23,9	24,2	23,56	23,8
	00:52:00	0,88	27,9	2,1	19,9	67,9	23,8	24	-0,2	23,4	24,5	23,8	24,2	23,51	23,73
	00:54:00	0,88	27,9	2,1	19,9	67,9	23,7	24	-0,3	23,5	24,4	23,8	24,1	23,43	23,68
	00:56:00	0,88	27,9	2,1	19,9	67,9	23,7	23,8	-0,1	23,3	24,3	23,7	24	23,39	23,63
	00:58:00	0,88	27,9	2,1	19,9	67,9	23,5	23,8	-0,3	23,2	24,3	23,6	24	23,34	23,58
	01:00:00	0,88	27,9	2,1	19,9	67,9	23,3	23,7	-0,4	23	24,1	23,6	23,9	23,31	23,53
	01:02:00	0,88	27,9	2,1	19,9	67,9	23,3	23,7	-0,4	23,1	24,2	23,5	23,8	23,26	23,48
	01:04:00	0,88	27,9	2,1	19,9	67,9	23,4	23,8	-0,4	23,3	24	23,5	23,8	23,24	23,43
	01:07:00	0,88	27,9	2,1	19,9	67,9	23,5	23,7	-0,2	22,9	24	23,4	23,7	23,19	23,36
	01:12:00	0,88	27,9	2,1	19,9	67,9	23,2	23,5	-0,3	22,8	23,8	23,3	23,5	23,09	23,21
	01:17:00	0,88	27,9	2,1	19,9	67,9	23,1	23,5	-0,4	22,7	23,8	23,3	23,5	23,02	23,12
	01:22:00	0,88	27,9	2,1	19,9	67,9	23,1	23,3	-0,2	22,5	23,6	23,1	23,3	22,97	23,04
	01:27:00	0,88	27,9	2,1	19,9	67,9	23	23,2	-0,2	22,4	23,4	23	23,2	22,87	22,92
	01:32:00	0,88	27,9	2,1	19,9	67,9	23,1	23,2	-0,1	22,4	23,4	23	23,2	22,8	22,82
	01:37:00	0,88	27,9	2,1	19,9	67,9	22,8	23,2	-0,4	22,3	23,1	22,9	23	22,7	22,72
	01:42:00	0,88	27,9	2,1	19,9	67,9	22,9	23,1	-0,2	22,1	23	22,8	22,9	22,65	22,62
	01:47:00	0,88	27,9	2,1	19,9	67,9	22,7	23,1	-0,4	22,3	22,7	22,8	22,9	22,57	22,55
	01:52:00	0,88	27,9	2,1	19,9	67,9	22,8	23,1	-0,3	22,4	22,7	22,8	22,8	22,48	22,45
	01:57:00	0,88	27,9	2,1	19,9	67,9	22,7	22,7	0	22,2	22,7	22,6	22,7	22,43	22,38
	02:02:00	0,88	27,9	2,1	19,9	67,9	22,7	22,7	0	22,2	22,8	22,7	22,7	22,38	22,33
	02:07:00	0,88	27,9	2,1	19,9	67,9	22,6	22,6	0	21,9	22,9	22,5	22,6	22,33	22,26
	02:12:00	0,88	27,9	2,1	19,9	67,9	22,4	22,5	-0,1	21,9	22,6	22,5	22,5	22,26	22,18
	02:17:00	0,88	27,9	2,1	19,9	67,9	22,1	22,3	-0,2	21,8	22,5	22,3	22,4	22,21	22,13
	02:22:00	0,88	27,9	2,1	19,9	67,9	22,2	22,2	0	21,8	22,5	22,2	22,3	22,13	22,06

C.4. – Specimen *WI*

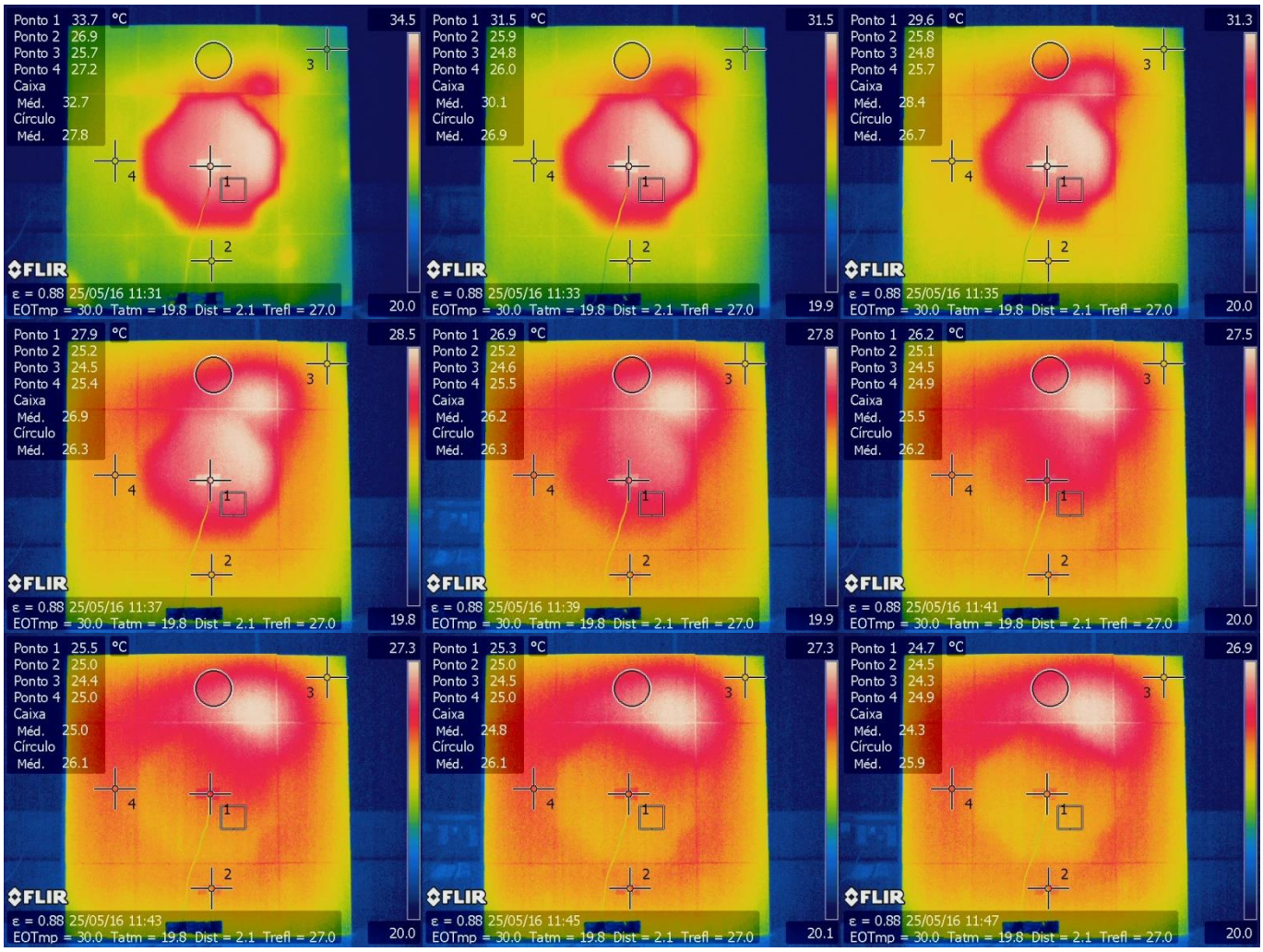

Figure B.4 –*WI* - Thermograms obtained during the first 18 min of survey

Table B.4 - Results from specimen WI

Phase	Accumulated time [hh:mm:ss]	Thermography												Thermocouples	
							Temperature [°C]							Temperature [°C]	
		ε	Trefl [°C]	Dist. [m]	Tamb [ºC]	Hr [%]	TDet	TAd	ΔT (Det-Ad)	Sp3	Sp4	Bx1	El1	TcDet	TcAd
Heating	00:00:00	-	-	-	-	-	-	-	-	-	-	-	-	20,07	20,07
	00:01:00	-	-	-	-	-	-	-	-	-	-	-	-	34,02	30,62
	00:02:00	-	-	-	-	-	-	-	-	-	-	-	-	34,4	31,18
	00:03:00	-	-	-	-	-	-	-	-	-	-	-	-	34,91	31,32
	00:04:00	-	-	-	-	-	-	-	-	-	-	-	-	35,46	31,42
	00:05:00	-	-	-	-	-	-	-	-	-	-	-	-	36	31,51
	00:06:00	-	-	-	-	-	-	-	-	-	-	-	-	36,5	31,66
	00:07:00	-	-	-	-	-	-	-	-	-	-	-	-	36,98	31,83
	00:08:00	-	-	-	-	-	-	-	-	-	-	-	-	37,39	31,97
	00:09:00	-	-	-	-	-	-	-	-	-	-	-	-	37,78	32,14
	00:10:00	-	-	-	-	-	-	-	-	-	-	-	-	38,14	32,33
	00:11:00	-	-	-	-	-	-	-	-	-	-	-	-	38,5	32,55
	00:12:00	-	-	-	-	-	-	-	-	-	-	-	-	38,81	32,74
	00:13:00	-	-	-	-	-	-	-	-	-	-	-	-	39,08	32,93
	00:14:00	-	-	-	-	-	-	-	-	-	-	-	-	39,37	33,13
	00:15:00	-	-	-	-	-	-	-	-	-	-	-	-	39,63	33,34
	00:16:00	-	-	-	-	-	-	-	-	-	-	-	-	39,87	33,54
	00:17:00	-	-	-	-	-	-	-	-	-	-	-	-	40,16	33,78
	00:18:00	-	-	-	-	-	-	-	-	-	-	-	-	40,4	34
	00:19:00	-	-	-	-	-	-	-	-	-	-	-	-	40,63	34,21
	00:20:00	-	-	-	-	-	-	-	-	-	-	-	-	40,87	34,43
Cooldown	00:21:00	0,88	27	2,1	19,8	66,5	33,9	26,9	7	25,7	27,3	32,7	27,8	33,13	26,85
	00:23:00	0,88	27	2,1	19,8	66,5	31,6	25,9	5,7	24,7	25,9	30,1	26,9	29,65	24,98
	00:25:00	0,88	27	2,1	19,8	66,5	29,6	25,9	3,7	24,7	25,6	28,5	26,7	27,88	24,61
	00:27:00	0,88	27	2,1	19,8	66,5	27,9	25,2	2,7	24,5	25,4	26,9	26,3	26,68	24,44
	00:29:00	0,88	27	2,1	19,8	66,5	27	25,3	1,7	24,6	25,5	26,2	26,4	25,77	24,34
	00:31:00	0,88	27	2,1	19,8	66,5	26,1	25,1	1	24,5	25	25,5	26,2	25,06	24,22
	00:33:00	0,88	27	2,1	19,8	66,5	25,8	25,2	0,6	24,5	25,1	25	26,2	24,57	24,15
	00:35:00	0,88	27	2,1	19,8	66,5	25,4	25	0,4	24,4	24,9	24,7	26,1	24,22	24,07
	00:37:00	0,88	27	2,1	19,8	66,5	24,7	24,9	-0,2	24,3	25	24,4	25,9	23,93	24
	00:39:00	0,88	27	2,1	19,8	66,5	24,6	24,8	-0,2	24,3	25	24,3	25,9	23,73	23,93
	00:41:00	0,88	27	2,1	19,8	66,5	24,4	24,8	-0,4	24,2	25	24,2	25,8	23,56	23,88
	00:43:00	0,88	27	2,1	19,8	66,5	24,1	24,8	-0,7	24,1	24,9	24	25,7	23,46	23,8
	00:45:00	0,88	27	2,1	19,8	66,5	24	24,6	-0,6	23,9	24,8	23,9	25,6	23,36	23,75
	00:47:00	0,88	27	2,1	19,8	66,5	24,1	24,4	-0,3	23,9	24,8	23,9	25,6	23,29	23,71
	00:49:00	0,88	27	2,1	19,8	66,5	24,3	24,6	-0,3	24	24,9	24	25,6	23,21	23,66
	00:51:00	0,88	27	2,1	19,8	66,5	24,2	24,6	-0,4	24	24,9	23,9	25,5	23,16	23,58
	00:53:00	0,88	27	2,1	19,8	66,5	23,6	24,2	-0,6	23,8	24,5	23,7	25,2	23,14	23,53
	00:55:00	0,88	27	2,1	19,8	66,5	23,6	24,2	-0,6	23,8	24,2	23,6	25,1	23,12	23,48
	00:57:00	0,88	27	2,1	19,8	66,5	23,7	24,1	-0,4	23,8	24,3	23,6	25,1	23,09	23,43
	00:59:00	0,88	27	2,1	19,8	66,5	23,7	24	-0,3	23,8	24,3	23,7	25,1	23,07	23,39
	01:01:00	0,88	27	2,1	19,8	66,5	23,6	24	-0,4	23,8	24,1	23,6	25	23,07	23,36
	01:03:00	0,88	27	2,1	19,8	66,5	23,6	24	-0,4	23,5	24,2	23,6	24,9	23,02	23,29
	01:06:00	0,88	27	2,1	19,8	66,5	23,6	24,1	-0,5	23,8	24,1	23,7	24,8	22,97	23,21
	01:11:00	0,88	27	2,1	19,8	66,5	23,7	24,1	-0,4	23,6	23,9	23,5	24,7	22,92	23,12
	01:16:00	0,88	27	2,1	19,8	66,5	23,9	23,9	0	23,4	23,9	23,5	24,5	22,89	23,04
	01:21:00	0,88	27	2,1	19,8	66,5	23,7	23,9	-0,2	23,1	23,9	23,5	24,4	22,85	22,94
	01:26:00	0,88	27	2,1	19,8	66,5	23,6	23,6	0	23,2	23,6	23,4	24,2	22,8	22,87
	01:31:00	0,88	27	2,1	19,8	66,5	23,3	23,6	-0,3	23,1	23,5	23,3	24,1	22,75	22,8
	01:36:00	0,88	27	2,1	19,8	66,5	23,4	23,7	-0,3	23,1	23,4	23,3	24,1	22,67	22,7
	01:41:00	0,88	27	2,1	19,8	66,5	23,3	23,2	0,1	22,8	23,3	23,2	23,8	22,65	22,65
	01:46:00	0,88	27	2,1	19,8	66,5	23,1	23,2	-0,1	22,8	23,3	23,1	23,7	22,57	22,55
	01:51:00	0,88	27	2,1	19,8	66,5	22,9	22,9	0	22,7	23,1	22,9	23,5	22,5	22,5
	01:56:00	0,88	27	2,1	19,8	66,5	23,1	23	0,1	22,6	23,2	22,9	23,5	22,48	22,45
	02:01:00	0,88	27	2,1	19,8	66,5	22,9	23	-0,1	22,4	22,9	22,7	23,2	22,4	22,35
	02:06:00	0,88	27	2,1	19,8	66,5	23	22,7	0,3	22,5	23	22,7	23,1	22,4	22,33
	02:11:00	0,88	27	2,1	19,8	66,5	23	23	0	22,4	22,8	22,8	23,2	22,3	22,23
	02:16:00	0,88	27	2,1	19,8	66,5	22,8	22,8	0	22,3	22,8	22,7	23,1	22,26	22,18
	02:21:00	0,88	27	2,1	19,8	66,5	22,6	22,4	0,2	22,4	22,5	22,5	22,9	22,23	22,13

C.5. – Specimen *BI*

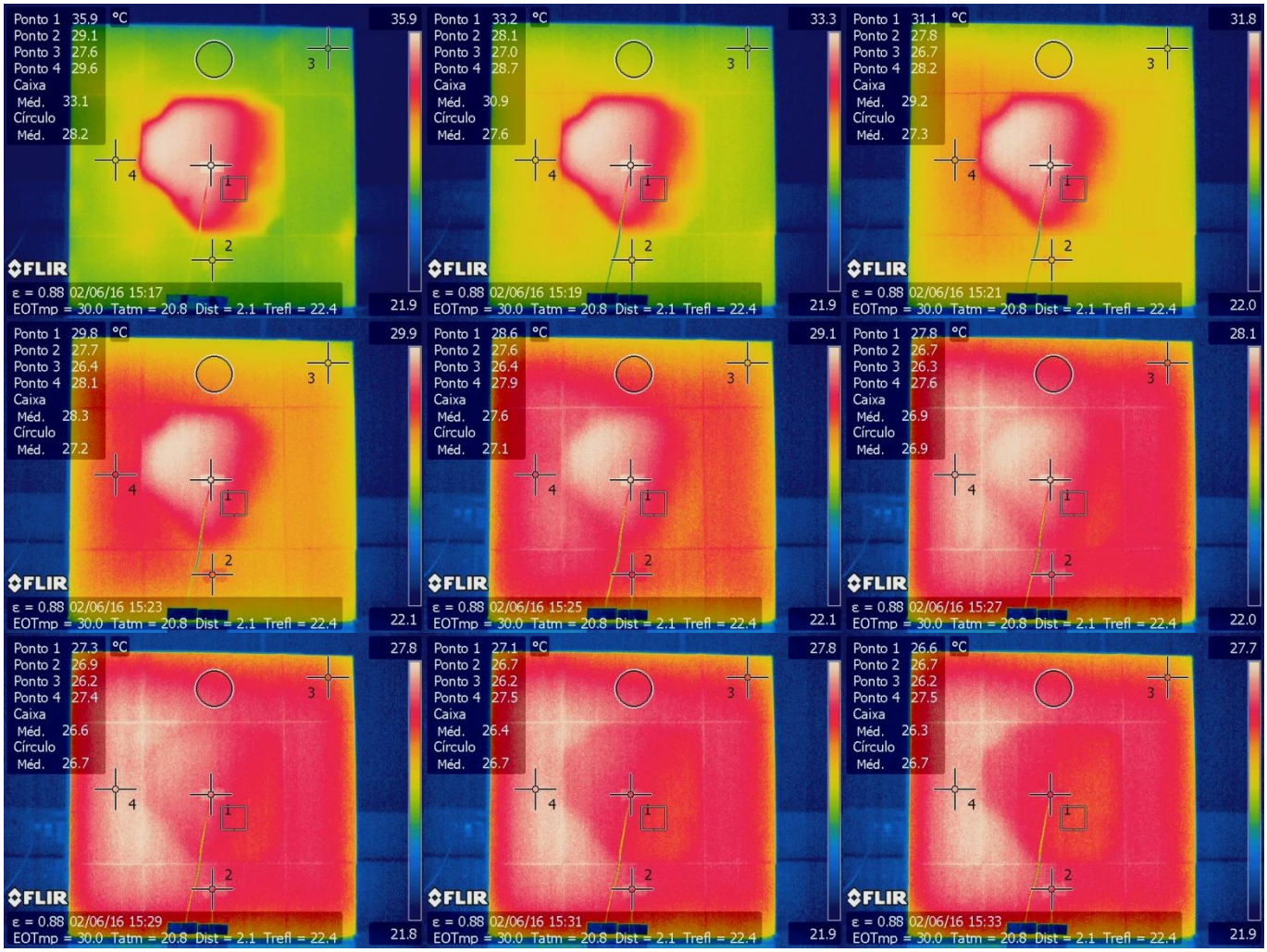

Figure B.5 – *BI* - Thermograms obtained during the first 18 min of survey

Table B.5 - Results from specimen Bl

Phase	Accumulated time [hh:mm:ss]	Thermography												Thermocouples	
							Temperature [°C]							Temperature [°C]	
		ε	Trefl [°C]	Dist. [m]	Tamb [ºC]	Hr [%]	TDet	TAd	ΔT (Det-Ad)	Sp3	Sp4	Bx1	El1	TcDet	TcAd
Heating	00:00:00	-	-	-	-	-	-	-	-	-	-	-	-	21,49	21,52
	00:01:00	-	-	-	-	-	-	-	-	-	-	-	-	34,86	29,87
	00:02:00	-	-	-	-	-	-	-	-	-	-	-	-	35,78	30,69
	00:03:00	-	-	-	-	-	-	-	-	-	-	-	-	36,62	31,03
	00:04:00	-	-	-	-	-	-	-	-	-	-	-	-	37,39	31,3
	00:05:00	-	-	-	-	-	-	-	-	-	-	-	-	38,07	31,49
	00:06:00	-	-	-	-	-	-	-	-	-	-	-	-	38,67	31,71
	00:07:00	-	-	-	-	-	-	-	-	-	-	-	-	39,2	31,9
	00:08:00	-	-	-	-	-	-	-	-	-	-	-	-	39,66	32,12
	00:09:00	-	-	-	-	-	-	-	-	-	-	-	-	40,16	32,4
	00:10:00	-	-	-	-	-	-	-	-	-	-	-	-	40,54	32,6
	00:11:00	-	-	-	-	-	-	-	-	-	-	-	-	40,89	32,86
	00:12:00	-	-	-	-	-	-	-	-	-	-	-	-	41,2	33,08
	00:13:00	-	-	-	-	-	-	-	-	-	-	-	-	41,44	33,3
	00:14:00	-	-	-	-	-	-	-	-	-	-	-	-	41,76	33,56
	00:15:00	-	-	-	-	-	-	-	-	-	-	-	-	42	33,78
	00:16:00	-	-	-	-	-	-	-	-	-	-	-	-	42,32	34,04
	00:17:00	-	-	-	-	-	-	-	-	-	-	-	-	42,56	34,26
	00:18:00	-	-	-	-	-	-	-	-	-	-	-	-	42,8	34,53
	00:19:00	-	-	-	-	-	-	-	-	-	-	-	-	43,04	34,77
	00:20:00	-	-	-	-	-	-	-	-	-	-	-	-	43,28	35,01
Cooldown	00:21:00	0,88	22,4	2,1	20,8	61	35,9	29	6,9	27,5	29,6	33,1	28,2	34,69	28,25
	00:23:00	0,88	22,4	2,1	20,8	61	33,2	28,1	5,1	26,9	28,7	30,8	27,6	30,84	26,43
	00:25:00	0,88	22,4	2,1	20,8	61	31	27,7	3,3	26,7	28,3	29,3	27,3	28,94	26,06
	00:27:00	0,88	22,4	2,1	20,8	61	29,6	27,6	2	26,5	28,2	28,2	27,2	27,66	25,87
	00:29:00	0,88	22,4	2,1	20,8	61	28,7	27,3	1,4	26,4	28	27,6	27,1	26,78	25,72
	00:31:00	0,88	22,4	2,1	20,8	61	27,8	26,8	1	26,3	27,5	26,9	26,9	26,11	25,67
	00:33:00	0,88	22,4	2,1	20,8	61	27,4	27,1	0,3	26,3	27,5	26,6	26,8	25,67	25,55
	00:35:00	0,88	22,4	2,1	20,8	61	26,9	26,8	0,1	26	27,4	26,4	26,7	25,33	25,42
	00:37:00	0,88	22,4	2,1	20,8	61	26,6	26,5	0,1	26,3	27,5	26,3	26,7	25,08	25,38
	00:39:00	0,88	22,4	2,1	20,8	61	26,5	26,7	-0,2	26,2	27,5	26,2	26,7	24,88	25,3
	00:41:00	0,88	22,4	2,1	20,8	61	26,4	26,7	-0,3	26,2	27,4	26,2	26,6	24,76	25,23
	00:43:00	0,88	22,4	2,1	20,8	61	26,1	26,5	-0,4	26	27,3	25,9	26,5	24,71	25,15
	00:45:00	0,88	22,4	2,1	20,8	61	26	26,7	-0,7	25,8	27,1	25,9	26,4	24,59	25,08
	00:47:00	0,88	22,4	2,1	20,8	61	26	26,4	-0,4	25,9	27	25,8	26,3	24,54	25,03
	00:49:00	0,88	22,4	2,1	20,8	61	25,9	26,4	-0,5	25,8	26,9	25,8	26,3	24,47	24,93
	00:51:00	0,88	22,4	2,1	20,8	61	26	26,6	-0,6	25,6	26,8	25,8	26,3	24,44	24,88
	00:53:00	0,88	22,4	2,1	20,8	61	25,9	26,3	-0,4	25,5	26,9	25,7	26,1	24,39	24,84
	00:55:00	0,88	22,4	2,1	20,8	61	25,8	26,3	-0,5	25,6	26,8	25,7	25,8	24,37	24,79
	00:57:00	0,88	22,4	2,1	20,8	61	25,8	26	-0,2	25,5	26,5	25,6	26	24,34	24,74
	00:59:00	0,88	22,4	2,1	20,8	61	25,8	26,1	-0,3	25,4	26,6	25,6	26	24,29	24,69
	01:01:00	0,88	22,4	2,1	20,8	61	25,8	26,3	-0,5	25,3	26,5	25,6	26	24,29	24,64
	01:03:00	0,88	22,4	2,1	20,8	61	25,8	26	-0,2	25,3	26,5	25,6	25,9	24,25	24,59
	01:06:00	0,88	22,4	2,1	20,8	61	25,8	26	-0,2	25,3	26,4	25,5	25,8	24,2	24,52
	01:11:00	0,88	22,4	2,1	20,8	61	25,5	26,1	-0,6	25,2	26,2	25,4	25,7	24,07	24,34
	01:16:00	0,88	22,4	2,1	20,8	61	25,5	25,7	-0,2	25	26	25,3	25,6	24,02	24,27
	01:21:00	0,88	22,4	2,1	20,8	61	25,4	25,6	-0,2	24,9	25,9	25,3	25,5	23,98	24,15
	01:26:00	0,88	22,4	2,1	20,8	61	25,3	25,4	-0,1	24,6	25,9	25,2	25,4	23,9	24,05
	01:31:00	0,88	22,4	2,1	20,8	61	25,4	25,5	-0,1	24,7	25,8	25,2	25,3	23,83	23,95
	01:36:00	0,88	22,4	2,1	20,8	61	25,4	25,6	-0,2	24,5	25,7	25,3	25,3	23,75	23,85
	01:41:00	0,88	22,4	2,1	20,8	61	25,4	25,5	-0,1	24,5	25,6	25,2	25,3	23,68	23,78
	01:46:00	0,88	22,4	2,1	20,8	61	25,2	25,4	-0,2	24,6	25,4	25,1	25,1	23,63	23,71
	01:51:00	0,88	22,4	2,1	20,8	61	25,1	25,1	0	24,6	25,1	25	25	23,53	23,61
	01:56:00	0,88	22,4	2,1	20,8	61	25,1	25,2	-0,1	24,5	25,2	25,1	25,1	23,53	23,56
	02:01:00	0,88	22,4	2,1	20,8	61	24,8	24,8	0	24,9	24,4	24,8	24,8	23,46	23,48
	02:06:00	0,88	22,4	2,1	20,8	61	24,8	24,9	-0,1	24,2	24,8	24,7	24,7	23,39	23,41
	02:11:00	0,88	22,4	2,1	20,8	61	24,8	24,9	-0,1	24,3	24,8	24,7	24,6	23,34	23,34
	02:16:00	0,88	22,4	2,1	20,8	61	24,8	24,7	0,1	24,2	24,8	24,6	24,6	23,29	23,29
	02:21:00	0,88	22,4	2,1	20,8	61	24,7	24,6	0,1	24,3	24,7	24,6	24,6	23,24	23,24

C.6. – Specimen *Bti*

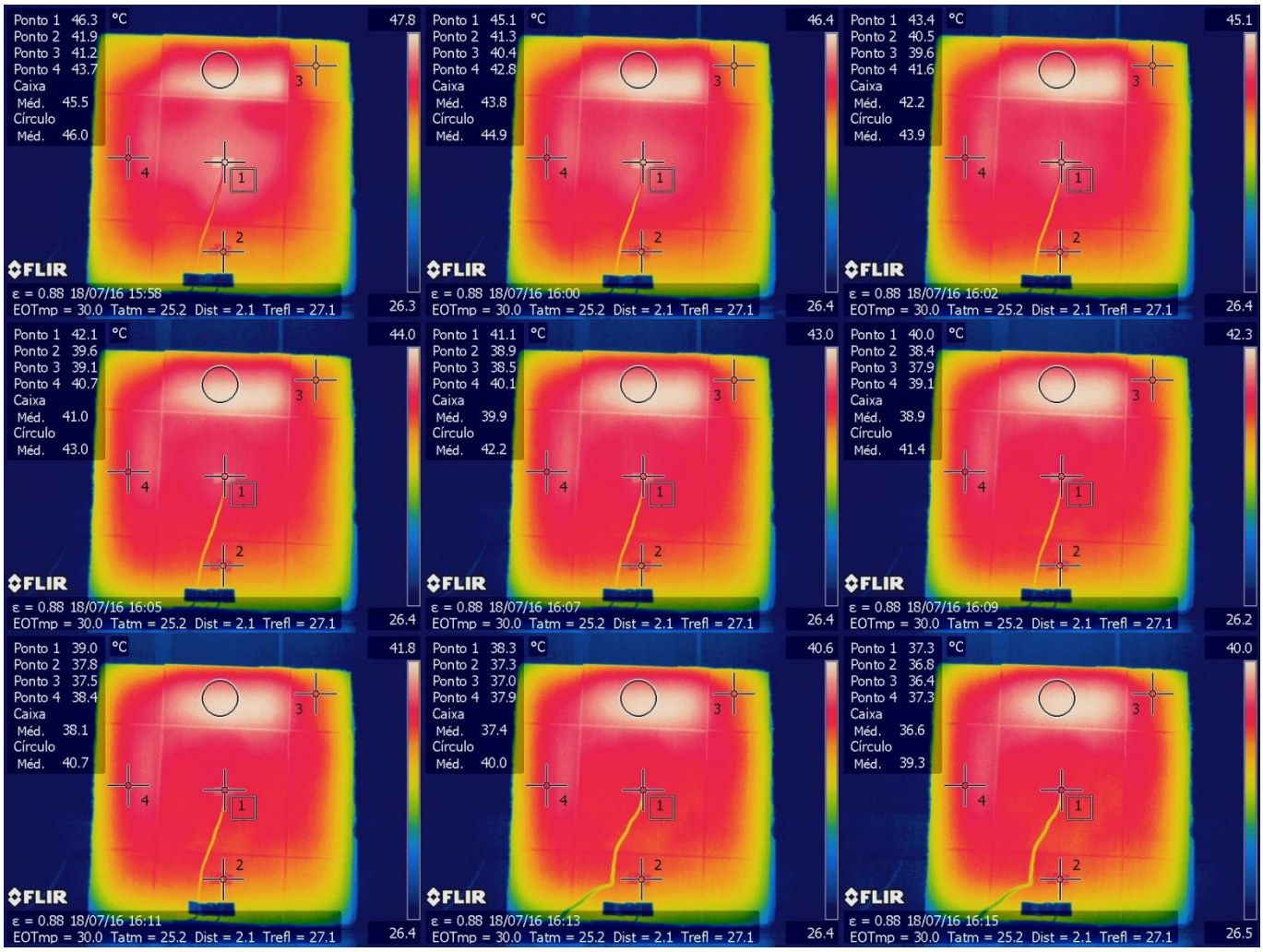

Figure B.6 – *Bti* - Thermograms obtained during the first 18 min of survey

Table B.6 - Results from specimen Bti

Phase	Accumulated time [hh:mm:ss]	Thermography												Thermocouples	
							Temperature [°C]							Temperature [°C]	
		ε	Trefl [°C]	Dist. [m]	Tamb [ºC]	Hr [%]	TDet	TAd	ΔT (Det-Ad)	Sp3	Sp4	Bx1	El1	TcDet	TcAd
Heating	00:00:00	-	-	-	-	-	-	-	-	-	-	-	-	25,5	25,67
	00:01:00	-	-	-	-	-	-	-	-	-	-	-	-	36,21	35,78
	00:02:00	-	-	-	-	-	-	-	-	-	-	-	-	37,06	36,6
	00:03:00	-	-	-	-	-	-	-	-	-	-	-	-	37,97	37,1
	00:04:00	-	-	-	-	-	-	-	-	-	-	-	-	38,86	37,68
	00:05:00	-	-	-	-	-	-	-	-	-	-	-	-	39,8	38,28
	00:06:00	-	-	-	-	-	-	-	-	-	-	-	-	40,68	38,89
	00:07:00	-	-	-	-	-	-	-	-	-	-	-	-	41,68	39,51
	00:08:00	-	-	-	-	-	-	-	-	-	-	-	-	42,48	40,14
	00:09:00	-	-	-	-	-	-	-	-	-	-	-	-	43,2	40,75
	00:10:00	-	-	-	-	-	-	-	-	-	-	-	-	44,08	41,36
	00:11:00	-	-	-	-	-	-	-	-	-	-	-	-	44,88	42
	00:12:00	-	-	-	-	-	-	-	-	-	-	-	-	45,68	42,64
	00:13:00	-	-	-	-	-	-	-	-	-	-	-	-	46,4	43,28
	00:14:00	-	-	-	-	-	-	-	-	-	-	-	-	47,28	43,92
	00:15:00	-	-	-	-	-	-	-	-	-	-	-	-	48	44,56
	00:16:00	-	-	-	-	-	-	-	-	-	-	-	-	48,72	45,12
	00:17:00	-	-	-	-	-	-	-	-	-	-	-	-	49,52	45,76
	00:18:00	-	-	-	-	-	-	-	-	-	-	-	-	50,24	46,4
	00:19:00	-	-	-	-	-	-	-	-	-	-	-	-	50,96	47,04
	00:20:00	-	-	-	-	-	-	-	-	-	-	-	-	51,68	47,6
Cooldown	00:21:00	0,88	27,1	2,1	25,2	59	47,3	42,5	4,8	41	43,8	45,5	46	43,76	40,07
	00:23:00	0,88	27,1	2,1	25,2	59	45,3	41,3	4	40,4	42,8	43,8	44,9	40,51	38,09
	00:25:00	0,88	27,1	2,1	25,2	59	43,5	40,6	2,9	39,7	41,7	42,2	43,9	39,06	37,3
	00:27:00	0,88	27,1	2,1	25,2	59	42,2	39,7	2,5	39,1	40,7	41	43	37,92	36,5
	00:29:00	0,88	27,1	2,1	25,2	59	40,9	39	1,9	38,4	40	39,9	42,2	36,93	35,85
	00:31:00	0,88	27,1	2,1	25,2	59	39,9	38,4	1,5	37,8	39,2	38,9	41,4	36,07	35,25
	00:33:00	0,88	27,1	2,1	25,2	59	39,1	37,7	1,4	37,5	38,5	38,1	40,7	35,34	34,65
	00:35:00	0,88	27,1	2,1	25,2	59	38,4	37,3	1,1	36,9	37,8	37,4	40	32,84	34,14
	00:37:00	0,88	27,1	2,1	25,2	59	37,4	36,9	0,5	36,5	37,3	36,6	39,3	31,87	33,63
	00:39:00	0,88	27,1	2,1	25,2	59	36,3	36	0,3	35,8	36,7	35,9	38,6	31,3	33,15
	00:41:00	0,88	27,1	2,1	25,2	59	35,9	35,6	0,3	35,5	36,2	35,4	38,1	30,86	32,74
	00:43:00	0,88	27,1	2,1	25,2	59	35,2	35,2	0	35	35,7	34,8	37,5	30,5	32,33
	00:45:00	0,88	27,1	2,1	25,2	59	34,6	34,7	-0,1	34,5	35,2	34,3	37	30,12	31,92
	00:47:00	0,88	27,1	2,1	25,2	59	34,2	34,3	-0,1	34,2	34,8	33,9	36,5	29,8	31,54
	00:49:00	0,88	27,1	2,1	25,2	59	33,5	33,9	-0,4	33,7	34,3	33,4	35,9	29,53	31,22
	00:51:00	0,88	27,1	2,1	25,2	59	33,2	33,5	-0,3	33,6	33,9	33	35,6	29,33	30,89
	00:53:00	0,88	27,1	2,1	25,2	59	32,6	32,7	-0,1	32,8	33,1	32,3	34,8	29,06	30,55
	00:55:00	0,88	27,1	2,1	25,2	59	32,1	32,3	-0,2	32,6	32,6	32	34,4	28,82	30,28
	00:57:00	0,88	27,1	2,1	25,2	59	31,9	32,3	-0,4	32,2	32,5	31,7	34	28,62	30,04
	00:59:00	0,88	27,1	2,1	25,2	59	31,5	31,9	-0,4	31,9	32,1	31,3	33,6	28,42	29,77
	01:01:00	0,88	27,1	2,1	25,2	59	31,3	31,5	-0,2	31,6	31,9	31,1	33,3	28,23	29,53
	01:03:00	0,88	27,1	2,1	25,2	59	30,9	31,3	-0,4	31,3	31,6	30,8	33	28,08	29,33
	01:06:00	0,88	27,1	2,1	25,2	59	30,6	31	-0,4	30,9	31,3	30,5	32,5	27,83	29,01
	01:11:00	0,88	27,1	2,1	25,2	59	30,2	30,4	-0,2	30,6	30,5	29,9	31,8	27,51	28,55
	01:16:00	0,88	27,1	2,1	25,2	59	29,7	30	-0,3	30,1	29,9	29,5	31,2	27,22	28,18
	01:21:00	0,88	27,1	2,1	25,2	59	29,3	29,6	-0,3	29,6	29,4	29,1	30,6	26,97	27,83
	01:26:00	0,88	27,1	2,1	25,2	59	29	29,1	-0,1	29,2	29,1	28,8	30,2	26,83	27,54
	01:31:00	0,88	27,1	2,1	25,2	59	28,8	28,9	-0,1	29,1	28,9	28,6	29,8	26,63	27,27
	01:36:00	0,88	27,1	2,1	25,2	59	28,4	28,7	-0,3	28,9	28,6	28,4	29,5	26,43	27,02
	01:41:00	0,88	27,1	2,1	25,2	59	28,1	28,5	-0,4	28,7	28,4	28,1	29,1	26,36	26,8
	01:46:00	0,88	27,1	2,1	25,2	59	28	28,2	-0,2	28,4	28,2	27,9	28,8	26,19	26,65
	01:51:00	0,88	27,1	2,1	25,2	59	27,8	28	-0,2	28,1	28	27,7	28,5	26,09	26,51
	01:56:00	0,88	27,1	2,1	25,2	59	27,8	27,9	-0,1	27,8	28	27,8	28,5	26,01	26,38
	02:01:00	0,88	27,1	2,1	25,2	59	27,5	27,8	-0,3	27,6	27,7	27,6	28,2	25,94	26,28
	02:06:00	0,88	27,1	2,1	25,2	59	27,4	27,6	-0,2	27,6	27,6	27,5	28	25,89	26,19
	02:11:00	0,88	27,1	2,1	25,2	59	27,4	27,6	-0,2	27,8	27,7	27,4	27,9	25,87	26,14
	02:16:00	0,88	27,1	2,1	25,2	59	27,3	27,4	-0,1	27,5	27,4	27,3	27,8	25,79	26,04
	02:21:00	0,88	27,1	2,1	25,2	59	27,4	27,5	-0,1	27,5	27,5	27,3	27,7	25,72	25,97

C.7. – Specimen *Wti*

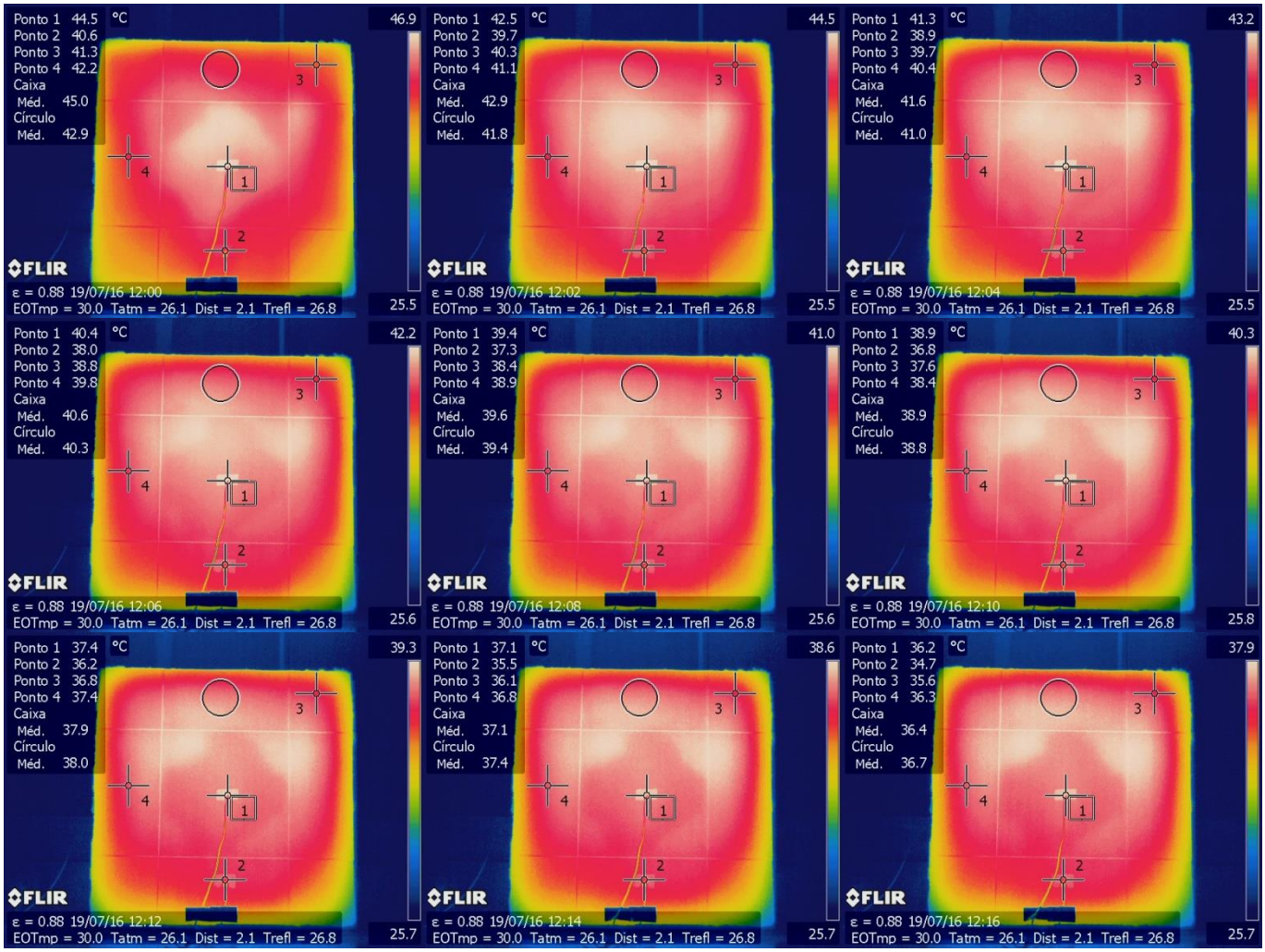

Figure B.7 – *Wti* - Thermograms obtained during the first 18 min of survey

Table 7 - Results from specimen Wti

Phase	Accumulated time [hh:mm:ss]	Thermography												Thermocouples	
							Temperature [°C]							Temperature [°C]	
		ε	Trefl [°C]	Dist. [m]	Tamb [ºC]	Hr [%]	TDet	TAd	ΔT (Det-Ad)	Sp3	Sp4	Bx1	El1	TcDet	TcAd
Heating	00:00:00	-	-	-	-	-	-	-	-	-	-	-	-	25,03	25,06
	00:01:00	-	-	-	-	-	-	-	-	-	-	-	-	39,13	36,04
	00:02:00	-	-	-	-	-	-	-	-	-	-	-	-	39,59	36,89
	00:03:00	-	-	-	-	-	-	-	-	-	-	-	-	40,18	37,42
	00:04:00	-	-	-	-	-	-	-	-	-	-	-	-	40,8	38
	00:05:00	-	-	-	-	-	-	-	-	-	-	-	-	41,44	38,62
	00:06:00	-	-	-	-	-	-	-	-	-	-	-	-	42,16	39,3
	00:07:00	-	-	-	-	-	-	-	-	-	-	-	-	42,88	39,97
	00:08:00	-	-	-	-	-	-	-	-	-	-	-	-	43,68	40,7
	00:09:00	-	-	-	-	-	-	-	-	-	-	-	-	44,4	41,36
	00:10:00	-	-	-	-	-	-	-	-	-	-	-	-	45,12	42
	00:11:00	-	-	-	-	-	-	-	-	-	-	-	-	45,84	42,72
	00:12:00	-	-	-	-	-	-	-	-	-	-	-	-	46,72	43,44
	00:13:00	-	-	-	-	-	-	-	-	-	-	-	-	47,36	44,08
	00:14:00	-	-	-	-	-	-	-	-	-	-	-	-	48,16	44,8
	00:15:00	-	-	-	-	-	-	-	-	-	-	-	-	48,88	45,44
	00:16:00	-	-	-	-	-	-	-	-	-	-	-	-	49,68	46,16
	00:17:00	-	-	-	-	-	-	-	-	-	-	-	-	50,4	46,8
	00:18:00	-	-	-	-	-	-	-	-	-	-	-	-	51,04	47,44
	00:19:00	-	-	-	-	-	-	-	-	-	-	-	-	51,76	48,16
	00:20:00	-	-	-	-	-	-	-	-	-	-	-	-	52,48	48,8
Cooldown	00:21:00	0,88	26,8	2,1	26,1	53	44,4	40,7	3,7	41,4	42,2	45	42,8	-	40,96
	00:23:00	0,88	26,8	2,1	26,1	53	42,6	39,7	2,9	40,4	41,2	42,9	41,8	-	39,15
	00:25:00	0,88	26,8	2,1	26,1	53	41,3	39	2,3	39,6	40,4	41,6	41	-	38,19
	00:27:00	0,88	26,8	2,1	26,1	53	40,4	38	2,4	38,8	39,8	40,6	40,2	-	37,3
	00:29:00	0,88	26,8	2,1	26,1	53	39,3	37,2	2,1	38,1	38,9	39,5	39,4	-	36,48
	00:31:00	0,88	26,8	2,1	26,1	53	38,3	36,7	1,6	37,5	38,1	38,7	38,7	-	35,73
	00:33:00	0,88	26,8	2,1	26,1	53	37,5	36,1	1,4	36,8	37,5	37,9	38	-	34,98
	00:35:00	0,88	26,8	2,1	26,1	53	37,1	35,5	1,6	36,2	36,8	37,1	37,4	-	34,36
	00:37:00	0,88	26,8	2,1	26,1	53	36,2	34,7	1,5	35,7	36,3	36,4	36,7	-	33,85
	00:39:00	0,88	26,8	2,1	26,1	53	35,8	34,2	1,6	35,2	35,8	35,8	36,2	-	33,42
	00:41:00	0,88	26,8	2,1	26,1	53	35,4	34,1	1,3	34,8	35,3	35,3	35,7	-	33,01
	00:43:00	0,88	26,8	2,1	26,1	53	35	33,8	1,2	34,3	34,8	34,8	35,2	-	32,38
	00:45:00	0,88	26,8	2,1	26,1	53	34,1	33,1	1	33,8	34,2	34,1	34,6	-	32
	00:47:00	0,88	26,8	2,1	26,1	53	33,8	33	0,8	33,5	33,8	33,8	34,2	-	31,59
	00:49:00	0,88	26,8	2,1	26,1	53	33,1	32,4	0,7	33	33,4	33,2	33,7	-	31,18
	00:51:00	0,88	26,8	2,1	26,1	53	32,9	32,1	0,8	32,8	33	32,9	33,4	-	30,86
	00:53:00	0,88	26,8	2,1	26,1	53	32,2	31,5	0,7	32,2	32,5	32,4	32,9	-	30,65
	00:55:00	0,88	26,8	2,1	26,1	53	32	31,2	0,8	31,9	32	32,1	32,6	-	30,19
	00:57:00	0,88	26,8	2,1	26,1	53	31,7	31,2	0,5	31,6	31,9	31,8	32,3	-	29,8
	00:59:00	0,88	26,8	2,1	26,1	53	31,4	30,7	0,7	31,4	31,6	31,4	32	-	29,68
	01:01:00	0,88	26,8	2,1	26,1	53	31	30,5	0,5	31,1	31,3	31,2	31,7	-	30,07
	01:03:00	0,88	26,8	2,1	26,1	53	30,9	30,2	0,7	30,9	31,1	30,9	31,4	-	29,23
	01:06:00	0,88	26,8	2,1	26,1	53	30,6	30	0,6	30,5	31	30,7	31,1	-	28,84
	01:11:00	0,88	26,8	2,1	26,1	53	30	29,6	0,4	30	30,2	30	30,4	-	28,3
	01:16:00	0,88	26,8	2,1	26,1	53	29,5	29,5	0	29,7	30	29,5	29,9	-	27,66
	01:21:00	0,88	26,8	2,1	26,1	53	29,1	28,8	0,3	29,2	29,3	29,1	29,5	-	27,54
	01:26:00	0,88	26,8	2,1	26,1	53	28,9	28,5	0,4	28,8	29	28,9	29,1	-	27,1
	01:31:00	0,88	26,8	2,1	26,1	53	28,4	28,4	0	28,5	28,8	28,6	28,9	-	27,05
	01:36:00	0,88	26,8	2,1	26,1	53	28,3	28,2	0,1	28,3	28,5	28,4	28,6	-	27
	01:41:00	0,88	26,8	2,1	26,1	53	28,3	28,2	0,1	28,1	28	28,1	28,3	-	26,43
	01:46:00	0,88	26,8	2,1	26,1	53	27,9	27,8	0,1	27,9	27,8	27,9	28	-	26,6
	01:51:00	0,88	26,8	2,1	26,1	53	27,7	27,7	0	27,7	27,8	27,7	27,8	-	26,41
	01:56:00	0,88	26,8	2,1	26,1	53	27,6	27,5	0,1	27,5	27,6	27,6	27,7	-	26,33
	02:01:00	0,88	26,8	2,1	26,1	53	27,5	27,4	0,1	27,4	27,6	27,5	27,6	-	26,14
	02:06:00	0,88	26,8	2,1	26,1	53	27,2	27,1	0,1	27,4	27,5	27,3	27,4	-	26,16
	02:11:00	0,88	26,8	2,1	26,1	53	27,4	27,2	0,2	27,2	27,5	27,3	27,3	-	26,21
	02:16:00	0,88	26,8	2,1	26,1	53	27,4	27,3	0,1	27,1	27,5	27,3	27,3	-	25,74
	02:21:00	0,88	26,8	2,1	26,1	53	27,1	27,2	-0,1	27,1	27,1	27,2	27,2	-	25,7

C.8. – Specimen *Blad*

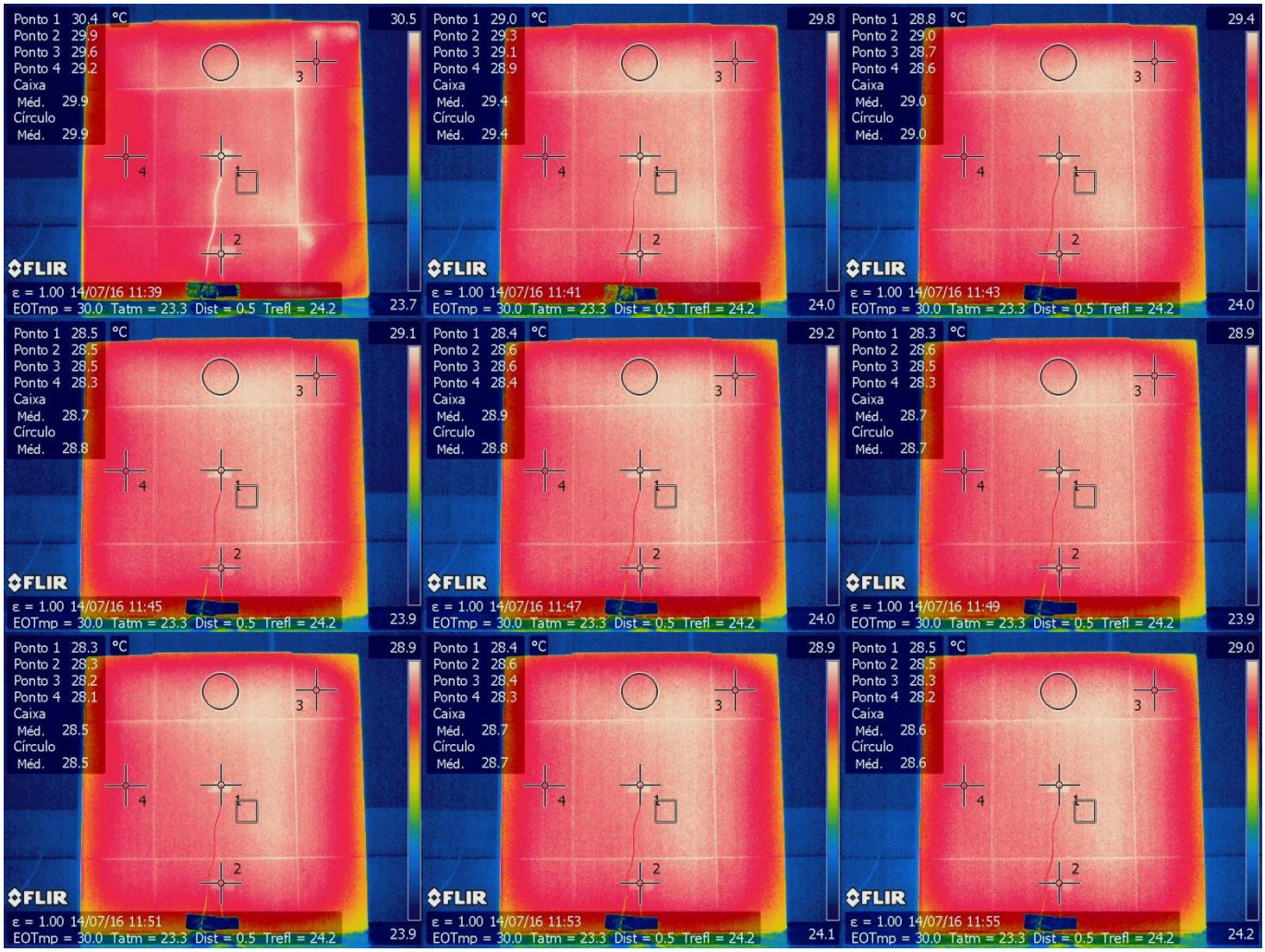

Figure B.8 – *Blad* - Thermograms obtained during the first 18 min of survey

Table B.8 - Results from specimen Bad

Phase	Accumulated time [hh:mm:ss]	Thermography											
							Temperature [°C]						
		ε	Trefl [°C]	Dist. [m]	Tamb [ºC]	Hr [%]	TDet	TAd	ΔT (Det-Ad)	Sp3	Sp4	Bx1	El1
Heating	00:00:00	-	-	-	-	-	-	-	-	-	-	-	-
	00:01:00	-	-	-	-	-	-	-	-	-	-	-	-
	00:02:00	-	-	-	-	-	-	-	-	-	-	-	-
	00:03:00	-	-	-	-	-	-	-	-	-	-	-	-
	00:04:00	-	-	-	-	-	-	-	-	-	-	-	-
	00:05:00	-	-	-	-	-	-	-	-	-	-	-	-
	00:06:00	-	-	-	-	-	-	-	-	-	-	-	-
	00:07:00	-	-	-	-	-	-	-	-	-	-	-	-
	00:08:00	-	-	-	-	-	-	-	-	-	-	-	-
	00:09:00	-	-	-	-	-	-	-	-	-	-	-	-
	00:10:00	-	-	-	-	-	-	-	-	-	-	-	-
	00:11:00	-	-	-	-	-	-	-	-	-	-	-	-
	00:12:00	-	-	-	-	-	-	-	-	-	-	-	-
	00:13:00	-	-	-	-	-	-	-	-	-	-	-	-
	00:14:00	-	-	-	-	-	-	-	-	-	-	-	-
	00:15:00	-	-	-	-	-	-	-	-	-	-	-	-
	00:16:00	-	-	-	-	-	-	-	-	-	-	-	-
	00:17:00	-	-	-	-	-	-	-	-	-	-	-	-
	00:18:00	-	-	-	-	-	-	-	-	-	-	-	-
	00:19:00	-	-	-	-	-	-	-	-	-	-	-	-
	00:20:00	-	-	-	-	-	-	-	-	-	-	-	-
Cooldown	00:21:00	0,88	24,2	2,1	23,3	49	30,3	29,9	0,4	29,6	29,2	29,9	29,9
	00:23:00	0,88	24,2	2,1	23,3	49	29,2	29,4	-0,2	29,3	28,9	29,5	29,4
	00:25:00	0,88	24,2	2,1	23,3	49	28,8	29	-0,2	28,8	28,7	29,1	29,1
	00:27:00	0,88	24,2	2,1	23,3	49	28,4	28,5	-0,1	28,5	28,4	28,8	28,8
	00:29:00	0,88	24,2	2,1	23,3	49	28,5	28,7	-0,2	28,6	28,4	28,9	28,9
	00:31:00	0,88	24,2	2,1	23,3	49	28,3	28,4	-0,1	28,5	28,2	28,7	28,6
	00:33:00	0,88	24,2	2,1	23,3	49	28,3	28,3	0	28,3	28,1	28,6	28,5
	00:35:00	0,88	24,2	2,1	23,3	49	28,5	28,5	0	28,4	28,3	28,7	28,6
	00:37:00	0,88	24,2	2,1	23,3	49	28,4	28,6	-0,2	28,4	28,3	28,7	28,6
	00:39:00	0,88	24,2	2,1	23,3	49	27,9	28,2	-0,3	28,1	28,1	28,5	28,4
	00:41:00	0,88	24,2	2,1	23,3	49	28	28,4	-0,4	28,1	28,1	28,5	28,4
	00:43:00	0,88	24,2	2,1	23,3	49	28	28,1	-0,1	28,1	27,8	28,3	28,3
	00:45:00	0,88	24,2	2,1	23,3	49	28,1	28,2	-0,1	28	27,8	28,3	28,3
	00:47:00	0,88	24,2	2,1	23,3	49	28,1	28,1	0	27,9	27,8	28,3	28,2
	00:49:00	0,88	24,2	2,1	23,3	49	28,1	28,2	-0,1	27,8	27,9	28,3	28,2
	00:51:00	0,88	24,2	2,1	23,3	49	27,7	27,9	-0,2	27,8	27,8	28,2	28,1
	00:53:00	0,88	24,2	2,1	23,3	49	27,9	28	-0,1	27,9	27,6	28,2	28
	00:55:00	0,88	24,2	2,1	23,3	49	27,9	27,9	0	27,8	27,6	28,2	28
	00:57:00	0,88	24,2	2,1	23,3	49	27,6	28	-0,4	27,9	27,8	28,2	28,1
	00:59:00	0,88	24,2	2,1	23,3	49	27,6	28	-0,4	27,8	27,8	28,2	28
	01:01:00	0,88	24,2	2,1	23,3	49	27,7	27,6	0,1	27,5	27,5	27,9	27,8
	01:03:00	0,88	24,2	2,1	23,3	49	27,7	27,7	0	27,5	27,6	27,9	27,8
	01:06:00	0,88	24,2	2,1	23,3	49	27,6	27,5	0,1	27,4	27,5	27,9	27,7
	01:11:00	0,88	24,2	2,1	23,3	49	27,5	27,5	0	27,1	27,3	27,7	27,6
	01:16:00	0,88	24,2	2,1	23,3	49	27,4	27,4	0	27,1	27,2	27,6	27,4
	01:21:00	0,88	24,2	2,1	23,3	49	27,4	27,3	0,1	27	27	27,4	27,3
	01:26:00	0,88	24,2	2,1	23,3	49	27,3	27	0,3	26,9	26,9	27,3	27,2
	01:31:00	0,88	24,2	2,1	23,3	49	27,3	27,1	0,2	26,9	26,9	27,3	27,2
	01:36:00	0,88	24,2	2,1	23,3	49	27	27,1	-0,1	26,7	27	27,2	27
	01:41:00	0,88	24,2	2,1	23,3	49	27,1	27	0,1	26,6	26,8	27,1	27
	01:46:00	0,88	24,2	2,1	23,3	49	27	26,7	0,3	26,6	26,5	26,9	26,8
	01:51:00	0,88	24,2	2,1	23,3	49	27	26,8	0,2	26,5	26,5	26,9	26,8
	01:56:00	0,88	24,2	2,1	23,3	49	26,8	26,6	0,2	26,1	26,3	26,7	26,6
	02:01:00	0,88	24,2	2,1	23,3	49	26,7	26,6	0,1	26,4	26,3	26,8	26,6
	02:06:00	0,88	24,2	2,1	23,3	49	26,7	26,5	0,2	26,3	26,3	26,7	26,6
	02:11:00	0,88	24,2	2,1	23,3	49	26,4	26,4	0	26,2	26,2	26,6	26,4
	02:16:00	0,88	24,2	2,1	23,3	49	26,7	26,4	0,3	26,1	26,4	26,6	26,5
	02:21:00	0,88	24,2	2,1	23,3	49	26,5	26,1	0,4	26,1	26,1	26,4	26,3

Apendix C – Results from the exterior laboratorial surveys

C.1. – Open joints survey

Result tables

Table C.1 - Results from panel C1_B (open joints)

Time	ε	Trefl [ºC]	Hr [%]	Tamb [°C]	Dist. [m]	Temperature [°C]		
						Ad	Det	ΔT
09:11	0,88	5,1	64,7	20,4	3,6	20,2	20,7	0,5
10:50	0,88	25,1	64,7	20,4	3,6	21,6	21,9	0,3
13:05	0,88	34,2	59,3	22,8	3,6	24,8	25,2	0,5
13:45	0,88	31,5	62,3	22,1	3,6	26,6	27,2	0,6
14:23	0,88	32,3	60,7	22,9	3,6	30,8	32,1	1,3
15:37	0,88	32,3	60,0	22,8	3,6	43,5	45,6	2,1
16:52	0,88	34,3	58,2	22,9	3,6	51,2	53,5	2,3
18:09	0,88	29,1	60,7	22,7	3,6	54,8	55,9	1,1
18:59	0,88	33,3	59,5	22,3	3,6	53,7	55,7	2,0
19:43	0,88	31,3	60,0	22,0	3,6	49,4	50,0	0,7
19:58	0,88	27,5	65,0	21,0	3,6	46,8	47,0	0,2
20:11	0,88	25,9	70,0	19,5	3,6	44,0	44,0	0,0
20:22	0,88	23,9	73,5	18,3	3,6	34,9	32,8	-2,1

Table C.2 - Results from panel C1_W (open joints)

Time	ε	Trefl [ºC]	Hr [%]	Tamb [°C]	Dist. [m]	Temperature [°C]		
						Ad	Det	ΔT
09:11	0,88	5,1	64,7	20,4	3,6	18,8	19,0	0,2
10:50	0,88	25,1	64,7	20,4	3,6	19,8	20,1	0,3
13:05	0,88	34,2	59,3	22,8	3,6	22,1	22,3	0,3
13:45	0,88	31,5	62,3	22,1	3,6	23,7	24,1	0,4
14:23	0,88	32,3	60,7	22,9	3,6	26,1	26,7	0,6
15:37	0,88	32,3	60,0	22,8	3,6	32,7	33,3	0,6
16:52	0,88	34,3	58,2	22,9	3,6	37,8	38,2	0,5
18:09	0,88	29,1	60,7	22,7	3,6	37,6	37,5	-0,1
18:59	0,88	33,3	59,5	22,3	3,6	36,3	36,4	0,1
19:43	0,88	31,3	60,0	22,0	3,6	32,6	32,0	-0,5
19:58	0,88	27,5	65,0	21,0	3,6	31,5	30,7	-0,8
20:11	0,88	25,9	70,0	19,5	3,6	30,1	29,1	-1,0
20:22	0,88	23,9	73,5	18,3	3,6	27,2	26,1	-1,1

Table C.3 - Results from panel C2_B (open joints)

Time	ε	Trefl [ºC]	Hr [%]	Tamb [°C]	Dist. [m]	Temperature [°C]		
						Ad	Det	ΔT
09:28	0,88	5,1	64,7	20,4	3,6	16,5	17,7	1,2
11:03	0,88	25,1	64,7	20,4	3,6	20,1	21,2	1,1
13:14	0,88	34,2	59,3	22,8	3,6	23,4	24,7	1,3
13:55	0,88	31,5	62,3	22,1	3,6	25,2	26,9	1,7
14:33	0,88	32,3	60,7	22,9	3,6	28,0	30,9	2,9
15:46	0,88	32,3	60,0	22,8	3,6	35,9	40,8	4,9
17:02	0,88	34,3	58,2	22,9	3,6	45,3	50,1	4,9
18:18	0,88	29,1	60,7	22,7	3,6	46,9	49,8	2,9
19:09	0,88	33,3	59,5	22,3	3,6	47,9	50,5	2,6
19:51	0,88	31,3	60,0	22,0	3,6	41,5	39,7	-1,8
20:04	0,88	27,5	65,0	21,0	3,6	37,0	33,2	-3,8
20:16	0,88	25,9	70,0	19,5	3,6	35,3	30,6	-4,7
20:28	0,88	23,9	73,5	18,3	3,6	32,9	28,7	-4,2

Table C.4 - Results from panel C2_W (open joints)

Time	ε	Trefl [ºC]	Hr [%]	Tamb [°C]	Dist. [m]	Temperature [°C]		
						Ad	Det	ΔT
09:28	0,88	5,1	64,7	20,4	3,6	14,7	15,3	0,6
11:03	0,88	25,1	64,7	20,4	3,6	17,8	18,8	0,9
13:14	0,88	34,2	59,3	22,8	3,6	21,2	22,0	0,9
13:55	0,88	31,5	62,3	22,1	3,6	22,5	23,6	1,2
14:33	0,88	32,3	60,7	22,9	3,6	23,9	25,7	1,8
15:46	0,88	32,3	60,0	22,8	3,6	28,5	31,0	2,5
17:02	0,88	34,3	58,2	22,9	3,6	34,6	36,9	2,4
18:18	0,88	29,1	60,7	22,7	3,6	35,2	36,1	0,8
19:09	0,88	33,3	59,5	22,3	3,6	34,4	34,7	0,3
19:51	0,88	31,3	60,0	22,0	3,6	31,7	30,7	-1,0
20:04	0,88	27,5	65,0	21,0	3,6	28,8	26,0	-2,8
20:16	0,88	25,9	70,0	19,5	3,6	28,0	25,3	-2,7
20:28	0,88	23,9	73,5	18,3	3,6	26,5	23,8	-2,7

Climacteric conditions during the day of the survey

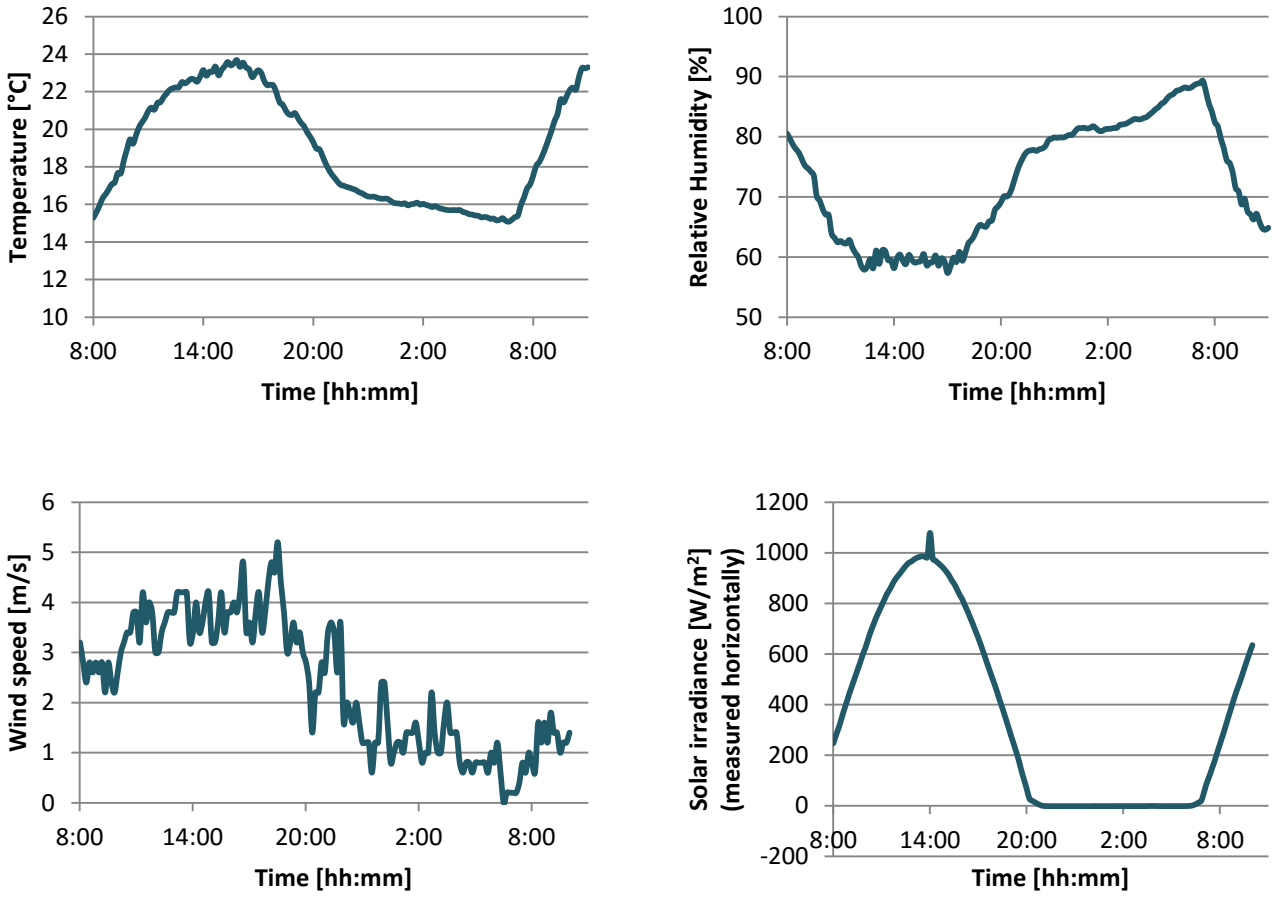

Figure C.1- Climacteric conditions during the survey (open joints)

Thermocouples Data

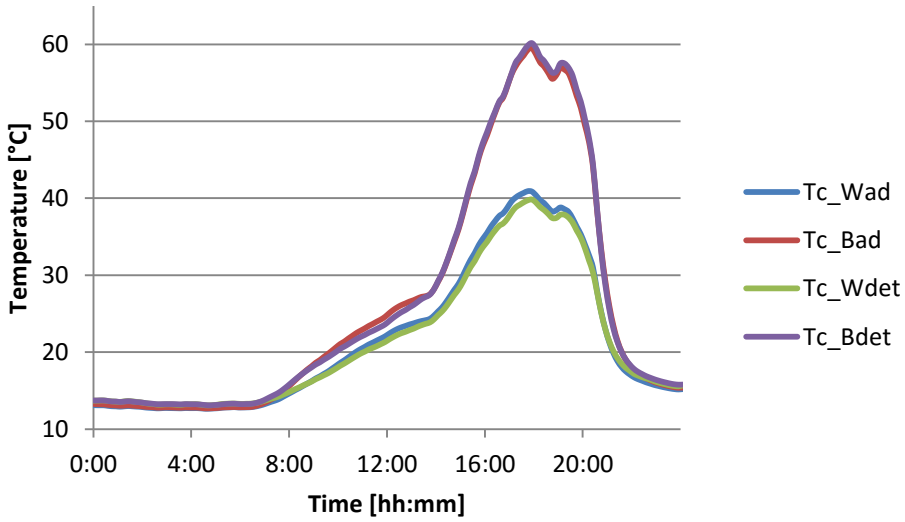

Figure C.2 - Thermocouples' readings on cell 1 (*Tc_Bad* – thermocouple under an **adherent black** tile; *Tc_Bdet* – thermocouple under a **detached black** tile; *Tc_Wad* – thermocouple under an **adherent white** tile; *Tc_Wdet* – thermocouple under a **detached white** tile) (open joints)

Thermograms obtained

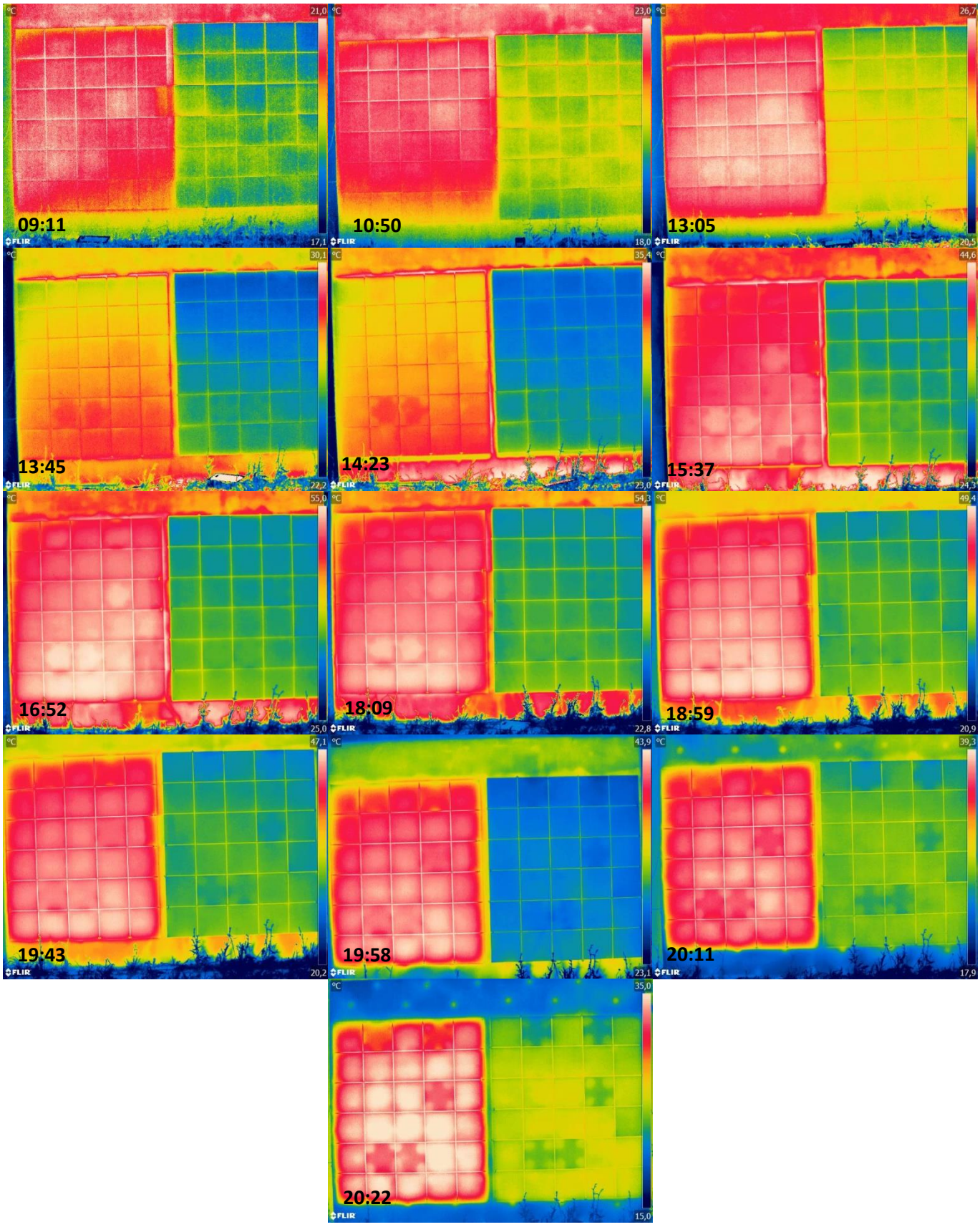

Figure C.3 – Thermograms from cell 1 (open joints)

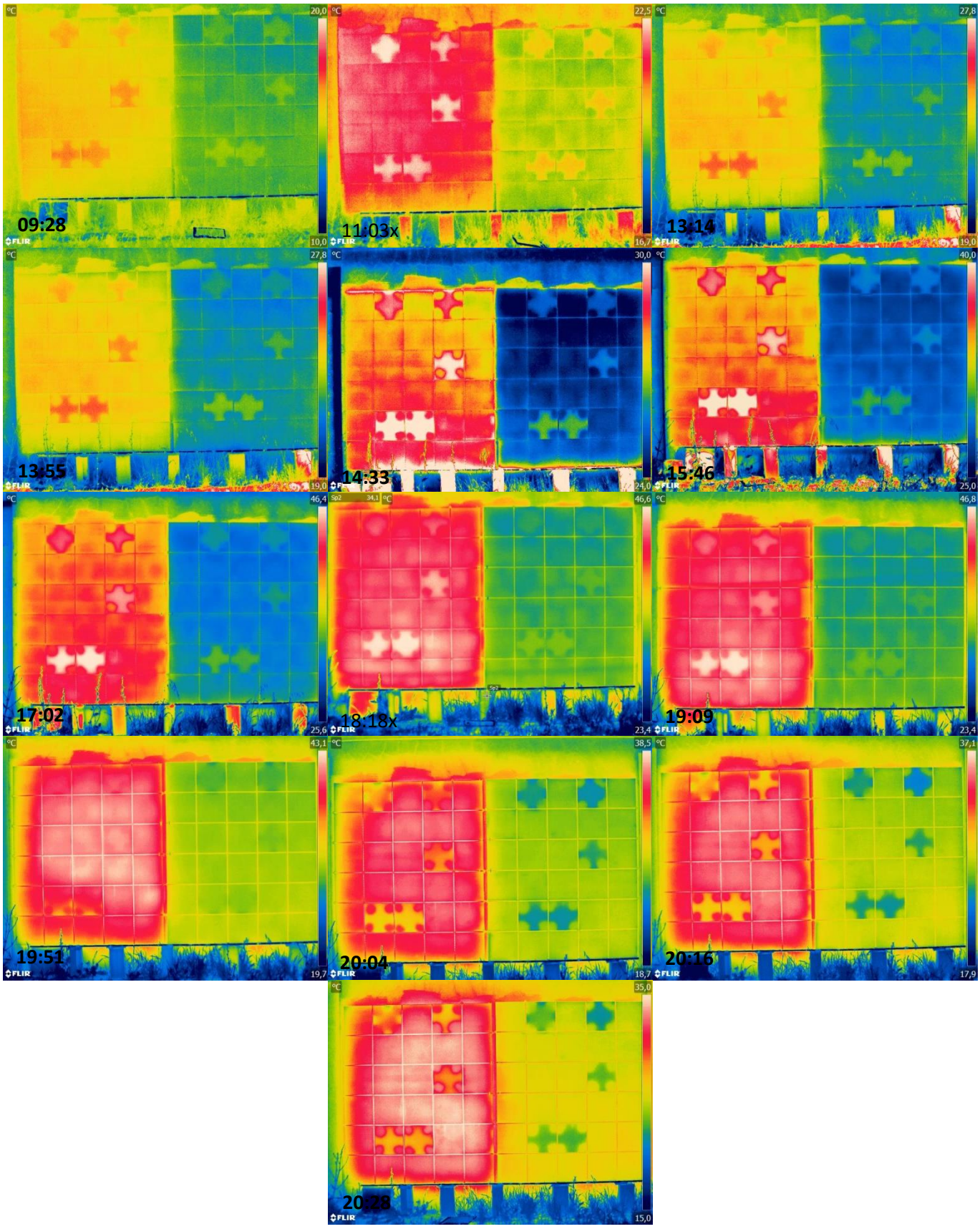

Figure C.4 - Thermograms from cell 2 (open joints)

C.2. – Closed joints survey

Result tables

Table C.5 - Results from panel C1_B (closed joints)

Time	ε	Trefl [ºC]	Hr [%]	Tamb [°C]	Dist. [m]	Temperature [°C]		
						Ad	Det	ΔT
09:40	0,88	18,0	61,0	23,5	3,6	24,7	25,0	0,4
10:37	0,88	19,0	59,1	24,2	3,6	26,4	26,7	0,3
11:39	0,88	20,0	53,0	25,7	3,6	28,9	29,0	0,1
12:30	0,88	23,2	49,0	26,8	3,6	31,7	32,2	0,5
13:01	0,88	25,2	49,3	26,6	3,6	33,6	34,2	0,7
13:23	0,88	25,2	49,3	27,7	3,6	34,8	35,4	0,6
13:45	0,88	24,8	45,0	27,9	3,6	35,8	36,3	0,5
13:54	0,88	26,2	45,0	28,2	3,6	36,7	37,3	0,6
14:07	0,88	28,4	44,4	28,4	3,6	37,3	38,2	0,9
15:34	0,88	30,6	39,5	30,2	3,6	52,1	53,6	1,5
16:48	0,88	28,1	41,8	28,9	3,6	60,0	61,3	1,3
17:54	0,88	21,0	44,1	27,5	3,6	63,1	64,3	1,3
18:40	0,88	19,1	47,6	26,4	3,6	62,9	64,2	1,4
19:37	0,88	20,4	54,4	25,0	3,6	58,0	58,9	1,0
19:46	0,88	19,8	57,4	24,4	3,6	56,6	57,3	0,7
19:58	0,88	18,6	59,0	24,2	3,6	53,7	54,2	0,5
20:07	0,88	19,5	58,7	24,7	3,6	50,7	51,2	0,4
20:15	0,88	15,5	60,7	23,9	3,6	49,2	49,5	0,3
20:24	0,88	17,4	61,9	23,7	3,6	44,5	44,7	0,1
20:31	0,88	13,5	63,2	22,9	3,6	40,4	40,0	-0,4
20:40	0,88	13,5	64,4	22,5	3,6	35,6	34,9	-0,8
21:01	0,88	13,7	68,2	21,4	3,6	28,8	28,0	-0,8
21:20	0,88	12,6	70,2	20,6	3,6	24,8	24,2	-0,6
21:44	0,88	13,1	69,5	20,5	3,6	22,2	21,9	-0,3
22:11	0,88	11,4	67,6	20,6	3,6	20,7	20,7	-0,1
08:48	0,88	11,2	66,7	21,3	3,6	23,1	23,4	0,3

Table C.6 - Results from panel C1_W (closed joints)

Time	ε	Trefl [ºC]	Hr [%]	Tamb [°C]	Dist. [m]	Temperature [°C]		
						Ad	Det	ΔT
09:40	0,88	18,0	61,0	23,5	3,6	22,2	22,3	0,1
10:37	0,88	19,0	59,1	24,2	3,6	24,6	24,7	0,1
11:39	0,88	20,0	53,0	25,7	3,6	27,0	27,1	0,2
12:30	0,88	23,2	49,0	26,8	3,6	29,2	29,7	0,5
13:01	0,88	25,2	49,3	26,6	3,6	30,8	31,1	0,4
13:23	0,88	25,2	49,3	27,7	3,6	31,8	32,2	0,4
13:45	0,88	24,8	45,0	27,9	3,6	32,4	32,9	0,4
13:54	0,88	26,2	45,0	28,2	3,6	33,0	33,5	0,5
14:07	0,88	28,4	44,4	28,4	3,6	33,3	33,9	0,6
15:34	0,88	30,6	39,5	30,2	3,6	40,6	41,4	0,8
16:48	0,88	28,1	41,8	28,9	3,6	44,6	45,1	0,6
17:54	0,88	21,0	44,1	27,5	3,6	45,7	46,0	0,3
18:40	0,88	19,1	47,6	26,4	3,6	44,8	45,0	0,2
19:37	0,88	20,4	54,4	25,0	3,6	41,3	41,3	0,0
19:46	0,88	19,8	57,4	24,4	3,6	39,6	39,6	0,0
19:58	0,88	18,6	59,0	24,2	3,6	37,8	37,5	-0,3
20:07	0,88	19,5	58,7	24,7	3,6	36,0	35,6	-0,4
20:15	0,88	15,5	60,7	23,9	3,6	35,2	34,7	-0,5
20:24	0,88	17,4	61,9	23,7	3,6	32,7	32,1	-0,6
20:31	0,88	13,5	63,2	22,9	3,6	30,9	30,0	-0,9
20:40	0,88	13,5	64,4	22,5	3,6	28,3	27,3	-1,0
21:01	0,88	13,7	68,2	21,4	3,6	24,5	23,8	-0,7
21:20	0,88	12,6	70,2	20,6	3,6	22,2	21,8	-0,4
21:44	0,88	13,1	69,5	20,5	3,6	20,6	20,4	-0,2
22:11	0,88	11,4	67,6	20,6	3,6	19,8	19,7	0,0
08:48	0,88	11,2	66,7	21,3	3,6	21,4	21,6	0,2

Table C.7 - Results from panel C2_B (closed joints)

Time	ε	Trefl [ºC]	Hr [%]	Tamb [°C]	Dist. [m]	Temperature [°C]		
						Ad	Det	ΔT
09:40	0,88	17,5	61,0	23,5	3,6	24,1	24,8	0,7
10:37	0,88	18,0	59,1	24,2	3,6	25,5	26,3	0,8
11:39	0,88	18,4	53,0	25,7	3,6	27,5	28,4	0,9
12:30	0,88	23,4	49,0	26,8	3,6	29,4	30,5	1,1
13:01	0,88	23,1	49,3	26,6	3,6	31,0	32,1	1,2
13:23	0,88	25,1	49,3	27,7	3,6	31,7	32,7	1,1
13:45	0,88	24,9	45,0	27,9	3,6	32,5	33,3	0,8
13:54	0,88	28,0	45,0	28,2	3,6	32,7	33,6	0,9
14:07	0,88	26,3	44,4	28,4	3,6	34,2	35,5	1,3
15:34	0,88	27,6	39,5	30,2	3,6	43,2	46,3	3,1
16:48	0,88	24,8	41,8	28,9	3,6	50,3	53,1	2,8
17:54	0,88	22,8	44,1	27,5	3,6	54,4	56,8	2,4
18:40	0,88	17,9	47,6	26,4	3,6	54,6	55,8	1,3
19:37	0,88	15,2	54,4	25,0	3,6	53,5	54,7	1,2
19:46	0,88	16,4	57,4	24,4	3,6	50,7	52,1	1,4
19:58	0,88	18,0	59,0	24,2	3,6	46,9	46,0	-0,9
20:07	0,88	12,4	58,7	24,7	3,6	45,1	42,7	-2,4
20:15	0,88	16,8	60,7	23,9	3,6	41,8	39,0	-2,8
20:24	0,88	15,3	61,9	23,7	3,6	41,0	37,9	-3,1
20:31	0,88	14,3	63,2	22,9	3,6	39,1	36,4	-2,6
20:40	0,88	10,7	64,4	22,5	3,6	38,5	35,7	-2,9
21:01	0,88	9,2	68,2	21,4	3,6	35,5	33,6	-1,9
21:20	0,88	8,0	70,2	20,6	3,6	33,9	32,1	-1,8
21:44	0,88	11,0	69,5	20,5	3,6	31,9	30,7	-1,2
22:11	0,88	11,9	67,6	20,6	3,6	30,1	29,2	-1,0
08:48	0,88	12,4	66,7	21,3	3,6	22,8	23,4	0,6

Table C.8 - Results from panel C2_W (closed joints)

Time	ε	Trefl [ºC]	Hr [%]	Tamb [°C]	Dist. [m]	Temperature [°C]		
						Ad	Det	ΔT
09:40	0,88	17,5	61,0	23,5	3,6	22,3	22,5	0,2
10:37	0,88	18,0	59,1	24,2	3,6	23,7	24,0	0,3
11:39	0,88	18,4	53,0	25,7	3,6	25,5	26,0	0,4
12:30	0,88	23,4	49,0	26,8	3,6	27,1	27,7	0,6
13:01	0,88	23,1	49,3	26,6	3,6	28,6	29,3	0,7
13:23	0,88	25,1	49,3	27,7	3,6	29,3	29,8	0,6
13:45	0,88	24,9	45,0	27,9	3,6	29,5	30,2	0,6
13:54	0,88	28,0	45,0	28,2	3,6	29,4	30,1	0,7
14:07	0,88	26,3	44,4	28,4	3,6	30,5	31,4	0,9
15:34	0,88	27,6	39,5	30,2	3,6	35,7	37,1	1,4
16:48	0,88	24,8	41,8	28,9	3,6	39,8	40,9	1,2
17:54	0,88	22,8	44,1	27,5	3,6	41,3	42,1	0,8
18:40	0,88	17,9	47,6	26,4	3,6	41,1	41,3	0,3
19:37	0,88	15,2	54,4	25,0	3,6	40,2	40,2	0,0
19:46	0,88	16,4	57,4	24,4	3,6	38,7	38,2	-0,5
19:58	0,88	18,0	59,0	24,2	3,6	37,8	36,6	-1,2
20:07	0,88	12,4	58,7	24,7	3,6	35,8	34,2	-1,6
20:15	0,88	16,8	60,7	23,9	3,6	34,1	32,1	-2,1
20:24	0,88	15,3	61,9	23,7	3,6	33,5	31,4	-2,1
20:31	0,88	14,3	63,2	22,9	3,6	32,5	30,5	-2,0
20:40	0,88	10,7	64,4	22,5	3,6	31,9	29,9	-2,1
21:01	0,88	9,2	68,2	21,4	3,6	30,5	28,6	-1,9
21:20	0,88	8,0	70,2	20,6	3,6	29,4	27,5	-1,9
21:44	0,88	11,0	69,5	20,5	3,6	28,0	26,6	-1,4
22:11	0,88	11,9	67,6	20,6	3,6	27,0	25,5	-1,5
08:48	0,88	12,4	66,7	21,3	3,6	20,4	20,7	0,3

Climacteric conditions during the day of the survey

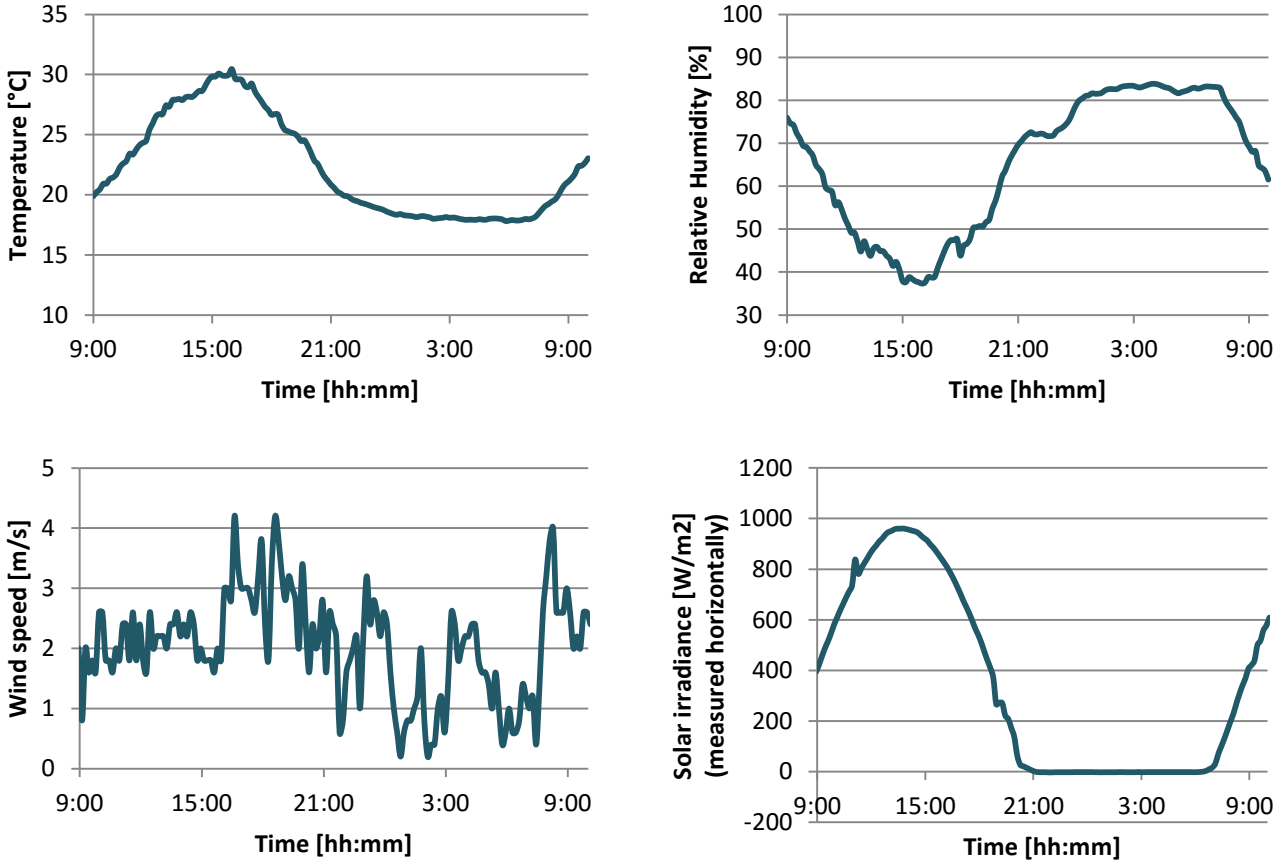

Figure C.5 - Climacteric conditions during the survey (closed joints)

Thermocouples Data

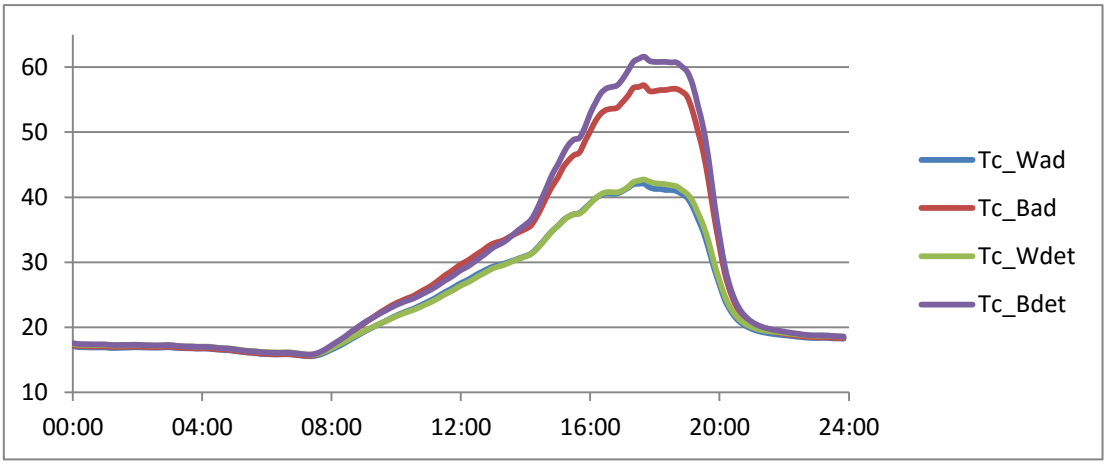

Figure C.6 - Thermocouples' readings on cell 1 (*Tc_Bad* – thermocouple under an **adherent black** tile; *Tc_Bdet* – thermocouple under a **detached black** tile; *Tc_Wad* – thermocouple under an **adherent white** tile; *Tc_Wdet* – thermocouple under a **detached white** tile) (closed joints)

Thermograms

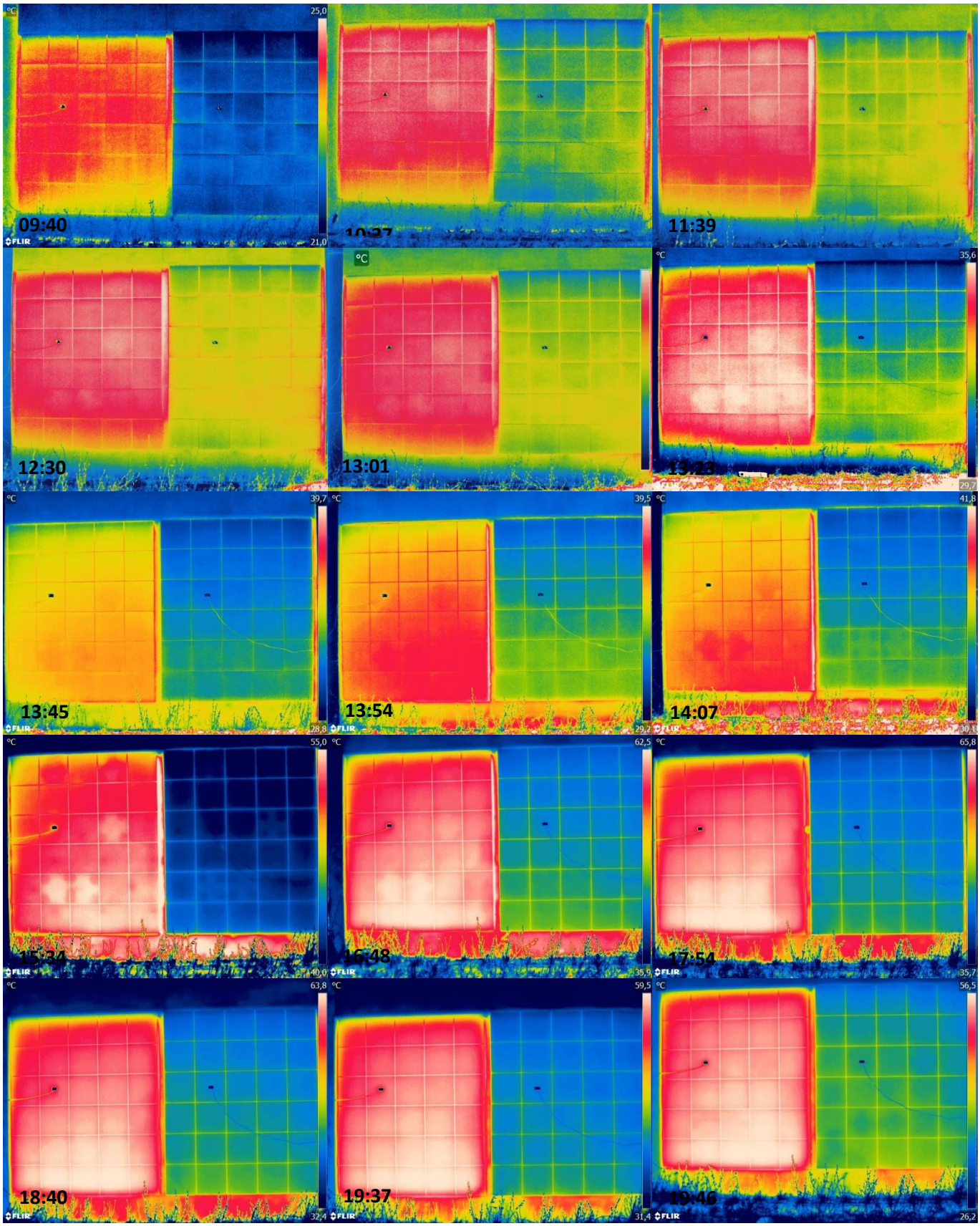

Figure C.7 - Thermograms from cell 1 (closed joints)

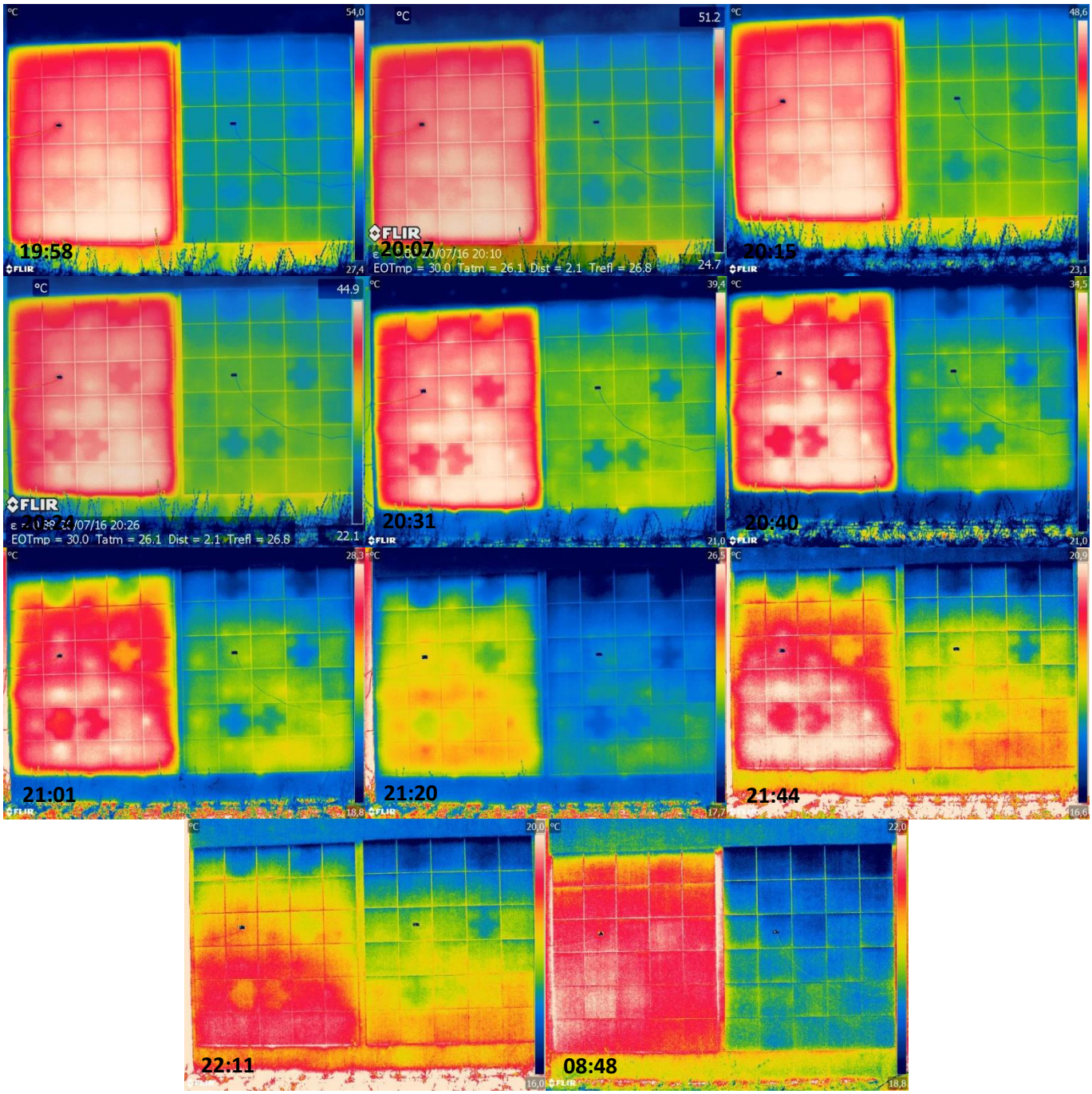

Figure C.8 - Thermograms from cell 1 (closed joints) (cont.)

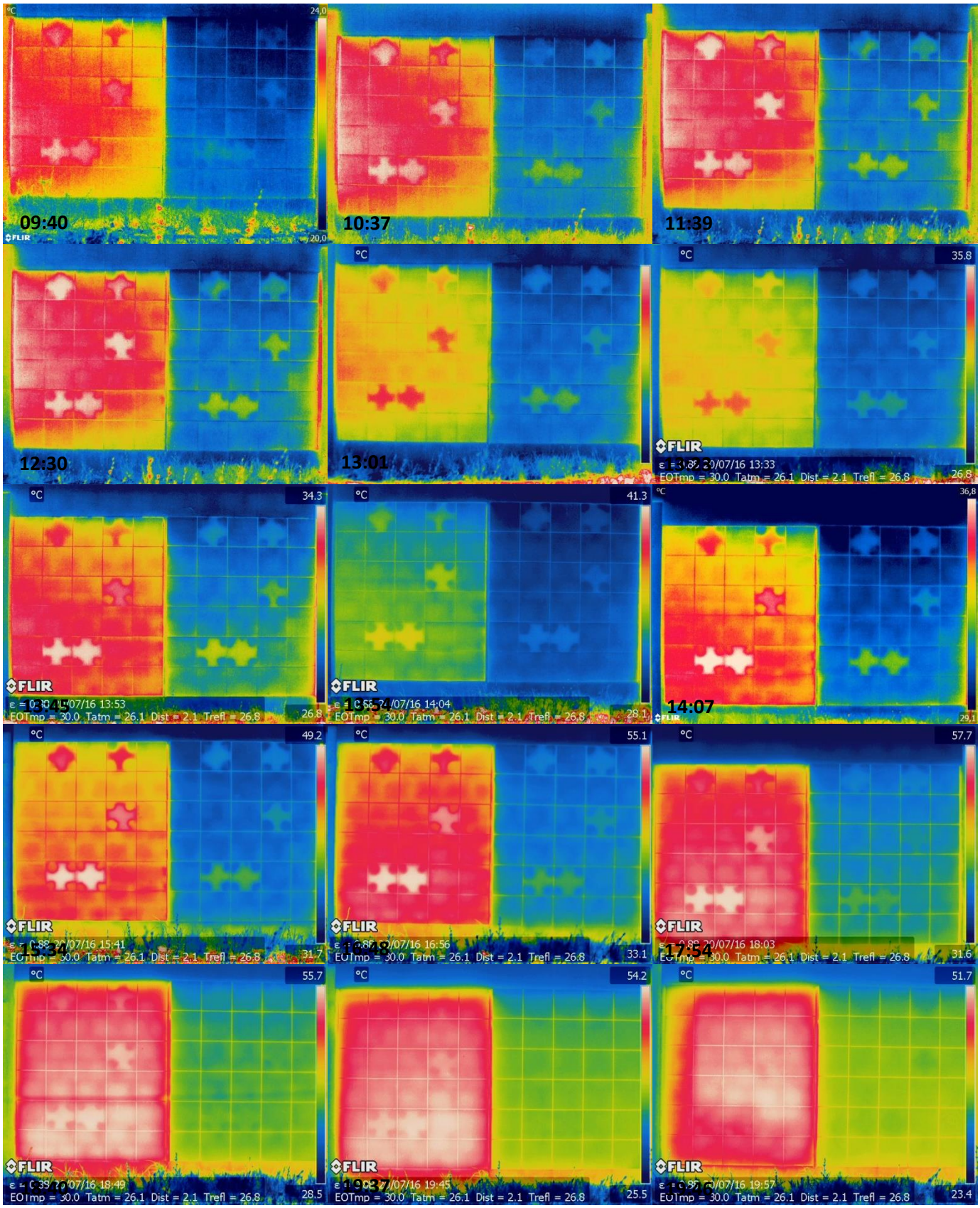

Figure C.9 - Thermograms from cell 2 (closed joints)

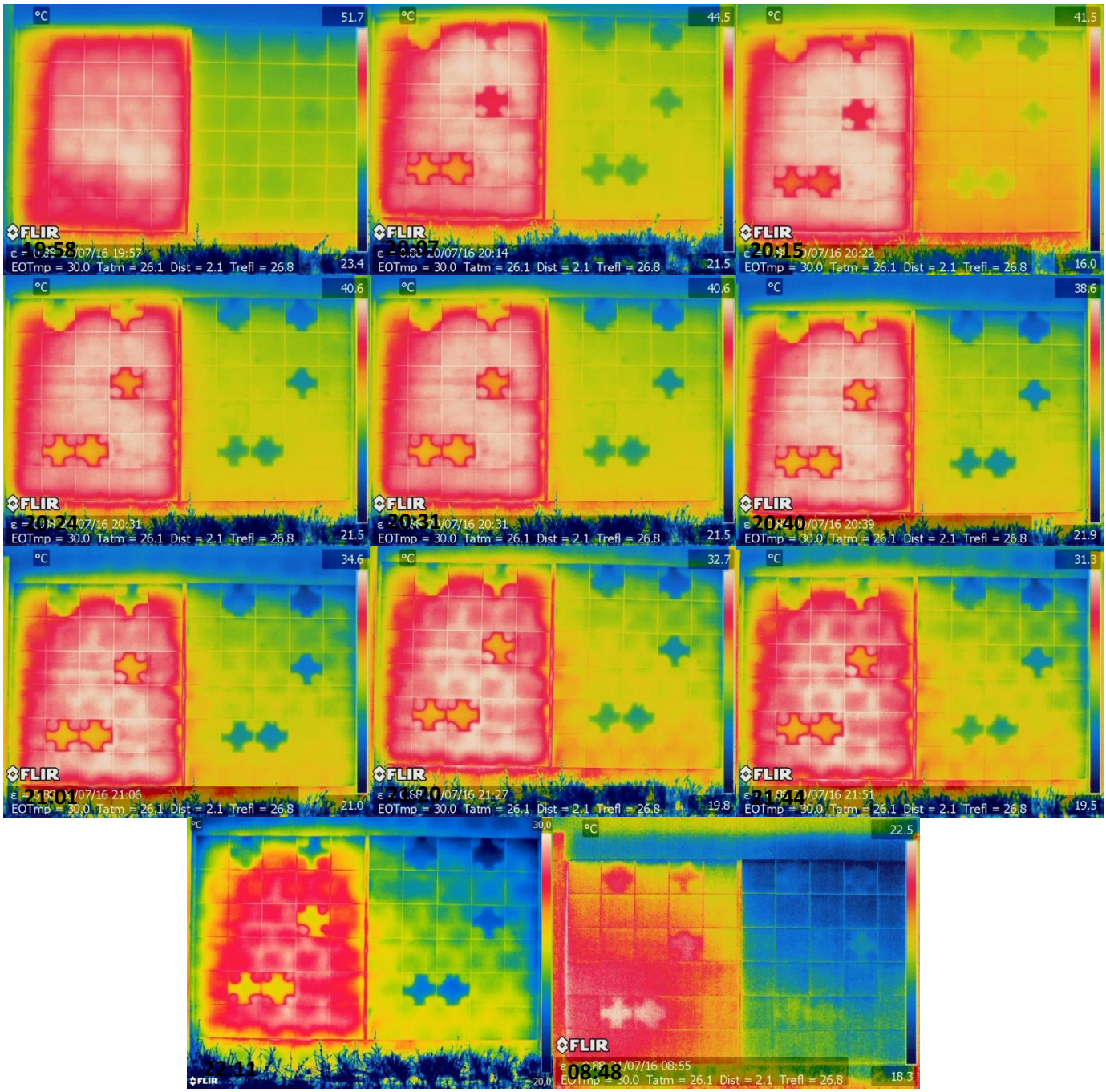

Figure C.10 - Thermograms from cell 2 (closed joints) (cont.)

C.3. – Humidity – first survey

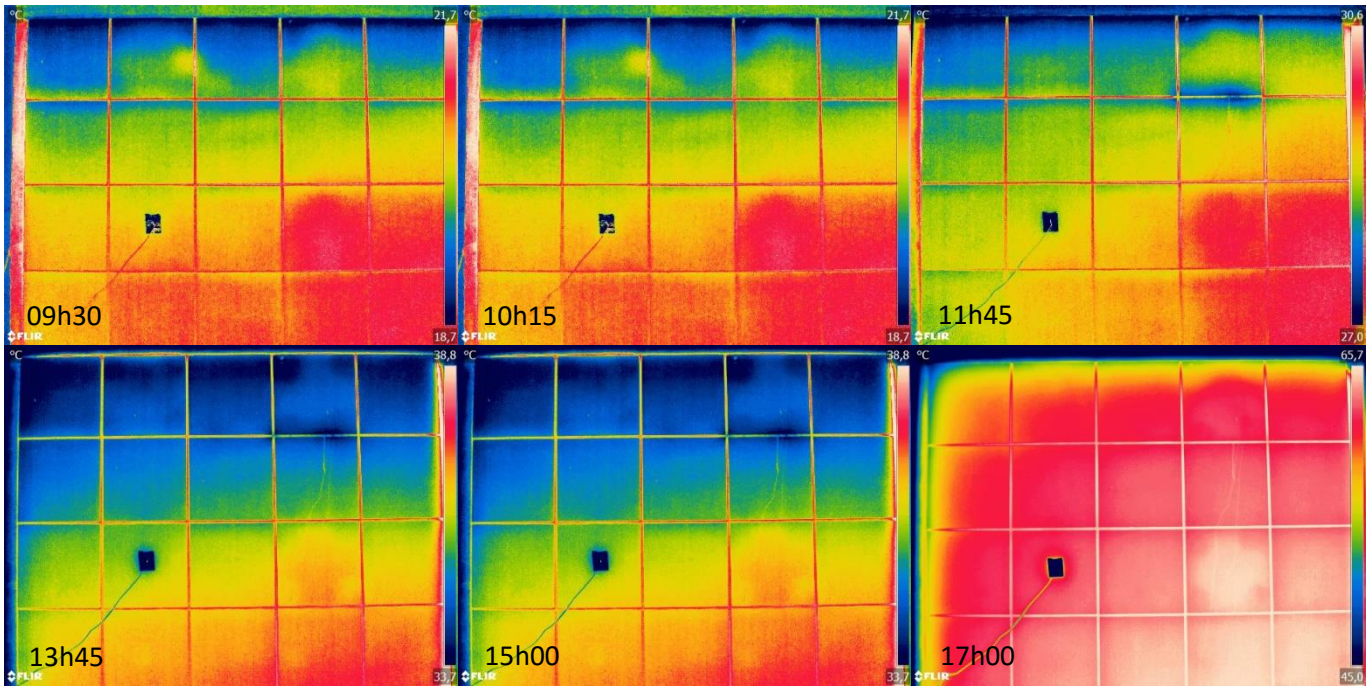

Figure C.11- First humidity survey C1_B

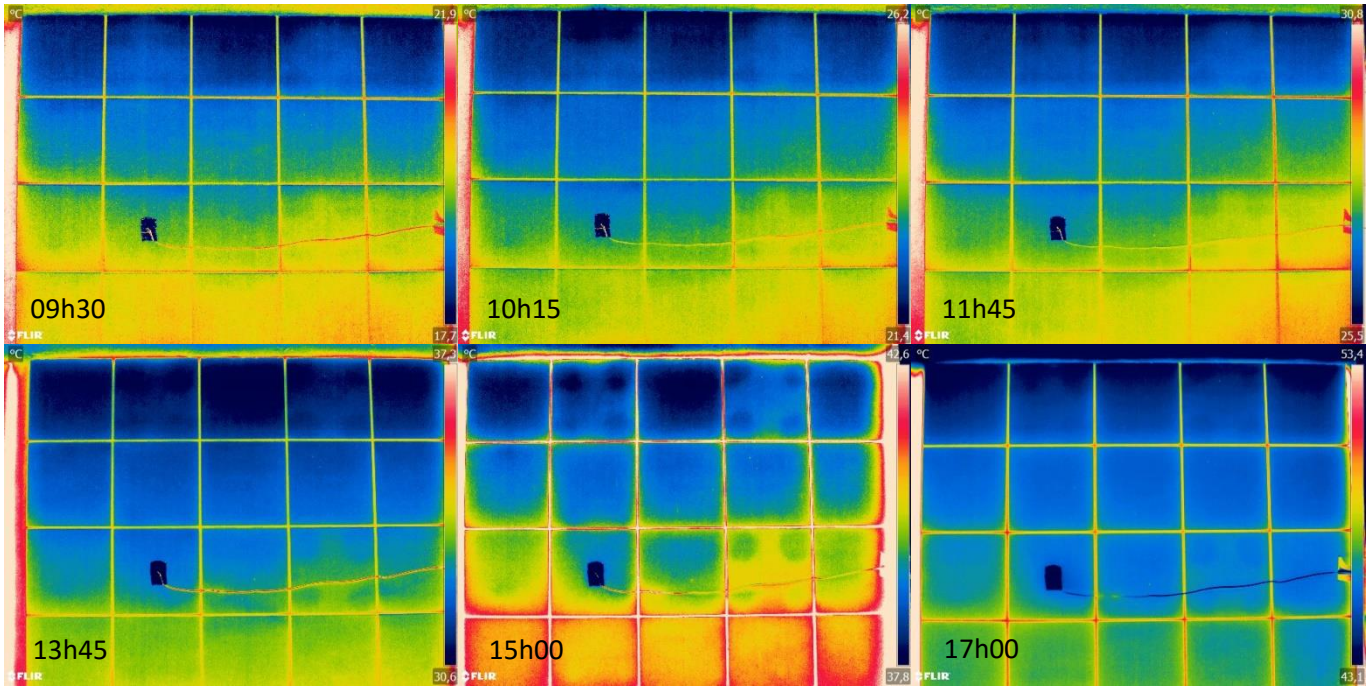

Figure C.12 - First humidity survey C1_W

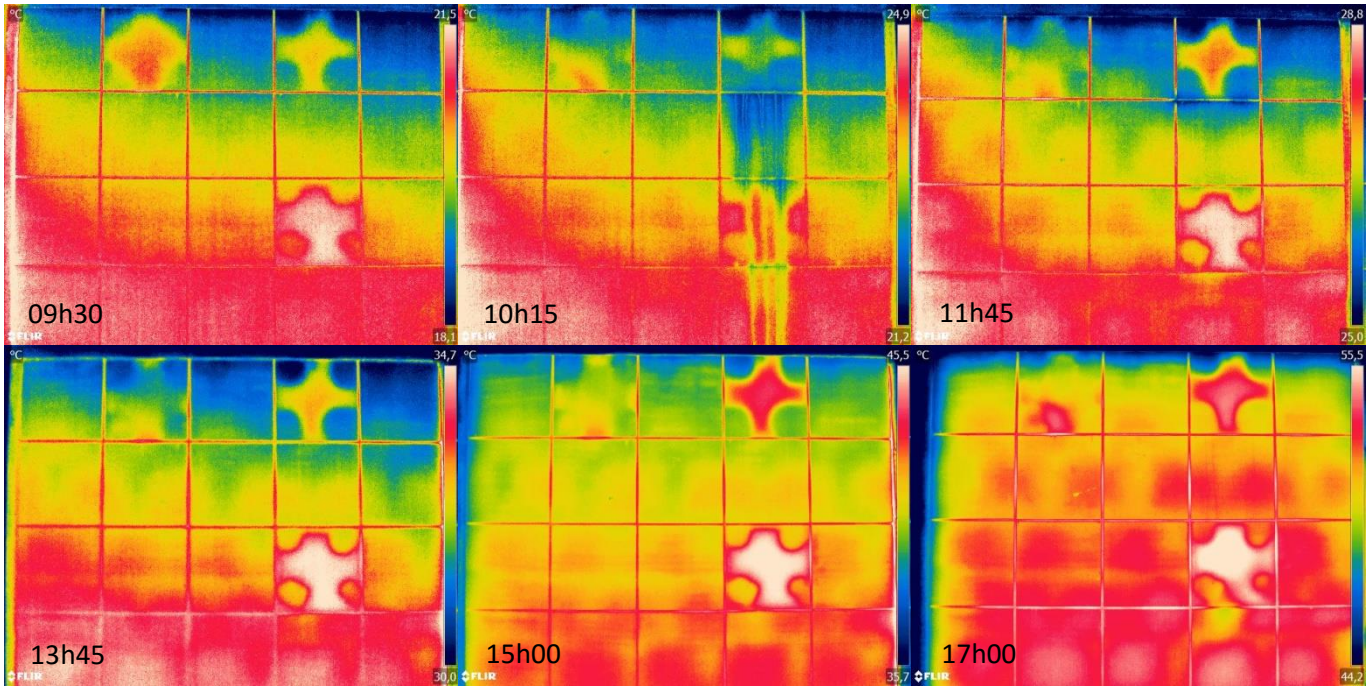

Figure C.13 - First humidity survey C2_B

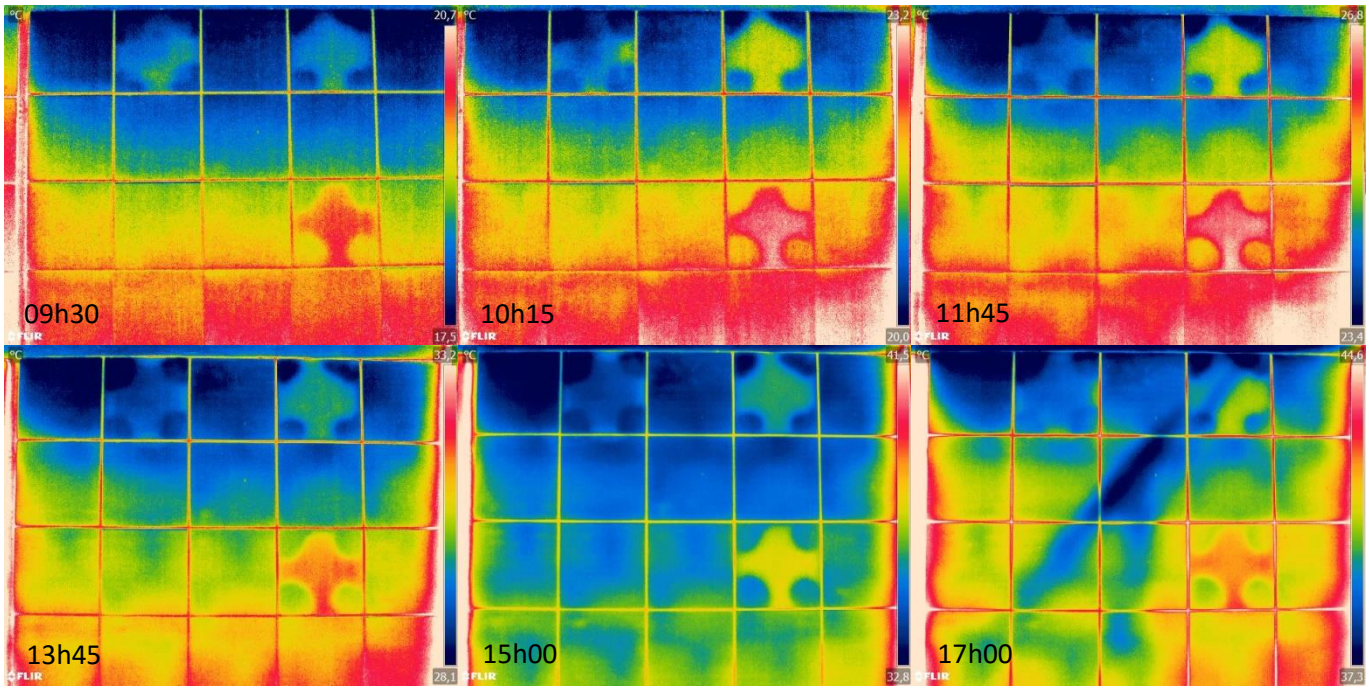

Figure C.14 - First humidity survey C2_W

C.4. – Humidity – second survey

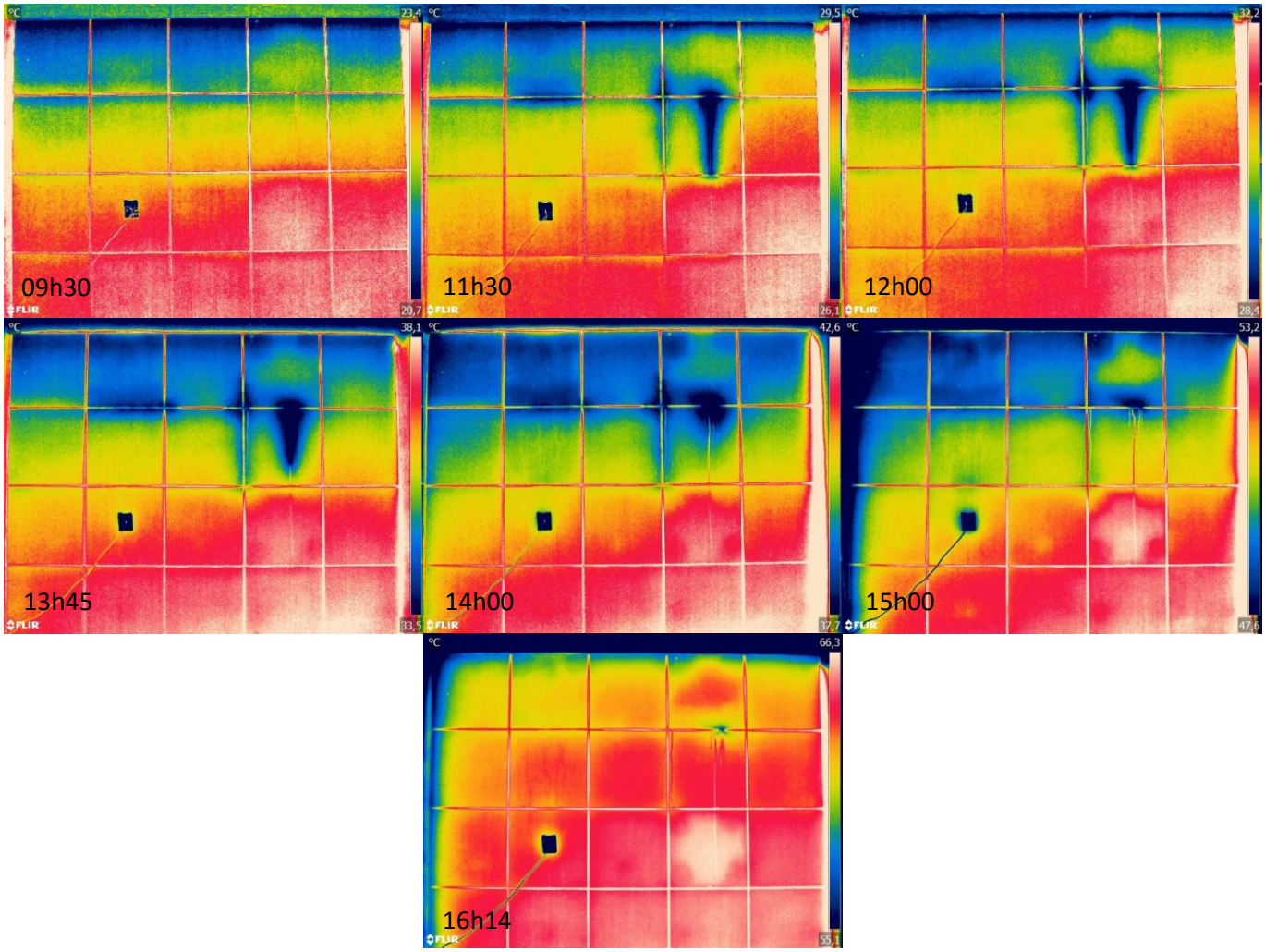

Figure C.15 – Second humidity survey C1_B

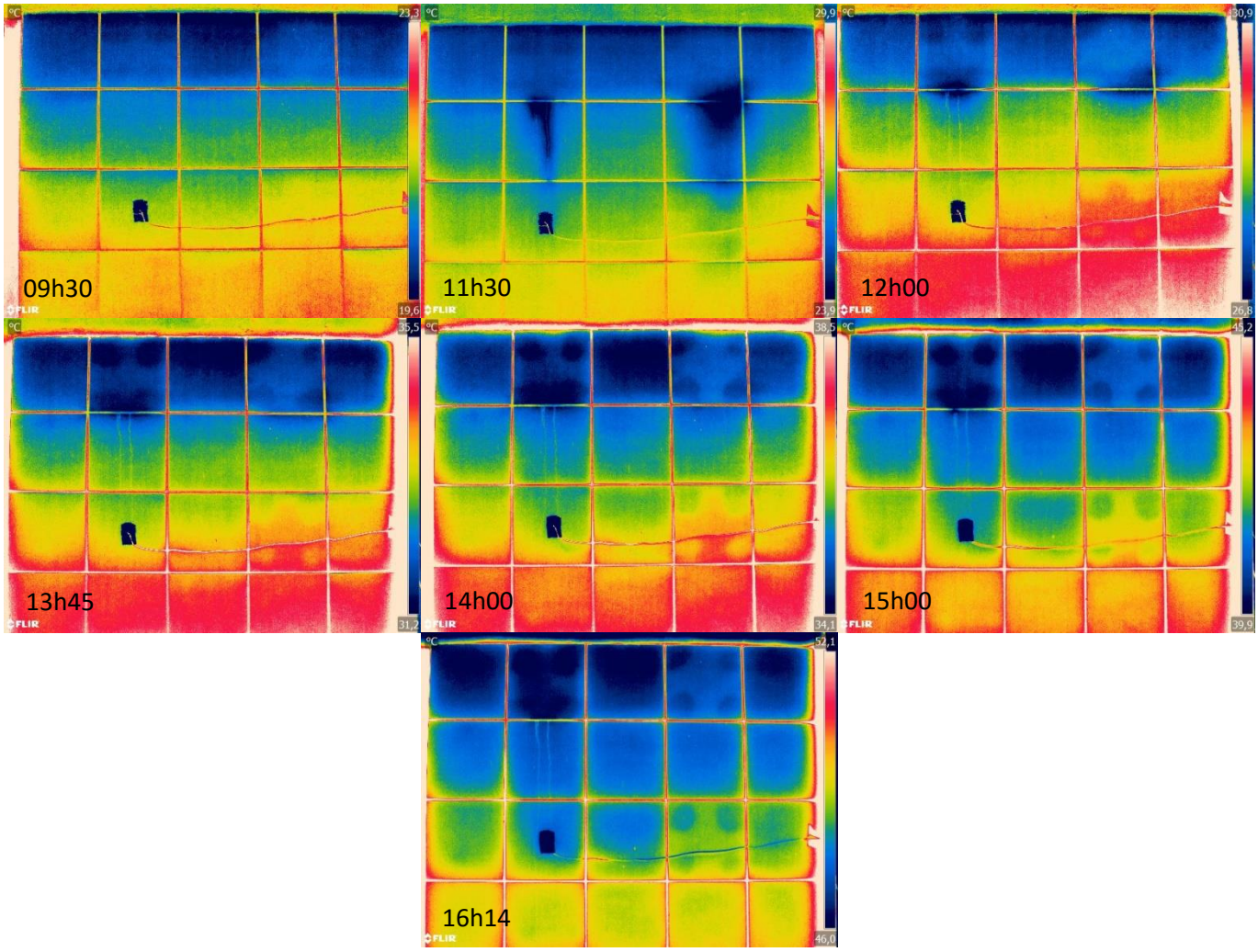

Figure C.16 - Second humidity survey C1_W

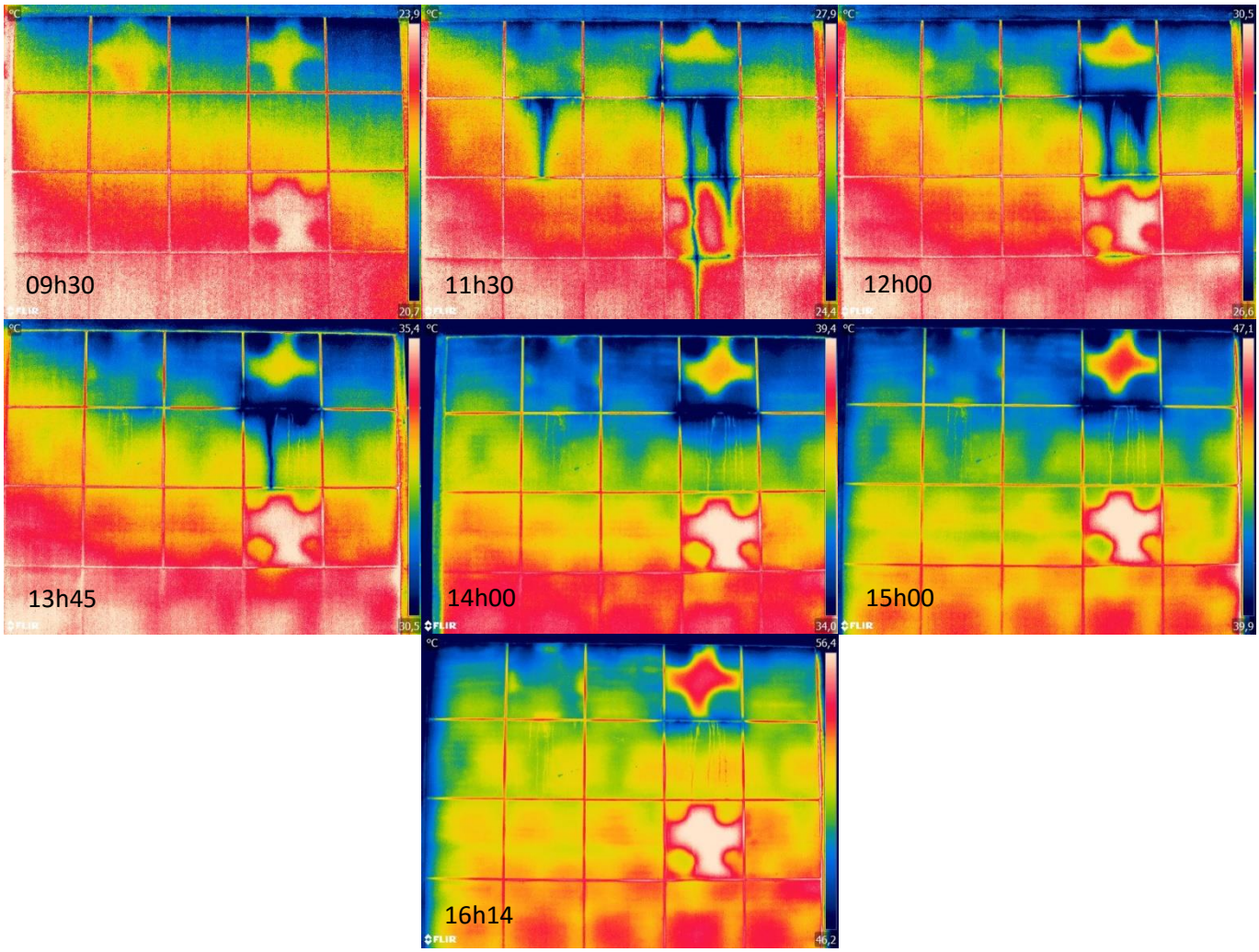

Figure C.17 - Second humidity survey C2_B

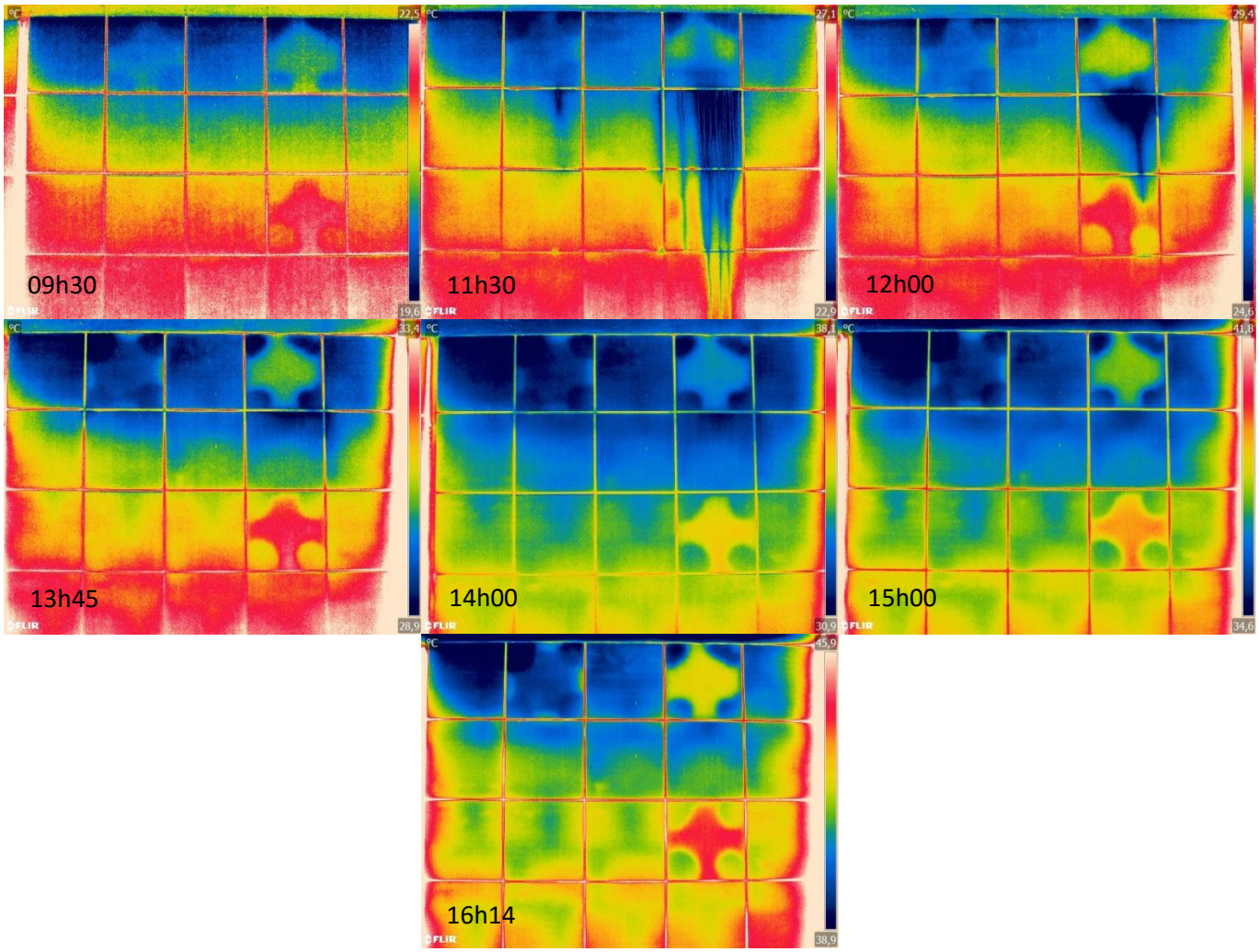

Figure C.18 - Second humidity survey C2_W

Appendix D – Case studies

A.1. Thermographic inspection in LNEC

Here the same thermograms presented in chapter 5 are presented in a higher scale for better perception.

FigureD.1 - Photo of the façade (*Edifício Manuel Rocha*)

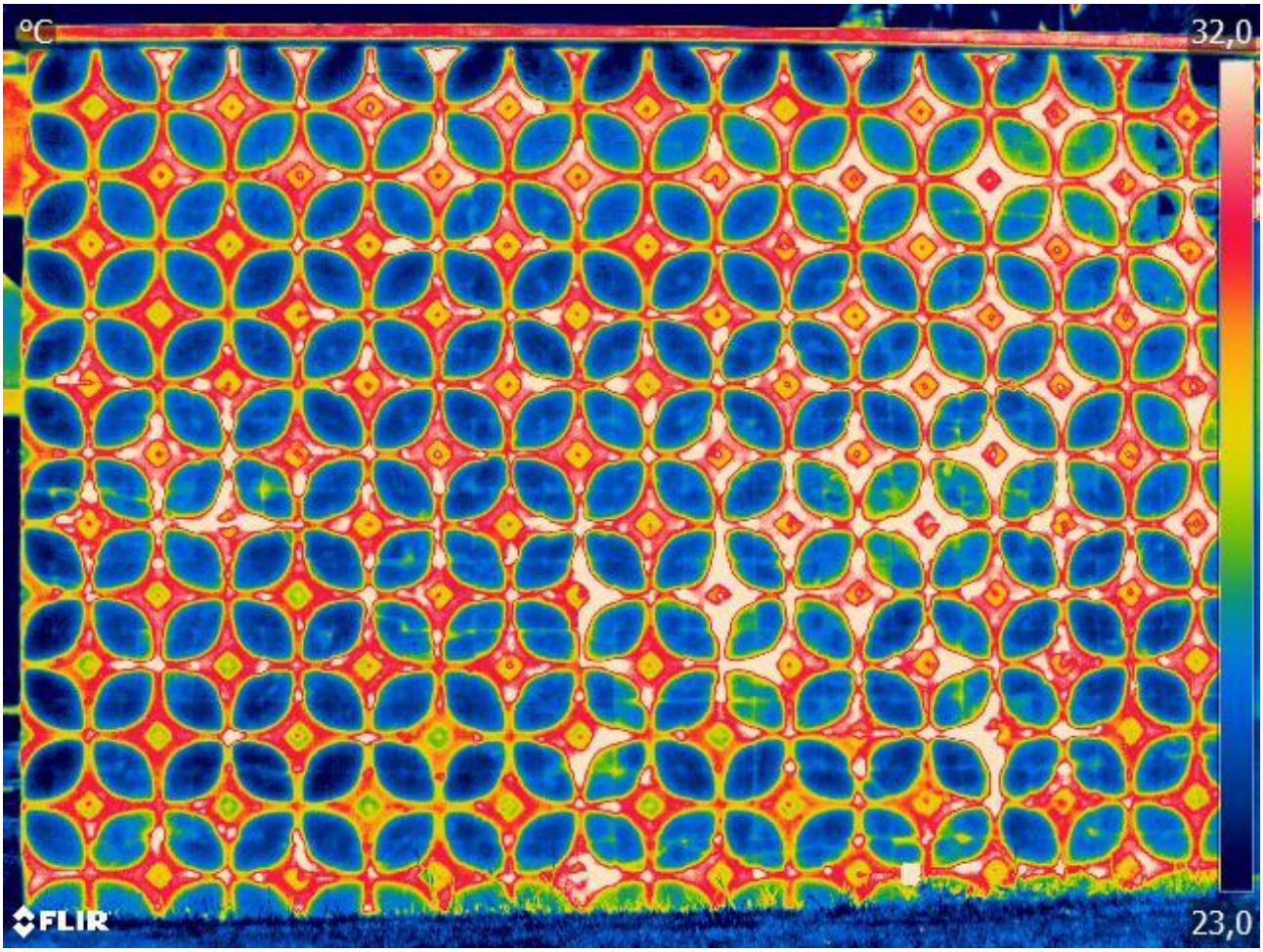

Figure D.2 - Untreated thermogram (*Edifício Manuel Rocha*)

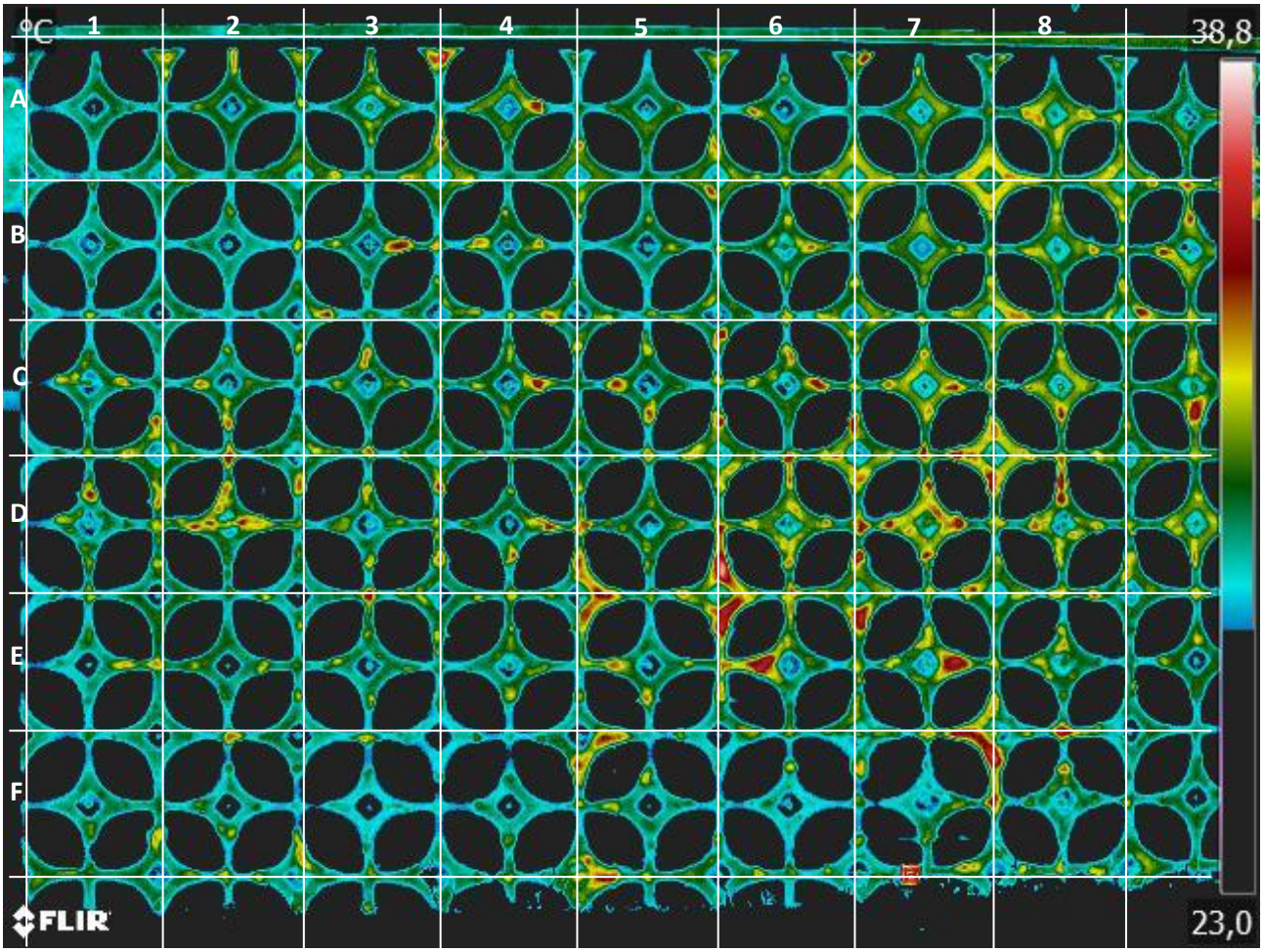

Figure D.3 - Thermogram treated to visualize anomalies in blue tile zones

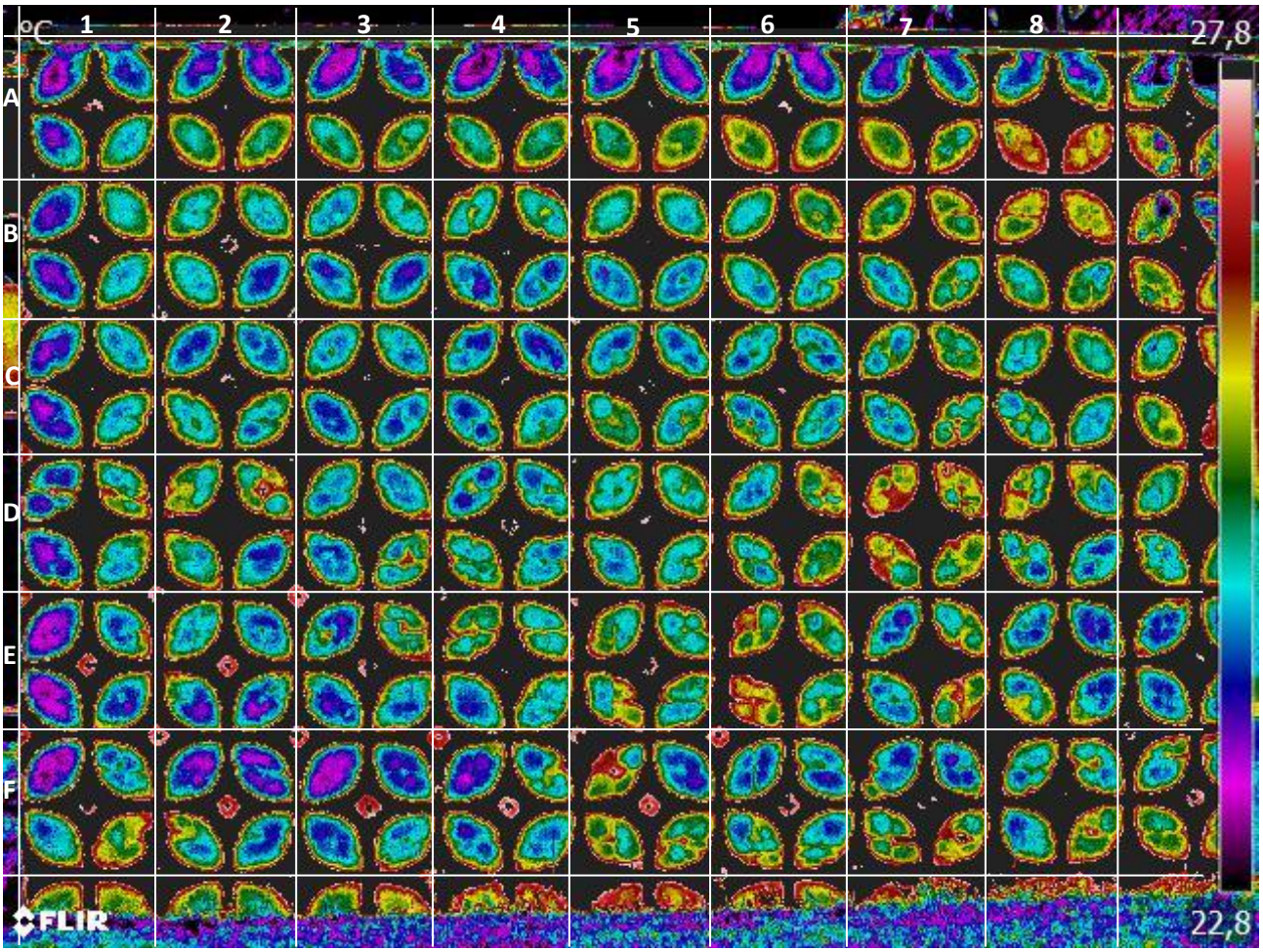

Figure D.4 - Thermogram treated to visualize anomalies in white tile zones

A.1. Thermographic inspection sheet – Case study 2

Building: Parque das nações

Address: Rua da Ilha dos Amores, 1990-118 Lisboa **Date of Inspection:** 21/07/2016

Year of construction: 2000 **Nº of floors:** 5 **Structural typology:** Reinforced concrete

Building's use: Residential building

Cladding(s): Stone and ceramic tilling systems

Material (ceramics): Klinker **Colour:** Ochre **Fixation:** Adhesive tiles

Estate of conservation: Good, apart from the cladding detachments.

Suffered interventions/rehabilitations: No **Where:**

Walls' description: Double leaf wall with thermal insulation

Shadowing elements (from the building): The building has balcanies both in the eastern and western façade's edges.

Shadowing elements (exterior): The western façade gets partially shadowed by the neighbour building.

Observations: Despite being relatively recent, the building suffers from detachments of ceramic tiles that can compromise security in such a way that the perimeter around the building is fenced to prevent people's passage. With the incidence of sideways solar radiation it is possible to visually identify flatness irregularities that might indicate detached zones. There are also some small areas where the tiles are either clearly about to fall or already did so.

Weather conditions:

Wind speed: Low **Sky:** Clean **Temperature:** 27°C **Relative humidity:** 55%

Thermograms' description:

1. Eastern façade (general)
2. Western façade (general)
3. East 1 (right to left)
4. East 2 (right to left)
5. East 3 (right to left)
6. East 4 (right to left)
7. East 5 (right to left)
8. West close-up 1
9. West shadowed zone
10. West 1 (collage)
11. West 2 (collage)
12. West 3 (collage)
13. West close-up 2
14. West (angled)
15.
16.
17.
18.
19.
20.
21.
22.

Thermogram nº: 1 **Thermograms:** 5886-5888

Time: 09h51 **Façade's orientation**: East

Shadows: No shadows

Sources of reflection: Balconies' guards

Observations: The possibly detached zones are circled in the figure on the right. The structural zones or shadowed zones were not considered as they are of difficut analysis using this scale.

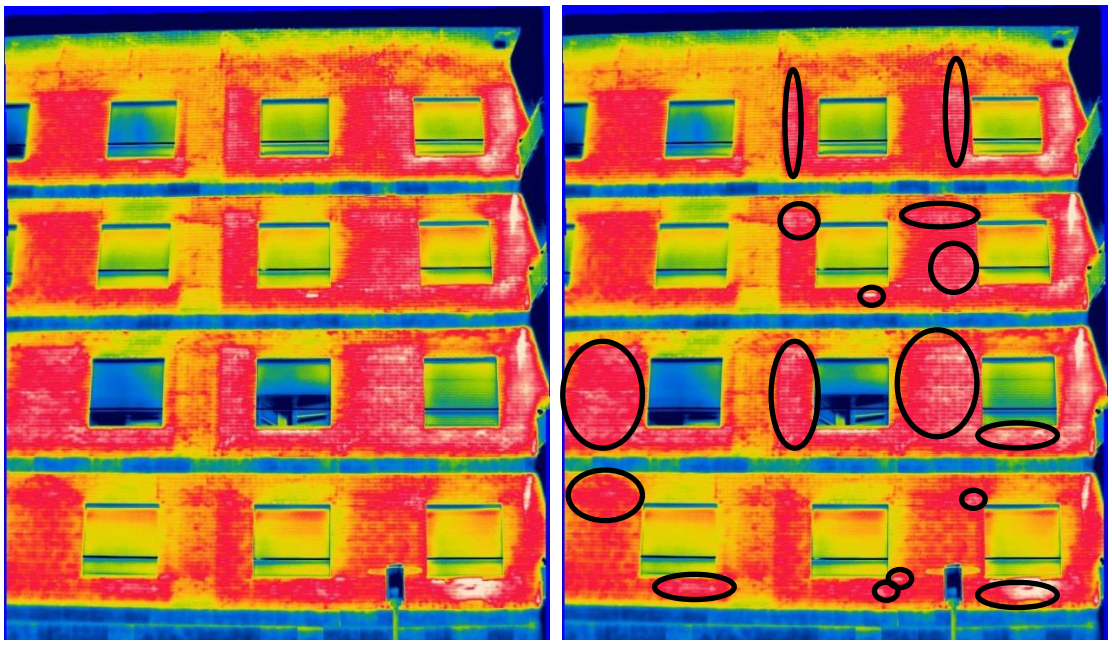

Thermogram nº: 2 **Thermograms:** 5882-5884

Time: 09h51 **Façade's orientation**: East

Shadows: No shadows

Sources of reflection: Balconies' guards

Observations: The possibly detached zones are circled in the figure on the right. The structural zones or shadowed zones were not considered as they are of difficut analysis using this scale.

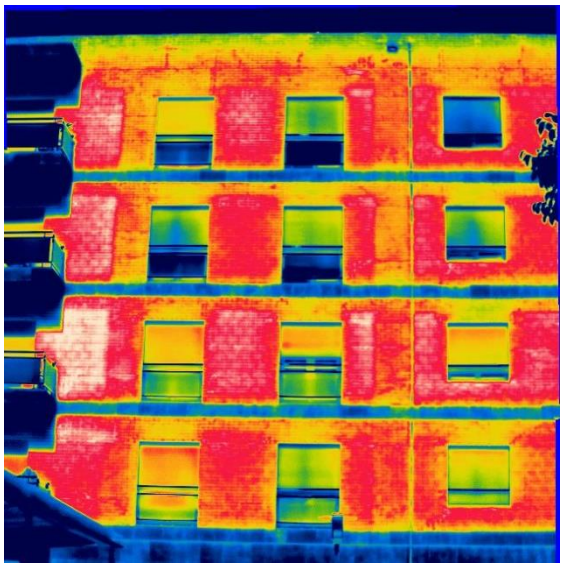

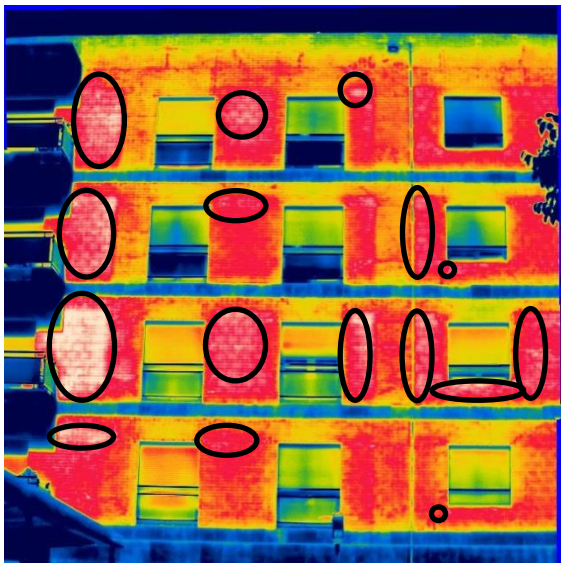

Thermogram nº: 3 **Thermograms:** 5924-5930

Time: 09h51 **Façade's orientation**: East

Shadows: No shadows

Sources of reflection: Balconies' guards

Wind: Low

Observations: This is a collage of 4 thermograms taken closer to the façade. The possibly detached zones are circled in the figure on the right. The structural zones, shadowed zones or zones who suffer reflections were not considered as they are of difficult analysis using this scale.

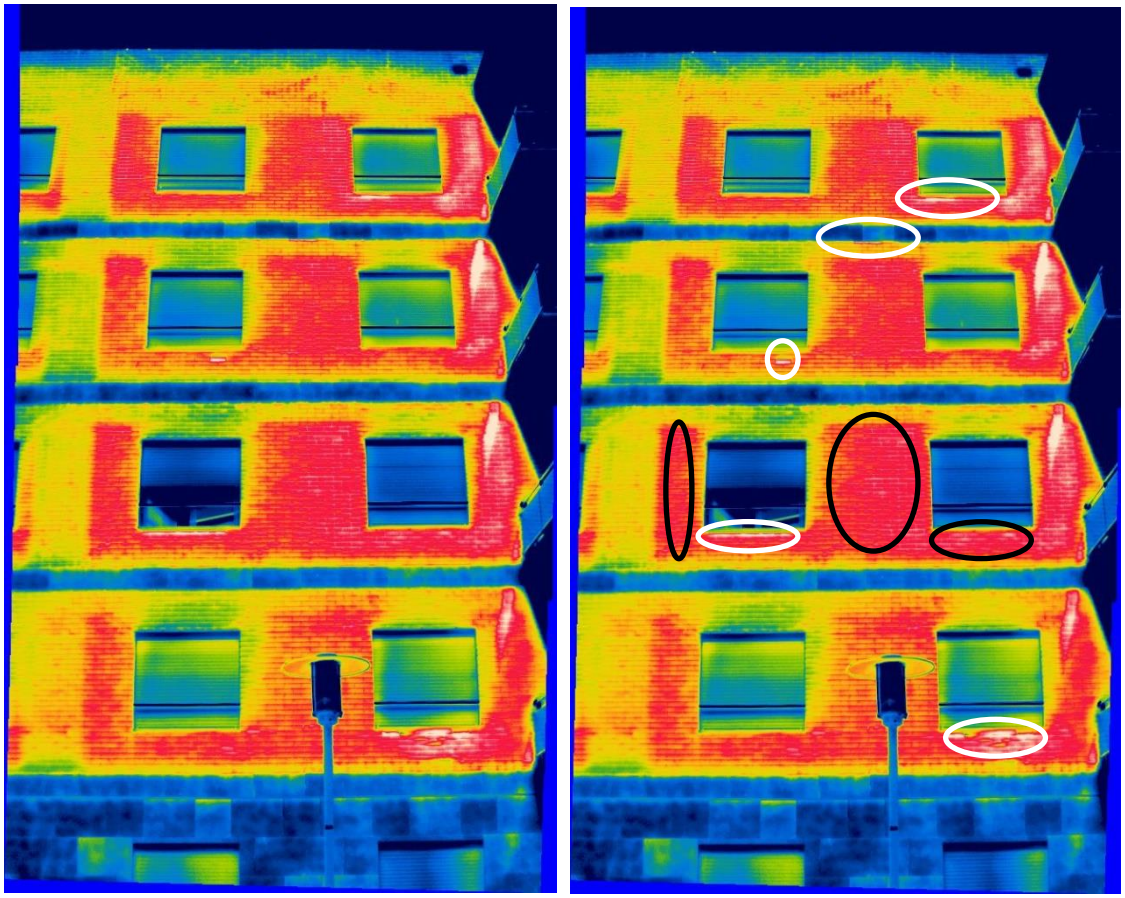

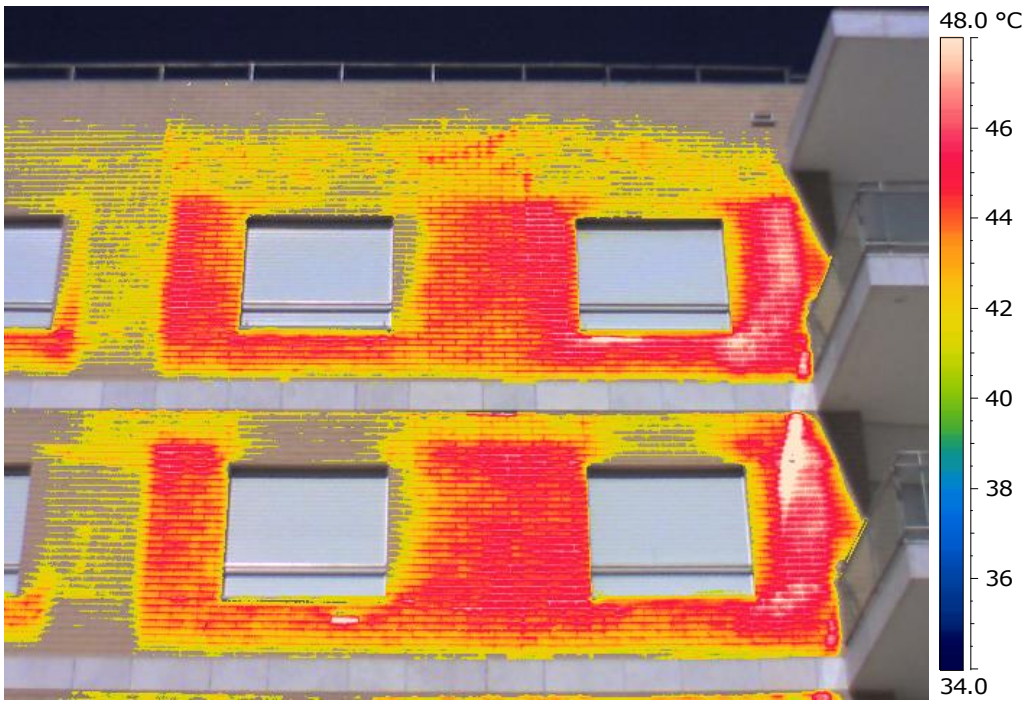
48.0 °C
46
44
42
40
38
36
34.0


48.0 °C
46
44
42
40
38
36
34
33.0


48.0 °C
46
44
42
40
38
36
34
33.0


48.0 °C
46
44
42
40
38
36
34
33.0

Thermogram nº: 4 **Thermograms:** 5932-5938

Time: 09h51 **Façade's orientation**: East

Shadows: No shadows

Sources of reflection: Balconies' guards

Observations: This is a collage of 4 thermograms taken closer to the façade. The possibly detached zones are circled in the figure on the right. The structural zones, shadowed zones or zones who suffer reflections were not considered as they are of difficult analysis using this scale.

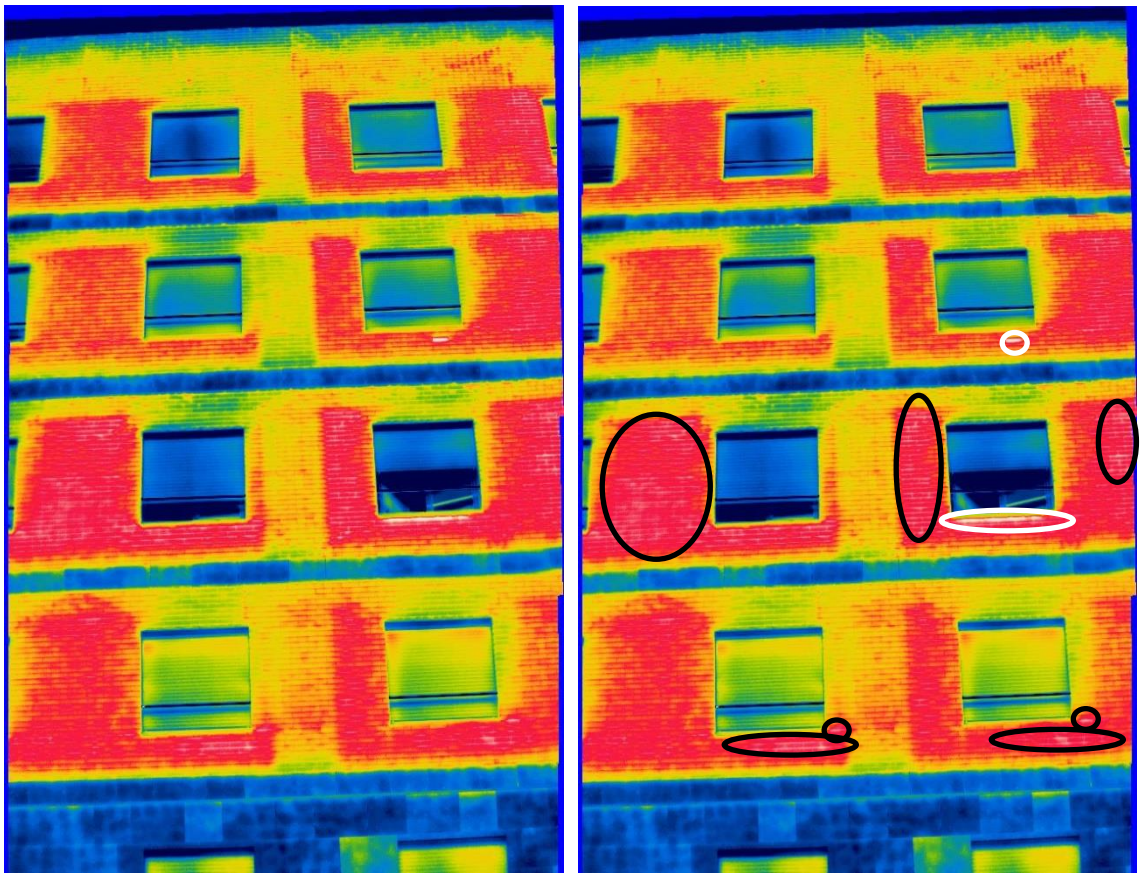


48.0 °C
46
44
42
40
38
36
34
33.0

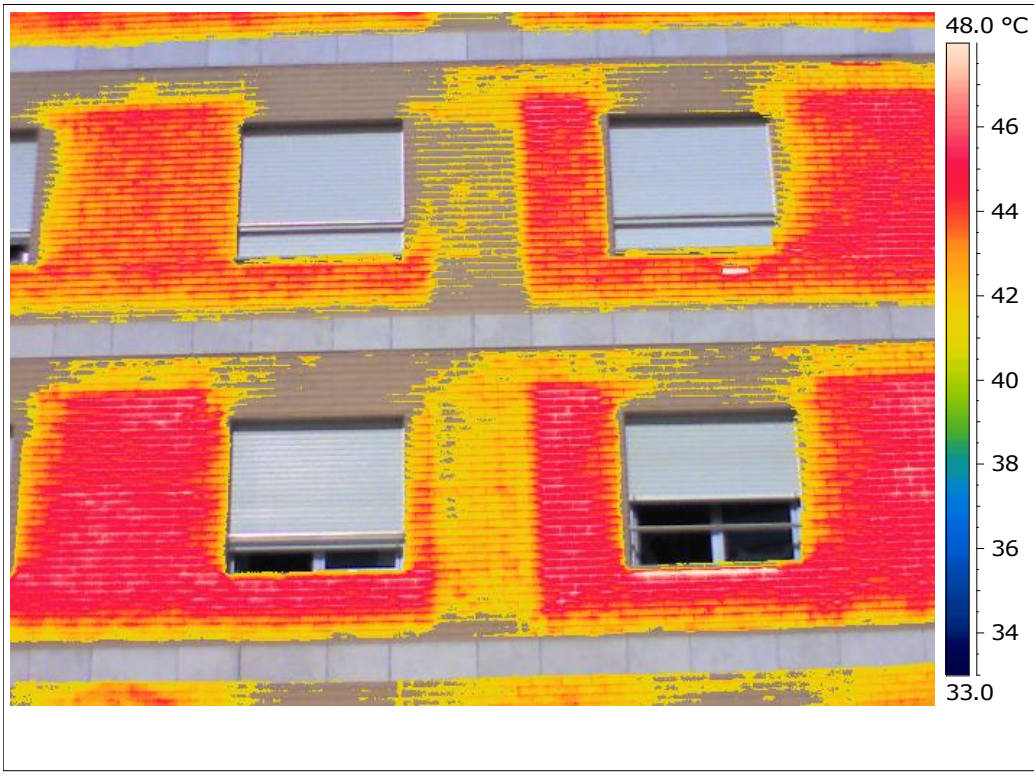
48.0 °C
46
44
42
40
38
36
34
33.0


48.0 °C
46
44
42
40
38
36
34
33.0


48.0 °C
46
44
42
40
38
36
34
33.0

Thermogram nº: 5 **Thermograms:** 5940-5946

Time: 09:51 **Façade's orientation**: East

Shadows: No shadows

Sources of reflection: Balconies' guards

Observations: This is a collage of 4 thermograms taken closer to the façade. The possibly detached zones are circled in the figure on the right. The structural zones, shadowed zones or zones who suffer reflections were not considered as they are of difficult analysis using this scale.

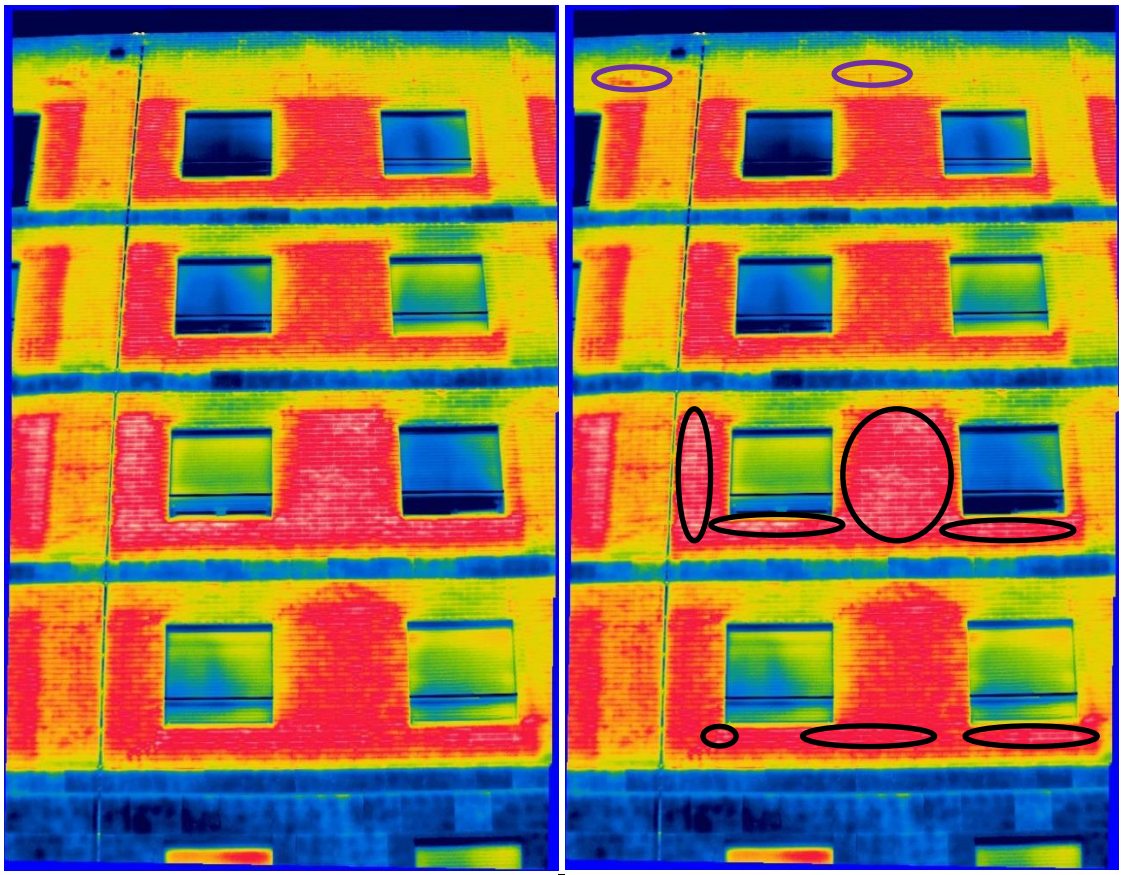


48.0 °C
46
44
42
40
38
36
34
33.0


48.0 °C
46
44
42
40
38
36
34
33.0


48.0 °C
46
44
42
40
38
36
34
33.0


48.0 °C
46
44
42
40
38
36
34
33.0

Thermogram nº: 6 **Thermograms:** 5948-5954

Time: 09h51 **Façade's orientation**: East

Shadows: No shadows

Sources of reflection: Balconies' guards

Observations: This is a collage of 4 thermograms taken closer to the façade. The possibly detached zones are circled in the figure on the right. The structural zones, shadowed zones or zones who suffer reflections were not considered as they are of difficult analysis using this scale.

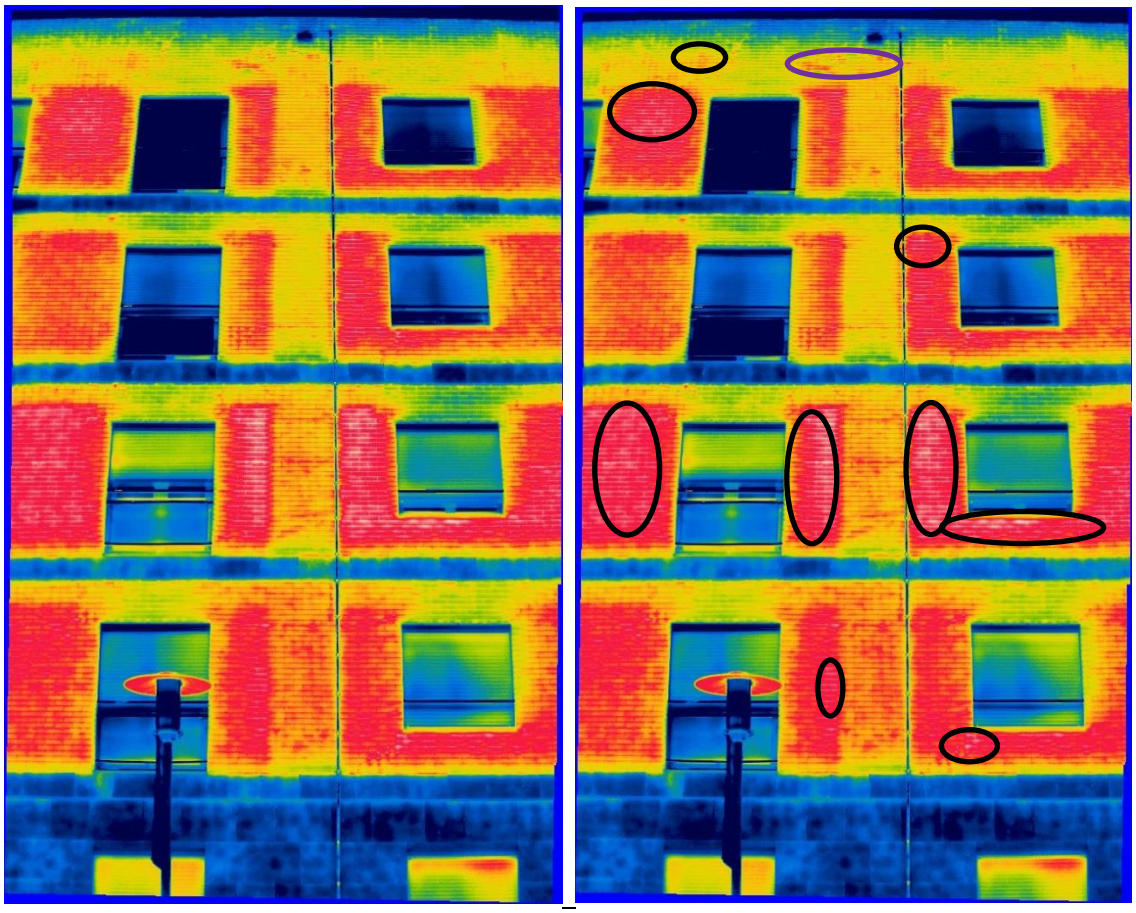


48.0 °C
46
44
42
40
38
36
34
33.0

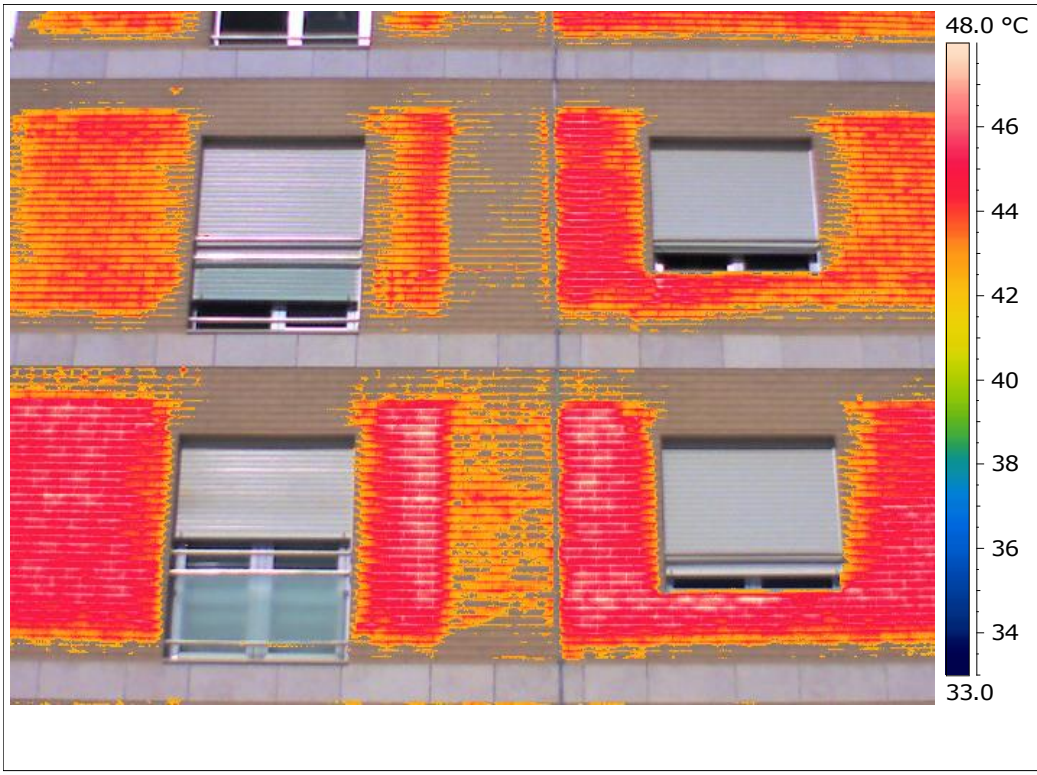
48.0 °C
46
44
42
40
38
36
34
33.0


48.0 °C
46
44
42
40
38
36
34
33.0

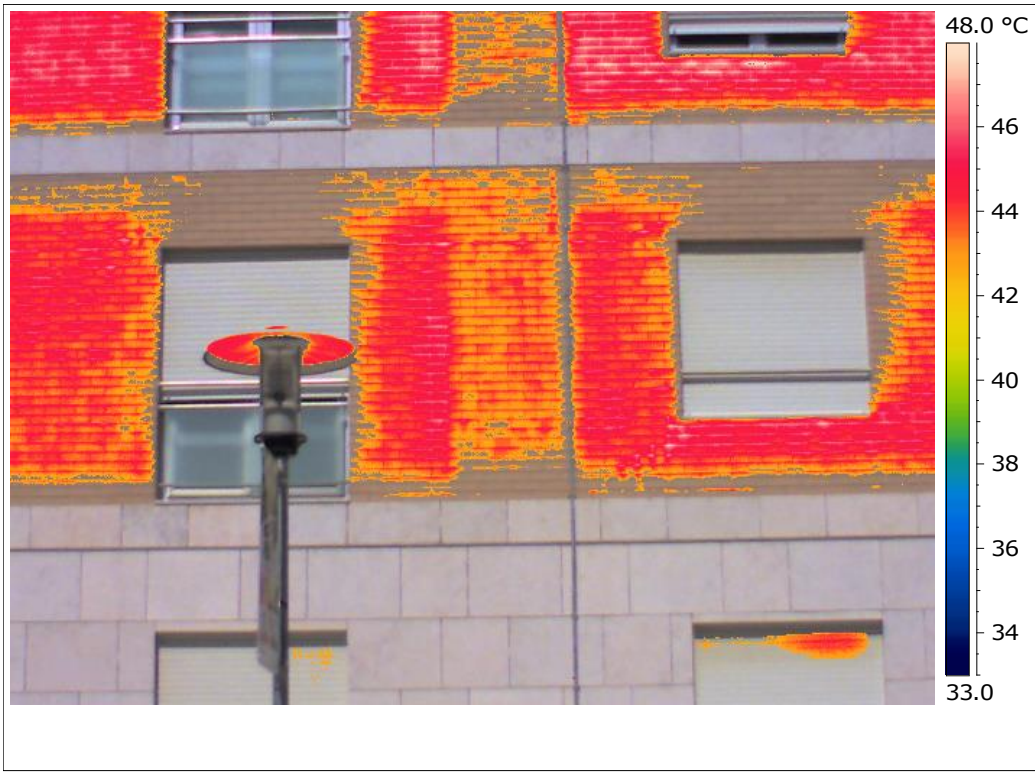
48.0 °C
46
44
42
40
38
36
34
33.0

Thermogram nº: 7 **Thermograms:** 5964-5970

Time: 09h51 **Façade's orientation**: East

Shadows: No shadows

Sources of reflection: Balconies' guards

Observations: This is a collage of 4 thermograms taken closer to the façade. The possibly detached zones are circled in the figure on the right. The structural zones, shadowed zones or zones who suffer reflections were not considered as they are of difficult analysis using this scale.

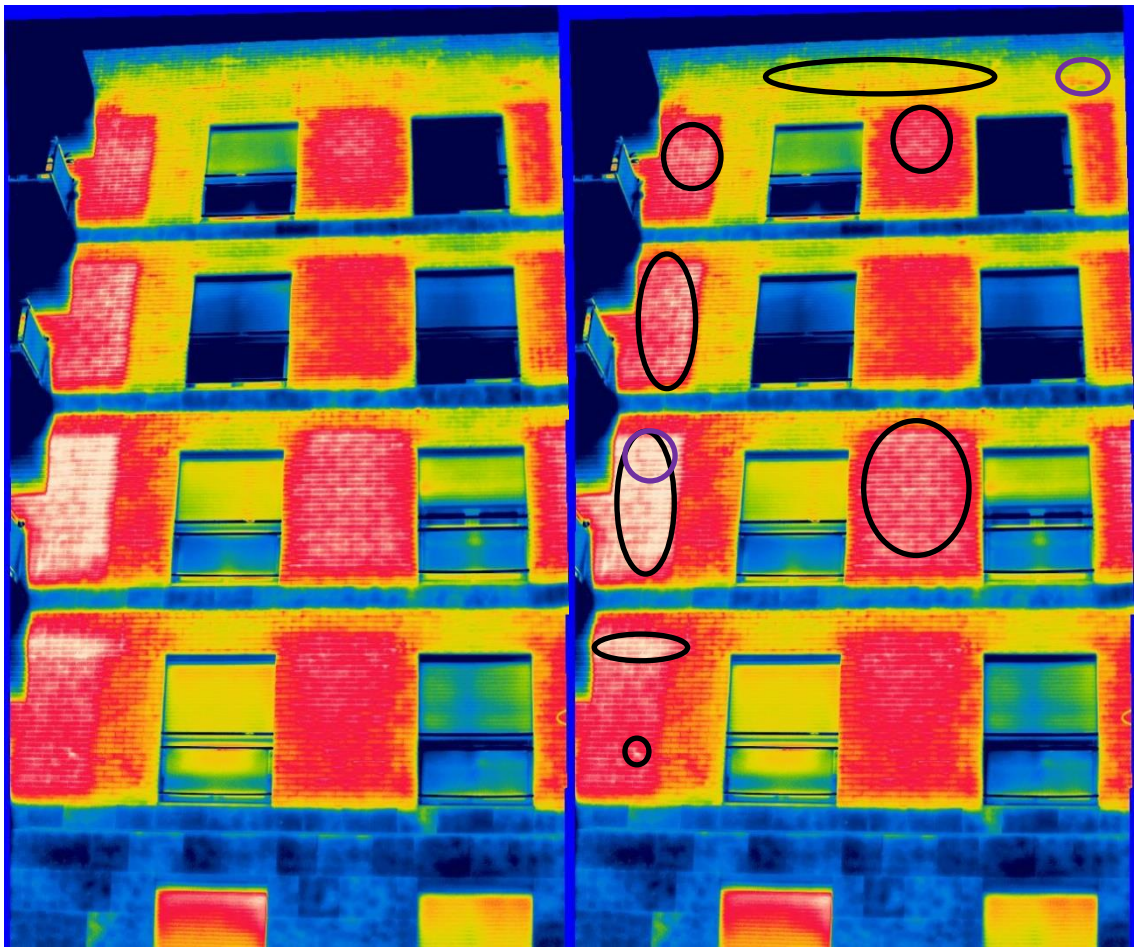


48.0 °C
46
44
42
40
38
36
34
33.0


48.0 °C
46
44
42
40
38
36
34
33.0


48.0 °C
46
44
42
40
38
36
34
33.0


48.0 °C
46
44
42
40
38
36
34
33.0

Thermogram nº: 8 **Thermograms:** 6024-6030

Time: 09h51 **Façade's orientation**: West

Shadows: No shadows

Sources of reflection: No Sources of reflection

Observations: This is a collage of 4 thermograms taken closer to the façade. The possibly detached zones are circled in the figure on the right. The structural zones, shadowed zones or zones who suffer reflections were not considered as they are of difficult analysis using this scale.

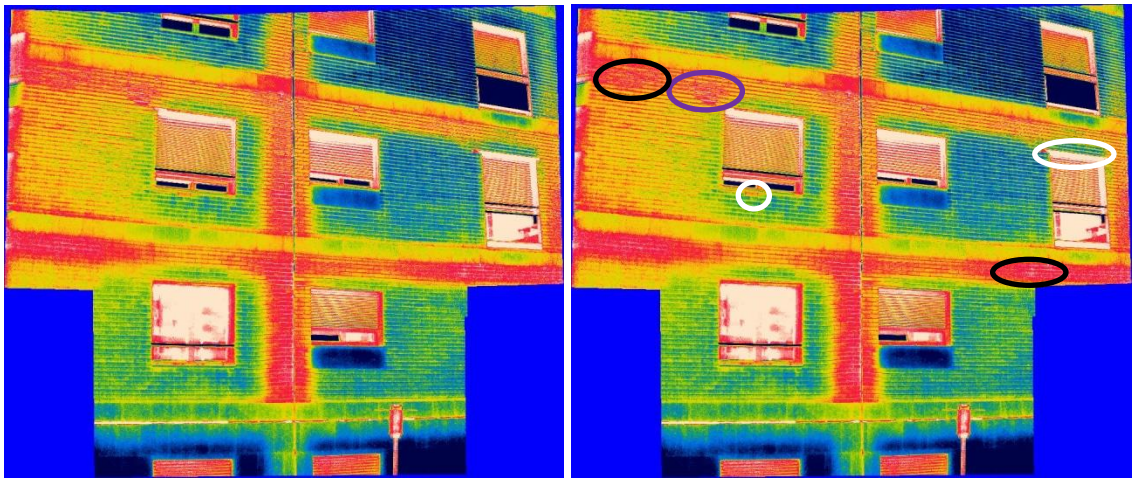

Thermogram nº: 9 **Thermograms:** 6088-6100

Time: 09h51 **Façade's orientation**: West

Shadows: Shadowed by the neighbour building

Sources of reflection: No Sources of reflection

Observations: This is a collage of 3 thermograms taken closer to the façade where two distinguishable zones are present (a cooler zone because of shadowing and a hotter zone that is being irradiated). This collage was made in order to understand if it is possible to visualize any anomalous zones right after shadowing. The possibly detached zones are circled in the figure on the right. The structural zones, shadowed zones or zones who suffer reflections were not considered as they are of difficult analysis using this scale.

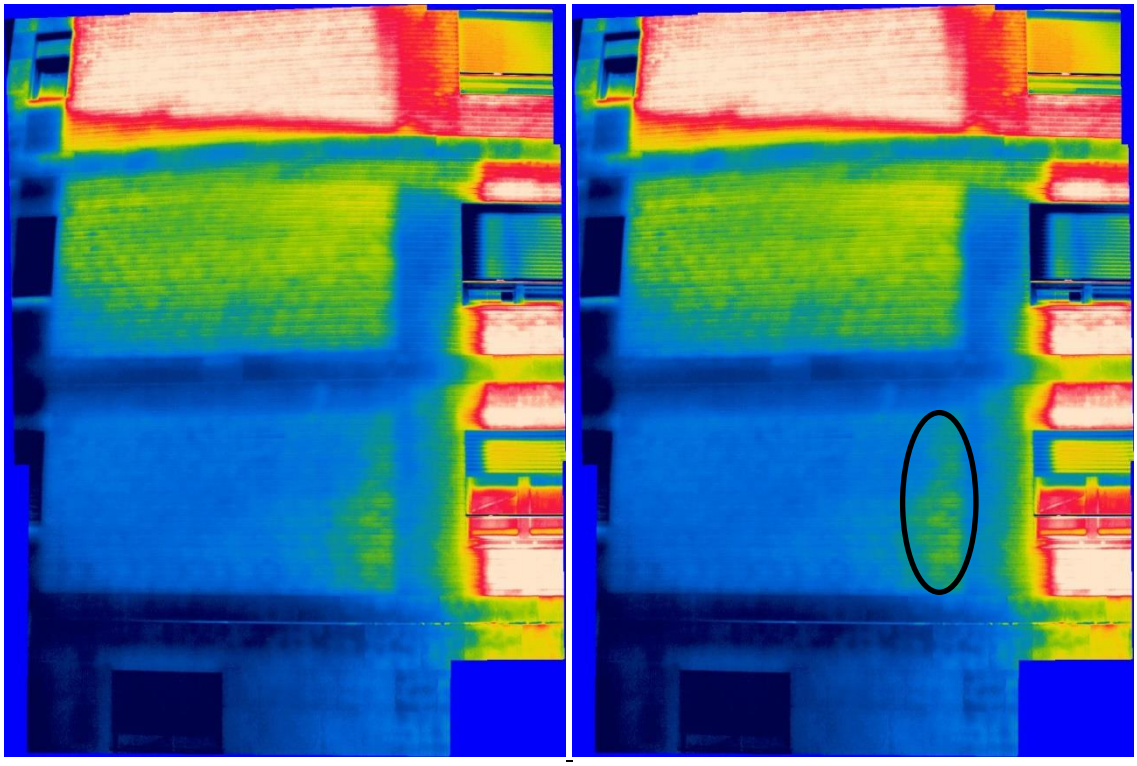

Thermogram nº: 10 **Thermograms:** 6032-6046

Time: 09h51 **Façade's orientation**: West

Shadows: Shadowed by the neighbour building

Sources of reflection: Reflections from the neighbour building

Observations: This is a collage of thermograms taken closer to the façade. The possibly detached zones are circled in the figure bellow. The structural zones, shadowed zones or zones who suffer reflections were not considered as they are of difficult analysis using this scale. The yellow circles represent reflections from the neighbour building.

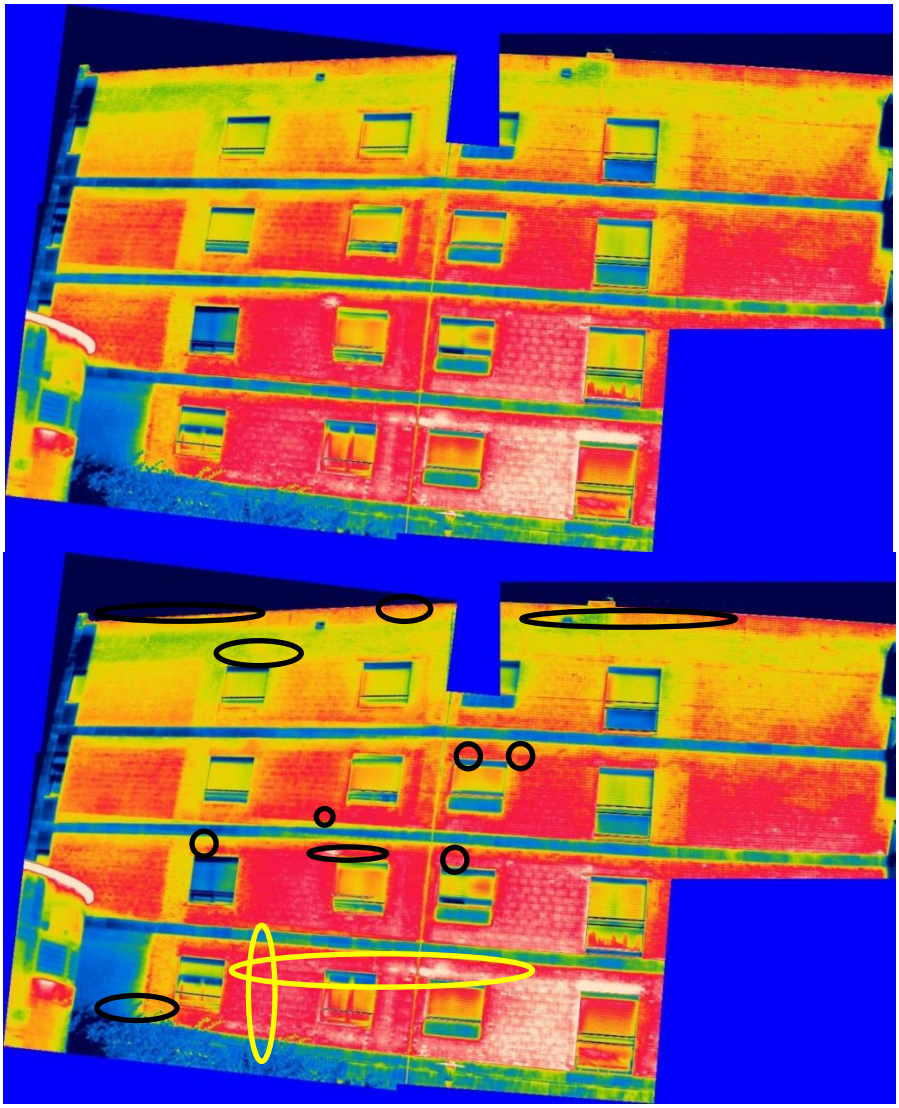

Thermogram nº: 11 **Thermograms:** 6040-6046

Time: 09h51 **Façade's orientation**: West

Shadows: No shadows

Sources of reflection: Reflections from the neighbour building

Observations: This is a collage of thermograms taken closer to the façade. The possibly detached zones are circled in the figure bellow. The structural zones, shadowed zones or zones who suffer reflections were not considered as they are of difficult analysis using this scale. The yellow circles represent reflections from the neighbour building.

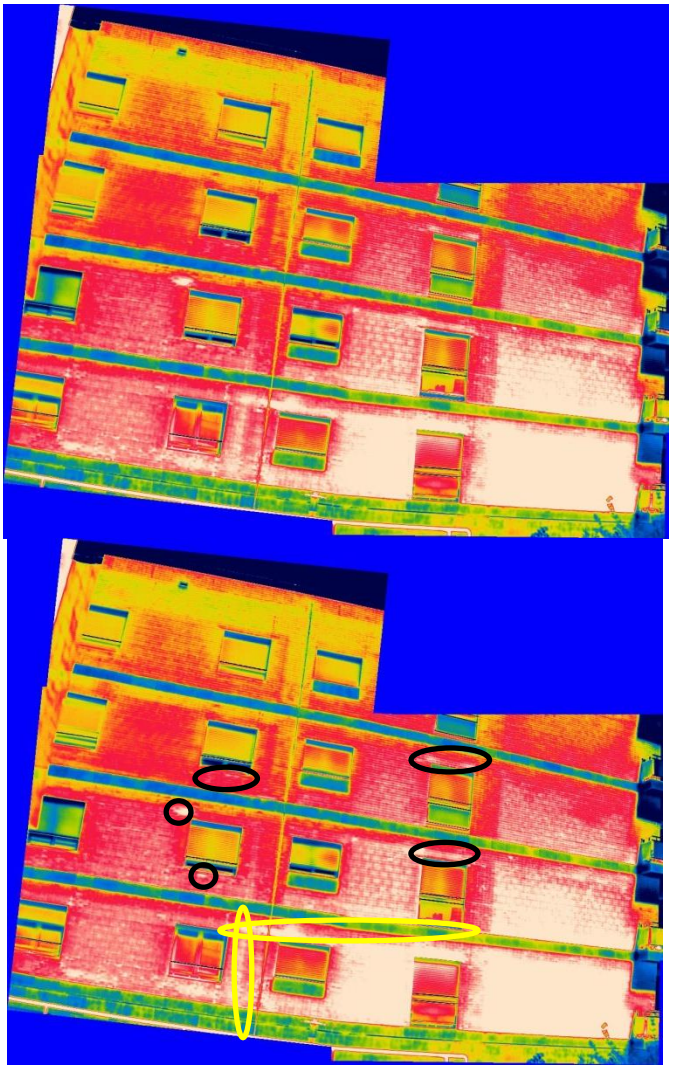

Thermogram nº: 12 **Thermograms:** 6072

Time: 09:51 **Façade's orientation**: West

Shadows: No shadows

Sources of reflection: Reflections from the neighbour building

Observations: This is a collage of thermograms taken closer to the façade. The possibly detached zones are circled in the figure on the right. The structural zones, shadowed zones or zones who suffer reflections were not considered as they are of difficult analysis using this scale. The yellow circles represent reflections from the neighbour building.

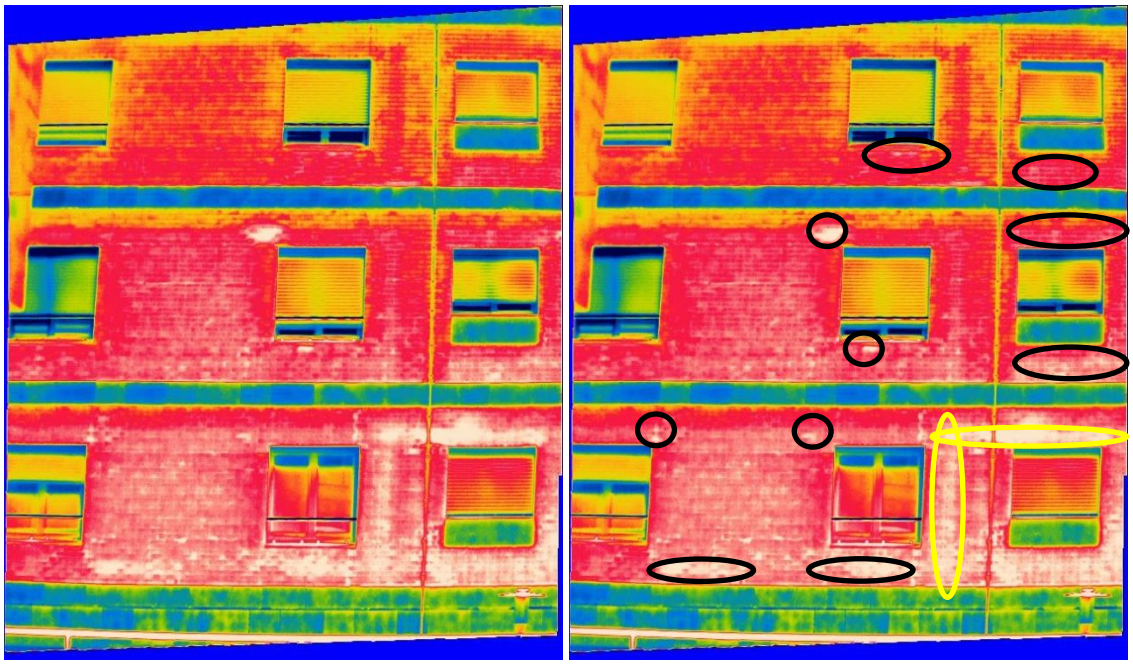

Thermogram nº: 13 **Thermograms:** 6074-6086

Time: 09h51 **Façade's orientation**: West

Shadows: No shadows

Sources of reflection: No Sources of reflection

Observations: This is a thermogram taken from a closer distance for a bette visualization of a clear detachment over the left window on the first floor. The possibly detached zones are circled in the figure on the right. The structural zones, shadowed zones or zones who suffer reflections were not considered as they are of difficult analysis using this scale.

Thermogram nº: 13 **Thermograms:** 6074-6086

Time: 09h51 **Façade's orientation**: West

Shadows: No shadows

Sources of reflection: Reflections from the neighbour building

Observations: This is a collage of thermograms taken from a diagonal position to the façade. The possibly detached zones are circled in the figure on the right. The structural zones, shadowed zones or zones who suffer reflections were not considered as they are of difficult analysis using this scale. The yellow circles represent reflections from the neighbour building. The angle from which the thermogram was taken might difficut its interpretation.

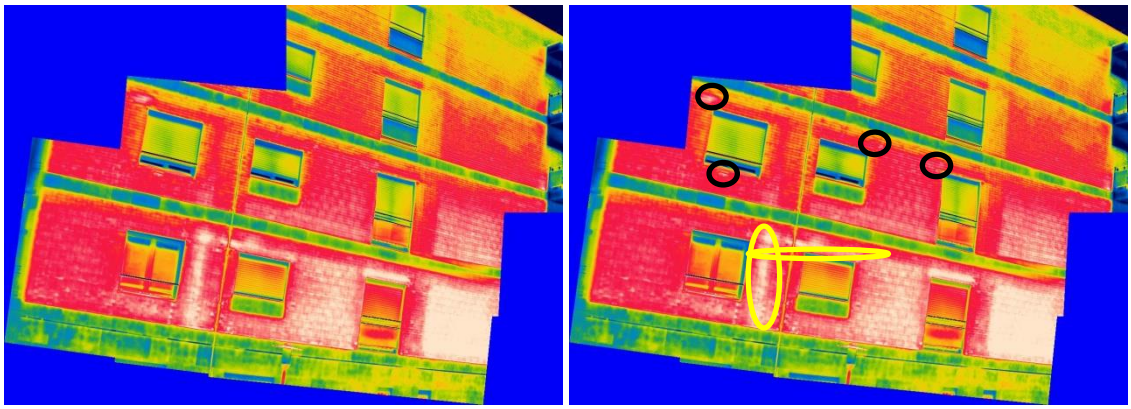

Anomalous zones schematic representation

Eastern façade

Western façade

Detachments both visible on photos: 

Detachments visualized on thermograms: